Journal of the
OPTICAL SOCIETY
of AMERICA

VOLUME 39, NUMBER 7 JULY, 1949

Image Contrast in Phase-Contrast Microscopy

PAUL H. KECK
Signal Corps Engineering Laboratories, Fort Monmouth, New Jersey,

AND

ARTHUR T. BRICE
Ross, California

(Received March 28, 1949)

The development of applications of the Zernike, or phase-contrast, principle in microscopy offers not only an image of the object more precisely resembling it than any other heretofore obtainable, but even a new method of perception, by means of which certain characteristics of objects heretofore invisible may be determined by immediate inspection. The application of the fullest capability of this method waits the development of procedures for more exactly determining the optical characteristics of objects, particularly the effect on the light of refraction and absorption characteristics combined at single points. The studies and conclusions reported in this paper represent an effort to simplify the evaluation procedure, and present a first approximation of the influence of the factors involved in phase-contrast image formation. They are no more than logical consequences of the Zernike principle.

I. INTRODUCTION

THE purpose of the phase-contrast method in microscopy is to increase the contrast of images of objects containing structures differentiated by only very small differences of absorption, as well as to give visible contrast to very small refraction differences in such structures where absorption may be entirely lacking and the structures are completely transparent.

As has been shown by F. Zernike[1] and others[2,3] two means of accomplishing these results are available:

(a) phase alteration of various orders of the diffraction spectrum occurring in the rear focal plane of the objective, by which transparent differences of phase produced by the object are converted into apparent amplitude differences at the image; and (b) absorption of a portion of the light transmitted at either the zero order maximum or at higher orders of the diffraction spectrum, by which a more favorable balance of distribution of the light as between the different orders of maxima may be obtained.

To secure maximum contrast in the image it is necessary to combine these two means in proper proportions, which are dependent on the absorption and refraction characteristics of the object. This can only be done with precision when such characteristics are known. A double integration process must be carried out; the first integration over the plane of the object; the second over the rear focal plane of the objective lens at which the diffraction pattern produced by the object structure appears. Actually as was pointed out by F. Zernike[4] early in the development of his theory unless the source of light is treated as a point in these calculations, a third integration over the area of the light source must be applied, so that precise mathematical treatment of the problem is subject to possible errors in the integrations and various physical outlooks. Calculations of this type, assuming a perfect grid structure as the object, have been published by F. Zernike,[1] and more recently by Christa and E. Menzel.[5]

[1] F. Zernike, "Phase contrast, a new method for the microscopic observation of transparent objects," Physica **IX**, 686–698 and 974–986 (1942).

[2] Bennett, Jupnik, Osterberg, and Richards, "Phase microscopy," Trans. Am. Microscopical Soc. **65**, No. 2, 99–131 (1946).

[3] Arthur T. Brice, "The phase principle in microscopy," Reports Division, Office of Technical Services, Dept. of Commerce, Washington 25, D. C., Report No. PB-78279 (1947).

[4] F. Zernike, "Das Phasenkontrastverfahren bei der mikroskopischen Beobachtung," Zeits. f. tech. Physik **16**, 454–457 (1935).

[5] Christa and E. Menzel, "Die Beugungserscheinungen optischer Gitter nach Intensität und Phase," Optik **3**, 247–259 (1948); also "Zur Abbildung optischer Gitter," *ibid.* **4**, 22–36 (1948).

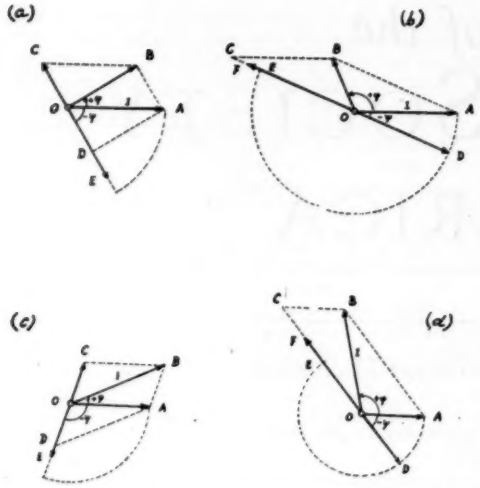

FIG. 1. Vector diagrams representing amplitude and phase relationships of various components of the light. (a) Brightfield objects with "*A*" type phase plates. (b) Brightfield objects with "*B*" type phase plates. (c) Darkfield objects with "*A*" type phase plates. (d) Darkfield objects with "*B*" type phase plates.

Lacking complete information as to the optical characteristics of the object, as is the case in many problems for microscopy, such precise mathematical treatment cannot be applied at all, and it therefore seems unlikely that microscopists will be able to make use of the fullest possible capability of the phase-contrast method for a long period of time. This, however, does not mean that the method has no immediate interest to microscopists or immediate practical applications—since it is evident from the practical microscopy that has already been done by it[6–8] that a vast improvement of images, and even a new method of perception, is provided by approximations to the theoretically optimum values. We may apply phase alteration and absorption of portions of the light, combined in such proportions as can be shown to produce the best contrast effects with the widest possible range of object optical characteristics, and rest content with less than maximum possible contrast in some details.

A paper by R. Richter[9] has suggested a basis for evaluation of the phase plate characteristics for known refraction characteristics of the object, assuming the details of interest to be very small and comparable in size to the resolving power of the optical system in use. In a former paper[10] we have also given some approximations of the optimum absorption to be incorporated in the phase plate ring for a wide variety of objects having inherent contrast characteristics based on only very small phase differences. The object of this study has been to extend these methods of analysis and to approximate for a wider range of objects the deviation from maximum possible contrast that may occur when the proportions of phase and absorption alteration incorporated in the phase plate do not meet the exactly calculated optimal values. In presenting our conclusions we make no claim to having given the subject a strict mathematical treatment. As stated above, such treatment can be applied only when the information as to the optical characteristics of the object is complete, as in the cases of artificially prepared test objects, or gratings.

The reasonable assumption upon which our study is based is that the image of a small object detail produced by the microscope can be characterized by the concept of contrast indicated by the brightness of the center of the image detail compared to the brightness of a surrounding area far enough away from the center so that the latter brightness may be considered a constant. This assumption permits us to simplify the evaluation by a vectorial method of analysis, and the conclusions based on it constitute, we believe, a first approximation of the influence of factors involved in the phase-contrast image formation. Such conclusions are only valid for small object details which give rise to an image diffraction disk having a central area of approximately constant brightness, that is to say, large enough so that they lie within the limits of resolving power of the optical system in use.

In describing the image of an object we shall speak of a "*Brightfield Object*" as an object which is more absorbing to light than its surroundings. Unless a reversal of contrast may be produced by the optical system, the image of such an object will be a "*Brightfield Image*" in which the object detail appears as darker against a brighter surrounding area. On the other hand, an object which absorbs less light than its surroundings will be referred to as a "*Darkfield Object*," and its image, if no reversal of contrast is produced by the optical system, will be a "*Darkfield Image*," in which the object will appear as brighter than its surroundings. In our discussion of the problem the following symbols will be used:

φ = A phase difference produced by refractive difference between the object detail and its surroundings. A minus (−) value indicates acceleration at the detail, i.e., refractive index of detail smaller than refractive index of its surroundings. A plus (+) value indicates retardation at the detail, i.e., index of detail greater than index of its surroundings.

ψ = A calculated optimal phase difference needed in the phase plate for maximum contrast effect with the object under con-

[6] Robert Barer, "Some applications of phase-contrast microscopy," Quarterly J. Microscopical Sci. **88**, Third Series, No. 4, 491–500 (1947).

[7] Ludford, Smiles, and Welch, "The study of malignant cells by phase-contrast and ultra-violet microscopy," J. Roy Microscopical Soc. **LXVIII**, Series III, Parts 1–4 (1948).

[8] C. R. Austin and J. Smiles, "Phase-contrast microscopy in the study of fertilization and early development of the rat egg," J. Roy. Microscopical Soc. **LXVIII**, Series III, Parts 1–4 (1948).

[9] R. Richter, "Eine einfache Erklärung des Phasenkontrast-mikroskopes," Optik **2**, 342–346 (1947).

[10] A. T. Brice and P. H. Keck, "The most favorable absorption of the phase plate in phase-contrast microscopy," J. Opt. Soc. Am. **37**, No. 8, 647–651 (1947).

sideration. A minus (−) value indicates acceleration at the area of the zero order maximum with respect to the higher orders. A plus (+) value indicates retardation at the zero order area.

$\psi \pm \delta$ = Any actual phase difference other than the optimum incorporated in the phase plate.

T_D = Transparency of a brightfield object referred to the transparency of its homogeneous surroundings as equal to 1.

T_S = Transparency of the surroundings of a darkfield object referred to the transparency of the object as equal to 1.

T_O = Calculated optimal transparency of the phase ring for maximum contrast effect with the object under consideration, referred to the transparency of the higher order area of the phase plate as equal to 1, when absorption is incorporated in the zero order area of the plate; described by Bennett, Jupnik, Osterberg, and Richards[2] as "*A*" type phase plates.

$\bar{T}_O$ = Calculated optimal transparency of the higher order area of the phase plate for maximum contrast effect with the object under consideration, referred to the transparency of the phase ring as equal to 1, when absorption is incorporated in the higher order area of the plate, described by Bennett, Jupnik, Osterberg, and Richards[2] as "*B*" type phase plates.

T_X = Any actual transparency of the phase ring other than optimum, when absorption is incorporated in the ring or zero order area of the phase plate, ("*A*" type).

$\bar{T}_X$ = Any actual transparency of the higher order area of the phase plate other than optimum, when absorption is incorporated in the higher order area of the plate ("*B*" type).

A_O = Absorption of the phase ring or zero order area of the phase plate as defined by $A_O = 1 - \bar{T}_O$.

$\bar{A}_O$ = Absorption of the higher order area of the phase plate as defined by $\bar{A}_O = 1 - T_O$.

K = Actual contrast of a brightfield object as defined by $K = 1 - T_D$.

K^* = Actual contrast of a darkfield object as defined by $K^* = 1 - T_S$.

K_X = Contrast of a brightfield image defined as the ratio of the brightness difference between the object and its surroundings to the brightness of the surroundings.

II. THE TRANSFORMATION OF A BRIGHTFIELD OBJECT OF LOW CONTRAST INTO A BRIGHTFIELD IMAGE OF HIGH CONTRAST

A. The Phase Plate Absorption and Its Influence on the Image Contrast

The first real image produced by the objective lens of the microscope comprises all essential image qualities, and therefore we can confine our consideration to that image, which, in turn, is the one usually viewed through the eyepiece.

If the object is assumed to consist of only a small detail, of constant refractive index and absorption, within a homogeneous surroundings, the light conditions at the object can be described by the vector diagram of Fig. 1a. OA represents the light amplitude corresponding to the uniformly bright background, and OB is assumed to describe the amplitude referring to the object detail. In a brightfield object the detail would be darker than the uniform surroundings. That is to say, since intensities correspond to the squares of amplitudes, that the amplitude OB is smaller than the amplitude OA by the factor $T_D^{\frac{1}{2}}$. Between OA and OB is a certain phase difference, φ, which may be caused by refraction differences occurring within the object. OB can be split by the parallelogram of forces into two components, one of which is equal to OA, and the other of which is represented by OC. As the component OA corresponds to the background in amplitude and phase we can imagine that the detail differs from its surroundings only by irradiating the component OC.

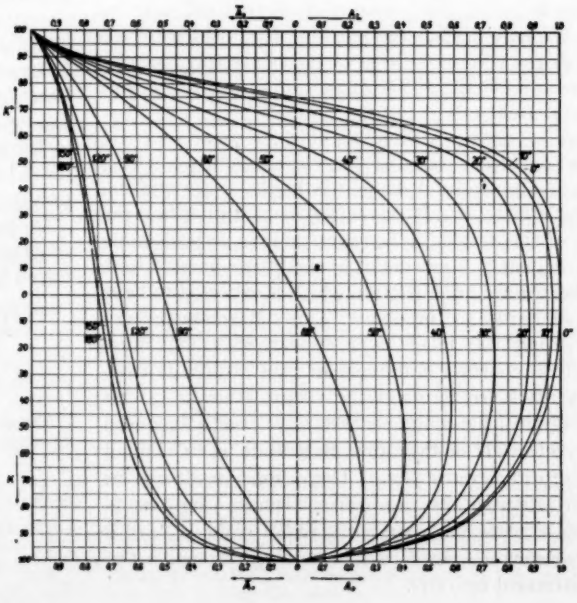

FIG. 2. Graphic representation of Eq. (3). Phase plate absorption and object contrast relationships for maximum brightfield image contrast. The curves illustrate these relationships for various values of phase difference produced at the object. (a) Quadrant I (upper right)—darkfield objects with "*A*" type phase plates. (b) Quadrant II (upper left)—darkfield objects with "*B*" type phase plates. (c) Quadrant III (lower left)—brightfield objects with "*B*" type phase plates. (d) Quadrant IV (lower right)—brightfield objects with "*A*" type phase plates.

TABLE I. For phase plates with absorption in the zero order ring ("A" Types)

Image contrast	Absorption less than optimum	Absorption greater than optimum
K_X	T_X/T_O	T_O/T_X
1	1	1
0.90	2.1	1.73
0.75	4	2.25
0.50	11.7	2.92
0.25	55.7	3.48
0.10	380	3.8

After leaving the object the component OA follows the usual geometrical optical path through the objective lens without suffering a diffraction, because it corresponds to a structureless object. For the same reason the total light flux concerned travels completely through the image of the light source formed in the rear focal plane of the objective lens, where the phase ring or zero order maximum of the Fraunhofer diffraction spectrum is located. Passing through this zero order area OA will appear at the image plane to be evenly distributed over it.

Contrary to OA, the component OC, being out of phase with the background illumination, will give rise to a Fresnel diffraction, dependent on the geometrical shape and size of the small object detail. If we assume a circular detail having a diameter of the magnitude of the resolving power of the optical system, the diffraction disk produced in the rear focal plane of the objective lens will have a diameter of approximately the size of the exit pupil of the objective. We may therefore assume, without making a great error, that the light flux corresponding to the component OC travels through the whole phase plate uniformly distributed over its area. We may neglect the portion of OC which travels through the zero order area of the phase ring, because this area is small, 3–10 percent, in comparison with the total area.

Thus we arrive, without making too great an error, at the conclusion that the flux corresponding to OC is passing completely through the higher order area of the phase plate, and is thereafter concentrated into the image of the detail. To be exact there is no such thing as a completely sharp detail in the image plane. There is rather a diffraction pattern which is expected to have some similarity to the object. This diffraction pattern constituting the image will appear with maximum brightfield contrast if its core or central area is completely black. In terms of the vector diagram 1a this would occur if the component OC were exactly balanced by a vector OD of the same magnitude as OC but of opposite direction or phase. The desired result can be brought about if the zero order or phase ring area of the phase plate incorporates a phase shift, ψ, and a transparency, T_O, such that in passing through it OA is transformed into OD.

Using the conception of contrast defined as the brightness difference between two adjacent areas divided by the greater brightness value of the two, we get an object contrast:

$$K=1-T_D, \tag{1}$$

and if the vector OA is supposed to be of unit length, we read from Fig. 1a:

$$\left.\begin{aligned} OB\cos\varphi+AB\cos\psi&=1\\ \text{and}\qquad OB\sin\varphi+AB\sin\psi&=0\end{aligned}\right\}, \tag{2}$$

with $OB=T_D^{\frac{1}{2}}=(1-K)^{\frac{1}{2}}$, and $OC=(-)OD=T_O^{\frac{1}{2}}$, Eqs. (2) become:

$$\left.\begin{aligned} (1-K)^{\frac{1}{2}}\cos\varphi+T_O^{\frac{1}{2}}\cos\psi&=1\\ \text{and}\qquad (1-K)^{\frac{1}{2}}\sin\varphi+T_O^{\frac{1}{2}}\sin\psi&=0\end{aligned}\right\}. \tag{2a}$$

Eliminating ψ results in:

$$T_O=2-K-2(1-K)^{\frac{1}{2}}\cos\varphi. \tag{3}$$

It is evident from Eq. (3) that the value of T_O becomes greater than 1 for certain values of K and φ. For such objects, instead of absorption in the zero order ring ("A" type phase plate) absorption of a portion of the light transmitted through the higher order area of the plate ("B" type) will be required. To calculate such values from Eq. (3), for any value of T_O greater than 1 we can substitute a corresponding value for transparency of the higher order area $\bar{T}_O=1/T_O$, smaller than 1. Transparency values may be converted into absorption values, $A_O=1-T_O$, and $\bar{A}_O=1-\bar{T}_O$. Equal values of $\cos\varphi$ whether positive or negative, or for any multiple of light wave-lengths, result in the same values of transparency or absorption.

Optimum absorption values for the phase plate, calculated from Eq. (3) for various K and φ characteristics of the object, are represented graphically in the lower half, quadrants III and IV of Fig. 2. The quadrant IV, lower right, represents phase plates with absorption in the zero order ring ("A" type). The quadrant III, lower left of Fig. 2, represents phase plates with absorption in the higher order area ("B" type).

Of particular interest is the region of small object contrast, let us say up to $K=10$ percent, as this is the region in which the phase-contrast method offers a new

TABLE II. For phase plates with absorption in the higher order area ("B" Types)

Image contrast	Absorption less than optimum	Absorption greater than optimum
K_X	$\bar{T}_X/\bar{T}_O$	$\bar{T}_O/\bar{T}_X$
1	1	1
0.90	1.73	2.1
0.75	2.25	4
0.50	2.92	11.7
0.25	3.48	55.7
0.10	3.8	380

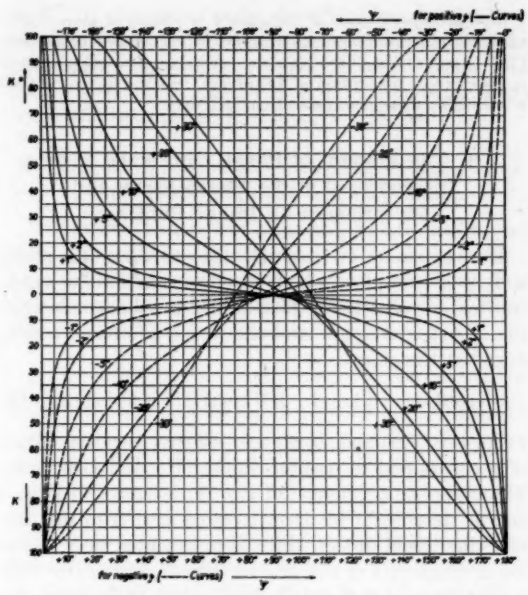

FIG. 3. Graphic representation of Eq. 9. Relationships between object contrast and optimal phase shift to be incorporated in the phase plate for various phase differences produced at the object of less than 30°. The solid line curves refer to $+\varphi$ and $-\psi$ values. The broken line curves are valid for $-\varphi$ and $+\psi$ values. The upper quadrants refer to darkfield objects. The lower quadrants refer to brightfield objects.

method of perception and markedly extends the sensitivity of the ordinary microscope. We learn from Fig. 2 that absorption in the zero order ring of the phase plate should be very high if the phase shift produced by the object happens to be very small. Small transparent object details, which produce phase shifts of only a few degrees, require absorption in the ring of more than 98 percent. With larger phase differences produced at the object the optimum phase plate absorption falls off rather rapidly, and where φ is larger than 60° absorption in the higher order area ("B" type plates), becomes more favorable.

The question may be raised as to how much loss of image contrast from its maximum attainable value results if the phase plate absorption may be greater or less than the optimum value? If instead of the transparency T_O any higher value T_X may be incorporated in the plate, the resulting image contrast is given by:

$$K_X=[T_X-(T_X^{\frac{1}{2}}-T_O^{\frac{1}{2}})^2]/T_X. \tag{4}$$

Equation (4) may be understood from Fig. 1a, where $OE=T_X^{\frac{1}{2}}$ cannot be completely compensated by the component $OC=T_O^{\frac{1}{2}}$.

It is interesting that K_X turns out to be a function of the ratio T_O/T_X only, and does not depend on φ or K.

Equation (4) may be transformed into:

$$T_O/T_X=[1-(1-K_X)^{\frac{1}{2}}]^2. \tag{5}$$

If absorption in the zero order area or ring of the phase plate is greater than optimum, and T_X is smaller than T_O, we obtain instead of Eq. (5) the expression:

$$T_O/T_X=[1+(1-K_X)^{\frac{1}{2}}]^2. \tag{6}$$

In Table I are given for different percentages of maximum attainable image contrast in the first column, some numerical values of Eq. (5) in the second, and of Eq. (6) in the last column.

The meaning of these figures may be demonstrated by an example: To bring about maximum image contrast of 1, from an object detail with intrinsic contrast of between 0 and 5 percent, resulting from absorption, and producing in the light a phase difference of $\varphi=10°$, would require according to Fig. 2 a phase plate ("A" type) with absorption in the zero order ring of 0.97, or $T_O=0.03$. Now if one may be satisfied with contrast of but 0.50 in the image of such an object, the corresponding lower phase plate absorption is found from the values of Table I: $T_X/T_O=T_X/0.03=11.7$, and $T_X=0.35$, or absorption of 0.65. To reduce the contrast to 0.50 by a higher than optimum absorption: $T_O/T_X=0.03/T_X=2.92$, and $T_X=0.01$, or absorption of 0.99.

Usually a deviation of the phase plate absorption toward smaller than optimum values is of greater interest than the converse. The fact that the ratio T_O/T_X turns out to be a function of K_X only, has another consquence also, *viz.*, only in the case where the optimum absorption is rather high is a deviation from this opti-

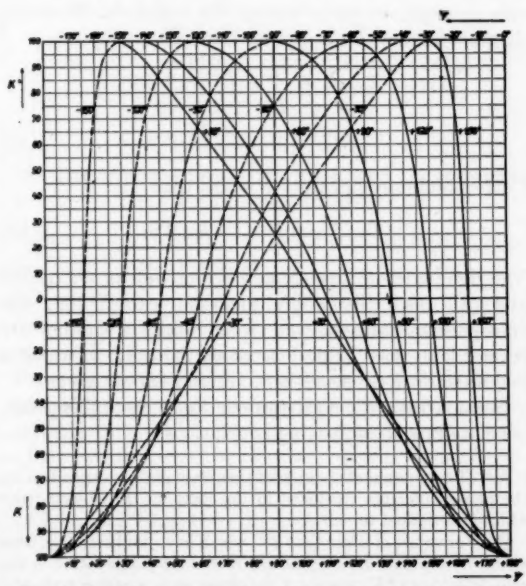

FIG. 4. Graphic representation of Eq. 9. Relationships between object contrast and optimal phase shift to be incorporated in the phase plate for various phase differences produced at the object of greater than 30°. The solid line curves refer to $+\varphi$ and $-\psi$ values. The broken line curves are valid for $-\varphi$ and $+\psi$ values. The upper quadrants refer to darkfield objects. The lower quadrants refer to brightfield objects.

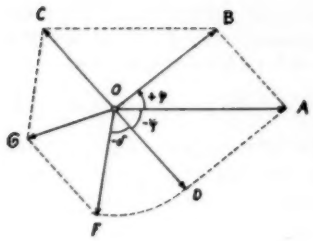

FIG. 5. Vector diagram representing the case of a phase plate shift of other than the optimal ψ value.

mum value of appreciable effect. This may be demonstrated by another example: Let us assume a phase plate of comparatively low absorption value, optimal to the object under consideration, of let us say 75 percent, or $T_O=0.25$. Making use of the figures of Table I, as in the former examples, we find that even though no absorption at all were incorporated in the plate, i.e., $T_X=1$, the image contrast would drop to no lower than 0.75 of its maximum attainable value.

The values of object contrast and phase shift represented in the lower left quadrant of Fig. 2, for which absorption in the higher order area of the phase plate ("B" types), is more favorable, are of less interest and importance. However, since the fullest possible application of the principle may be required for the study of objects, certain or all of the structures of which may fall within this region, it may be noted that analysis of the vector diagram 1b, which covers such cases, by methods corresponding to the above, may be applied, and indicate corresponding conclusions: We read from the vector diagram in case $\bar{T}_X$ is greater than $\bar{T}_O$:

$$K_X=1-[(\bar{T}_X/\bar{T}_O)^{\frac{1}{2}}-1]^2,$$

or

$$\bar{T}_X/\bar{T}_O=[1+(1-K_X)^{\frac{1}{2}}]^2. \quad (7)$$

Correspondingly in case $\bar{T}_X$ is less than $\bar{T}_O$:

$$\bar{T}_X/\bar{T}_O=[1-(1-K_X)^{\frac{1}{2}}]^2. \quad (8)$$

The right sides of Eqs. (5) and (7), as well as of Eqs. (6) and (8), respectively, are identical, except that the transparency ratios as well as the ranges of validity are reversed, so that Table I becomes Table II, in which a few numerical values of Eqs. (7) and (8) are given.

Summarizing the results of our study up to this point, we can draw the following conclusions:

(a) The optimum absorption of the phase plate is dependent on the phase difference produced in the light by the object detail which it is desired to observe.

(b) For values of φ less than 20°, which have not heretofore been visible by the ordinary microscope, the required absorption in the zero order ring ("A" types), of the phase plate is rather high, and the image contrast is highly dependent on its being exactly optimum.

(c) For values of φ between 20° and 60° weaker absorption in the zero order area or ring ("A" types), of the phase plate, or none at all, is required, and the image contrast is only slightly dependent on the characteristic of the instrument.

(d) For improvement of the quality of images of more highly refractile objects weaker absorptions in the higher order area ("B" types) of the phase plate are favorable. The value need in no case exceed absorption of 75 percent, and the image contrast is not highly dependent on this characteristic.

B. The Amount of Phase Difference to be Incorporated in the Phase Plate, and Its Influence on Image Contrast

If we eliminate T_O from Eqs. (2a) we obtain the phase shift ψ of the plate which results in maximum image contrast of value 1. The phase difference ψ depends upon the object contrast K and the phase difference φ produced at the object:

$$\cot\psi=(-)[1-(1-K)^{\frac{1}{2}}\cos\varphi]/(1-K)^{\frac{1}{2}}\sin\varphi. \quad (9)$$

From Eqs. (2a) and (9) we can see that negative values of ψ correspond to positive values of φ and vice versa. The graphical expression of Eq. (9) is shown in Figs. 3 and 4. Here again we are interested at first in the case of a brightfield object which is represented only in the lower quadrants of the graphs. Figure 3 indicates that within the range of small object phase differences the optimum phase difference ψ varies rather rapidly with the object contrast. However, for larger object phase differences, Fig. 4, the values of ψ change only slowly in dependence on object contrast.

It is interesting to inquire how the image contrast may be changed if, instead of the most favorable value ψ, the phase plate may actually produce a phase shift of $\psi\pm\delta$, other than optimal. The vector diagram Fig. 5 represents such a case, in which the component OD has been rotated as a result of the additional plate shift δ to the position OF. Addition of the vectors OC and OF results in the vector OG, which therefore represents the light oscillation at the core of the image detail. The image contrast K_X in this case turns out to be:

$$K_X=\{(OF)^2-[(OF)^2+(OC)^2-2(OF)(OC)\cos\delta]\}/(OF)^2$$

or:

$$K_X=[2(OF)(OC)\cos\delta-(OC)^2]/(OF)^2. \quad (10)$$

If we assume that the phase plate transparency is optimum, $OC=OF$ and we obtain:

$$K_X=2\cos\delta-1. \quad (11)$$

This result is interesting in that it indicates that the decrease from maximum of image contrast is a simple function of the deviation δ from optimum phase plate difference ψ, and is independent of all of the other variables. Equation (11) is represented graphically in Fig. 6 by the curve $T_X/T_O=1$. It is clear that relatively large values of δ are permissible if a slight decrease in image contrast may be accepted. If 75 percent of the maximum attainable contrast may be accepted the deviation δ from optimum value of phase plate shift may be as large

as 30°. If the phase plate deviation from optimum is greater than 40° the image contrast decreases rapidly, and reaches zero when $\delta = \pm 60°$. For deviation from optimum values of δ larger than 60° the contrast in the image will be reversed in comparison to the object.

C. The General Case of Deviation of the Phase Plate Characteristics from Optimum

The general case in which the phase plate data deviate from the optimum transparency value T_O as well as from the most favorable phase shift ψ, is easily deduced if we substitute in Eq. (10) $OF = (T_X)^{\frac{1}{2}}$ and $OC = (T_O)^{\frac{1}{2}}$. The resulting image contrast becomes:

$$K_X = [2(T_X \cdot T_O)^{\frac{1}{2}} \cos\delta - T_O]/T_X. \qquad (12)$$

Equation (12) becomes Eq. (4) when $\delta = 0$, and Eq. (11) when $T_X/T_O = 1$. Figure 6 shows the curves which represent Eq. (12) for the values $T_X/T_O = 2.1$, and $T_X/T_O = 4$, examples in which the absorption of the zero order ring of the phase plate is less than optimum. It may be noticed that the combined effect of deviations from the most favorable phase plate data is somewhat less than the algebraic sum of both components. For large values of deviation from optimum phase shift the image contrast when T_X is greater than T_O, i.e., the phase plate absorption is less than optimum, is even higher than when $T_X = T_O$, i.e., when the phase plate absorption is exactly optimum.

The corresponding curves for examples in which the absorption in the zero order ring ("*A*" type) is greater than optimum, $T_O/T_X = 1.73$, and $T_O/T_X = 2.25$, are also shown in Fig. 6. In these cases the decrease in image contrast with increasing deviation of phase shift of the plate from optimum is more rapid.

We conclude from these findings that when the phase shift of the plate is not exactly optimum for the object under consideration it is better to have a lower than optimum absorption in the ring rather than a higher one.

For the cases of absorption in the higher order area of the phase plate ("*B*" types) we must substitute in Eq. (12) $T_X = 1/\bar{T}_X$, and $T_O = 1/\bar{T}_O$, and the converse of the above findings is deduced, a greater than optimum absorption in the higher order area of the plate being more favorable when the phase shift of the plate is other than optimum.

We may further summarize the results of our studies at this point as follows:

(a) The image contrast is not very sensitive to deviations from correct phase shift incorporated in the plate, until such deviations exceed about 30°± from the optimum. ±30° represents, therefore, the range over which a particular phase plate may be expected to give good results in microscopy.

(b) The image contrast is only sensitive to deviations from correct absorption in the plate in the range of objects characterized by rather high relative transparency and low relative refraction.

(c) The image contrast is not highly sensitive to deviations from correct absorption in the phase plate in the range of objects of relatively high refraction, such as those which produce the so-called diffraction images by the ordinary microscope.

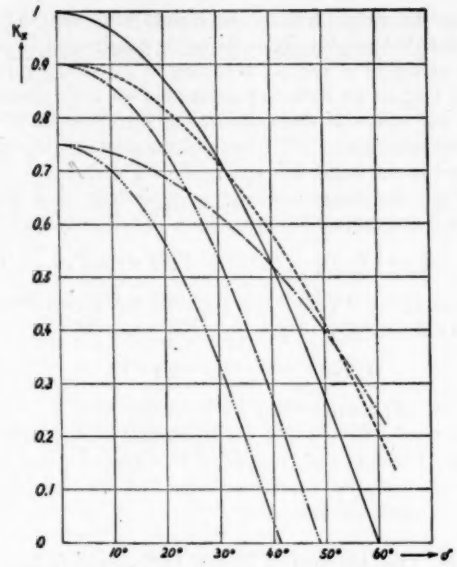

FIG. 6. Illustrating the effect on image contrast of deviation from optimum phase plate shift, for selected phase plate absorption values greater and less than optimum. Graphic representation of Eq. 12. — $T_X/T_O = 1$; - - - $T_X/T_O = 2.1$ —·— $T_X/T_O = 4$; —·· $T_O/T_X = 1.73$ —···— $T_O/T_X = 2.25$.

(d) The image contrast in the range of comparatively highly refractile objects which require absorption in the higher order areas ("*B*" types), of the phase plate is more sensitive to lower than optimum absorption in the plate than to higher.

III. TRANSFORMATION OF A DARKFIELD OBJECT OF LOW CONTRAST INTO A BRIGHTFIELD IMAGE OF HIGH CONTRAST

A. The Phase Plate Absorption and Its Influence on Image Contrast

The vector diagrams 1c and 1d describe these cases. Our basic assumption is simply reversed and the vectors *OB* representing the light oscillations from the object detail are considered to be of unit length, whereas the vectors *OA* representing the background are smaller. Using T_S to represent the transparency of the surroundings with respect to the object detail, we have $OA = T_S^{\frac{1}{2}}$, and $OC = (T_S \cdot T_O)^{\frac{1}{2}}$. The object contrast is given by:

$$K^* = 1 - T_S, \qquad (13)$$

and we read from the diagram:

$$\left.\begin{aligned} &\cos\varphi + (1-K^*)^{\frac{1}{2}} T_O^{\frac{1}{2}} \cos\psi = (1-K^*)^{\frac{1}{2}} \\ \text{and} \quad &\sin\varphi + (1-K^*)^{\frac{1}{2}} T_O^{\frac{1}{2}} \sin\psi = 0 \end{aligned}\right\}. \qquad (14)$$

The elimination of ψ results in:

$$T_O = 1 - [2(1-K^*)^{\frac{1}{2}} \cos\varphi - 1]/(1-K^*). \qquad (15)$$

These T_O values for various values of φ and K^* are represented graphically in the upper quadrants of Fig. 2. For values of φ and K^* resulting in T_O values greater than 1 again we have to substitute $\bar{T}_O = 1/T_O$ to calculate the values of absorption to be incorporated in the higher order area ("B" types), of the phase plate, represented in the upper left quadrant of Fig. 2.

When the image contrast is dependent on a phase plate transparency T_X other than T_O we have:

$$K_X = [T_X T_S - (T_X^{\frac{1}{2}} T_S^{\frac{1}{2}} - T_S^{\frac{1}{2}} T_O^{\frac{1}{2}})^2]/T_X T_S. \quad (16)$$

Canceling out T_S from this equation we obtain a result identical with Eq. (5):

$$T_O/T_X = [1-(1-K_X)^{\frac{1}{2}}]^2, \quad (5)$$

and Eq. (6) results when T_X is smaller than T_O. From these results we see that the numerical values given in Tables I and II can be applied here again for darkfield objects, and the conclusions reached for brightfield objects again are indicated.

B. The Amount of Phase Difference to be Incorporated in the Phase Plate and Its Influence on Image Contrast

The elimination of T_O from Eq. (14) results in:

$$\cot\psi = (-)[(1-K^*)^{\frac{1}{2}} - \cos\varphi]/\sin\varphi, \quad (17)$$

which is represented graphically in the upper quadrants of Figs. 3 and 4. The conclusions are obviously similar to those for a brightfield object.

To evaluate the effect on image contrast produced by phase differences in the plate other than optimum we derive from Fig. 5 modified to correspond to diagram 2c:

$$K_X = [T_S T_X - (T_S T_X + T_S T_O - 2T_S T_X^{\frac{1}{2}} T_O^{\frac{1}{2}} \cos\delta)]/T_S T_X. \quad (18)$$

T_S again can be canceled out yielding Eq. (12), and the curves of Fig. 6 again describe the conditions, and give rise to similar conclusions.

We have treated in this Chapter III the case of a reversal of contrast as between object and image, analyzing the conditions under which a brightfield image of high contrast may be produced by an object detail which is less absorptive of the light than its surroundings and of low contrast. From the vector diagrams of Fig. 1 we can conclude that in order to produce a high contrast darkfield image of such an object, the vector OA must not be rotated to the position OD but into the opposite direction OC. The most favorable phase plate shift for maximum contrast is therefore given by the supplements of the ψ values shown graphically in Figs. 3 and 4. Independently of the absorptive and refractive characteristics, of course, as has been known for long before the discovery of the Zernike or phase-contrast principle and the development of the phase-contrast method of illumination, the darkfield image of greatest contrast of any object may be attained by complete absorption of the zero order maximum of the diffraction spectrum, which is the arrangement of illumination commonly known as central darkfield.

A Photoelectric Method of Measuring the Atmospheric Attenuation of Brightness Contrast Along a Horizontal Path for the Visible Region of the Spectrum*

HOWARD S. COLEMAN, FRED J. MORRIS, HAROLD E. ROSENBERGER,
The Optical Research Laboratory, The University of Texas, Austin, Texas

AND

MARSHALL J. WALKER
Physics Department, Pennsylvania State College, State College, Pennsylvania

(Received April 11, 1949)

A satisfactory method has been developed for measuring the attenuation of brightness contrast by the atmosphere along horizontal paths for the visible region of the spectrum. The method consists of the measurement of the apparent brightness of "black" and "white" test objects (referred to hereafter as targets) located at different distances from a photoelectric telephotometer. The method is being used in an ONR sponsored research program at the University of Texas. In this program seven pairs of "black" and "white" targets are being used. These are rectangular in shape and subtend practically the same angle with respect to the telephotometer. The targets range in size from 0.65×1.30 ft. to 33×66 ft. These are located approximately along a horizontal line running nearly due East starting at a point located about eight miles east of Austin, Texas, and cover a range of nearly 9 miles in the vicinity of the Colorado River. This location of the target range provides a means of making atmospheric attenuation measurements for different azimuth angles between the path of observation and the position of the sun. In addition, the location is such that fogs and dust haze occur fairly frequently as well as a highly clear atmosphere. The data obtained during the first year of operation indicate that, for "white light," the brightness contrast is exponentially attenuated and that the attenuation coefficient is surprisingly insensitive to the naturally occurring local variations in illumination along the observation path.

INTRODUCTION

THERE is an obvious need for quantitative information about the limitations imposed by the atmosphere on the visibility of objects viewed through it for such weather conditions as are of civil and military interest. It is the purpose of this paper to describe an objective method of experimentally determining such limitations. The reason that reliable information is not available on this important subject is directly relatable to the great cost and the magnitude of the effort required to conduct studies in the field under the conditions of actual interest. This is particularly difficult in visibility studies because factors of interest to be measured are the weather conditions themselves, and hence, no simple orderly experiments can be conducted in which the operations can be prescheduled. For this reason it is necessary to design an experiment in which,

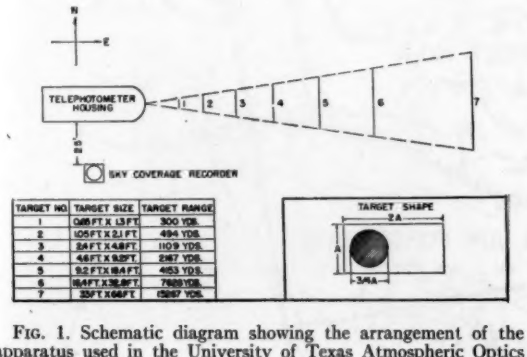

FIG. 1. Schematic diagram showing the arrangement of the apparatus used in the University of Texas Atmospheric Optics Project.

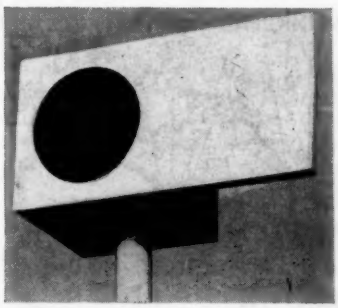

FIG. 2. University of Texas visibility target No. 2. Target size—1.05 ft.×2.1 ft. Target range—494 yd.

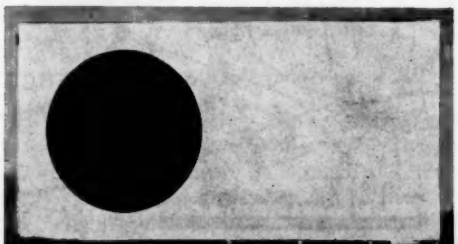

FIG. 3. University of Texas visibility target No. 7. Target size—33 ft.×66 ft. Target range—15,267 yd.

* The work described in this paper was performed as a part of Task IX of Contract N6onr-266 between the ONR and the University of Texas and as a part of Task IV of the ONR Contract N6onr-269 at Pennsylvania State College.

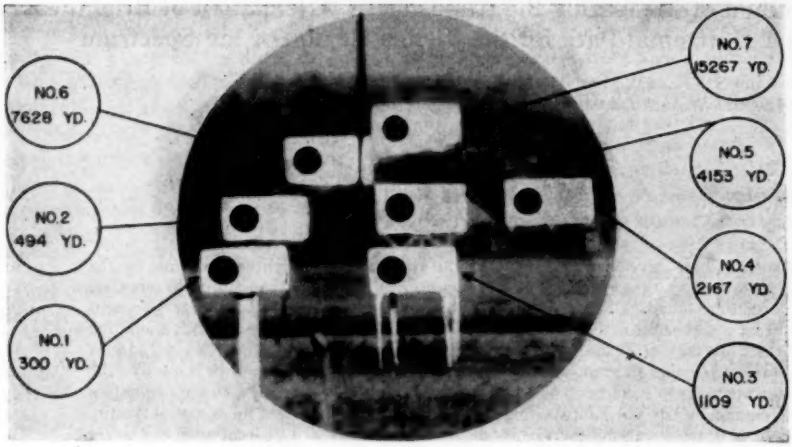

FIG. 4. Telephotograph of the University of Texas visibility targets at 5:30 p.m., April 5, 1949. Subtense of black targets = 54.0×10^{-4} radians (1.86 min.). Meteorological range = 60,000 yd.

no matter how the weather changes, such changes can be used to further the progress of the experiment.

The limitations imposed by the atmosphere on the "visibility" of objects through it can be considered in terms of two processes. First, the light from an object is attenuated by scattering, absorption, refraction, and diffraction, as it proceeds toward an observer. Second, if the column of air along the line of observation is illuminated by light such as from the sky, the sun, and the ground, a certain amount of this illuminant is scattered toward the point of observation. This tends to "cast a veiling glare" over the object from the point of view of an observer. This latter process is difficult to consider because the illumination generally varies along

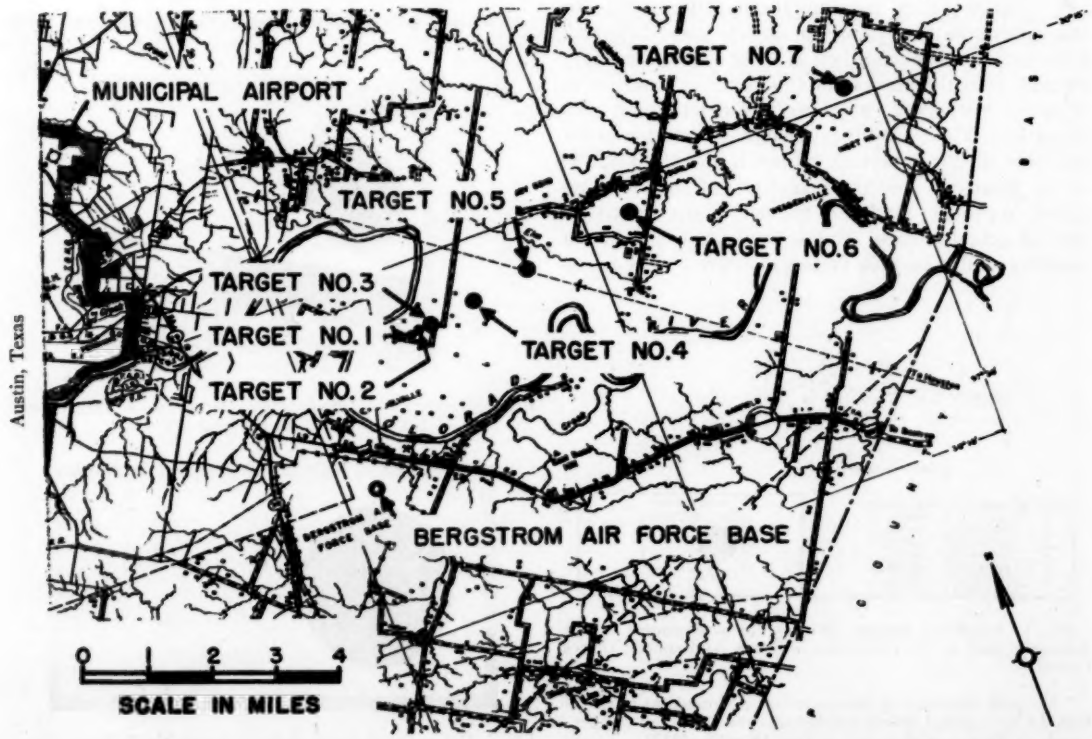

FIG. 5. Map showing location of University of Texas visibility targets.

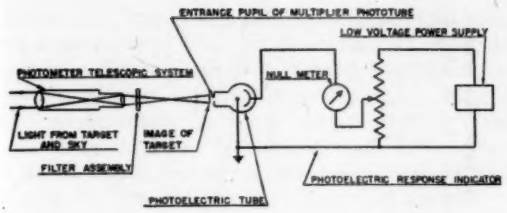

FIG. 6. Schematic diagram of the photoelectric telephotometer.

a path of observation of any practical length and the air along it may be neither homogeneous nor isotropic. Because of the existence of these non-uniform conditions, and the probable discontinuities associated with them, the development of even an approximate attenuation theory is almost hopeless without some experimental facts that can be used as a guide. With this situation in mind, an apparatus and a procedure were developed to yield quantitative data about the light reaching the point of observation from an object and the effect of the light scattered along the line of sight by the atmosphere regardless of its state or the illumination conditions that prevail.

As might be expected for a subject as important as this, a considerable amount of theoretical and some experimental work has been reported in the literature. From a practical point of view, most of this work was published about 1924 by Koschmieder[1] and, subsequently, by him and his associates in Germany up through 1947. These studies consisted primarily of the development and testing of a theoretical expression derived assuming Bouguer's law[2] and using a considerable number of necessary simplifying assumptions which rarely hold, if ever, in nature. Because it would be beyond the intended scope of this paper, a survey of the results of these will not be given in detail here. However, it might be mentioned that Koschmieder and his successors, in attempting to confirm the theoretical law derived, were able to obtain "usable" data on only twenty-eight days in over a year and a half, and these varied within limits as much as ±30 percent of average values. This has cast doubt as to the extent to which the theoretical law holds as well as its usefulness in practice (in which case attenuation data must be determined to an accuracy of at least 5 percent).

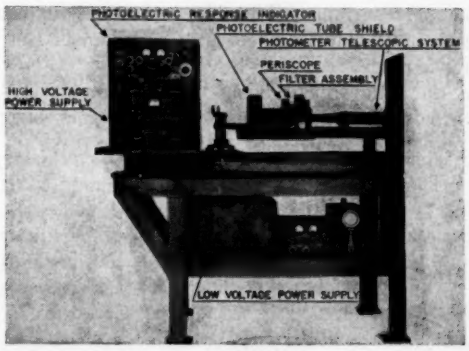

FIG. 7. The photoelectric telephotometer.

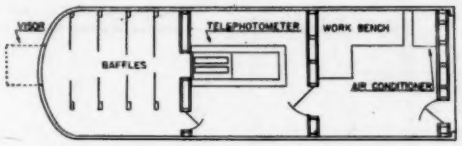

FIG. 8. Schematic arrangement of equipment in telephotometer housing for atmospheric attenuation studies (top view).

In discussing the quantities to be measured in a study of the limitations imposed by the atmosphere, it is convenient to use some of the concepts and definitions used by Koschmieder and subsequent investigators. These may be summarized as the following equations:

B_O = the inherent brightness of an object (i.e., at zero range). (1)

B_H = the apparent brightness of the background of the object. (2)

R = the distance between the object and the point of observation. (3)

B_R = the apparent brightness of an object at range, R. (4)

β = the attenuation coefficient. (5)

R_m = the meteorological range (i.e., the horizontal distance at which an object of zero inherent brightness would have to be from the point of observation to have an apparent brightness of 98 percent of the brightness of its horizon background). (6)

$C_O = (B_O - B_H)/B_H$ = the inherent brightness contrast of the object. (7)

$C_R = (B_R - B_H)/B_H$ = the apparent brightness contrast. (8)

Bouguer's law:

$B_R = B_O e^{-\beta R}$ (i.e., the attenuation of light from the target). (9)

Koschmieder's law:

$$B_R = B_O e^{-\beta R} + B_H(1 - e^{-\beta R}). \quad (10)$$

Since the purpose of studying the limitations imposed by the atmosphere on the visibility of objects is to be able to quantitatively predict the range at which any object is visible under any conditions of the weather and general illumination, it is necessary to discover some parameter which describes the state of the atmosphere under all conditions of interest. Of those parameters which might be used, the attenuation coefficient

[1] Harald Koschmieder, "Theorie Der Horizontalen Sichtweite," Beitr. z. Phys. d. Freien Atm. 12, 33–53, 171–181 (1924, 1925).

[2] Pierre Bouguer, "Essai d'Optique, sur la Gradation de la Lumiere" (1760), pp. 44–45. (First announced in 1729.)

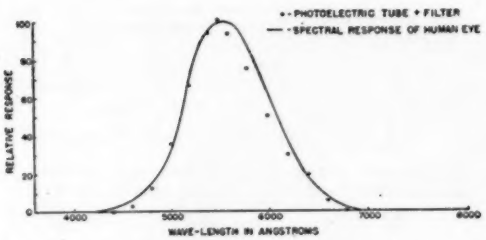

FIG. 9. Spectral response of telephotometer using 2.76-mm Y_2 filter.

(or the meteorological range which is related to it) appears to be most suitable. In order to obtain a numerical value for the attenuation coefficient, it is necessary to define it in terms of something that can always be measured. For this purpose it is convenient to rewrite Koschmieder's law in terms of contrast, making the simplifying assumption that the background brightness is that of the horizon. It is further assumed that the horizon brightness is not a function of the range. For many distances of practical interest this is likely true. In this form, Koschmieder's law can be expressed as follows:

$$C_R = C_0 e^{-\beta R} \tag{11}$$

$$C_R = C_0 \exp(-3.912R/R_m) \tag{12}$$

$$\mathrm{Log}_e C_R = \mathrm{Log}_e C_0 e^{-\beta R} = \mathrm{Log}_e C_0 - \beta \mathrm{R}. \tag{13}$$

Thus, from Eq. (13) it is evident that if Koschmieder's law were to hold, a plot of the Logarithm of the apparent contrast *vs.* range of objects of known inherent brightness should yield a straight line, the slope of which is the attenuation coefficient. Since it is reasonable to expect that Koschmieder's law should hold for a sufficiently limited range, the experimental procedure was designed, using it as a guide as to the quantities to be measured and as a means of defining the attenuation coefficient to be used as a parameter. In this regard the operation of obtaining β (or its related quantity R_m), will be referred to hereafter as "the determination of the attenuation of brightness contrast by the atmosphere."

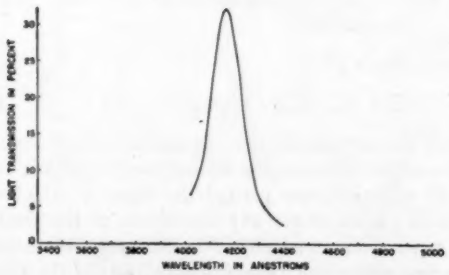

FIG. 10. Light transmission *vs.* wave-length for "violet" filter used in telephotometer. $\lambda_{max} = 4170$A, $HW = 160$A, $T = 32$ percent.

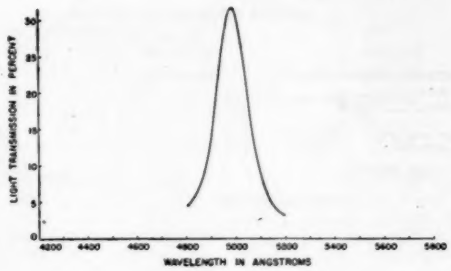

FIG. 11. Light transmission *vs.* wave-length for "blue" filter used in telephotometer. $\lambda_{max} = 4980$A, $HW = 160$A, $T = 31.5$ percent.

THE APPARATUS

The apparatus used to determine the atmospheric attenuation of brightness contrast can be regarded as consisting of the following parts: (1) the targets, (2) the telephotometer, (3) the target illumination meters, and (4) the sky coverage recorder.

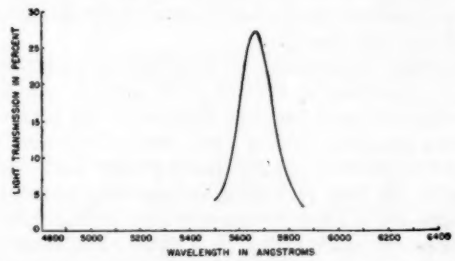

FIG. 12. Light transmission *vs.* wave-length for "green" filter used in telephotometer. $\lambda_{max} = 5670$A, $HW = 170$A, $T = 27.5$ percent.

The Targets

The objects used in the atmospheric attenuation studies are referred to as targets. Since there is a wide range of reflectance of objects of interest, "black" targets and "white" targets are used to cover this reflectance range.

In the arrangement being used at present (1949), seven pairs of targets are used. These targets range in

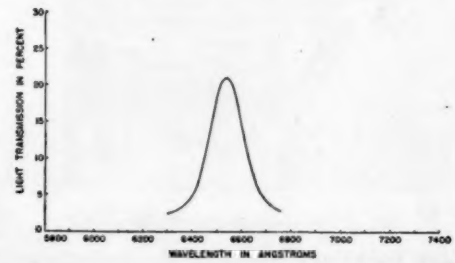

FIG. 13. Light transmission *vs.* wave-length for "red" filter used in telephotometer. $\lambda_{max} = 6540$A, $HW = 180$A, $T = 21$ percent.

size such that they subtend the same angle (1.86 min.) with respect to the point of observation as shown in Fig. 1. The details of one of the smaller targets and the largest target are shown photographically in Figs. 2 and 3. As is evident, the "black" targets are really holes in the faces of white "bill boards" with a black box behind the hole to reduce changes in their luminance as the azimuth of the sun changes throughout the day.

The targets are located in the bottom land near the Colorado River and are practically along, and normal to, the path of observation as is shown in Fig. 4. The targets are erected along a line running nearly due East, starting at a point about eight miles east of Austin, Texas, as shown in Fig. 5. With arrangement of targets described, in the morning periods of observations, the white targets are often darker than their background when the sun is behind them, and are often brighter than their background in the afternoon when the sun is in front of them. This makes it possible to make atmospheric attenuation measurements for targets having a range of inherent contrasts from -1 to approximately 4. In addition, the location selected is such that "river" fogs, dust haze, and highly clear atmospheric conditions occur frequently enough to study the influence of a wide variety of weather conditions on atmospheric attenuation.

The Telephotometer

The device used to measure the apparent brightnesses of the targets and their backgrounds is referred to as a "telephotometer." The telephotometer, shown schematically and photographically together with its housing in Figs. 6, 7, and 8, consists of four parts: (1) the telescopic system, (2) the filter assembly, (3) the photoelectric tube, and (4) the response indicator.

The telescopic system is essentially a $20\times60\times2°$ telescopic system of high optical quality provided with diaphragms which reduce the stray light in it practically to zero. The magnification is such that the telescopic system forms images of the targets that are approximately four times the diameter of the entrance pupil leading to the photoelectric tube.

A series of filters, referred to as the filter assembly, is used in the telephotometer. These filters are mounted in an enclosed turret near the exit pupil of the telescopic system. Five filters are used. One is used to render the spectral response of the photoelectric tube similar to that of the human eye, with the result as shown in Fig. 9. The other filters are used to limit the light falling on the photoelectric tube to four practically monochromatic regions of the spectrum. These latter filters are of the interference type and are designated as "violet," "blue," "green," and "red," having the spectral transmissions shown in Figs. 10, 11, 12, and 13.

The photoelectric tube used is of the commercially available multiplying type and was selected from a number available for its high sensitivity and the stability of its linear response.

FIG. 14a. The sky coverage recorder used in the University of Texas Atmospheric Optics Project.

The photoelectric responses are measured by means of a potentiometer type circuit referred to as "the response indicator," the principle of which is shown in Fig. 6. This unit and the power supplies for the photoelectric assembly were designed and constructed by Professor Wayne B. Nottingham of the Massachusetts Institute of Technology.

The Target Illumination Meters

One of the most important items to be considered in an atmospheric study of the type discussed here, is the influence of variations in illumination along the path of observation on the value of the attenuation coefficient being measured. If the attenuation coefficient is particularly sensitive to such variations, from a practical

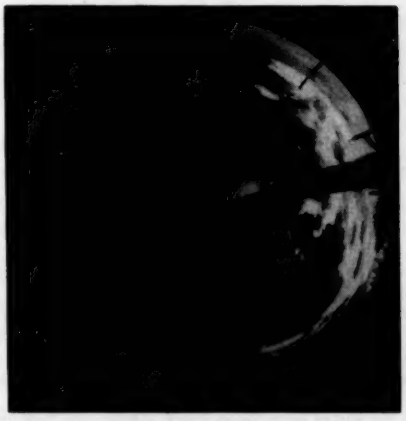

FIG. 14b. Photograph of sky.

TABLE I. Variation of target illumination as a function of time (February 9, 1949)

Time C.S.T. Hr.	Min.	Sec.	Target No. 1	Target No. 4	Target No. 5	Target No. 7
16	40	00	2520	2250	2300	4640
	41	00	2800	2140	2160	3790
	42	00	2190	2410	2600	2180
	43	00	3110	2710	2160	2270
	44	00	3360	2850	3720	2040
	45	00	5600	3400	3310	3500
	46	00	6750	6460	5000	4170
	47	00	6730	6110	6420	3220
	48	00	7310	6390	6140	3500
	49	00	7340	6870	6370	5210
	50	00	7620	6890	6900	6060
	51	00	5810	7170	7000	6200
	52	00	4890	4640	6600	6720
	53	00	6980	5190	4140	7670
	54	00	5730	6070	5400	7480
	55	00	6600	5840	5590	7670
	56	00	6420	6570	6280	4830
	57	00	5480	6300	5890	6060
	58	00	5350	4780	5000	5590
	59	00	4890	4870	4600	6630

point of view, either methods must be developed to make allowances for such variations or some other "less sensitive" parameter would have to be discovered which would describe the state of the atmosphere. In order to study this matter, the illumination is measured as a function of time along the target range during the course of the telephotometer measurements. This is done by means of commercially available illumination meters used in conjunction with stop watches synchronized with a "master clock" located in the telephotometer housing.

The Sky Coverage Recorder

The principal cause of non-uniform illumination along a line of observation is the unequal distribution and types of clouds between the sky and the observation path. In order to be able to study this situation, a device referred to as "the sky coverage recorder" has been developed which photographically records the cloud coverage during the attenuation measurements. This device and a sample cloud record are shown in Figs. 14a and 14b.

THE PROCEDURE

The procedure used in studying the attenuation of brightness contrast by the atmosphere is as follows:

(1) The apparent brightnesses of the black targets, the white targets, and the horizon, are measured, using the telephotometer for each of the filters mentioned. In these measurements the time is recorded for each brightness measurement. Such a group of measurements is referred to as a "set."

(2) The illumination on the six largest targets is recorded at the end of each 30-sec. interval during the period in which the telephotometer measurements are being made.

(3) At the end of each set of brightness measurements a record is taken of the sky coverage.

(4) At the end of each day in which attenuation measurements are made, such meteorological data are collected as were recorded at two weather stations in the vicinity of the target range during the time in which the telephotometer measurements were made.

(5) The brightness data and the meteorological data mentioned above are then recorded, as shown in Fig. 15, for each filter used. The target illumination data are recorded as shown in Table I. The data in these forms are referred to as basic data.

(6) The aging of the white paint used on the targets is recorded by making periodic spectral reflectance curves of detachable paint specimens located at each target.

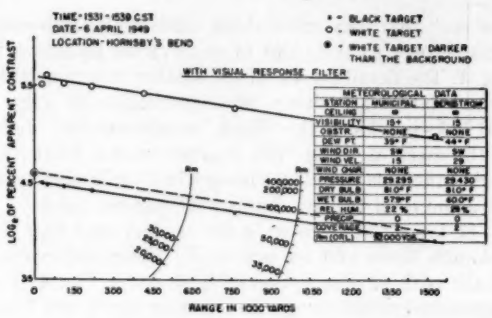

FIG. 15. Log$_e$ of percent apparent contrast *vs.* range.

THE TREATMENT OF THE DATA

Since the basic data mentioned are to be used to determine the limitations imposed by the atmosphere for various weather conditions, they are analyzed, for each spectral region, for any possible correlation with the target illumination and the meteorological data recorded. This analysis consists of four parts. The first consists in determining the meteorological range for targets of zero inherent brightness. This is done by drawing a dashed line through the log$_e$ 100 point on the basic data graphs such that it is parallel to the line obtained by plotting the contrast data for the black targets (which are not of zero luminance). The second

TABLE II. Sample meteorological range and relative humidity data.

Meteorological range	Relative humidity % Municipal airport weather station	Relative humidity % Bergstrom A.F. weather station	Observation date
4600	91	95	Jan. 12, 1949
6000	97	92	Jan. 13, 1949
7000	96	99	Jan. 11, 1949
9000	96	99	Jan. 11, 1949
12000	97	93	Jan. 11, 1949
15000	100	96	Jan. 10, 1949
25000	95	92	Jan. 11, 1949
35000	97	95	Jan. 10, 1949
50000	26	33	Jan. 6, 1949
60000	39	49	Jan. 5, 1949
70000	32	37	Jan. 7, 1949
80000	71	69	Jan. 8, 1949
90000	34	41	Jan. 3, 1949
100000	56	50	Jan. 18, 1949
140000	28	31	Jan. 6, 1949
200000	58	54	Jan. 18, 1949

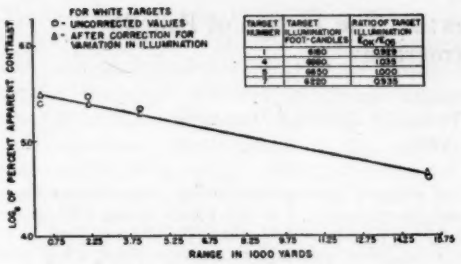
FOR WHITE TARGETS
O - UNCORRECTED VALUES
Δ - AFTER CORRECTION FOR VARIATION IN ILLUMINATION
TARGET NUMBER
TARGET ILLUMINATION FOOT-CANDLES
RATIO OF TARGET ILLUMINATION
LOG10 OF PERCENT APPARENT CONTRAST
RANGE IN 1000 YARDS

FIG. 16. Graph showing the influence of target illumination on measurements of atmospheric attenuation of brightness contrast at a time when the meteorological range was found to be 58,000 yd. Observations made 1503–1508 C.S.T. (February 11, 1949).

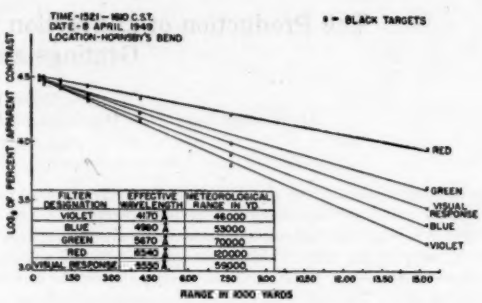

FIG. 17. Log$_{10}$ of percent apparent contrast *vs.* range using different filters in the telephotometer.

consists of listing the data obtained from the weather stations in order of increasing meteorological range as shown in the example for relative humidity in Table II. Such lists are analyzed by statistical methods. The third consists of correcting the basic data for the white targets, when necessary, to the inherent brightness they would have had if the illumination along the path had been constant. The results of such corrections are shown in Fig. 16. The fourth step in analyzing the data consists of comparing the results obtained using the four interference filters for possible regular trends relative to the meteorological elements. A sample of basic telephotometer data used for this purpose is shown in Fig. 17.

DISCUSSION AND CONCLUSIONS

The method and equipment described for measuring the atmospheric attenuation of brightness contrast along a horizontal path for the visible region of the spectrum have been used daily for a period of nearly a year. During this period, the equipment and procedure have proven satisfactory. The data collected during this period are being used to determine the meteorological factors which influence visibility. The present indications are that these data may be used as a basis for the development of a simple and reasonably accurate method for determining the range at which objects are visible for different weather and illumination conditions of interest.

Perhaps the most important advantage of the photoelectric method described for making the atmospheric attenuation of brightness contrast measurements is that the data obtained can be related directly to the meteorological conditions and their changes during the actual course of the observation periods.

The preliminary atmospheric attenuation data obtained show that the atmospheric attenuation of brightness contrast is an exponential function for a wide range of weather conditions and illumination conditions. This suggests that from a practical point of view Koschmieder's theoretical attenuation law holds for far more cases of interest than the many simplifying assumptions used in its derivation would be expected to permit. This results in the conclusion that the attenuation coefficient (and hence the meteorological range, R_m is surprisingly insensitive to many factors which cannot be controlled and for which "corrections" would be difficult to make if they were required. This is fortunate from a practical point of view since the meteorological range may be used as a parameter for describing the state of the atmosphere and hence, to predict visibility ranges. The explanation of the mechanism by means of which the attenuation coefficient is so insensitive to illumination conditions indicates a need for further theoretical considerations of the problem of the scattering of light by the atmosphere.

ACKNOWLEDGMENTS

A considerable number of individuals have contributed to the program being conducted using the methods described in this paper. Among those who should be mentioned are the members of the Atmospheric Optics Sub-Committee of the Armed Forces Vision Committee. Also acknowledgment is made of the interest and help given by members of The Optical Research Laboratory at the University of Texas, including Mr. George W. Arnold, Dr. Madeline F. Coleman, Mr. George W. Crawford, Mr. Robert B. West, Mr. H. D. Weisser, Mr. Otto H. Hill, Mr. David L. Fridge, and Mr. Martin T. Love. In addition to The Optical Research Laboratory personnel mentioned, acknowledgment is made of the assistance received from Dr. C. P. Boner, Director of The Defense Research Laboratory, Mr. Jack G. Taylor, Investment Officer of the University of Texas, and Mr. Ralph Huber of the Supervising Architects Office at the University of Texas, who are largely responsible for handling the complex legal and constructional details involved in the erecting of the visibility targets described.

In addition to the above-mentioned individuals, special acknowledgment should be made of the interest and help received from the ONR, including Mr. Frank B. Isakson, Mrs. Elizabeth K. Kelley, and Mr. George F. Kucera.

The Production of Diffraction Gratings: II. The Design of Echelle Gratings and Spectrographs[1]

GEORGE R. HARRISON
Spectroscopy Laboratory, Massachusetts Institute of Technology, Cambridge, Massachusetts

(Received January 5, 1949)

In seeking to circumvent the difficulties that have limited production of ruled gratings having resolving powers in excess of 400,000, it is observed that resolving power at a given wave-length depends only on the ruled width of the grating and the angles of illumination and observation, and not specifically on the number of ruled grooves. The reflection echelon is a grating of high resolving power in which groove separation has been increased to a degree involving extreme sacrifice of free spectral range. It is suggested that much could be gained by producing a grating with only as many reflecting grooves per inch as are needed to give sufficient free spectral range to avoid difficulties arising from overlapping of orders. For the study of Zeeman effects, hyperfine structure, and complex atomic and molecular spectra, 20 wave numbers of free spectrum should suffice, which would require use of about 100 grooves per inch. Such gratings, having a simple step groove form that reflects light of all orders in a narrow bundle, and designed to be used at an angle of incidence greater than 45° and normal to the narrow side of the "step," may be designated "echelles," as intermediate in character between the echellette and the echelon. Echelles should lend themselves to production of very powerful compact spectrographs giving single-exposure coverage of broad spectral ranges. A 10-inch echelle having 1000 grooves of width 0.25 mm, each with one flat side 0.05 mm deep, gives at 5000A a theoretical resolving power of one million, a free spectral range of 5A and a plate factor of 0.2 A/mm, when used with a lens or mirror of only 250 cm focal length. It should thus be as powerful as a 10-inch concave grating of 42 ft. radius having 30,000 grooves per inch when used in the third order, and would be much faster even though used with a lens of less than 75 mm aperture. When crossed with a suitable prism or grating of low dispersion this echelle should, without overlapping of orders, produce spectrograms having a range of 10,000 wave numbers or more on a single plate, instead of the 5 to 25 plates required by the equivalent orthodox grating in the Paschen-Runge mount. The echelle spectrograph would also offer great gains in stability and portability. Problems and possibilities of the production of original and replica echelles are discussed, and it is shown that the reduction of ruling time from weeks to hours makes interferometric control of groove spacing in gratings appear feasible for the first time.

IN a previous paper[1] the need for more and larger diffraction gratings was emphasized. Gratings ruled with from 90,000 to 180,000 grooves usually give maximum useful resolution not in excess of 300,000, and even so are not available in the numbers desired. For such important spectroscopic fields as the Zeeman effect, hyperfine and isotope structures of spectrum lines, and the precise measurement of wave-lengths in the spectra of complex atoms and molecules, resolving powers ranging upward to one million are needed. The problem of ruling satisfactory gratings of such high resolving power on a reliable basis has not yet been solved.

It has been tacitly assumed that the solution to this problem lies in the development of improved engines capable of ruling from 120,000 to 300,000 very uniform grooves on concave blanks eight or ten inches wide. The resolving power of such a grating should be matched to that of a fast photographic emulsion, which for a plate that will resolve 40 lines/mm requires that the grating be used at about $f/50$. Hence a grating 10 inches wide should be ruled on a blank having a radius of from 35 to 50 ft., depending on the mounting to be used. To obtain the broad spectral coverage needed for extensive spectroscopic programs it would be desirable to mount such a grating in an unobstructed room some 40 to 60 ft. long instead of the 25 to 40 ft. now used for 6-inch gratings. The isolation of such space from thermal and mechanical disturbances presents difficulties that have in the past been considered unavoidable. In addition, at the dispersion available in the second order of a 10-inch 42-ft. grating ruled with 30,000 g/in., the spectrum between 10,000 and 2000A would cover more than 60 ft., requiring for its registration some three dozen plates each 20 inches long. The difficulty of producing such gratings, arising largely from the requirement of ruling such large numbers of equally spaced grooves, combined with the magnitude of the task of operating so large a spectrograph, makes consideration of alternative methods desirable.

The grating formulas are ordinarily written $R=mN$, where R is the resolving power $\lambda/d\lambda$, m is the order of interference, and N is the number of grooves in the grating; and $m\lambda=W/N(\sin\alpha\pm\sin\beta)$, where W is the ruled width of the grating and α and β are the angles of incidence and diffraction. These equations and their derivatives give rise to the statements commonly seen in textbooks that the resolving power of a grating depends on the number of grooves it contains, while the dispersion depends on the spacing between grooves. However, we may combine the equations to eliminate these variables, as follows:

$$R=\frac{W}{\lambda}(\sin\alpha\pm\sin\beta).$$

When a grating is to be used at the highest resolution and dispersion we illuminate it at large angles of incidence and diffraction, using the Littrow or the Eagle mounting,[2] in which case $\alpha=\beta$. Then $R=(2W\sin\beta)/\lambda$,

[1] Based on an invited paper presented before the New York meeting of the Optical Society of America, March 11, 1949. See Part I: "Development of the Ruling Art," J. Opt. Soc. Am. 39, 413 (1949).

[2] Harrison, Lord and Loofbourow, *Practical Spectroscopy* (Prentice-Hall, Inc., New York 1948), pp. 72, 83.

and the dispersion $d\beta/d\lambda=(2\tan\beta)/\lambda$. Thus resolving power at a given wave-length is seen to depend fundamentally only on the ruled width W of the grating and the angle at which light is taken from it, while dispersion depends on the latter alone.

These equations suggest making N, the number of grooves, anything we please, a consideration that doubtless led Michelson to the design of the echelon interferometer.[3] If we increase W/N too much, however, difficulties arise from the overlapping of orders, and we should consider the importance of free spectral range, F, the spectrum interval lying between successive orders of any wave-length. This quantity is given by the formulas $F_\sigma=1/2t$ and $F_\lambda=\lambda^2/2t$, in terms of wave numbers and wave-lengths respectively. F_σ is constant over the entire spectrum and depends only on $2t$, the optical path difference between successive interfering beams, which is related to the order of interference by the formula $m=2t/\lambda$.

Taking one extreme value of t, we consider a reflection echelon that consists of only two reflecting steps 10 inches apart. Then $F_\sigma=0.02$ cm^{-1}, giving at 5000A a free spectral range of only 0.005A, a value much too low for spectrographic usefulness. If we go toward the other extreme and use 30,000 steps (grooves) per inch, as in a typical concave grating, F_σ is more than 6000 cm^{-1}, a value unnecessarily large.

The reflection echelon, as first successfully produced by Williams[4] from the early design of Michelson, is a grating having a practical maximum of some 40 steps, each about 7 mm deep and 1 mm wide. Here the order of interference $2t/\lambda=28{,}000$ at 5000A, and $R=1{,}120{,}000$, but the free spectral range is a mere 0.72 cm^{-1}, which at 5000A is only 0.18A. This causes much overlapping of even narrow hyperfine patterns, and has given rise to the incorrect statement frequently made in textbooks that the dispersion of the reflection echelon is low. Actually it is extremely high, but since almost all the light of any wave-length band is thrown into a single narrow order only one or two spectrum lines wide, the spectrum needs high magnification for easy observation. This very circumstance, however, suggests what might be done to realize an instrument superior in many ways to either the concave grating or the reflection echelon.

What minimum free spectral range would be satisfactory? Few Zeeman patterns, when produced in fields of 100,000 gauss or less, spread over more than 10 wave numbers; hyperfine and isotope-structure patterns spread even less broadly, and for wave-length measurements overlapping of orders has only secondary importance. A value of F_σ sufficiently great to eliminate most difficulties arising from overlapping orders would appear to be 20 cm^{-1}, or 20A at 10,000A, 5A at 5000A, and 0.8A at 2000A. Substituting in either formula for F, $t=0.25$ mm. Thus we need a grating or an echelon in which the successive beams are delayed by optical steps $2t$ of about 1/50 inch. We shall then be working in the order $m=1000$ at 5000A, and to obtain a resolving power of 10^6 in the 1000th order require interference of 1000 beams.

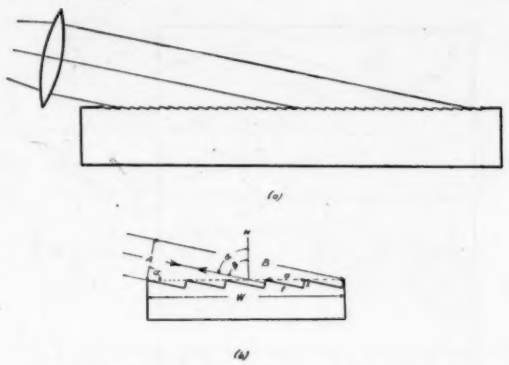

FIG. 1. (a) Mode of illumination of the echelle. (b) Groove shape and constants of the echelle. The aperture A, the optical depth B, and the ruled width W are respectively N times the step width s, the step depth t, and the groove separation a.

The reflection echelon as now made is one of the most difficult optical devices to construct, and hence one of the most expensive. The maximum number of flat plates that have been assembled in optical contact without distortion is about 40; also, flats have not been worked optically to the necessary uniformity of 1/80 wave in thicknesses less than 7 mm.[5] Assembly of 1000 plates each 1/100 inch thick into an echelon appears quite impracticable. It should not be impossible, however, to produce a grating having grooves or steps of the desired shape if only 100 g/inch are needed.

R. W. Wood[6] early ruled coarse gratings of controlled groove form, and the echelette grating originated by him has long been used in infra-red work. Wood's echelettes were ruled with approximately 1000 or 2000 g/inch, the cutting tool being so shaped as to throw the light into only a few orders. Echelettes of as few as 25 lines per inch have been ruled at the University of Michigan by Randall and Barker, but these have been for use at low resolution with long infra-red waves, and the groove forms would not be sufficiently precise for use with the shorter waves of length 10,000 to 2000A. The present problem calls for a grating somewhat coarser than the usual echelette in groove number, but considerably finer than this in groove form, approaching in surface precision the $\frac{1}{10}$ fringe of the assembled echelon. Such precision does not appear to be impossible of attainment; in fact, modern methods of controlling ruling engines now under investigation in various laboratories should lend themselves even more directly to producing such special gratings than to producing ordinary gratings.

[3] A. A. Michelson, Astrophys. J. 8, 37 (1898); Proc. Am. Acad. 35, 111 (1899).
[4] W. E. Williams, Proc. Phys. Soc. London 45, 699 (1933).
[5] S. Tolansky, *High Resolution Spectroscopy* (Methuen and Company, Ltd., London, 1947), p. 227.
[6] R. W. Wood, Phil. Mag. 20, 770 (1910).

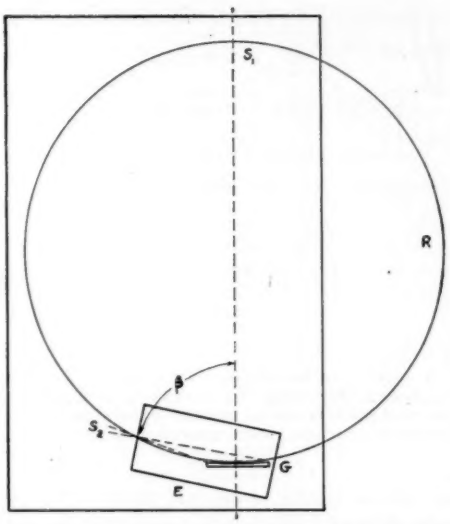

FIG. 2. How compactness is achieved in the echelle spectrograph. G is a 10-inch grating or echelle. R is the Rowland circle, of 16 m radius for such a grating in an ordinary mount. S_2 is the position of the slit of a concave grating used at large angle β in the Eagle mount, or of an echelle spectrograph designated by the rectangle E.

For convenience in discussion, it is desirable to give such special gratings a name. The term *echelle** will be used here, as indicating possession of characteristics lying between those of the echelon and the echelette, yet differing markedly from both.

DESIGN OF THE ECHELLE

Figure 1 shows a typical groove form for an echelle, and its mode of illumination. Only the steep side s of the groove is used, and this side is illuminated at or near the normal. Let us assume for the moment that echelles can be made available for installation in spectrographs, so that suitable characteristics may be determined.

The dispersion of any dispersive device is equal to its theoretical resolving power divided by its linear aperture A. Considering the echelle as a grating the dispersion $d\beta/d\lambda=(2W\sin\beta)/A\lambda=(2\tan\beta)/\lambda$, since $A/W=\cos\beta$. Considering the echelle as a reflection echelon, the dispersion $d\beta/d\lambda=m/s=2t/\lambda s$. These two forms are equivalent since $t/s=\tan\beta$, as shown in Fig. 1. It thus becomes apparent that the reflection echelon has the high dispersion of any grating used at a very large angle ($t=7$ mm, $s=1$ mm, $t/s=\tan\beta=7$, $\beta=82°$). Similarly, its high resolving power may be thought of as arising from the use at a large angle of a grating of width W. (For a typical echelon having 40 plates, $W=11.5$ inches.)

We associate high resolving power with large aperture in ordinary gratings. However, the above discussion emphasizes the possibility of separating the effective aperture A from $W\sin\beta$, the optical depth B, responsible for spectroscopic resolving power. This separation of function was well recognized by Michelson when he designed the echelon, but the possibility of its utilization with ordinary plane gratings appears to have been ignored. In the echelle we contemplate a device to be used always at a fixed large angle β, so a small lens will serve for collimation.

Figure 2 shows how compactness, broad spectral coverage, high dispersion, and great resolving power are achieved with the echelle. Let the large circle represent the Rowland circle of a 10-inch 16-meter concave grating. To reach high values of resolving power we move to a large angle β on the circle, thus bringing spectrum plate and grating closer together. To eliminate the astigmatism of the concave grating we substitute a plane grating and a lens. To obtain all desired wave-lengths at the exit slit by means of overlapping orders we reduce the number of grooves in the grating to the minimum that will still give us the necessary free spectral range. To increase speed we use a flat-sided groove that reflects most of the radiation in the desired direction. Having recognized the independence of aperture A and optical depth B, we substitute a lens of small aperture for the large lens needed with the grating at smaller angles of incidence. Finally, we cross the dispersion of the echelle with that of a spectrograph of moderate dispersion to separate overlapping orders. The resulting spectrogram should appear as in Fig. 3. The vertical linear dispersion $dl/d\lambda$ obtained on the photographic plate is the product of the angular dispersion $d\beta/d\lambda$ and the projection distance P, in this case the focal length of the collimator lens used. Hence $dl/d\lambda=(2P\tan\beta)/\lambda=(2Pt)/\lambda s$. The length l of the useful part of a vertical cycle on the plate can be determined by multiplying the free spectral range F_λ by this linear dispersion, which gives $l=P\lambda/s$.

If the photographic emulsion on which the spectrum is to be recorded can resolve two lines r mm apart, optimal results will be obtained by using a spectroscopic system having an aperture ratio $P/A=r/\lambda$. Since the

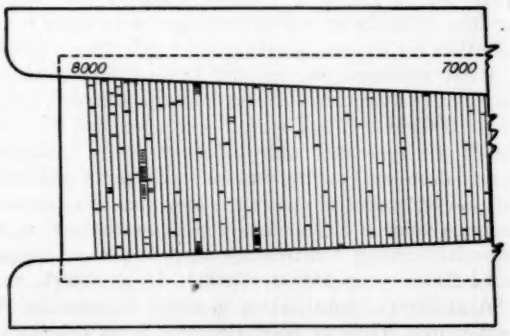

FIG. 3. Drawing of a section of a spectrogram of the type to be obtained by crossing an echelle with a stigmatic spectrograph of low dispersion. The inclined jaws are adjusted to restrict the vertical spectra to one order in each cycle.

* In French: a "ladder, scale, or pair of steps."

factor r varies approximately with λ, a single value of P/A, the aperture ratio, will serve for an entire plate. With modern fast emulsions 40 lines/mm can be resolved, so P/A may be taken as $f/50$. If we choose to use a collimator lens of 50 mm diameter, a size which can readily be constructed to be sufficiently achromatic throughout the range 10,000 to 2000A, P becomes 250 cm, and the echelle spectrograph has a theoretical resolving power of 500,000 at 10,000A, one million at 5000A, and 2.5 million at 2000A. The optical depth B is $1000t$ or 250 mm; since 1000 groves are to cover not more than a width $A=50$ mm, we have $s=A/1000$, or 0.05 mm. The groove separation a along the grating surface is $(s^2+t^2)^{\frac{1}{2}}$, and since $W=1000a$, $W=255$ mm, or slightly over 10 inches. Substituting in the formula for dispersion, we find this to be 5 mm/A at 5000A. The equivalent plate factor of 0.2A/mm is equal to that of a 10-inch concave grating of 42 ft. radius having 30,000 grooves per inch when used in the third order.

The echelle considered above was designed for high resolution in the visible and ultraviolet, but the constants of echelle design can be varied over a wide range to suit many applications. An echelle should be useful to increase the dispersion of an ordinary spectrograph for certain types of analytical work, for example. In this case a broader spectral range than that used above may be desirable, coupled with resolving power similar to that of a 6-inch concave grating. Setting the free spectral range at 100 wave numbers, the step-depth t becomes 0.05 mm. If the resolving power is to be 250,000, say, at 5000A, the optical depth B must be 62.5 mm, since $B=R\lambda/2$. B/t gives the number of grooves N as 1250. If a small spectrograph is to be used to give the crossed dispersion, we may set A at 40 mm, whereupon we determine s, which is A/N, as 0.032 mm. At numerical aperture $f/50$, P becomes $50A=2$ meters, and the linear dispersion at 5000A $dl/d\lambda=Pm/s=1.25$ mm/A. The length l of a free vertical cycle on the plate is 31.3 mm at 5000A.

If, as seems probable, the echelle proves capable of rapid multiplication by the improved methods now used for producing replicas, it should be possible to obtain readily families of echelles of different characteristics to be used in a given spectrograph. Since they are mounted in parallel light, interchangeability of echelles without the necessity of careful refocusing should be straightforward.

THE ECHELLE SPECTROGRAPH

In addition to high resolution and great speed and compactness of spectrographs, it is becoming increasingly desirable to have available broad spectral coverage in a single exposure, as the problems of spectroscopy become more difficult owing to the smallness of the available sample of material emitting light, or the complexity of operation of large magnets and similar auxiliary source equipment. It therefore becomes of great importance to take full advantage of the broad range of the echelle. This requires careful selection of the spectrograph used to give auxiliary dispersion.

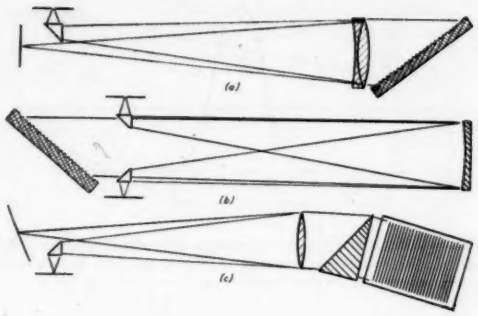

FIG. 4. Mountings that have been used with the reflection echelon, which could be adapted for use with the echelle. (a) Williams external mounting with achromatic lens; (b) Ritschl external mounting with concave mirror; (c) Jackson internal mounting.

R. W. Wood[7] has exhibited the advantage of crossing the spectrum from an ordinary grating with that of an echelette, as suggested by Shane, thus making possible photography of a spectrum several feet long on a single rectangular plate by using several horizontal cycles. In an echelle spectrum the cycles are vertical, like those long obtained in crossing an etalon or echelon with a prism or grating spectrograph of moderate dispersion. The design of a spectrograph to contain an echelle may well be patterned on experience obtained with the echelon.[8]

To obtain great flexibility the echelle may be mounted in a case of its own, with a short horizontal entrance slit and a vertical exit slit perhaps 25 mm long. An achromatic collimator must be used in this mounting, shown in Fig. 4a, because all wave-lengths covered must be brought to a sharp focus on the exit slit. This can then be used as the entrance slit of an ordinary spectrograph which gives the desired horizontal dispersion, or the light from the exit slit can be focused with an achromatic lens or mirror on the slit of the second instrument.

Ritschl[9] has used concave mirrors for the collimation of light on an echelon, achieving high resolution as a result of the absence of chromatic aberration but losing considerably in intensity from the four reflections used in addition to that at the echelon (Fig. 4b). Some of these reflections can probably be eliminated with the echelle, since it will require no large vacuum-tight case for the shifting of orders, and the geometry is simplified.

A prism spectrograph produces the crossed dispersion needed with an echelle more effectively than does a grating, because its dispersion is more nearly uniform on a wave number scale than is that of the latter. The vertical echelle cycles have uniform wave number cover-

[7] R. W. Wood, J. Opt. Soc. Am. **37**, 733 (1947).
[8] W. E. Williams, reference 4; K. W. Meissner, J. Opt. Soc. Am. **32**, 185 (1942); reference 5, p. 231.
[9] R. Ritschl, Zeits. f. Physik **79**, 1 (1932).

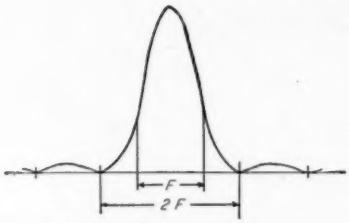

FIG. 5. Intensity envelope of energy diffracted from an echelon or echelle. The distance between the inner minima is two orders; the order used falls in that portion of the curve marked *F*.

age in each free spectral range, and hence plate space is used most effectively when the horizontal dispersion is uniform on a wave number basis. The wave number dispersion of the large Littrow quartz spectrograph manufactured by Bausch & Lomb varies by a factor of only 2.7 between 5300A and 2225A, averaging about 45 wave numbers per mm. This would serve admirably to give the auxiliary dispersion for an echelle having a free spectral range of 50 wave numbers. It may prove possible to mount such an echelle directly behind the Littrow prism, as in Fig. 4c, the coated backing of the prism having been removed. Preliminary calculations indicate that the loss in resolving power at the ends of an inclined 10-inch plate, which would subtend not more than 4 inches from the position of the echelle, should be not more than 10 or 15 percent.

With an echelle having a free spectral range of 50 wave numbers, a range of 12,500 wave numbers (as from 10,000A to 4500A) could theoretically be photographed without overlapping on a single plate with the Littrow spectrograph considered above, using a slit 1 mm long. This slit length has been found ample when echelons and other interferometers are crossed with spectrographs of low power.

D. L. MacAdam has found it useful to place the dispersion of a reflection echelon parallel to that of the spectrograph, and this might on occasion be desirable with the echelle. The latter should lend itself effectively to use in the vacuum ultraviolet, where echelles having from 300 to 600 grooves per inch would be especially valuable if sufficiently accurate groove forms can be produced. MacAdam found that the greatest drawback to use of the echelon in the vacuum region, for which it had been vigorously touted as the only available interferometric instrument, was the very high orders of interference resulting when such short waves were used. A combination of fluorite prism with a suitably ruled echelle should effectively overcome this difficulty, and make possible a very compact yet powerful vacuum spectrograph.

The large number of short lines concentrated on a single echelle spectrogram may appear to lead to difficulties in the identification and measurement of spectrum lines. The broad spectral coverage available on one plate would make it worth while to provide a transparent sheet bearing a precise wave-length grid in two dimensions with which rapid interpolation of wave-lengths to within 0.01A should be possible. A small spectrum-viewing eyepiece with internal scale could then be used for more precise wave-length interpolation, and for the highest precision a two-dimensional comparator of the type used for star-position determinations would be useful. The Winmac,[10] a scanning and computing comparator developed for use in reducing etalon spectrograms, could readily be adapted to the automatic measurement of echelle spectrograms.

GHOST AND LINE INTENSITY CONSIDERATIONS

Since the intensities of the Rowland ghosts of a grating are commonly said to increase relative to their parent lines as the square of the order m, the echelle, used in very high orders, might be expected to require undue freedom from periodic errors of groove spacing. Rowland[11] gives for the ratio of intensity of ghosts of first order to their parent line $G=(\pi^2m^2e^2)/a^2$, where e is the amplitude of periodic sinusoidal displacement of the grooves, and a is the normal groove separation. Setting $\alpha=\beta$ in the grating formula, we have $m\lambda=2a\sin\beta$, so $G=(4\pi^2e^2\sin^2\beta)/\lambda^2$. Thus the ghost intensity produced at a given wave-length by a periodic error of amplitude e is a function of the angle β only. Though the echelle will be more sensitive to periodic errors of ruling than an ordinary grating used near the normal, its sensitivity will be the same as that of any grating used at the angle necessary to achieve equivalent fundamental dispersion. Since the requirements for optical precision set by the Rayleigh criterion for resolution are much less stringent than those set by the need for low ghost intensity, there appears to be a real advantage in seeking a method of groove production in which unavoidable errors of position will be random rather than periodic.

An echelle spectrograph can be expected to be from four to 20 times as fast as an ordinary concave grating spectrograph of equivalent dispersion and resolving

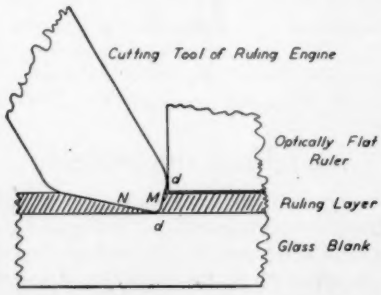

FIG. 6. Suggested method of ruling echelles, with two optical surfaces guiding the cutting tool near its point.

[10] G. R. Harrison, J. Opt. Soc. Am. **36**, 644 (1946).
[11] H. A. Rowland, *Collected Physical Papers* (Johns Hopkins Press, Baltimore, Maryland), p. 525; Phil. Mag. **35**, 397 (1893).

power, because of its lack of astigmatism and its high concentration of light in the desired order. All rays used pass through the lens in directions close to the normal, so aberrations can be kept relatively low at high numerical apertures if desired.

The expected distribution of intensity from an echelle is shown in Fig. 5. This was plotted from the formula

$$I = A^2 \frac{\sin^2\theta}{\theta^2},$$

where $\theta = (\pi s\beta)/\lambda$. Such a curve represents the envelope of the intensity diffracted by any number of equally spaced equivalent rectangular apertures of width s.[12] Most of the light is thrown into a narrow angle covering only two orders F, and a large percentage falls into the single order that is to be used. In the case of the reflection echelon the apertures are so wide (1 mm) that the very narrow intensity envelope contains only one or two lines, and great distortions in the apparent shape of the line and displacements of its center of gravity result from the steeply varying intensity curve. The narrower steps of the echelle produce a wider and more uniform envelope of illumination, corresponding to the greater free spectral range. In the first echelle discussed above, at the linear dispersion used, radiation will be concentrated in a band varying in vertical length $2l$ from 100 mm at 10,000A to 16 mm at 2000A, and the central half of each band will be used.

Though variations of intensity across a single spectrum line produced by an echelle can be expected to be negligible, lines at the top and bottom of the used portion of each vertical cycle will be less than half as intense as those at the center.** In cases where this effect is objectionable, a filter of suitably varying density made by evaporating aluminum, inconel, or some other approximately neutral absorber on a thin sheet of transparent plastic, could be put in front of the plate.

THE PRODUCTION OF ECHELLES

The optical requirements on the grooves of a high quality echelle for use in the visible and near ultraviolet are that they be flat on the active side s to within $\frac{1}{10}$ fringe and that no part of this side deviate by more than $\frac{1}{10}$ fringe from its proper position relative to the first groove ruled, even though this be 10 or more inches away. Probably the greatest difficulties in producing the desired groove shape will arise from natural strains in, and plastic flow of, the material being cut, and storage in it of residual elastic energy.

A possible method of producing large echelles that is now being tested, is as follows. A large optical flat, worked in circular form to a thickness not less than $\frac{1}{6}$ of its diameter, will be cut into two rectangular blanks each approximately 3 inches wide. Each blank will be coated to a uniform depth on its flat side with gold, silver, or aluminum, with an organic plastic, or as suggested by Cartwright[13] for lamellar gratings, with dictating record wax. The thickness of soft material will be made equal to the depth of cut desired, so that the cutting tool, having a sliding surface on its bottom as in Fig. 6, will be constrained vertically by the flat glass surface. Another optical flat will be used as a straightedge, a smooth portion of the tool sliding on this and being constrained laterally while cutting a groove with the sharp, optically straight, edge M, and the edge N which may be of any convenient shape.

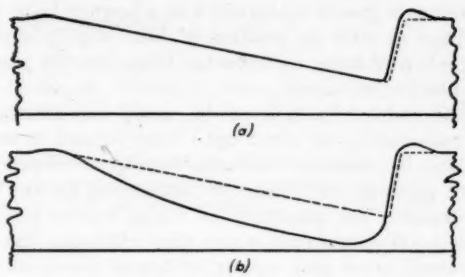

FIG. 7. (a) Expected groove form after the first cut is taken; dotted lines show the desired groove form. (b) Use of a deeper groove to relieve the cut.

In preliminary experiments carried out by J. C. Anderson and the writer, a free motion up to 5 inches in amplitude, with no lateral motion greater than 0.1 fringe, of a tool sliding against an optical flat was produced in a ruling engine. Direct two-dimensional sliding constraint on the tool should make possible the exertion of large forces without deflecting the tool from the proper line of cut.

After most of the material has been removed under carefully controlled conditions from each of the grooves, it is expected that the groove form will appear roughly as in a of Fig. 7. It should be possible to shape the cutting edge of the tool somewhat to compensate for plastic flow. If desired, the groove may be cut deeper than necessary, as in b of Fig. 7. The critical part of the groove to form will probably be the thin apex of the land between grooves. A study of the groove form after the echelle has been rough cut can be made by microscopic observation of a transverse groove cut across the rulings, by use of a plano-interferometer, and by observation of the distribution of light in the diffraction patterns from individual grooves or groups of grooves. The echelle can then be remounted on the ruling engine, the standard ruling conditions reestablished, and a burnishing tool used to straighten up the sides of the grooves and leave them at the proper spacing. Finally, it should be possible

[12] Reference 5, p. 220.

** Meissner suggests making the intensity distribution more uniform by employing angles of incidence slightly in excess of the normal, so a part of each step will be occulted. A slightly rounded groove could also probably be used to control intensity distribution; both methods would involve some loss of intensity.

[13] C. H. Cartwright, J. Opt. Soc. Am. **21**, 785 (1931).

to test each groove separately with a beam of light, and perhaps to alter its position or form slightly during inspection to bring its diffracted beam into the proper phase with the others.

The completed echelle can be coated with aluminum by evaporation, for direct use, or can be used to make replicas by standard methods, already developed for plane gratings, which are now undergoing marked improvement. The possibility of ruling master echelles directly on optical flats of soft steel which can then be hardened, or on gold, copper, or bronze plates, should not be overlooked.

While the problem of shaping the side of a groove to the required optical precision is admittedly difficult, certain great simplifications over the ruling of ordinary gratings appear with the echelle. Whereas the ruling of a 300,000-line grating can be expected to take from two to three weeks, one set of 1000 cuts across an echelle should take only a few hours. The problems of temperature control and of uniform lubrication are vastly simplified by this shortening of the ruling period. Also a large groove can be more carefully controlled in shape than a small one, for single grooves can be more readily studied.

Perhaps most important of all, interferometric control of the ruling engine over large widths of ruling appears practicable in echelle manufacture. The greatest problem to be solved in designing such control systems has been to insure that the interferometer plates remain in constant adjustment to $\frac{1}{10}$ fringe or better during the entire ruling period. While such adjustments can easily be maintained for a period of several hours, no one has yet claimed success in holding them to the required tolerance over several weeks. Of secondary importance, barometric pressure changes affect the wave-length of the light used with an interferometer, and if periods of more than a few hours are used for interferometric ruling devices designed to compensate for pressure variation must be introduced.

I am grateful to Professor K. W. Meissner for checking the calculations of this paper, and for pointing out the desirability, on occasion, of using the dispersion of an echelle in parallel with that of an ordinary spectrograph, rather than crossed with it.

Book Review

Absorption Spectrophotometry

G. F. LOTHIAN, Hilger and Watts, Ltd., London (Jarrell-Ash Company, Boston), 1949. Pp. 196, price $7.60.

This book is the third edition of a book previously credited to other authors (F. Twyman and C. B. Allsopp) entitled *The Practice of Spectrophotometry with Hilger Instruments*. The second edition was published in 1934. A welcome change in viewpoint in this edition, over that in the earlier editions of this work and other similar contributions from Hilger and Watts, Ltd. (formerly Adam Hilger, Ltd.), has been a greater recognition of other instruments and methods than those produced by or used with Hilger instruments. While major emphasis is still on Hilger manufactured equipment, at least an effort has been made to include some competitive and complementary equipment with some comparison of quality and character.

One senses the slow evolution in absorption spectra nomenclature which is taking place in the change in terminology in this last edition of "light" to "radiation." There is also a trend toward molecular absorption data, ϵ, which is reflected in current journal practice. There has been a reduction of the space allotted to the photographic spectrophotometric techniques but not a proportional expansion in the descriptive photoelectric devices (Beckmann, Cary, Hardy-GE, etc.) which have been responsible for this change in methods.

The greatest increase has been in the treatment of infrared instrumentation, technique, and application. There is an extended discussion on the "conditions for securing accuracy in spectrophotometry." Although much of the earlier edition material is reproduced without change, there has been a reorganization in the method of presentation with separate sections on the (a) principles, (b) applications, and (c) technique of spectrophotometry with sufficient new material to justify the new edition.

The paper and illustrations are good, as should be expected from the price. There is an improved bibliography combined with the author index.

WALLACE R. BRODE
National Bureau of Standards, Washington, 25, D. C.

JOURNAL OF THE OPTICAL SOCIETY OF AMERICA VOLUME 39, NUMBER 7 JULY, 1949

The Image Orthicon in Spectroscopy*

R. E. Benn, W. S. Foote, and C. T. Chase
The Franklin Institute, Laboratories for Research and Development, Philadelphia, Pennsylvania

(Received April 21, 1949)

Use of the image orthicon tube as a detector in spectroscopy provides rapid response at controlled instants and, for short exposure times, greater light sensitivity than the photographic plate. The application of the orthicon spectrograph to the study of transient or rapidly varying light sources is discussed.

INTRODUCTION

RECENT advances in electronics, especially in the field of television, have so far found little application in the spectroscopic laboratory. The traditional photographic plate has in some instances been assisted or replaced by photocells or photomultiplier tubes; these cells may play the role of the thermocouple or bolometer in infra-red spectrographs where the intensity of radiation as a function of wave-length is obtained point by point, or more often they may find application in microphotometers or recording densitometers.

Modern electronic techniques, applied to spectroscopy, not only enable one to overcome certain limitations of the photographic plate or film; they also make possible the instantaneous observation or recording of spectral intensity as a function of both wave-length and time throughout a wide spectral region. One such application, in which the image orthicon replaces the photographic plate in the spectrograph, is discussed in the present paper.

The image orthicon, RCA Type 2P23, is a recently designed television pick-up tube having high luminous sensitivity in the approximate range 3500A to 10,000A, with a peak in sensitivity near 4200A. As a detector in spectroscopy the tube has a number of advantages of which three are outstanding. (1) For short exposure times it is much more sensitive to light of low intensity than any available photographic emulsion, since its signal-to-noise ratio is considerably greater than the ratio of density to background for the plate under these conditions. (2) It is sensitive not only in the visible region but also in the near-infra-red region. (3) It can be made to respond to illumination, and provide a corresponding signal response, at any predetermined instant or succession of instants, and it exhibits, over fairly short times, a cumulative characteristic which for short exposures to weak illumination may be more linear than is the case for the photographic plate.

The output signal appears on an oscilloscope as a curve of intensity *vs.* wave-length in any range up to the limits, 3500A and 10,000A, imposed by tube sensitivity. If more than one signal is desired, a number of traces, separated in time by small predetermined amounts, may be photographed by means of a high-speed camera, or separated on the oscilloscope screen and photographed in a single exposure. This feature is of particular value in the study of rapidly varying or transient sources, especially where the illumination is so faint that a moving plate or film cannot be used in the spectrograph.

DESCRIPTION AND MODE OF OPERATION

A schematic diagram of the image orthicon is shown in Fig. 1. Incident radiation passes through a glass window on the inside of which is a semi-transparent photosensitive surface. Electrons emitted from this surface are accelerated toward a thin specially prepared glass target by an axial electric field and focused on the target by an axial magnetic field. The accelerated electrons, upon striking the target, emit secondary electrons which are collected by a fine-mesh screen. The characteristics of the glass target are such that the number of secondary electrons emitted is greater than the number of primary electrons incident on the target. Thus an intensified charge pattern of the original light pattern is left on the surface of the target facing the photosensitive surface. The magnification of the image is unity.

A stabilized beam of electrons, originating in the electron "gun" and focused by an axial magnetic field, strikes the other side of the target, the velocity of this beam being so low that few secondary electrons are emitted. In operation, the electron beam is swept across the target by means of a magnetic deflection coil. A negative charge is thus deposited on this side of the target equal to the positive charge on the opposite side. The electrons in the beam in excess of the number needed to neutralize the positive charge are reflected and return back toward the source, where they enter a five-stage secondary-emission electron multiplier. The anode current of the multiplier, consisting of the amplified current of reflected electrons, is passed through a load resistance, generating the output signal voltage. Since this signal is referred to that obtained when the tube is dark and all the beam current is reflected, the output signal is proportional to the intensity of light incident on the photosensitive surface at a position corresponding to the instantaneous position of the electron beam. Finally, electrons on the gun side of the glass target move through the target and neutralize the positive charge on the opposite side.

* Based on work performed under contract with the Office of the Chief of Ordnance, Department of the Army.

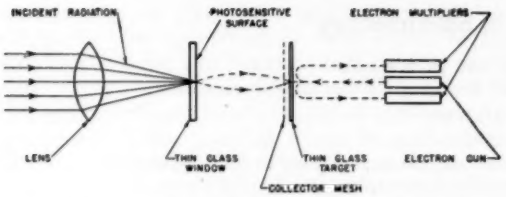

FIG. 1. Schematic diagram of image orthicon.

The spectrum is focused on the photosensitive surface. The signal response may be obtained by one of three methods: (1) The tube can be exposed continuously and the signal then obtained in one scan, giving the integrated radiation at each wave-length. (2) The signal can be obtained at intervals, each scan giving the integrated radiation for the time since the previous scan. (3) The signal can be obtained at intervals but with the electron beam displaced a small amount normal to the scanning direction between scans. In this case the beam scans a new section of the target each time and each signal is proportional to the integrated radiation from the beginning of exposure to the respective time of scan.

Presentation of the signal is by means of an oscilloscope, the electron beam of which is synchronized in the horizontal direction with the scanning electron beam of the image orthicon. The signal amplitude appears as a vertical deflection on the oscilloscope screen, giving a plot of intensity *versus* wave-length. Further scans provide information on changes of spectral distribution with time.

A scanning time of 63.5 microseconds, conventional in television practice, has been adopted. Successive sweeps may follow each other continuously, or they may be spaced by various desired intervals from 1 to 100 milliseconds. Although it might appear that triggering of a single sweep on the orthicon by a signal from a transient light source would be desirable, it should be remembered that the orthicon was designed for continuous sweeping, as in television operation. If allowed to remain quiescent too long, charges will accumulate which destroy the focus conditions. Operation with spaced sweeps and a synchronized output signal for initiating a combustion process obviates the difficulty and provides for timing control between the recording system and the source.

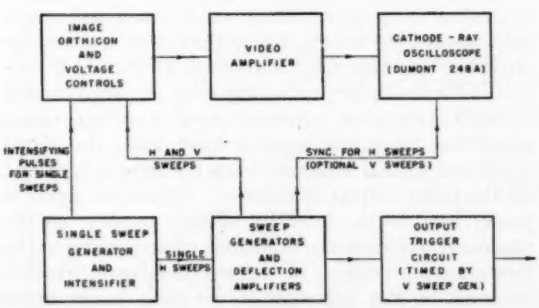
IMAGE ORTHICON AND VOLTAGE CONTROLS
VIDEO AMPLIFIER
CATHODE - RAY OSCILLOSCOPE (DUMONT 248A)
INTENSIFYING PULSES FOR SINGLE SWEEPS
H AND V SWEEPS
SYNC. FOR H SWEEPS (OPTIONAL V SWEEPS)
SINGLE SWEEP GENERATOR AND INTENSIFIER
SINGLE H SWEEPS
SWEEP GENERATORS AND DEFLECTION AMPLIFIERS
OUTPUT TRIGGER CIRCUIT (TIMED BY V SWEEP GEN.)

FIG. 2. Block diagram of electronic system for orthicon spectrograph.

The block diagram of Fig. 2 shows how the various components of the electronic system are connected. Output signals from the orthicon are fed through a video amplifier to the vertical deflection plates of the oscilloscope. Sweep voltages and intensifying pulses for the orthicon are provided by separate units, which also furnish synchronizing signals and, if desired, a vertical sweep (trace separation) voltage for the oscilloscope. Provision is made for continuously repeated scans of the orthicon target or for single scans at predetermined intervals. In either case the scanning beam may be displaced between scans by the vertical sweep voltage applied to the orthicon. When spaced sweeps are used, the orthicon scanning beam is blanked out between sweeps to prevent damage to the target, and intensifying pulses are provided for the duration of each scan. An output circuit, which contains a thyratron, furnishes a pulse to ignite the gas in a combustion bomb or other tansient source at a suitable time with respect to the instantaneous values of the scanning voltages applied to the orthicon.

A spectrograph of large aperture, designed to utilize either the orthicon or a photographic plate for recording, is shown in Fig. 3 and a spectrum of the high pressure mercury arc, obtained by using continuously repeated sweeps, appears in Fig. 4. A single sweep would have provided the same trace, with less noise. Calibration of the instrument to allow for spectral sensitivity and focus conditions is necessary before measurements made on such a trace can be accurately converted to luminous intensities.

DETAILS OF OPERATION

In normal television practice, for which the orthicon was designed, each horizontal scan of the image has a duration of 63.5 microseconds, and the entire image is covered in $33\frac{1}{3}$ milliseconds. Accordingly, each portion of the target is scanned at intervals of $33\frac{1}{3}$ msec. During each scan, as mentioned above, enough electrons are removed from the beam to equalize the positive charge on the far side of the target representing the optical image, the remainder returning to the multipliers, and appearing as the output signal. In approximately 30 msec. these charges on the target become neutralized by motion of the negative charge through the target. Thus, if a single portion of the target is scanned too frequently, a portion of the previously added negative charge remains on the target and the output signal will be reduced. Under continuous illumination, positive charge will accummulate while the decay process is going on, and conditions are not suitable for accurate observation. Greatest accuracy with respect to measurements of intensity appears to result if the target is

allowed to store up positive charge for about 30 msec. Accordingly, when conditions permit, the same portion of the target should be scanned each time, and the interval between scans should be approximately 30 msec.

A related question concerns the spectral sensitivity of the orthicon as a function of position. Preliminary observations indicate that the relative amplitudes of the output signals corresponding to two spectral lines of different color depend on position, which might possibly indicate different spectral sensitivity characteristics at different positions on the photosensitive surface or variation in target characteristics, but more probably indicates an effect of focus on the various streams of electrons. Calibration is required, but this becomes much simpler if the same portion of the target is scanned each time. If the desired information can only be obtained by scans repeated oftener than about 30 per second, it is probably better to scan the same portion of the target each time. One then loses a little accuracy because of target characteristics as just explained but avoids extreme precautions in the stabilization and adjustment of the various focusing voltages and currents.

Data supplied with the tube indicate a linear relation between the output signal current and the illumination on the tube face when this lies between 0.0015 and 0.05 foot candle, assuming that scans of the same target region are repeated at the rate of 30 per second. For greater intensities the signal amplitude is constant, and the tube is usable but signal amplitude is no longer proportional to illumination. Under conditions which are optimum for the orthicon, its response may thus be more linear than that of the photographic plate. Fortunately these conditions are approached most closely in cases where the orthicon can be most useful, that is, in a study of combustion where spectral distribution of radiant energy is desired as a function of time.

The relation between the spacing of spectrum lines on the face of the orthicon and spacing of the corresponding peaks on the oscilloscope depends on the degree of stability of the power supplies and circuit components. With moderate care in this regard, calibrations can be reproduced to a degree sufficient for studies of combustion but probably not to the extent required for the most accurate quantitative analysis. But if a few prominent and well-spaced lines are available, the rapid response and the ability to make observations at predetermined instants outweigh other considerations.

The electronic circuit components, which though complex do not involve details unfamiliar in television or radar practice, must be designed and constructed for stability. The temperature of the orthicon tube itself should be maintained between 35°C and 45°C. Further points of interest are furnished in a bulletin supplied with the tube.

Resolving power depends largely on circuit stability. The tube is designed for resolution of 500 lines per inch or better, which is of the order of the resolution

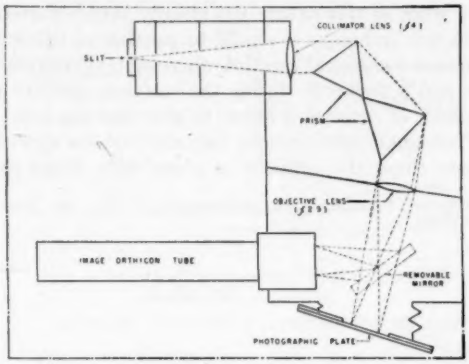

FIG. 3. Diagram of orthicon spectrograph.

obtainable with plates or film. To achieve this resolution, the power supplies and circuit components should be stable and the video amplifer should have a passband 5 megacycles wide. Such amplifiers are not unusual in television practice and their design presents no difficulties. Strong spectrum lines will of course produce spreading of the response peak which becomes wider with a flat top. As in the case of the plate, weak neighboring lines may be masked.

CONCLUSION

The application of the orthicon to spectroscopy was originally made in order to study a gaseous combustion process in which a few prominent spectral lines and bands were available. The time variation of the intensities of these lines and bands, unobtainable in many cases on a moving plate or film because of low intensities, is observable with ease and accuracy. Prelimi-

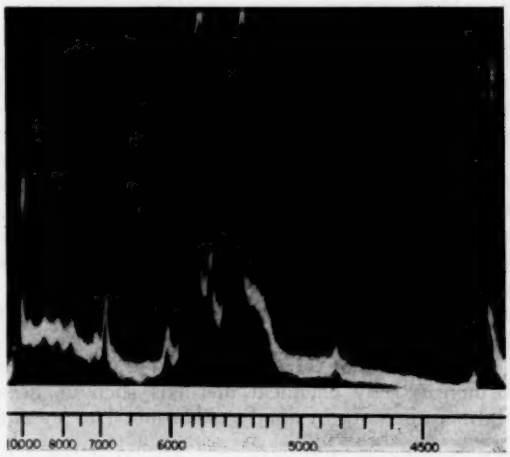

FIG. 4. Mercury spectrum as observed with recurrent sweeps on the orthicon spectrograph. (A scale of wave-lengths in angstrom units is attached.)

nary work of this nature has already been reported.** With this technique it should be possible to follow the course of a chemical reaction where certain radicals are free and active only during the reaction, and are not available or detectable before or after the reaction.

Preliminary observations indicate that for short exposure times the orthicon is about fifty times more sensitive than the photographic plate, if the orthicon response is measured above noise and the plate response above background. The orthicon has the further advantage that the entire region between 3500A and 10,000A can be covered at the same time—no single photographic emulsion will provide this coverage. Errors due to the use of several plates of different types, especially if used at different times, or to low sensitivity in the overlap regions, are thus avoided.

** Agnew, Franklin, Benn, and Bazarian, J. Opt. Soc. Am. 39, 409 (1949).

JOURNAL OF THE OPTICAL SOCIETY OF AMERICA VOLUME 39, NUMBER 7 JULY, 1949

On the Preparation of Hard Oxide Films with Precisely Controlled Thickness on Evaporated Aluminum Mirrors*

GEORG HASS
Engineer Research and Development Laboratories, The Engineer Center and Fort Belvoir, Fort Belvoir, Virginia
(Received April 7, 1949)

By increasing the thickness of the natural oxide film on evaporated aluminum mirrors, a much better surface protection can be achieved. Heat treatment in air is not practical for producing protective coatings on aluminum because the temperature required is more than 400°C and oxide films formed at this temperature are rough. Oxide films with precisely controlled thickness can be produced on evaporated aluminum mirrors by anodic oxidation in electrolytes such as ammonium tartrate. The thickness of the oxide layer formed in a given time increases linearly with the applied voltage and is 13.0 *A*-units/volt for 2 minutes anodizing time. The current efficiency of the anodic process in ammonium tartrate is in the neighborhood of 80 percent. The thickness of the oxide coatings is 1.38 times thicker than that of the aluminum layer replaced. The anodic oxide films formed in ammonium tartrate are amorphous and free of pores. They exhibit no noticeable absorption in the ultraviolet, visible, and infra-red. Their refractive index between $\lambda = 3000$A and $\lambda = 6000$A varies from 1.67 to 1.62. Anodized aluminum mirrors show excellent abrasion resistance. To obtain highest reflectivity in the visible the anodic oxidation must be performed with 120 volts for 2 minutes. The precisely controlled uniform anodic coatings on opaque aluminum mirrors are suitable for the preparation and investigation of reflection type interference filters. The thickness of a pure aluminum film can be determined by the voltage required for complete oxidation.

INTRODUCTION

THE fact that evaporated aluminum mirrors do not tarnish in normal atmosphere is a result of the good protective qualities of their natural oxide films. For many mirror applications, however, the natural oxide film is too thin to furnish sufficient mechanical and chemical protection. Therefore, various methods have been developed to coat the aluminum mirror surface with a hard and adherent dielectric layer. Since the extremely thin natural oxide film has a relatively good protective effect, a very satisfactory protection of evaporated aluminum mirrors must be expected after increasing the thickness of their oxide coating. Electrolytically brightened massive aluminum reflectors show very good scratch and corrosion resistance due to their hard anodically produced surface layer of aluminum oxide.[1]

The thickness of the oxide film on aluminum can be increased by chemical methods such as heat treatment in air or by anodic oxidation. The present paper presents data on the formation and properties of oxide films produced on evaporated aluminum mirrors at various temperatures in air and by anodic oxidation in ammonium tartrate. The applications of anodically produced films, the thickness of which can be precisely controlled, will be discussed.

I. ON THE OXIDATION OF EVAPORATED AL-MIRRORS IN AIR AT VARIOUS TEMPERATURES

The thickness of oxide layers formed in air on evaporated aluminum films was studied by Drude's optical polarization method. The special vacuum apparatus in which the films can be evaporated and examined before and after initial exposure to air has been described in a previous paper.[2] The oxide film formed on aluminum when exposed to air at normal temperature for two hours is about 10 *A* thick. It continues to grow very slowly and stops almost completely in about one month. The thickness is then about 45 *A*. The same thickness for the oxide film formed on evaporated aluminum

* Presented at the Winter Meeting of the Optical Society of America, New York, New York, March 10–12, 1949.

[1] J. D. Edwards, Trans. I. E. S. **29**, 351 (1934), and N. D. Pullen, J. Inst. Metals (London) **59**, 151 (1936).

[2] G. Hass, Zeits. f. anorg. allgen. Chemie **254**, 96 (1947).

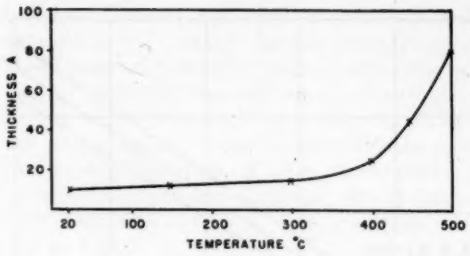

FIG. 1. Thickness of oxide film formed on evaporated Al-mirror after two hours exposure to air as function of temperature.

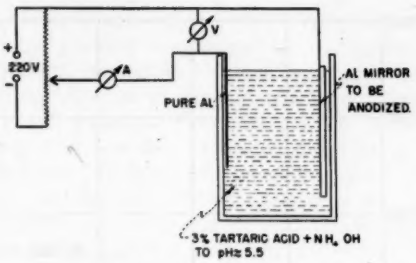

FIG. 2. Sketch of arrangement used to anodize evaporated Al-mirrors.

was calculated from the increase of the electrical resistance caused by oxidation in air. The fact that the oxide film on aluminum reaches a limiting thickness of about 45 *A* is in good agreement with the theory of the formation of oxide films on metals developed by Mott.[3]

Figure 1 shows the thickness of oxide films formed on aluminum at different temperatures after two hours exposure to air. The rate of oxidation of a fresh aluminum surface changes very little below 300° C. From 300° C, it increases slowly and from 450° C very rapidly. An increase of humidity in the air increases the rate of oxidation and shifts the beginning of more rapid oxidation to lower temperatures. By introducing steam into the oxidation furnace a rapid oxidation could be detected at 350° C. The oxidation of aluminum in oxygen at various temperatures and pressures has been studied by Gulbransen and Wysong.[4] They, too, found a rapid increase of oxidation rates at high temperature beginning at about 475° C. The fact that high humidity increases the rate of oxidation of aluminum slightly at low and strongly at higher temperatures has been reported previously.[5] The electron diffraction investigations of aluminum oxide films showed the following results. The oxide films formed on poly-crystalline aluminum at a temperature region where the oxidation rate is low are amorphous and those formed at higher temperatures are crystalline consisting of γ-Al_2O_3 with $a=7.90$ *A*. At low humidity the formation of crystalline γ-Al_2O_3 begins at about 450° to 500° C, while in the presence of steam γ-Al_2O_3 and rapid oxidation can be found at 350° C. The change in structure of the aluminum oxide film seems to be responsible for the rapid change in oxidation rates with increasing temperature. Furthermore, the electron diffraction investigations showed that during the formation of crystalline γ-Al_2O_3 in air at higher temperatures the lattice constant of the underlying aluminum increased from 4.04 *A* to 4.10 ± 0.02 *A*. The increase of the Al-lattice constant must be caused by the diffusion of oxygen into aluminum and may be considered as the first oxidation step.

Heat treatment in air is not a practical method for producing protective coatings on evaporated aluminum mirrors. The temperature required for producing the desired thickness of oxide is very high, and the films thus produced are rough and non-uniform resulting in diffuse reflection.

II. ON THE ANODIC OXIDATION OF EVAPORATED ALUMINUM MIRRORS IN 3 PERCENT AMMONIUM TARTRATE

Unlike aluminum oxide films produced by oxidation at high temperatures, those formed anodically in a suitable bath are smooth and uniform and can be prepared in precisely controlled thicknesses. The method used to anodize evaporated aluminum mirrors and data on the properties of Al_2O_3-films thus formed, together with their applications, are given in the following.

1. METHOD FOR ANODIZING EVAPORATED ALUMINUM FILMS

When aluminum is made the anode in an electrolyte containing oxygen-bearing anions, a coating consisting predominantly of aluminum oxide is formed on its surface as long as a current flows. The electrolytes used for the anodic oxidation must be divided into two classes: Those which have an appreciable solvent effect on the oxide films formed,

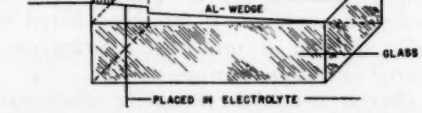

FIG. 3. Al-wedge to measure thickness of anodic coatings as function of voltage and time.

[3] N. F. Mott, Trans. Faraday Soc. **36**, 472 (1940), and **43**, 429 (1947).

[4] E. A. Gulbransen and W. S. Wysong, J. Phys. and Colloid Chem. **51**, 1087 (1947).

[5] H. Rohrig and G. Lux, *Korrosion metallischer Werkstoffe Band 3* (Verlag S. Hirzel, Leipsig, 1940), and N. Cabrera and J. Hammon, C. R. Acad. Sci., Paris **225**, 59 (1947).

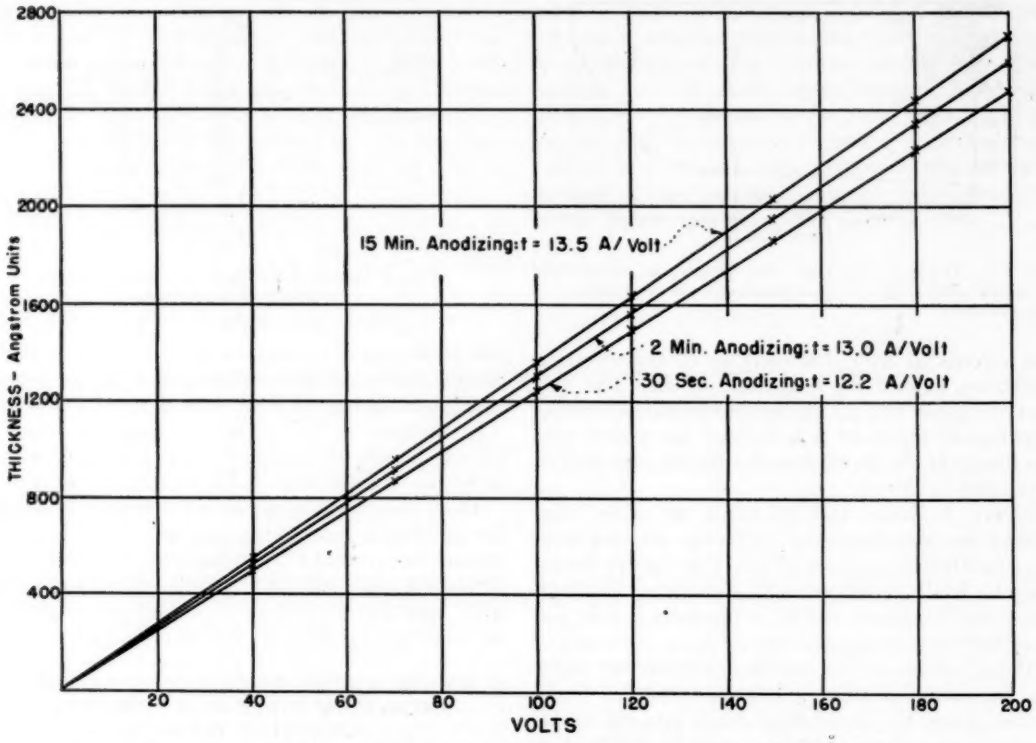

FIG. 4. Thickness of anodic coating formed in 3 percent ammonium tartrate as function of voltage for 30 sec., 2 min., and 15 min. anodizing time.

such as dilute sulfuric and oxalic acid, and those which have no solvent action on aluminum oxide, such as boric acid and solutions of acidified organic ammonium salts. The oxide films formed in electrolytes such as dilute sulfuric acid are characterized by substantial thickness and porous structure. Within quite a wide range, these oxide coatings continue to grow as long as potential is applied and film thicknesses of more than 100 microns can be attained under suitable conditions. In electrolytes in which the aluminum oxide is insoluble the dielectric coating forms rapidly and the high initial current which flows when contact is first made decreases to less than 1 ma/dm² in a few minutes, indicating that the growth of the coating has almost ceased. The thickness of the oxide films produced in a given time depends only on the applied anodizing voltage and therefore can be controlled. This type of oxide film is non-porous and is called an anodic barrier-layer. It has been found to be especially suitable as protective coating on thin evaporated aluminum mirrors.

The electrolyte used for producing anodic barrier-layers on evaporated aluminum is a solution of 3 percent tartaric acid with ammonium hydroxide added to make the *p*H about 5.5. It permits the formation of uniform films up to about 5000 *A* thick on evaporated aluminum mirrors of any size.

Figure 2 is a sketch of the anodizing arrangement. The evaporated aluminum surface is made the anode in the electrolyte and a plate of aluminum is used as cathode. The strong initial current is limited to 2 amperes by a resistor. As the oxidation increases, the current decreases to a few ma/dm² in one minute. Continued application of the applied voltage after the first minute produces little change in film thickness.

The glass form on which the aluminum film is evaporated must be extremely clean; otherwise, the aluminum film will loosen during the anodic oxidation process. Also impurities will cause pinholes by the anodic treatment. Thus, the anodic oxidation provides an excellent means for checking the adherence and purity of evaporated aluminum mirrors.

2. THICKNESS OF THE ANODIC COATINGS PRODUCED IN 3 PERCENT AMMONIUM TARTRATE

The thickness of Al_2O_3-layers formed in 3 percent ammonium tartrate as a function of voltage and time was determined by means of multiple reflec-

tion fringes. This optical method was developed by Tolansky[6] and is based on the consideration of these fringes as Newton's rings greatly sharpened through a multiple-beam action between two highly reflecting surfaces placed close together. The extreme sharpness of these fringes permits a very accurate determination of film thicknesses. The thicknesses of the Al_2O_3-coatings thus determined are accurate to about 10 *A*. The technique is illustrated in Fig. 3.

A wedge of aluminum is evaporated on a flat glass plate while a narrow central area of the glass is shielded. The top of the wedge is increased in thickness to furnish good contact for the anodizing process. The wedge coated glass is immersed in the ammonium tartrate bath and the aluminum oxidized anodically with constant voltage. The thinner part of the aluminum wedge becomes transparent and completely oxidized in a few seconds. The boundary up to which the evaporated aluminum is completely changed to its oxide moves rapidly during the first 10 seconds and then slower and slower up to the thicker part of the aluminum film. The thickness of the coating on glass at this boundary represents the thickness of the aluminum oxide film formed under the applied voltage and time. It is measured by the relative fringe displacement, which is observed at the boundary of the narrow uncoated central area after a high reflecting Al-film is evaporated over the whole plate and a similar plate with a 90 percent reflecting silver coating is placed close to it. Thus, the thickness of the anodic coatings produced with various voltages in various times was determined. The results are presented in Fig. 4. The thickness of the oxide layer formed in a given time on aluminum in 3 percent ammonium tartrate increases linearly with the applied voltage. Layers produced in two minutes have a thickness of 13.0 *A*-units/volt. The thickness increase in the next 15 minutes is only 5 percent. After about 40 minutes the anodizing current reaches a constant very small value resulting in a constant increase in thickness of only about 1 percent per hour. Walkenhorst[7] determined the thickness of anodic barrier-layers formed on Al in ammonium citrate to be 13.7 *A*-units/volt, and Taylor and Edwards[8] found for films produced in aqueous solution of boric acid a thickness of about 11.6-*A*/volt. The thickness of oxide coatings formed in different electrolytes in which aluminum oxide is insoluble seems to be in the same order of magnitude.

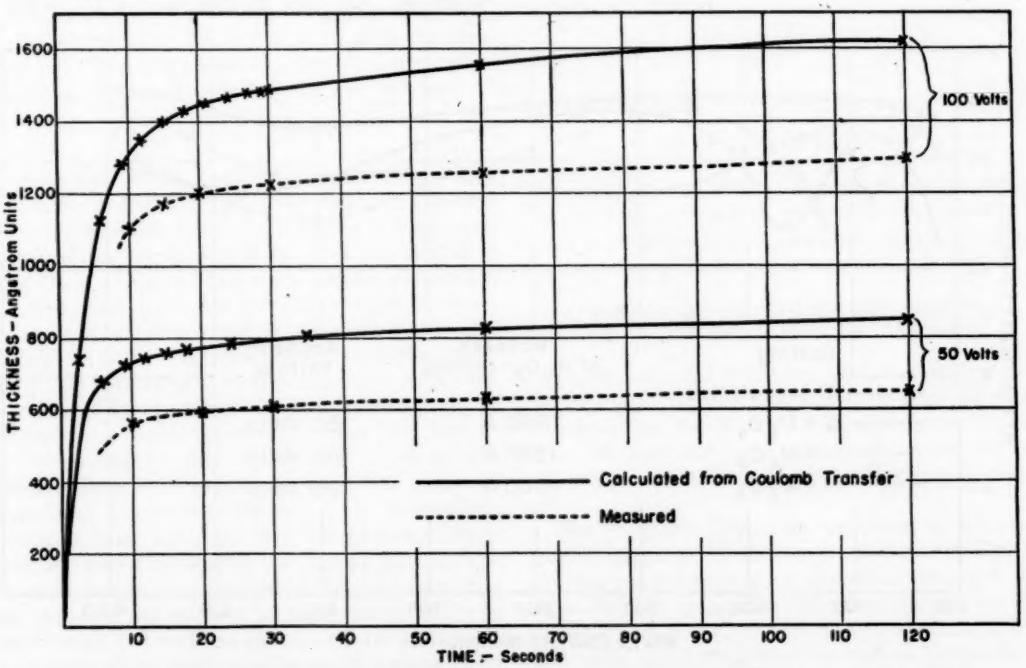

FIG. 5. Calculated and measured thickness of Al_2O_3-coating formed in 3 percent ammonium tartrate as function of time for 50 volts and 100 volts anodizing voltage.

[6] S. Tolansky, J. Sci. Instr. **22**, 161 (1945).
[7] W. Walkenhorst, Naturwiss. **34**, 373 (1947).
[8] C. S. Taylor and J. D. Edwards, Heating, Piping and Air Conditioning **11**, 59 (1939).

3. CURRENT EFFICIENCY OF THE ANODIC PROCESS

The amount, m, of Al_2O_3 formed on aluminum during the anodic oxidation should be, according to Faraday's law, proportional to the quantity of electricity passing through the electrolyte: $m = Ite$. The electrochemical equivalent e for Al_2O_3 is 17.6×10^{-5}g/amp.-sec.

This means that the thickness of the oxide coating increases with the amount of electricity according to the following relation:

$$t_{Al_2O_3}\ (\text{in } A\text{-units}) = \frac{17.6It(\text{ma-sec.})}{\rho_{Al_2O_3}F}$$

where $\rho_{Al_2O_3}$ = density of Al_2O_3 in g/cm³ and F = area of the aluminum surface to be anodized in cm². The density of γ-Al_2O_3 calculated from x-ray data is 3.62 g/cm³.[9] The values measured for anodic coatings are smaller, about 3.0 g/cm³ for the porous type of films[10] and between 3.1 and 3.3 g/cm³ for nonporous anodic barrier layers.[11] Assuming the density is 3.2 g/cm³ for the films formed in 3 percent ammonium tartrate, their thickness may be calculated from:

$$t_{Al_2O_3}\ (\text{in } A\text{-units}) = \frac{5.50It(\text{ma-sec.})}{F(\text{cm}^2)}.$$

In electrolytes which have a solvent effect on Al_2O_3 the increase in thickness must be smaller, while in those in which the coating formed is insoluble an agreement with the values calculated by Faraday's law may be expected. The amount of amp.-sec. was measured with a recently described coulometer[12] and checked with a fast recording ammeter. Figure 5 shows the measured and the theoretical thickness increase of Al_2O_3-films as function of time for formation voltages of 50 volts and 100 volts. The apparent current efficiency is in the neighborhood of 80 percent only, though no solvent effect on Al_2O_3 by ammonium tartrate could be measured after 65 hours of exposure.

4. RELATION BETWEEN THICKNESS OF ANODIC COATING FORMED AND THICKNESS OF ALUMINUM LAYER REMOVED

If all of the aluminum reacting appears as oxide, the thickness ratio of the oxide film formed to the aluminum layer replaced should be:

$$\frac{t_{Al_2O_3}}{t_{Al}} = \frac{M_{Al_2O_3}\rho_{Al}}{2M_{Al}\rho_{Al_2O_3}} = 1.60,$$

where $M_{Al_2O_3}$, the molecular weight of Al_2O_3 = 101.94, M_{Al}, the atomic weight of Al = 26.97,

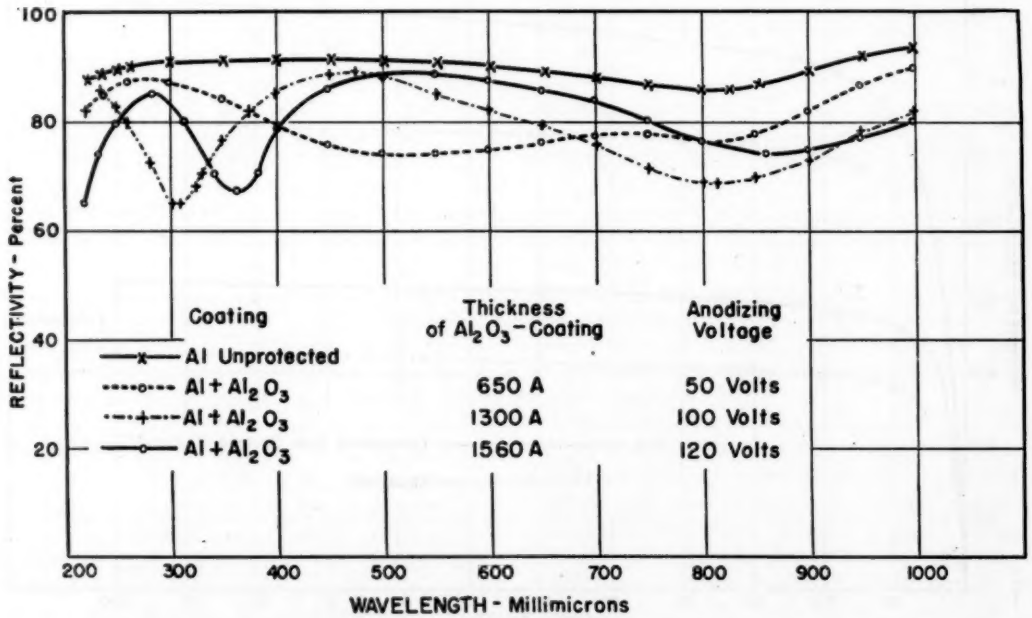

FIG. 6. Reflectivity of evaporated Al-mirrors coated with anodic Al_2O_3-films of different thicknesses as function of wave-length from 220 mμ to 1000 mμ.

[9] E. J. W. Verwey, Zeits f. Krist. 91, 65 (1935).
[10] J. D. Edwards, Proc. A. S. T. M. 40, 14 (1940).
[11] Burgers, Claasen, and Zernike, Zeits f. Physik 74, 593 (1932).
[12] E. L. Abers and R. F. Newton, J. Phys. and Colloid Chem. 52, 955 (1948).

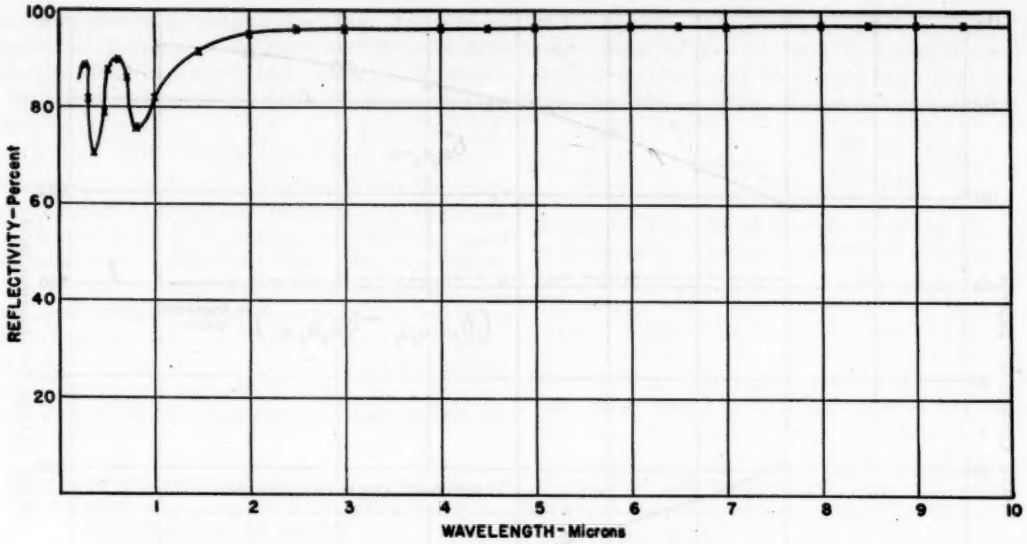

FIG. 7. Reflectivity of evaporated Al-mirror coated with an anodic Al_2O_3-film 1560 A thick as function of wave-length from 0.2μ to 10μ.

ρ_{Al}, the density of Al = 2.7 g/cm³, (aluminum films produced by fast evaporation under good vacuum conditions have, according to Walkenhorst,[13] normal density), $\rho_{Al_2O_3}$, the density of Al_2O_3 = 3.2 g/cm³.

By measuring the thickness of 10 different film before and after complete oxidation in ammonium tartrate the thickness ratio was determined to:

$$(t_{Al_2O_3}/t_{Al}) = 1.38 \pm 0.03.$$

The measured value is considerably smaller than the theoretical one. An agreement between the two values could be obtained by assuming a density of 3.70 g/cm³ for the anodic films. But this value is higher than any one known for anodic aluminum oxide films and since the refractive index of these films is very low (see later) this assumption is not justified. The fact that the thickness of the oxide is only 1.38 instead of 1.60 times greater than that of the aluminum from which it is formed may be explained by a theory recently developed by Anderson[14] According to this theory one third of the anodizing current is carried through the anodical barrier-layer by Al-ions and the rest is transported by oxygen ions, and only two out of every three aluminum ions that leaves the parent metal combine with oxygen ions to form Al_2O_3 while one diffuses through the oxide film into the electrolyte, where it may become lost for oxide formation. The loss of one out of three aluminum ions during the oxide formation would lead to a thickness ratio which is agreeable with the one measured here.

[13] W. Walkenhorst, Zeits. Tech. Physik. 22, 14 (1941), and Diss. Hannover (1940).
[14] Scott Anderson, J. App. Phys. 15, 477 (1944).

The thickness of an evaporated aluminum film t_{Al} can be readily determined from the voltage required for its complete oxidation in ammonium tartrate, since

$$t_{Al} = 0.725 t_{Al_2O_3}$$

and

$$t_{Al_2O_3} \text{ (in } A) = 12.2 \times \text{volts for 30 sec. anodizing time,}$$

$$t_{Al} \text{ (in } A) = 8.85 \times \text{volts.}$$

For complete anodic oxidation of an aluminum film that is just opaque to a bright tungsten filament, a 30-second application of about 70 volts is required. Its thickness is therefore about 620 A.

5. STRUCTURE OF THE ANODIC COATINGS PRODUCED IN AMMONIUM TARTRATE

Anodic coatings produced with various voltages (10 to 150 volts) were released from their substrate by dissolving the aluminum in a solution of mercuric chloride and were examined by the electron diffraction method and with the electron microscope.

The electron diffraction patterns of all these anodic coatings consists only of diffuse rings indicating an amorphous, or glass-like structure. The films become crystalline when subjected to temperatures of 700° C or higher. The electron diffraction patterns of films heat treated at temperatures between 700° and 950° C correspond with those for γ-Al_2O_3 while at higher temperatures α-Al_2O_3 is formed.

The electron micrographs show no evidence of pores or structure in the oxide layer even at mag-

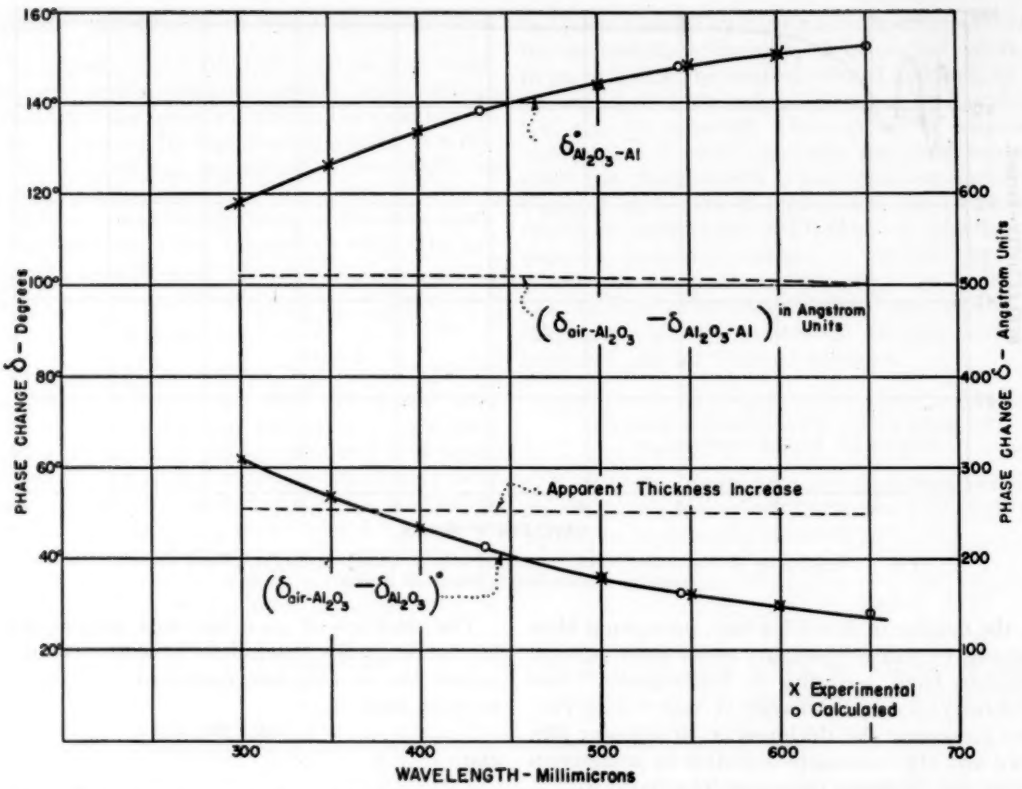

FIG. 8. Phase changes occurring on reflection at Al_2O_3 coated Al as function of wave-length from 300 mμ to 650 mμ.

nifications of 50,000 diameters. A characteristic grain structure appears only when the films are heated to more than 700° C. They are therefore suitable as temperature-resistant support films for electron diffraction and electron microscope investigations.[15] When used for this purpose the films are made 100 *A* to 200 *A* thick.

6. PROPERTIES OF ALUMINUM OXIDE PROTECTED ALUMINUM FRONT SURFACE MIRRORS

Figures 6 and 7 show the reflectivity in the wave-length region from 0.22μ to 10μ of evaporated aluminum mirrors protected by anodic films of various thicknesses. The interference maxima and minima which shift with increasing thickness of the aluminum oxide coating to longer wave-length can be adjusted to a desired position by the applied anodizing voltage. To obtain highest reflectivity in the visible, the anodic oxidation must be performed with 120 volts (2 minutes). The oxide film formed with this voltage is 1560 *A* thick and yields a first order maximum at λ = 550 mμ. Front surface mirrors for use in the ultraviolet and infra-red can be advantageously protected with an anodic coating because the thin layer of aluminum oxide used for protection does not show any appreciable absorption. The infra-red reflectivity from 2μ to 10μ (see Fig. 7) is therefore practically the same as that of an unprotected aluminum mirror, since the Al_2O_3 coating is too thin to produce any interference minimum in this region.

The abrasion resistance of evaporated aluminum mirrors protected with aluminum oxide is very good. They cannot be damaged by strong rubbing with rough linen and are extremely resistant to scratching with most metal points. They are, however, more sensitive to boiling water and salt spray than silicon monoxide protected aluminum mirrors.

7. REFRACTIVE INDEX OF THE ANODICALLY PRODUCED AL_2O_3 FILMS

The refractive index of the anodic coatings was determined by dividing the difference in optical thickness, $n(t_2-t_1)$ of two films produced with different voltages by their actual difference in thickness, t_2-t_1. To eliminate the phase change on reflection from the calculations, the thickness of

[15] G. Hass and H. Kehler, Kolloid Zeits. 95, 26 (1941), and 97, 27 (1941).

the oxide films were adjusted so that interference maxima or minima of different orders were produced at the same wave-length. Thus the difference in optical thickness of two films can be calculated from:

$$n(t_2-t_1)=\lambda/4(m_2-m_1)$$

where m_2-m_1 represents the difference in the interference order. The actual difference in thickness was determined by the difference in voltage used for the anodic oxidation. The refractive index, which was determined to be $n=1.62$ for $\lambda=600$ mμ, increases uniformly with decreasing wave-length to $n=1.67$ for $\lambda=300$ mμ. These values are smaller than those known for γ-Al_2O_3 ($n=1.73$ for $\lambda=589$ mμ[16]) but are in agreement with the refractive indices for anodic coatings as determined by Edwards.[17]

8. ABSOLUTE PHASE CHANGE OF LIGHT WAVES AT BOUNDARY AL_2O_3–AL AND ITS EFFECT ON THE POSITION OF REFLECTION MINIMA AND MAXIMA

If light is reflected at normal incidence from a metal surface covered with a thin dielectric film of the optical thickness n_1t the spectral position of reflection minima and maxima can be calculated by the following equation:

$$2n_1t+\delta_1-\delta_2=m(\lambda/2), \qquad (1)$$

where m is the interference order, δ_1 the absolute phase change at the boundary air-dielectric film, and δ_2 the absolute phase change at the boundary dielectric film-metal surface. While δ_1 has a constant value of $\lambda/2$ or 180°, δ_2 depends upon the optical constants of the metal n, κ and the refractive index n_1 of the dielectric and is defined by:

$$\tan\delta_2=\frac{2n_1n\kappa}{n_1^2-n^2-(n\kappa)^2} \qquad (2)$$

δ_2 can be determined directly from Eq. (1) where it is the only unknown quantity and can be calculated from Eq. (2) using the optical constants of aluminum, which have been reported in a recent paper.[18] Figure 8 shows the δ-values in degrees and A-units (units of the wave-length) for the system $Al+Al_2O_3$ as function of wave-length from 300 to 650 mμ. There is a good agreement between the calculated and directly determined δ-values. ($\delta_{air\text{-}Al_2O_3}-\delta_{Al_2O_3\text{-}Al}$) in A-units is almost fixed throughout the wave-length region studied and behaves like a constant increase in optical thickness of the Al_2O_3-film of 250 A. Therefore Eq. (1) becomes simple for this special case: $2(n_1t+250)=m(\lambda/2)$. (t and λ in A-units.)

9. REFLECTION TYPE INTERFERENCE FILTERS WITH AL_2O_3 DIELECTRIC LAYER

A reflection type interference filter consists in its normal form of a highly reflecting opaque mirror coating on which is first applied a thin layer of dielectric material and then a very thin semi-transparent metal film.[19] The spectral positions of minimum and maximum reflection and the shape

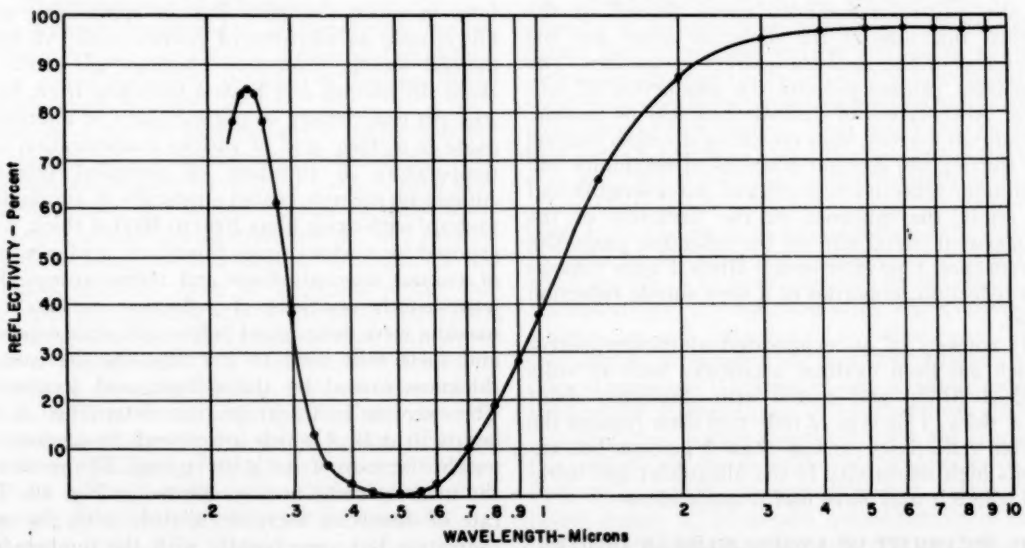

FIG. 9. Reflectivity of reflection-type interference filter as function of wave-length from 0.2μ to 10μ. Filter consists of Al (opaque)+Al_2O_3 (580 A thick)+Al (transparent appr. 50 A thick).

[16] E. Kordes, Zeits f. Krist. **91**, 193 (1935).
[17] J. D. Edwards, Monthly Rev. Am. Electroplater' Soc. **26**, 513 (1939).
[18] G. Hass, Optik **1**, 2 (1946).
[19] L. N. Hadley and D. M. Dennison, J. Opt. Soc. Am. **37**, 451 (1947) and **38**, 483 (1948).

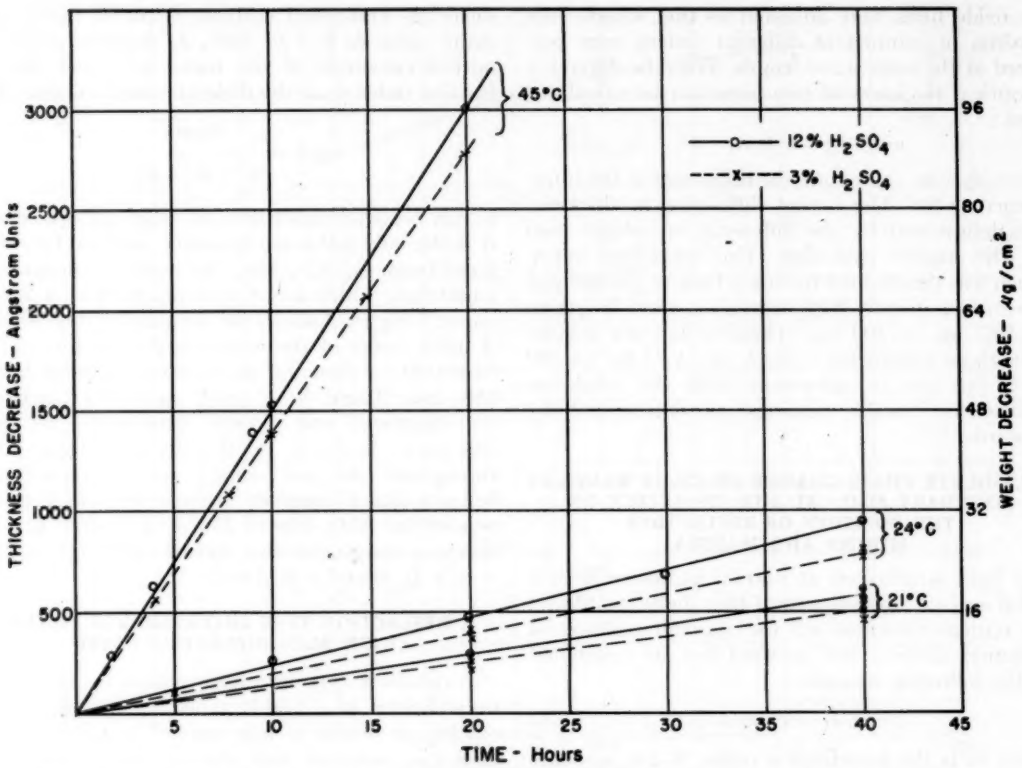

FIG. 10. Dissolving rates of anodic Al_2O_3-films in H_2SO_4-solutions of various concentrations and temperatures.

of the spectral reflectivity curve depend on the optical thickness of the dielectric layer and the thickness of the semi-transparent metal film. The anodizing process permits the production of uniform Al_2O_3-layers of desired thickness on opaque aluminum mirrors, thus providing a simple method for shifting the spectral positions of maximum and minimum reflectivity to desired wave-lengths and to study the influence of the thickness of the transparent metal film on the reflection properties of reflection type interference filters. Figure 9 shows the reflection properties of a very simple reflection filter.

It consists of an evaporated aluminum mirror which has been oxidized anodically with 45 volts (585 *A* Al_2O_3) and coated with aluminum about 50 *A* thick. This type of reflection filter reduces the visible reflectivity to less than 2 percent but exhibits high reflectivity in the ultraviolet and infrared where it may have useful applications.

10. SOLUBILITY OF ANODIC FILMS IN DILUTE SOLUTIONS OF SULFURIC ACID

As mentioned above very thick coatings of aluminum oxide can only be produced in electrolytes in which the oxide has an appreciable solubility, such as solutions of sulfuric acid. All commercial anodic protective coatings are made in these electrolytes and have a thickness from 2μ to 20μ. An exact study of the solubility of aluminum oxide in sulfuric acid of various concentration and temperature is therefore of technical interest. Aluminum mirrors, coated anodically in ammonium tartrate with oxide films 2000 to 4000 *A* thick, were exposed for various times to sulfuric acid solutions of various concentrations and temperatures. The wave-length positions of reflection minima and maxima were determined before and after exposure and their shift used to calculate the decrease in thickness caused by the sulfuric acid treatment. The decrease in thickness thus determined is accurate to ± 20 *A* which corresponds to accuracy in weight decrease of $\pm 6 \times 10^{-7}$ g/cm^3. The results of the measurements are represented in Fig. 10. The rate of dissolving increases slightly with the concentration but very rapidly with the temperature of the sulfuric acid solution. The aluminum oxide films decrease very uniformly in thickness during their exposure to sulfuric acid.

JOURNAL OF THE OPTICAL SOCIETY OF AMERICA VOLUME 39, NUMBER 7 JULY, 1949

A Method of Measuring High Intensities at the Focus of a Parabolic Reflector with Large Relative Aperture

GEORGE E. DAVIS
Material Laboratory, New York Naval Shipyard, Brooklyn, New York
(Received April 12, 1949)

A method of measuring very high intensities in the focus of a highly convergent beam is described. A receiving cell with special stops is used to determine the energy distribution thermoelectrically. The sources of error with two different types of aperture are discussed. Errors due to heat radiated from the stop are minimized by using short exposures and by substituting a reflector for the stop immediately after the exposure. A suitable mount and adjusting mechanism for the cell are described.

IN the measurement of radiation of very high intensity at points within an extended image formed at the focus of a parabolic reflector with large relative aperture, difficulties are encountered due to the wide angular distribution of the reflected rays.

Our particular problem was to measure the distribution of intensity in the focus of a 24-inch parabolic mirror when this reflected parallel or nearly parallel rays from a 5600-watt carbon arc. Since the source was not a point, and because of small departures from perfect optical geometry, the focal image was extended and somewhat diffuse, with the energy concentrated mainly on a circular area of 4- or 5-mm radius, but extending several mm farther. There was approximate radial symmetry of intensity distribution, so that in this particular case it was possible to find the distribution from measurements of the energy falling upon concentric circular areas with various radii. However, the method used is equally well suited to point-to-point measurements, and such determinations also were made.

The focused rays formed a 127-degree cone. That is, when the rays were received on a plane surface normal to the axis of the mirror, the angle of incidence of the peripheral rays was 63.5°.

Because of the very high intensity at the focus, it was not possible to use a thermocouple or other small device which could be moved from point to point. A much more massive receiver was devised, so that its temperature rise would be small during exposures of 1 or 2 seconds. It was necessary for this receiver to retain, for the period of recording, nearly all the radiant energy incident upon it, regardless both of the angle of incidence and the cross-sectional area of the incident beam at the point of measurement. The receiver could be used (a) to measure the energy falling upon circular areas of various radii, concentric with the axis of the mirror, by use of stops with apertures of various sizes; or (b) to find the energy falling upon equal small areas at different positions in the image, by using a single stop with small aperture, placed successively at the various points.

ACTION OF STOPS

In the case of rays collimated at the point of measurement, accurate results may be obtained by use of a black-body receiving cavity with a stop made of sufficiently thick material with low thermal conductivity. But if the rays are converging or diverging, difficulties are introduced, as is seen by reference to Fig. 1, in which the action of each of two different types of stop is shown. In both (A) and (B), the stop *DD* is of any desired thickness. It admits a selected portion of the converging beam to the black-body cavity (not shown) of the receiving cell *C*. The upper surface S_1 is placed in the plane in which the intensity is to be found; in the present case, in a plane normal to the axis of the mirror and passing through the focus.

First consider a stop shaped as in (A). Some of the rays fall upon surface S_1, heating it. Some rays strike the inner surface S_3 of the aperture and are reflected one or more times before entering the cell. The radiant energy recorded as heat in the cell is the amount entering the aperture, modified by the following principal energy losses and gains: (a) losses by absorption at S_3 and by re-radiation through the aperture from S_4; (b) gains by re-radiation from S_2 and S_3, with heat conducted from S_1 to these surfaces and, at S_3, also absorbed directly from the radiation. The heat gained as noted in (b) may be very considerable when the incident radiation is of high intensity, even with a stop made of heat insulating material and with exposures as short as a second or less. Thickening the stop reduces conduction of heat to surfaces S_2 and S_3 but increases the absorption losses at S_3. The energy losses and gains may be reduced by surfacing the stop with polished, highly reflecting metal but cannot be made negligible by this means.

Calculation of the absorption at S_3, which introduces a direct loss and, through (b), an indirect gain, must take account of variation of the following factors with angle of incidence: (1) projected area of entrance end of aperture; (2) fractional part of entering beam striking S_3 rather than passing directly through the aperture; (3) intensity of the radiation; (4) reflectivity of S_3. Factors (1) and (2) are geometrical only. Factor (3) is caused mainly (a) by angular non-uniformity of emission from the surface of the source, this non-uniformity itself varying in type with the contour of the surface; and (b) to variations of reflectivity with angle of incidence on the collimating mirror or lens and on the

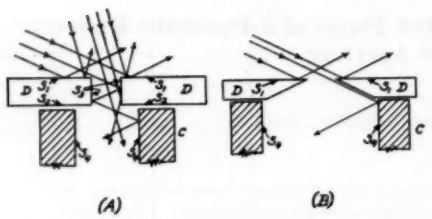

FIG. 1. Action of stops in admitting oblique radiation to a cell. C, receiving cell. DD, stop. S_1, S_2, S_3, S_4, surfaces of stop and cell.

focusing mirror. Factor (4) involves two different uncertainties; namely, the variation of reflectivity with angle of incidence on S_3, and the reflectivity at normal incidence. The former can be calculated only if the surface is very highly polished and the latter is known. The latter must be determined experimentally in every case (handbook values are generally unreliable when applied to any surface which is not known to conform exactly to the specified conditions) and moreover tends to change because of surface effects induced by the high-intensity radiation.

Estimation of the amount of heat conducted to surfaces S_2, S_3, and thence radiated to the receiving cell involves similarly great difficulties, since it must take account of (a) non-uniform heating of surface S_1, the intensity of the rays and the amount absorbed varying from point to point, due to angular and positional non-uniformity of emission of the source, and to variation of absorption with angle of incidence and condition of surface; (b) the effect of the shape and dimensions of the stop, on the flow of heat through it; both (a) and (b) to be considered under varying temperature conditions.

It is seen that with the stop shaped as in (A), Fig. 1, the difficulties of making corrections for the energy losses and gains preclude its use under the experimental conditions here considered, unless only rough measurements are to be made or some experimental method of reducing the errors can be applied.

Next consider a stop shaped as in (B), Fig. 1. With the proper angle of bevel at the aperture, none of the rays strike its inner surface, so that one of the two principal sources of error discussed in considering type (A) is eliminated. Radiation of heat from stop to cell is increased, however, since the part of the stop adjacent to the aperture is thinner and so is more highly heated during exposure and more readily conducts heat to the surfaces facing the cell. Therefore, to determine the net effect of beveling the edge of the aperture, the heat losses and gains would have to be calculated or measured for both types of aperture and for various materials, thicknesses and shapes.

TABLE I. Exposure time, 0.5 sec. in all cases

Diameter of aperture (mm)	Errors caused by heat from stop: Stop left in position (%)	Stop removed after exposure (%)
3.0	75	9
4.0	40	6
5.0	23	3.7
7.0	9	1.7
9.0	4.7	0.9
13.0	2.0	0.4
16.0	1.5	0.3

This was made unnecessary by finding an experimental method which reduces to negligible values the errors due to radiation of heat from stop to cell, although not greatly reducing the uncertainties due to radiation striking surface S_3 when the stop is of type (A). The choice then was clearly a stop of type (B), which does not introduce this latter difficulty.

The necessity of reducing the errors due to heat radiated from stop to cell was shown by measurements on stops of type (B) made of polished stainless steel $\frac{1}{32}$-inch thick, backed with a $\frac{1}{8}$-inch layer of "transite," a heat-resisting material with low thermal conductivity. Heat radiated to the cell was shown by large variations in the time required for the cell to reach maximum temperature after the exposure, the time increasing with increased heating of surface S_1. The heating of S_1 in any given exposure time varies with size of aperture. Large errors were indicated for readings taken with small apertures.

EXPERIMENTAL METHOD

The method of reducing these errors to negligible values consists mainly in removing the heated stop immediately after the exposure, replacing it with a thin polished reflector with no aperture. This reflector prevents most of the loss of heat by radiation from the inner surface of the cell, while the parts of the massive cell are coming to thermal equilibrium. The heat capacity of the thin reflector is small, favoring rapid attainment of approximate thermal equilibrium with the cell. The reflector used was polished aluminum foil cemented onto thin cardboard. The foil without the cardboard probably would have done as well. The amount of heat radiated to the cell while the stop was in position was minimized by using exposures shorter than 1 sec.

The stops finally used were like those described above except that the backing layer of transite was omitted, to reduce the diameter of cell required for stops with the larger apertures. The insulating material should reduce the errors, but for our purposes these could be made sufficiently small using stops of polished $\frac{1}{32}$-inch stainless steel alone. The stop and the reflector to replace it were mounted on a metal slide which brings them into position 1.6 mm from the end of the cell, with air space between.

To test the method, exposures of equal duration were made with apertures of various sizes, then with the stops replaced by a disk exactly similar to them except that it had no aperture, so that no direct radiation

entered the cell. Correction was made for the energy falling on the area normally occupied by the aperture. The stop was replaced by the reflector immediately (about $\frac{1}{2}$ sec.) after the exposure, by manually moving the slide on which they were mounted. The results are shown in Table I.

It is seen that by removing the heated stop immediately after the exposure and substituting the aluminum reflector, the errors are reduced to negligible values except for the smallest apertures. The remaining errors are due to heat coming from the stop before it was removed. These could be reduced by using an electrically controlled device to remove the stop more quickly than can be done by hand, and by using still shorter exposures.

CONSTRUCTION OF CELL

Construction of the receiving cell is shown in Fig. 2. It was made from a solid copper cylinder, drilled and

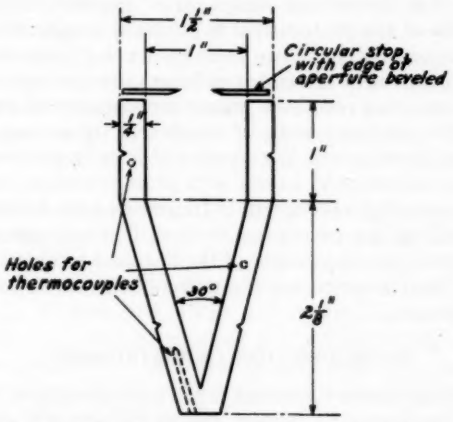

FIG. 2. Receiving cell, with stop in position. Shown in section.

shaped to have a $\frac{1}{4}$-inch wall, with a 30-degree taper over about $\frac{2}{3}$ of its length. The inner surface was polished, then blackened with a smooth coat of carbon ink ("India ink"). Most of the rays entering the cell are reflected 6 or more times, the remainder 4 or 5 times, before emerging. The loss by reflection thus is negligible. The outside of the cell also is polished, to reduce heat losses. For mounting the cell, two grooves are cut around it, as shown in Figs. 2 and 3.

Three holes, $\frac{1}{16}$-inch in diameter, are drilled to receive copper-constantan thermocouples, in the positions shown. Each couple is soldered to the end of a cylindrical copper plug about $\frac{1}{4}$-inch long, with rounded ends and slightly less than $\frac{1}{16}$-inch in diameter, so that it fits the hole closely after receiving a thin coat of electrical insulating material. Good thermal contact is insured by sealing the plugs in with paraffin. When in position, the

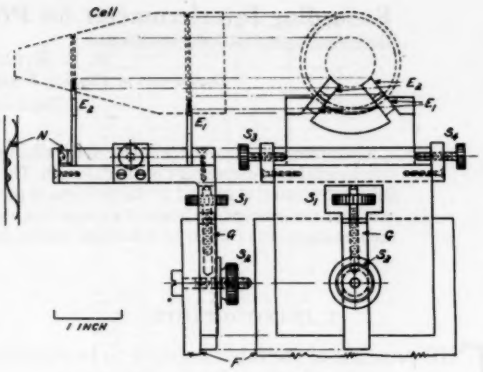

FIG. 3. Adjustable mount for receiving cell.

couples are $\frac{1}{4}$-inch or more from the outer ends of the holes and about equally distant from the inner and outer surfaces of the cell. The three couples are connected to a galvanometer in parallel, with the three lead-wire resistances equal. The time required for maximum response of the cell was not measured but was observed to be not more than 20 sec., probably much less, for exposures of the order of 1 sec. Because of the large heat capacity, the temperature rise is never more than a few degrees but sufficient for accurate thermoelectric determination. After heating, the temperature decreases very slowly.

MOUNT FOR CELL AND STOP

The cell is mounted as shown in Fig. 3. To minimize heat losses by conduction, it is supported on four sharp edges formed by tapering the ends of narrow steel strips E_1, E_2. Vertical adjustment is made by means of screw S_1, loosening S_2 to allow motion along the fixed guide strip G. Transverse adjustment is effected by means of screws S_3, S_4, with play eliminated by spring N. The distance of the cell from the focusing mirror is adjusted by means of a screw (not shown) which moves the support F.

The stop, Fig. 2, is mounted on a brass slide which can be moved horizontally in a guide attached to the front of the cell mount, Fig. 3 (guide not shown). The slide also carries the thin aluminum reflector which replaces the stop immediately after the exposure. When moved out of position, the heated stop is brought behind a part of the support on which the slide is mounted, so that its heat cannot be radiated to the cell, while the reflector automatically comes into position in front of the cell.

It is obvious that the method we have described is not restricted in application to rays from parabolic reflectors but can also be used advantageously in measuring very high intensities in any highly convergent or divergent beam.

Recording Interferometer for Precision Wave-Length Determinations*

W. R. SITTNER** AND E. R. PECK
Department of Physics, Northwestern University, Evanston, Illinois
(Received April 15, 1949)

A recording interferometer is described which permits the precise measurement of an angle by means of interferometric measurement of chord length. The present instrument, working in conjunction with a recording spectrometer, is applied to the problem of precise wave-length determinations. Preliminary results indicate that the average deviation of a single measurement is 0.044A. The application of this interferometer to the measurement of linear or rotational motion is discussed.

I. INTRODUCTION

THE principle of the interferometer to be described was suggested by one of us[1] as a means of obtaining the precision in wave-length measurement which was expected to be attainable with the completion of a recording infra-red spectrometer. It was expected that the spectrometer, when in final form, would permit a precision of wave-length measurements of 1 part in 10^6.

A diagram of the new interferometer is shown in Fig. 1. It is seen to be similar to the Michelson interferometer except that each of the two plane reflecting mirrors is replaced by a pair of mirrors mounted to form a right angle. The useful property is that optical path difference is independent of rotation of either mirror pair about the intersection line of its two surfaces.

The interferometer works in conjunction with the spectrometer described by Nelson.[2] The optical arrangement is that of Pfund, and the spectrum is scanned by rotation of a plane grating through the medium of a precision bearing, lever arm, nut, and precision screw.

In operation, mirror M_1 of the interferometer is mounted on the rotating lever arm, and the remainder of the interferometer is mounted on the frame of the spectrometer. M_1 moves on the arc of a circle as the spectrum is scanned, hence the order of interference changes progressively. The direction of view also changes as M_1 rotates, and, if M_1 passes through the image of M_2 at zero order, the change in the direction of view is one-half the angle of rotation of M_1. A telescope is provided which projects the fringe system on a diaphragm having an aperture which lets some of the flux contained in the central fringe fall on a detector. The telescope rotates with half the angular velocity of M_1, thus the detector always "sees" the central fringe. A plot of the photocurrent is produced simultaneously with the spectrum under investigation on a paper chart. A measurement of number of fringes between points in the spectrum permits a precise measurement of chord length and hence angle of rotation of the grating between these points. If a number of lines on the record have wave-lengths known with great precision, a formula relating wave-length to fringe count can be determined. In this comparison method, it is not necessary to know the wave-length of the line used to illuminate the interferometer, nor the radius of the arc on which M_1 moves.

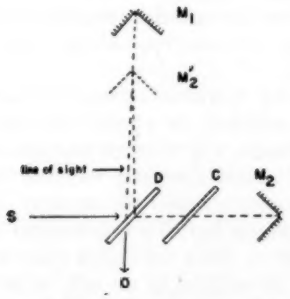

FIG. 1. Diagram of new interferometer.

S = Source. M_2, M_1 = Mirror Pairs.
D = Dividing Plate. M_2' = Image of M_2.
C = Compensating Plate. O = Observer.

II. DESCRIPTION OF INSTRUMENT

An arc source containing argon and cadmium is used for illumination. A housing around the source is water cooled in order to minimize changes in temperature of the interferometer and/or spectrometer during operation. The 6438.47A spectral line of cadmium is isolated by means of color filters and the photoelectric threshold of the detector.

The interferometer is shown in Fig. 2. It is seen that four positioning pins define the planes of the two front surface mirrors of each pair. These pins were burnished to approach a right angle using as criterion the coincidence of the two images seen by reflection in a mirror pair. Fine adjustment is made by elastic deformation of the positioning pins and/or glass of the mirror by means of the leaf springs seen in the photograph. The criterion here is quality of the fringes.

The adjusting screws on M_1 allow the intersection line of M_1 to be rendered parallel to its axis of rotation. The adjusting screws on the fixed portion of the interferometer are used to complete the interferometer adjustment as described in reference 1. The radial position of M_1 on the lever arm can be precisely adjusted in

* This work was supported by the Bureau of Ships, U. S. Navy.
** Now at Bell Telephone Laboratories, Murray Hill, New Jersey.
[1] E. R. Peck, J. Opt. Soc. Am. 38, 66 (1948).
[2] R. C. Nelson, J. Opt. Soc. Am. 39, 68 (1948).

FIG. 2. View of interferometer and telescope.

order to make its intersection line pass through the image of the intersection line of M_2 at zero order.

The lens, diaphragm, and shielded detector, L, D, and T, respectively, are shown in Fig. 2. The detector is an electron multiplier phototube (RCA type 931A). The platform which carries the telescope is rotated by the lever arm through a mechanical linkage.

A block diagram of the circuits used with this instrument is shown in Fig. 3. A potential of about 2 volts is developed across the 10 megohm load resistor. Amplifier A_1 produces about 4 volts across the low impedance magnetic penmotor G which records the individual fringes on the paper chart. Fringe frequencies of 1 and 2 per second are encountered at the spectrum scanning speeds used.

Since a large number of fringes are normally recorded between spectral lines, a means of automatically counting the fringes and recording the count on the fringe record is provided by means of a three decade scaling circuit. At each 10th, 100th, and 1000th count a sharp pulse of adjustable amplitude is impressed on the penmotor which then records a fiducial mark. The amplitude of the fiducial mark is adjusted to distinguish the 1000, 100, and 10 counts.

A long shielded cable is used between the detector in the spectrometer room and the relay rack housing the circuits, which is in another room. Some electrical pick-up by this cable is present. Also a small signal at a frequency of 15–20 cycle sec.$^{-1}$ is sometimes present due to residual vibration of M_1 with respect to M_2. Selective

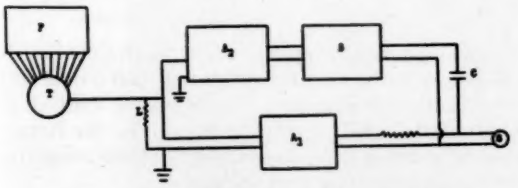

FIG. 3. Block diagram of circuits used with recording interferometer.

T = Multiplier Phototube Detector (RCA Type 931A).
P = Power Supply (1000 v d.c.).
A_1 = a.c. Amplifier (Brush Development Company Type BL 905).
G = High Speed Galvanometer (Brush Development Company Type BL 902. Magnetic Penmotor).
A_2 = Tuned Amplifier.
S = Electronic Counter (Potter Instrument Company Type 330B, modified for this application).
L, C = Load Resistor and Coupling Condenser.

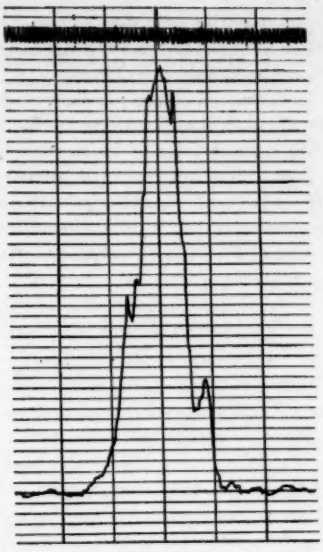

FIG. 4. Typical interferometer fringes, counter marks, and spectral line.

amplifier A_2 is tuned to 1 or 2 cycle sec.$^{-1}$ as desired, thus preventing false counts due to pick-up or vibration.

Our experience in the development of this instrument indicates that the following additional requirements merit careful consideration.

(1) The relative motion of M_1 and M_2 due to vibration must not be greater than one microinch.
(2) Relatively constant angular velocity of M_1 is necessary.
(3) The lateral "play" in the bearing carrying M_1 must be quite small.

III. RESULTS

Figure 4 shows a typical fringe record, counter marks, and spectral line. This record was made with spectrometer slits having an equivalent width of 0.4A.

TABLE I. Comparison of wave-lengths measured with recording interferometer and with Fabry-Perot étalons.

Position on fringe scale	Wave-length observed here	Wave-length due to Humphreys	Wave-length difference
116.2 fringes	8104.410A	Kr 8104.3660A	+0.044A
355.8	Standard	Kr 8112.9023	
2531.8	8190.032	Kr 8190.0570	−0.025
3704.7	8231.609	Xe 8231.6348	−0.026
4597.1	Standard	Kr 8263.2412	
5581.0	8298.116	Kr 8298.1091	+0.007
19240.2	Standard	Kr 8776.7498	
20452.4	8819.286	Xe 8819.412	−0.126
23568.7	8928.636	Kr 8928.6934	−0.057
24241.1	8952.231	Xe 8952.254	−0.023
30180.8	Standard	Xe 9162.654	
		Mean deviation =	0.044A

In order to test the precision obtainable with this instrument a number of the stronger arc lines of krypton and xenon have been recorded. The wave-length of these lines has been determined very precisely by Humphreys[3] using Fabry-Perot étalon interferometers. Some of the lines were taken as standards, the wave-lengths of the remaining lines calculated by interpolation along the fringe scale, and then compared with Humphreys' values. The results are given in Table I.

Examination of Fig. 4 shows that the uncertainty in determination of the position of the peak of such a line is about $\frac{1}{10}$ of the width. Since the width is 0.4A, a mean deviation smaller than 0.044A is not to be expected. To increase the precision it is necessary to decrease the instrumental width, which implies narrower slits. These could be used if one or more of the following conditions were fulfilled: more intense source, more sensitive detector, larger grating area, and higher reflectivity or possibly echelette effect in the grating. When instrumental width has been reduced, fractions of a unit on the fringe scale should become more significant. The dispersion in terms of fringes is now 0.035A/fringe. However, a larger number of fringes can be recorded for a given grating rotation by using radiation of shorter wave-length for illumination or by increasing the radius of the circle on which M_1 moves. The velocity of the paper chart would then be increased to provide convenient measurement.

The mean deviation of 0.044A obtained here is to be compared with a standard deviation of 0.1A obtained with this spectrometer when the conventional commutator method of producing fiducial marks for a wave-length scale is used.[2] It should be noted that while the precision obtained with the commutator method is probably a maximum, that obtained by use of the interferometer method is limited by the instrumental width of the recorded lines and not by the interferometer itself.

With the present design of interferometer a single fringe represents a motion of M_1 of about 12 microinches. A motion of one microinch, which may be due to either a linear or rotational motion, is easily detected. Thus the use of such an instrument is to be considered whenever very small displacements are to be measured, or whenever measurements must be made with great precision and/or accuracy.

IV. ACKNOWLEDGMENT

It is a pleasure to acknowledge the assistance of Messrs. J. W. Petzel and Joseph Grzybowski in the construction of the interferometer and of Mr. W. R. Wilson for suggesting the circuit of the tuned amplifier. Special thanks are also due Dr. W. S. Huxford, director of the project under which the work was done.

[3] C. J. Humphreys, Bur. Stand. J. Research 5, 1041 (1930).

JOURNAL OF THE OPTICAL SOCIETY OF AMERICA VOLUME 39, NUMBER 7 JULY, 1949

Interference Phenomenon in the Schlieren System*

E. L. GAYHART AND ROCHELLE PRESCOTT
Applied Physics Laboratory, Johns Hopkins University, Silver Spring, Maryland
(Received April 13, 1949)

A diffraction phenomenon has been discovered in the schlieren system which makes possible a quantitative schlieren method. In this method bands are observed in the schlieren field. These bands represent regions in the schlieren through which the optical path length is constant and different from the schlieren free portion of the field by $(N+\frac{1}{2})$ wave-lengths of the light used (where N represents an integer). It has been demonstrated that, within the experimental accuracy, these bands have the same meaning as those observed in the Mach-Zender type of interferometer when that instrument is adjusted so that one fringe covers the entire field.

INTRODUCTION

TOEPLER'S schlieren method has long been used for the study of phenomena involving temperature variations and compressibility effects in gases. This method was placed on a quantitative basis by Schardin[1] who showed that the brightness variation in the schlieren image was related quantitatively to a component of the optical path gradient in the corresponding portion of the schlieren field. Schardin's analysis was based on geometrical optics and left much to be desired. As a quantitative research tool the method is difficult to standardize and depends on densitometric methods for analysis. In addition, the results are in the form of density gradient components which require integration in many cases before they are useful.

The phenomenon to be described in the present paper is observed in the customary two-mirror schlieren system when the light source (preferably monochromatic) is reduced in size to approximate a "line" or "point" source. Under these conditions some of the light passing through the schlieren field is diffracted to form a fringe system near the central minimum of the Fraunhofer

* Operating under NOrd Contract 7386 with the Bureau of Ordnance, U. S. Navy.
[1] Hubert Schardin, *Das Toeplersche Schlierenverfahren*, (VDI-Forschungsheft 367, Berlin, 1934).

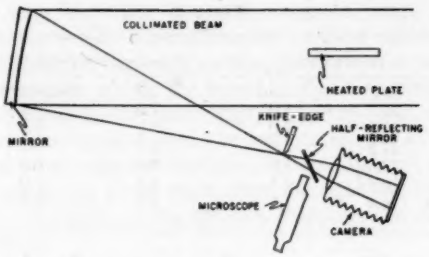

FIG. 1. Drawing of experimental arrangement of apparatus.

pattern in the "knife-edge" plane. If, under these conditions, the central maximum of the Fraunhofer pattern is stopped by the "knife-edge" or preferably by a small wire, then the light which is not stopped in this plane will give rise to a series of bands in the image of the schlieren fields. Data are given which indicate that, within experimental error, these bands represent regions of constant optical path length which differ from the optical path length in the ambient air by $(N+\frac{1}{2})$ wavelengths of the light used, where N is an integer.

APPARATUS

The arrangement of the apparatus shown in Fig. 1. represents an ordinary two-mirror schlieren system less the light source and collimating mirror. In this type of system the light source is placed off the axis of the first paraboloidal mirror such a distance that the collimated beam of light reflected from the mirror just misses the light source. The object giving rise to the schlieren to be observed is placed in the collimated beam as shown. After passing through the schlieren the light falls on the second mirror whose axis is parallel to the axis of the first mirror. In the focal plane of this second mirror is formed an image of the light source. The "knife-edge" is adjusted exactly in the plane of this image. A camera is so located behind the knife-edge that that portion of the light not stopped by the knife-edge forms an image of the plane containing the schlieren on the focusing screen of the camera. In the present apparatus provision is made to introduce a half-reflecting mirror between the knife-edge and the camera lens. This allows direct observation of the knife-edge plane with the microscope indicated in the figure simultaneously with the observation of the schlieren image on the camera focusing screen.

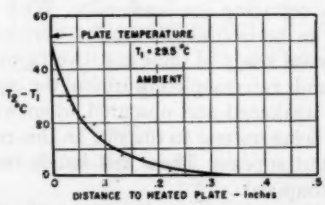

FIG. 2. Air temperature as a function of distance from plate (thermocouple).

The light source consists of a General Electric mercury vapor arc (type H-4) focused through a condensing system on a Gaertner Spectrograph slit which is adjustable to widths of only a few microns. A Wratten 77A filter may be used to restrict the light substantially to the 5461 angstrom line. Alternatively, a tungsten filament lamp may be substituted for the mercury arc to provide white light.

DESCRIPTION OF EXPERIMENTS

The schlieren consist of the density gradients set up in the air near the vertical face of a heated plate. In the convection flow rising at the surface of the plate there is a temperature gradient extending from the boundary of the flow to the surface of the plate where the temperature is a maximum. Thus there results a schlieren in which the optical path length varies, becoming a minimum at the plate.

In the course of the present investigation the temperature distribution was determined in one case by means of a thermocouple. Precautions were taken to reduce heat losses along the thermocouple leads and radiation to the thermocouple. This latter effect must be negligible as the ambient temperature was indicated at only a very short distance from the plate, at which distance the radiation from the plate to the thermocouple would not have diminished appreciably. The

FIG. 3. Fringes in knife-edge plane.

FIG. 4. Bands in convective flow at plate.

FIG. 5. Bands on both sides of plate—wire substituted for knife-edge.

resulting plot of temperature *versus* distance to the plate is shown in Fig. 2.

When, with the apparatus as described above, screens were placed in the collimated beam so that only a portion of the beam (approximately one inch in height opposite the face of the plate nearest the observer) was allowed to fall on the second mirror, then an examination of the slit image showed that a considerable amount of light fell in the region of the knife-edge plane to the observer's left. This is the schlieren phenomenon as described by Schardin.[1] If the horizontal dimension of the source was then reduced to approximately 30 microns or 0.001 inch, fringes could be observed in this diffracted light. These were superimposed upon the normal Fraunhofer pattern which could be seen alone either with the plate at room temperature or removed. The number of fringes and the width of the pattern appeared to vary directly as the plate temperature. It was found that if the light on the opposite side of the plate was allowed to pass under conditions similar to the above then a similar fringe pattern appeared on the opposite side of the source image. This type of fringe pattern is shown in Fig. 3 in which the knife-edge has been placed so as to stop the central image of the source. A wire 0.016 inch in diameter was introduced for scaling purposes. It was further observed that if the light were allowed to pass both faces of the plate simultaneously then the fringes nearest the knife-edge on either side broke up into a finer pattern. It was also observed that if the height of the beam was increased beyond approximately one inch the fringes lost contrast and definition, disappearing for appreciably greater heights.

TABLE I.

6-inch plate		Ambient temp. 304.4°A	
ΔT	Count	ΔN	Difference
37.6	8.0	7.8	0.2
32.8	7.0	6.9	0.1
27.8	5.8	5.9	−0.1
23.0	5.0	5.0	0.0
20.5	4.5	4.5	0.0
18.4	3.5	4.0	−0.5

Changing the point of observation to the focusing screen of the camera it was observed that, if the right-hand knife-edge was brought up so that the central slit image was just stopped, the area of the image next to the heated surface of the plate (which would normally be bright in ordinary schlieren observation) contained a number of bright bands nearly parallel to the face of the plate and extending out to the boundary of the convection flow (see Fig. 4). It was noted that if the knife-edge was advanced farther into the fringe system in its plane the bands in the camera image moved into the plate disappearing one by one until the outermost band was adjacent to the plate before it too disappeared.

In observations on the camera screen it was not necessary to restrict the mirror aperature with a screen to prevent confusion of the bands in the schlieren image. It was noted, however, that the bands only showed in that portion of the image which would have appeared brighter than the schlieren free field in ordinary schlieren observations; the portion containing schlieren which would appear darker were indistinguishable from the dark field. Of course, bands would appear in these portions if the left-hand knife-edge were used. In order to observe both sets of schlieren simultaneously (i.e., those on both sides of the plate), a wire 0.004 inch in diameter was substituted for the knife-edge. When this was adjusted to stop only the central image then both sets of bands could be seen as shown in Fig. 5. To determine more of the nature of these bands a heated pipe placed axially to the beam was substituted for the vertical plate with the results shown in Fig. 6. with the wire again replacing the knife-edge. With the source slit and wire horizontal the results were as shown in Fig. 7. Careful study of these last two figures indicates that the bands run completely around the pipe although somewhat weakened and obscured when within a few degrees of being normal to the slit. In this region a new type of band appears. These last bands turn into the pipe and disappear.

In any of the above experiments either the monochromatic or tungsten light source could be used. How-

FIG. 6. Bands around pipe using vertical wire as knife-edge.

FIG. 7. Bands around pipe using horizontal wire wire as knife-edge.

FIG. 8. Photograph of heated plate with knife-edge brought up to central maximum but not stopping it.

ever, with the light from the tungsten lamp, chromatic effects were observed similar to those observed in interferometry, i.e., each wave-length formed a pattern of its own in which the fringe or band spacing was proportional to the wave-length. If more than a few fringes were present only the few nearest the ambient temperature were separate and distinct. Figure 8 shows the appearance of the plate when the right-hand knife-edge is brought up to, but not stopping, the central slit image.

To determine more completely the conditions under which these bands in the schlieren image and fringes in the knife-edge plane would appear the plate and knife-edge were arranged as in Fig. 1. The right-hand knife-edge was brought up just to stop the central source image. A small screen one inch high was then brought up from the side of the plate nearest the observer. It was observed that when the screen apparently just touched the first band all the bands between the screen and the plate disappeared, being replaced by a more or less uniformly illuminated area. The portions of the bands above and below the screen were unchanged. If the screen was replaced by a vertical wire the same result was noted. Apparently the light just outside the schlieren was necessary for the production of the bands.

If the arrangement described for observation of the fringes in the knife-edge plane was used in the above screen and wire experiment, it was noted that these fringes disappeared simultaneously with the disappearance of the bands. In the use of the wire positions could be found on further entrance of the wire into the schlieren, at which the bands reappeared.

TABLE II.

12-inch plate		Ambient temp. 304.4°A	
ΔT	Count	ΔN	Difference
28.6	13.0	13.3	−0.3
20.8	10.0	10.0	0.0
16.1	8.0	7.9	0.1
11.2	5.8	5.6	0.2
8.9	4.5	4.4	0.1
6.6	3.3	3.3	0.0

QUANTITATIVE RESULTS

On the basis of the above-described experiments which indicated that the bands might correspond to constant optical path lengths, a quantative study of the phenomenon was undertaken. The study to be described was an attempt to determine whether or not this is the case. Rather similar experiments using a Mach-Zender type interferometer were described by Kennard.[2] Starting with the Lorenz-Lorentz equation for the index of refraction of a gas

$$\frac{n^2-1}{n^2+2}=C\rho, \tag{1}$$

where n is the index of refraction of the gas, ρ is the density of the gas, and C a constant, Kennard derived the equation

$$T_2-T_1=T_1\frac{\Delta N}{(n_1-1)\frac{L}{\lambda_0}-\Delta N}, \tag{2}$$

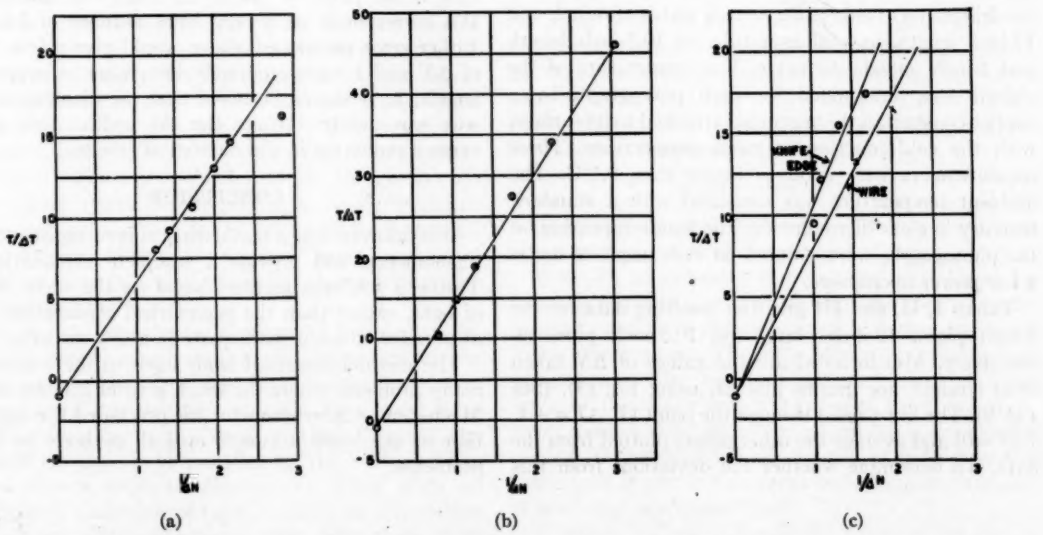

FIG. 9. (a) 6-inch plate. See Table I. (b) 12-inch plate. See Table II. (c) 10.5-inch pipe. See Table III. Graphs of $T/\Delta T=(k/\Delta N)-1$. T=air temperature (ambient), and N=band number.

[2] R. B. Kennard, *Temperature Distribution and Heat Flux in Air by Interferometry; Temperature, Its Measurement and Control* (Reinhold Publishing Corporation, New York, 1941).

TABLE III.

10.5-inch pipe		Ambient temp. 301°A	
	Horizontal knife-edge		
ΔT	Count	ΔN	Difference
31.8	10.0	10.9	−0.9
24.7	9.0	8.7	0.3
19.5	7.5	7.0	0.5
17.3	6.0	6.2	−0.2
	Horizontal wire		
22.7	6.5	6.5	0.0
18.1	5.0	5.0	0.0
13.3	4.3	3.9	0.4
7.2	2.0	2.1	−0.1

in which T_1 is the ambient temperature (absolute), T_2 the temperature along the light path in question, L the length of the path through the gas at this temperature, λ_0 the wave-length of the light in vacuum, and ΔN the difference in path in wave-lengths between the optical path length in question and that in the ambient air of index of refraction n_1.

A simple transformation gives

$$\frac{T}{\Delta T}=\frac{k}{\Delta N}-1, \tag{3}$$

where

$$T \text{ is } T_1,\ \Delta T \text{ is } T_2-T_1, \text{ and } k=(n_1-1)L/o. \tag{4}$$

The above equation describes a straight line if the variables plotted are $T/\Delta T$ and $1/\Delta N$.

In order to determine whether this equation actually described the fringe number, a series of photographs of the fringes was made using heated plates of 6-inch and 12-inch length, as well as a tube of 10.5-inch length and 4-inch outside diameter. The temperature of the objects was determined for each photograph by a copper-constantan thermocouple attached to its surface, with the cold junction at room temperature. These measurements were good to better than 0.1°C. The ambient temperature was measured with a standard mercury in glass thermometer. The bands appearing on the photographs were counted on each negative under a low power microscope.

Tables I, II, and III give the resulting data for the 6-inch plate, 12-inch plate, and 10.5-inch pipe, respectively. Also included are the values of ΔN taken from straight line graphs plotted, using Eq. (3). (See Fig. 9). The line passed through the point ($T/\Delta T=-1$, $1\Delta N=0$) and average the other points plotted from the data. To determine whether the deviations from this line were within the probable error in the count the ΔN for each temperature as read from this graph is also given as well as the difference between this value and the actual count. This result indicates that only one count differed from the average by more than 0.5 band. Most counts were well within this value.

TABLE IV.

Object	End correction*
6-inch plate	−6 mm
12-inch plate	20 mm
10.5-inch pipe	−30 mm
10.5 Horizontal wire	−78 mm

* To be added to true length to check length determined from K in formulas (3) and (4).

As a check, the equivalent length of each object was computed to determine the end correction from Eq. (4), using the value of k determined from the corresponding graph. The correction is to be applied to the length of the heated object to arrive at the equivalent length determined from the experiment. These are given for the experiments listed in Table IV.

It will be noted that these values show inconsistencies particularly for the pipe. Looking back at Kennard's formula (1) we notice that a low fringe count will give rise to a low equivalent length. Such a low count may arise from two sources; it is very difficult to estimate the last fringe as the fringe spacing decreases rapidly as the plate is approached and also the number of fringes may be decreased by the knife-edge being brought in farther than the amount necessary just to darken the field. (It should be noted that in neither case is the point ($T/\Delta T=-1$, $1/\Delta N=0$) affected as this corresponds to a very large number of fringes.) Either error mentioned above would give a low value of ΔN and a correspondingly low value of equivalent length, L. It should be noted that the diameter of the wire was nearly 4 times the slit width. This would cause a reduction in the number of fringes.

CONCLUSION

It is believed that a mathematical investigation of the phenomenon will provide a complete explanation of Toepler's schlieren method based on the wave theory of light, rather than the geometrical explanation used at present[1] which is inadequate in many respects.

The method described lends itself to the solution of many problems where the much greater expense of the Mach-Zender interferometer has precluded the application of the more accurate optical methods to these problems.

Optical Characteristics of Sheets of Scattering Materials*

R. L. LONGINI
Westinghouse Research Laboratories, East Pittsburgh, Pennsylvania

(Received January 31, 1949)

There are a number of articles on the optical properties of sheets of scattering materials where the fundamental equations relating to such sheets have been derived or checked by experiment. These equations have, in general, two constants related to the materials involved. Except in the case of opal glasses these coefficients have not been related to the bulk properties and size of these materials. It is here shown, by geometric considerations, that for large particles two properly selected coefficients are independent, and their relationship to particle size is shown. The scattering coefficient proves to be inversely proportional to particle size while the absorption coefficient is independent of particle size. These coefficients can be measured accurately, and measurement of the scattering coefficient may prove a reliable means of checking particle size. The general expressions for the transmission and reflection of the sheets can be much simplified for thin sheets of material having low absorption.

IN many cases sheets of scattering materials are composed of tightly packed particles large enough so that light can be considered to obey the laws of geometric optics in and around them. Ryde,[1] in his excellent treatise on opal glasses, limits his treatment to the case where the scattering particles are many wave-lengths apart so that the scattering due to each particle can be considered independently. His treatment is only applicable to particles of low refractive index and very small absorption. Ryde's paper evaluates the scattering constant of Schuster's equations in terms of particle size and the bulk optical constants of the materials involved. It will here be shown that the dependence on particle size, at least, is much more general than can be gathered from an examination of his derivation.

In the case considered by Ryde we can assume that an elementary layer could be thick enough to contain whole particles since they are so far apart that the chance is very small of scattering of a single ray by more than one particle in the layer. In the case now under consideration, on the contrary, any elementary layer of thickness large enough to contain whole particles would have much multiple scattering within the layer between its particles. Furthermore, such elementary layers would of necessity have boundaries cutting through particles constituting the layer.

Let us now consider an elementary layer of thickness dx (much smaller than the diameters of the scattering particle but still large enough to be in the range of "geometric" optics). This layer is to be bounded by two planes cutting through the crystals of the sheet parallel to the surface. The figure shows such an elementary layer with an example of a number of rays incident on it from one side. Note that reflections and refractions take place only at particle surfaces. The layer is thin enough so that the probability of two scattering processes for one ray of light is negligibly small.

Of the rays incident on one side a fraction sdx is scattered out the same side while the fraction $1-sdx$ is transmitted if the material is non-absorbing. The coefficient s will be called the reflectancy.[2]

Now suppose that the material is unchanged in in geometry but is made slightly absorbing. This will have a negligible effect on the reflection coefficients of the particle surfaces, thus the same fraction of rays will be reflected and refracted as before. If wdx is the attenuation then the transmittance will be

$$(1-sdx)(1-wdx)=1-(s+w)dx. \qquad (1)$$

The reflectance, however, is more complicated. The reflected part will be diminished by absorption of the same nature, but with a different mean value, as that reducing the transmitted light. The fraction not absorbed will be $1-w_1dx$ where w_1 is the mean absorptancy[2] for these rays. Thus the reflectance of the elementary layer is

$$sdx(1-w_1dx)=sdx, \qquad (2)$$

neglecting second order terms. Thus we see that the reflectancy s is unchanged by absorption.

Now let us consider the changes introduced by varying particle size. Let us suppose that our elementary layer is increased by a factor m in all linear dimensions. The new elementary layer will be geometrically similar, but m times as large linearly. Thus the new thickness of the elementary layer is $dx'=mdx$. Since the geometry is unchanged except for lengths of path, angles of reflection and refraction at particle surfaces remaining unchanged, it is at once apparent that

$$sdx=s'dx'=s'(mdx)$$

* Taken in part from Ph.D. Thesis, University of Pittsburgh. Pittsburgh, Pennsylvania. Contribution 1-P-49, Physics Dept,

[1] J. W. Ryde, Proc. Roy. Soc. **131A**, 451 (1931).

[2] American Standards Association Report on American Standard Letter Symbols for Heat and Thermodynamics Including Heat Flow, p. 18, ASA, Z 10.4, 1943.

thus

$$s' = s/m.$$

However the absorption $w'dx'$ must be m times as great as before as the absorption is a function of lengths of path rather than of angles. Thus

$$m(wdx) = w'dx' = w'(mdx)$$

giving

$$w' = w.$$

In words, the reflectancy is inversely proportional to particle size whereas the absorptancy is independent of particle size. Unfortunately, the relationships between s and w cannot be evaluated simply directly from theory. It can be stated, however, that s increases with increase of the index of refraction of the scattering material and that w increase with increased absorption coefficient of the bulk material. Both the particle shape and the three dimensional random distribution of ray directions enter into these relationships.

A comparison of Eqs. (3) and (4) with those of Ryde show that the reflectancy s is equal to Ryde's NB where N is the number of particles per unit volume and B is the back scattering per particle. Now, for large particles, Ryde finds B is proportional to the square of the diameter of the particles. In the case here considered N is inversely proportional to the volume of the particles, or to D^3. Thus Ryde's NB for our case would be inversely proportional to the particle diameter, as we find for s from geometric considerations.

When one calculates the absorptancy from an elementary layer such as described here he finds that for diffuse incident light the absorption is twice that of columnated light normal to the surface. This ratio of two is rigorous in the case of opal glass calculated by Ryde (though Ryde uses the same absorptancy both for normal columnated and for diffuse light). In our present case, however, this might be in error due to the coherence of adjacent elementary layers.

The differential equations for transmission and reflection have been set up and solved by Coltman *et al.*,[3] Schuster,[4] and others.[5] The reflectance R and transmittance T for the entire sheet have been found by Coltman to be, in our notation,

$$R = \frac{(s/p)\sinh pt}{\cosh pt + [(s+w/p)]\sinh pt} \tag{3}$$

[3] Coltman, Ebbighausen, and Altar, J. App. Phys. **18**, 530 (1947).

[4] Schuster, Astrophys. J. **21**, 1 (1905).

[5] Hamaker, Philips Res. Rep. **2**, 55 (1947); G. M. Dreosti, Thesis, Utrecht, 1930; P. Kubelka and F. Munk, Z. Tech. Phys. **12**, 593 (1931); J. Spijkerboer, Thesis, Utrecht, 1917; K. Schwarzschild, Berl. Ber., p. 1183 (1914); L. V. King, Phil. Trans. Roy. Soc. **A212**, 375 (1912); D. B. Judd with collaborators, Harrison, Sweo, Hickson, Eickoff, Shaw, Paffenberger, National Bureau of Standards Research Paper, RP 1026, J. Research Nat. Bur. Stand. **19**, 287 (1937).

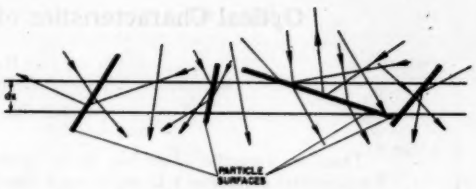

FIG. 1. A number of typical paths of light rays are shown incident on one side of an elementary layer. Reflections and refractions take place at surfaces only.

and

$$T = \frac{1}{\cosh pt + [(s+w/p)]\sinh pt} \tag{4}$$

where $p \equiv [w(2s+w)]^{\frac{1}{2}}$ for brevity, and t is the sheet thickness.

An interesting side line of this attack is that the reflectancy s can be evaluated quite well by measurement of R/T which is related to s by

$$R/T = (s/p)\sinh pt. \tag{5}$$

This was pointed out by Coltman *et al.*, in their paper. Since s is independent of absorption and is inversely proportional to particle size, materials assumed otherwise constant, measuring s should prove a good method of measuring or comparing particle size.

For the cases of very small absorptancy Eqs. (3) and (4) reduce to

$$R = st/(1+st) \quad \text{and} \quad T = 1/(1+st). \tag{6}$$

Now if we let the thickness t be given by $t = CD$, where C is the mean number of particle "diameters" D of sheet thickness, and s be given by $s = h/D$, where h is a proportionality constant, then, from (6)

$$R = Ch/(1+Ch) \quad \text{and} \quad T = 1/(1+Ch). \tag{7}$$

Thus R and T are dependent in this case only on the mean thickness expressed in particle "diameters," C, and on a constant of the materials involved through h. These equations are useful for thin layers where the absorption is small, for example, in the screens of ordinary cathode ray tubes.

G. M. Dreosti (Thesis, Utrecht, 1930) concluded from some observations that the reflectancy was apparently influenced by the addition of a non-scattering absorbing dye to the fluid between particles. The correctness of this conclusion seems highly doubtful as the reflection at a boundary is affected by absorption only if the absorptancy is tremendous. Such a very large absorptancy will, however, have a greater than expected effect on the reflectance of a layer as the outer surface will probably be relatively poor in scattering particles.

But, due to high absorption, this outer surface will prevent the light from penetrating into the more highly scattering part of the layer, and thus might lead one to the conclusion that the reflectancy was reduced. Actually, of course, the reflectancy measured in this case would be of material poor in scattering particles, not of the average material of the layer. Thus, contrary to the conclusion of Hamaker, who quoted Dreosti's results, there does not seem to be any reason for believing that the reflectancy and absorptancy are closely interrelated. This lack of dependence was experimentally found in another case by Judd, who with Paffenberger reports no change in reflectancy when nonscattering black pigment was added to white cement.

JOURNAL OF THE OPTICAL SOCIETY OF AMERICA VOLUME 39, NUMBER 7 JULY, 1949

The Resolving Power of a Coated Objective

HAROLD OSTERBERG AND J. ERNEST WILKINS, JR.
American Optical Company, Scientific Instrument Division, Buffalo 15, New York

(Received April 25, 1949)

A theoretical method is described for reducing the diameter of the central bright disk in the diffraction pattern produced by an objective from an unresolved pinhole as object. On the basis of the Airy criterion the limit of resolution is therefore improved. The method offers a systematic approach for discovering how to coat the exit pupil of the objective with light absorbing and refracting materials so as to reduce the diameter of the central bright disk and yet obtain favorable energy distribution in the diffraction rings. The method selects that family of diffraction patterns whose amplitude and phase distribution can be expressed as a series of Sonine Diffraction Integrals. The coefficients of this series automatically determine both the characteristics of the diffraction pattern and of the corresponding coating which must be applied to the exit pupil. The numerical results obtained for a simple series involving Bessel Functions of the first and second orders are included. In this case the radius of the bright disk is 77 percent of that of the usual Airy disk when the energy density at the diffraction head is 21 percent of that of the classical Airy disk. The radius of the central bright disk can be reduced still further at the expense of serious reduction of the energy density at the diffraction head and a corresponding increase in the energy content of the diffraction rings.

I. INTRODUCTION

LUNEBERG[1] has pointed out one manner in which the resolving power of an objective for two particles can be increased by applying a coating to its exit pupil in such a way as to reduce the diameter of the central bright disk in the diffraction pattern produced by the objective from an unresolved, illuminated pinhole as object. This result is based upon the assumption that the Airy criterion for the limit of resolution remains valid even when the relative energy content of the diffraction rings has been increased.

The problem is to discover how to coat the exit pupil so as to obtain a diffraction pattern having diffraction rings with low and favorably distributed energy density. This problem can be attacked in many ways. The following method applies to coatings which alter both the amplitude and phase distribution over the exit pupil of the objective and includes that family of diffraction patterns which can be expressed as a series of what we shall call Sonine Integrals. To each series of Sonine Integrals there corresponds a unique and simply determined coating function which describes the amplitude and phase transmission of the absorbing and refracting materials with which the exit pupil is coated. Objectives which have been coated in this manner will be called Sonine type objectives. The series of Sonine Integrals can be expressed if desired as a series of Lambda functions which have been discussed by G. Lansraux.[2] The analysis has many points of contact with that presented by Lansraux but the purpose and points of view are different.

The amplitude and phase distribution $U(x, y)$ in the X, Y plane which is conjugate to the object plane containing an unresolved pinhole on the optical axis, as indicated in Fig. 1, is given[3] by

$$U(x, y)=\int_{-\infty}^{\infty}\int_{-\infty}^{\infty} P(p, q)\exp[2\pi i(px+qy)]dpdq. \quad (1)$$

Here the variables of integration are the optical direction cosines p, q in the image space of the axial bundle traced (see Fig. 1) from the pinhole. The complex pupil function $P(p, q)$ includes the distribution of amplitude and phase over the spherical wave converging upon the point $x=y=0$ and is required to vanish when

$$p^2+q^2>n^2\sin^2\vartheta_m=\sin^2\vartheta_m\equiv\rho_m^2,$$

where ρ_m is the maximum numerical aperture of the objective in the image space. The pupil function $P(p, q)$

[1] R. K. Luneberg, *Mathematical Theory of Optics* (Brown University Press, Providence, 1944), pp. 391–395.

[2] G. Lansraux, Revue D'Optique **26**, 24–45 (1947).

[3] R. K. Luneberg, *Mathematical Theory of Optics* (Brown University Press, Providence, 1944), p. 386, Eq. (50.11).

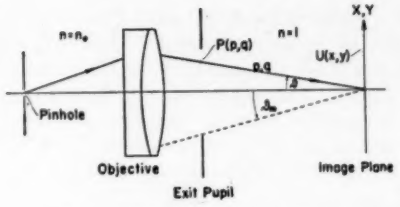

FIG. 1. Optical system and notation.

may be written as the product

$$P(p, q)=c(p, q)\psi(p, q) \tag{2}$$

of a function $c(p, q)$, called the coating function, which determines the change in the amplitude and phase transmission of the exit pupil when the absorbing and refracting coating is applied, and a function $\psi(p, q)$ which is equal to $P(p, q)$ in the absence of an applied coating, i.e., when $c(p, q)=1$. The function $\psi(p, q)$ will be discussed in greater detail in the next section. It includes effects due to spherical aberration, to the weakening of the transmitted axial bundle by reflection and absorption losses, to alteration of the amplitude distribution of the axial bundle by refraction and to the amplitude variations over the incident axial bundle. In general, $|\psi(p, q)|\neq 1$. The function $\psi(p, q)$ will be regarded as known from the properties of the uncoated system. When $P(p, q)$ has been determined, the coating function $c(p, q)$ is calculated from Eq. (2). The coordinates x, y in Eq. (1) are distances measured in terms of wavelengths of the incident light.

If the system has axial symmetry, Eq. (1) may be written as

$$U(r)=2\pi\int_0^{\rho_m} P(\rho)J_0(2\pi r\rho)\rho d\rho, \tag{3}$$

in which $P(\rho)=c(\rho)\psi(\rho)$, ρ is the zonal numerical aperture in the image space, $r=(x^2+y^2)^{\frac{1}{2}}$ is the distance from the optical axis in the image plane measured in wave-lengths of the incident light and J_0 is the Bessel function of the first kind and order zero.

II. THE FUNCTION $\psi(\rho)$

Let unit spheres be drawn about the axial points O_0 and O in the object and image space of the objective, respectively, as in Fig. 2. The unit sphere about the point O_0 is regarded as the incident wave front of reference having the amplitude A_0 which is in general a function of the polar angle ϑ_0 and the azimuthal angle ϕ_0. The unit sphere about the point O is considered to be the locus of the corresponding spherical wave converging upon O. The problem is to find the amplitude and phase relations between the wave front chosen as reference in the object space and the spherical wave converging upon point O. It will be supposed at first that the objective has no spherical aberration. The spherical wave converging upon O is then a wave front. It will also be supposed at first that the amplitude transmission of the objective is unity and that the exit pupil is uncoated. Let A_1 denote the amplitude over the spherical wave front converging upon O. Then according to Luneberg[4]

$$A_1=A_0(n_0/n)^{\frac{1}{2}}(d\sigma_0/d\sigma)^{\frac{1}{2}}, \tag{4.1}$$

in which $d\sigma_0$ and $d\sigma$ are the corresponding areas upon the two wave fronts as in Fig. 2. Furthermore,

$$\begin{aligned} d\sigma_0&=\sin\vartheta_0 d\vartheta_0 d\phi_0;\\ d\sigma&=\sin\vartheta d\vartheta d\phi; \end{aligned} \tag{4.2}$$

with $d\phi_0=d\phi$. It will be assumed that the objective satisfies the Abbe sine condition so that

$$\begin{aligned} nM\sin\vartheta&=n_0\sin\vartheta_0,\\ nM\rho&=n_0\rho_0. \end{aligned} \tag{4.3}$$

It follows from Eqs. (4.1), (4.2), and (4.3) that

$$\begin{aligned} A_1&=(n/n_0)^{\frac{1}{2}}A_0M(\cos\vartheta/\cos\vartheta_0)^{\frac{1}{2}},\\ A_1(\rho)&=(n/n_0)^{\frac{1}{2}}MA_0(\rho_0)k(\rho); \end{aligned} \tag{5}$$

$$k(\rho)\equiv(1-\rho^2)^{\frac{1}{2}}/[1-(nM\rho/n_0)^2]^{\frac{1}{2}}. \tag{6}$$

If spherical aberration is present, one may define a function $W(\rho)$ which describes the corresponding phase variation over the spherical wave converging upon O. One may determine the amplitude transmission function $T(\rho)$ of the objective for the axial bundle of rays by triangulating this axial bundle and computing the losses due to Fresnel reflection and to absorption in the lenses. The amplitude and phase introduced by coating the exit pupil has been defined as $c(\rho)$. Let $A(\rho)$ be a complex number which specifies the amplitude and phase distribution over the spherical wave converging upon O. Then

$$A(\rho)=A_1(\rho)T(\rho)c(\rho)\exp[2\pi iW(\rho)]. \tag{7}$$

From Eqs. (5), (6), and (7)

$$A(\rho)=M(n/n_0)^{\frac{1}{2}}A_0(nM\rho/n_0)k(\rho)T(\rho)c(\rho)\times\exp[2\pi iW(\rho)]. \tag{8}$$

The relation between the pupil function $P(\rho)$ and the amplitude and phase variation $A(\rho)$ over the spherical wave converging upon O is given[5] by

$$P(\rho)=A(\rho)/(1-\rho^2)^{\frac{1}{2}}. \tag{9}$$

In summary, from Eqs. (2), (9), and (8)

$$\psi(\rho)=M(n/n_0)^{\frac{1}{2}}A_0(nM\rho/n_0)k(\rho)T(\rho)\times\exp[2\pi iW(\rho)]/(1-\rho^2)^{\frac{1}{2}}, \tag{10}$$

[4] R. K. Luneberg, *Mathematical Theory of Optics* (Brown University Press, Providence, 1944), p. 51, Eq. (12.28).

[5] R. K. Luneberg, *Mathematical Theory of Optics* (Brown University Press, Providence, 1944), pp. 373 and 375, Eqs. (47.58) and (48.33). When the wave front is spherical or very nearly spherical and when the index of the image space is unity $(n_1^2|LN-M^2|)=(1-\sin^2\vartheta)^{-\frac{1}{2}}=(1-\rho^2)^{-\frac{1}{2}}$. Luneberg's quantity $\phi\exp[ikW]$ is proportional to $A(\rho)$ of this paper. The factors of proportionality are constants which may be set equal to unity without essential loss of generality.

with $k(\rho)$ defined by Eq. (6). If the incident light is unpolarized and if the amplitude variation over the incident wave front has not been distorted by the presence of non-uniform filters or by other lenses,

$$A_0(nM\rho/n_0)=\text{constant}=A_0. \tag{10.1}$$

If the maximum values of ϑ or ϑ_0 in the axial cone do not exceed 40° and if absorption in the objective is negligible, approximately

$$T(\rho)=\text{constant}=T, \tag{10.2}$$

where T is the paraxial amplitude transmission of the objective. Constant factors which appear in Eq. (10) are not of direct importance in the present problem and may therefore be set equal to unity. For example, if the physical conditions leading to Eqs. (10.1) and (10.2) are satisfied, it is sufficient to take

$$\psi(\rho)=k(\rho)\exp[2\pi iW(\rho)]/(1-\rho^2)^{\frac{1}{4}}, \tag{10.3}$$

with $M(n/n_0)^{\frac{1}{2}}A_0T=1$. If, in addition, the objective is free from spherical aberration,

$$\psi(\rho)=k(\rho)/(1-\rho^2)^{\frac{1}{4}}$$
$$=1/(1-\rho^2)^{\frac{1}{4}}[1-(nM\rho/n_0)^2]^{\frac{1}{4}}. \tag{10.4}$$

This equation applies therefore to aberration free objectives of low numerical aperture.

It is of practical interest to note that even with aberration free objectives of low numerical aperture $P(\rho)=1$ only when the exit pupil is coated such that

$$c(\rho)=(1-\rho^2)^{\frac{1}{4}}[1-(nM\rho/n_0)^2]^{\frac{1}{4}}. \tag{10.5}$$

This means that aberration free objectives of low numerical aperture will not be of the Airy type, that is, will not produce the classical diffraction pattern whose energy distribution is proportional to $[2J_1(ar)/ar]^2$ unless the exit pupil is coated with absorbing materials in accordance with Eq. (10.5). If the exit pupil is uncoated, the amplitudes of the outer zones of the wave front converging upon the axial point O, Fig. 2, are too large with objectives of low numerical aperture. With objectives of sufficiently high numerical aperture, however, there may exist a $\rho=\rho_s$ such that $T(\rho)<[k(\rho)/(1-\rho^2)^{\frac{1}{4}}]^{-1}$ when $\rho>\rho_s$. For such objectives the amplitudes of the outer zones of the wave front converging upon O are too small. With telescope objectives $\psi(\rho)$ is more nearly equal to unity than with microscope objectives. Consequently, the aberration free telescope objective should produce diffraction patterns which approach the classical Airy type pattern more closely than is the case with uncoated microscope objectives.

When A_0 and T assume their maximum value at $\rho=0$, it is convenient to normalize $\psi(\rho)$ by dividing $\psi(\rho)$ as given in Eq. (10) by the value of the product $M(n/n_0)^{\frac{1}{2}}A_0(nM\rho/n_0)T(\rho)$ at the paraxial point $\rho=0$. This normalized form of $\psi(\rho)$ may then be used in the usual equation

$$P(\rho)=c(\rho)\psi(\rho). \tag{11}$$

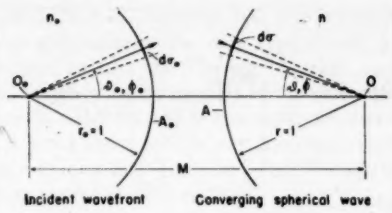

FIG. 2. The incident wave front and the converging spherical wave.

From the definition of the coating function it follows that for physical reasons

$$|c(\rho)|\leqq 1, \quad 0\leqq\rho\leqq\rho_m. \tag{12}$$

If therefore $P(\rho)$ is determined so as to obtain a desired distribution $U(r)$ as calculated from Eq. (3), the calculated distribution $U(r)$ will have physical significance only when $P(\rho)$ is so chosen that both Eqs. (11) and (12) are satisfied.

III. SONINE DIFFRACTION INTEGRALS

It will now be shown that when the pupil function $P(\rho)$ is suitably chosen, $U(r)$ is expressible as a series of Sonine Integrals. Sonine's integral formula[6] is the following:

$$J_{\mu+\nu+1}(z)=\frac{z^{\nu+1}}{2^\nu\Gamma(\nu+1)}\int_0^{\pi/2}J_\mu(z\sin\alpha)$$
$$\times\sin^{\mu+1}\alpha\cos^{2\nu+1}\alpha d\alpha. \tag{13}$$

This equation is an identity connecting Bessel functions of different order and the gamma-function which was proved by Sonine in 1880 and is valid provided that the real parts of μ and ν are greater than -1. Since Eq. (3) involved a Bessel function of order zero under the integral sign, we shall be interested in Eq. (13) only when $\mu=0$. In this case it reduces to

$$\int_0^{\pi/2}J_0(z\sin\alpha)\sin\alpha\cos^{2\nu+1}\alpha d\alpha$$
$$=2^\nu\Gamma(\nu+1)J_{\nu+1}(z)/z^{\nu+1}. \tag{14}$$

If we introduce the notation

$$\rho=\rho_m\sin\alpha; \quad z=2\pi r\rho_m \tag{15}$$

into equation (14), we find that

$$\int_0^{\rho_m}J_0(2\pi r\rho)\left[1-\left(\frac{\rho}{\rho_m}\right)^2\right]^\nu\rho d\rho$$
$$=\rho_m{}^2 2^\nu\Gamma(\nu+1)J_{\nu+1}(2\pi r\rho_m)/(2\pi r\rho_m)^{\nu+1}. \tag{16}$$

[6] G. N. Watson, *Bessel Functions* (Cambridge University Press, London, 1945), p. 373.

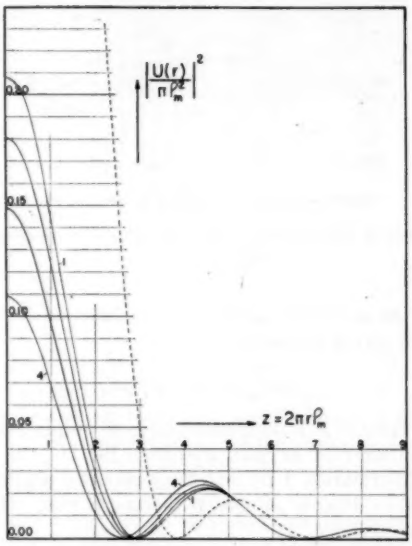

FIG. 3. Comparison of four Sonine type diffraction curves. The curves 1 to 4, in the order indicated, have been drawn respectively for values of r_0 such that $2\pi r_0\rho_m=2.95$, 2.87, 2.76, and 2.59. The broken curve is a portion of the diffraction curve for the Airy type objective.

When the integrands of Eqs. (3) and (16) are compared, it is seen that they are identical provided that

$$P(\rho)=[1-(\rho/\rho_m)^2]^\nu, \tag{17}$$

and in this case we see that

$$U(r)=\pi\rho_m{}^2 2^{\nu+1}\Gamma(\nu+1)J_{\nu+1}(2\pi r\rho_m)/(2\pi r\rho_m)^{\nu+1}. \tag{18}$$

In other words, whenever the pupil function $P(\rho)$ is described by Eq. (17), the corresponding amplitude and phase distribution in the image plane is described by what we shall call the Sonine diffraction integral of Eq. (18).

IV. IMPROVEMENT OF RESOLVING POWER

If $P(\rho)$ is constant, ν must equal zero in Eq. (17). In this case $U(r)$ is seen from Eq. (18) to be proportional to $J_1(z)/z$ in which $z=2\pi r\rho_m$, and this is recognized as the usual solution for the Airy type objective. For other values of ν, $U(r)$ is proportional to $J_{\nu+1}(z)/z^{\nu+1}$. Now it is known[7] that the smallest positive zero of $J_{\nu+1}(z)$ increases as ν increases. This means that the Sonine diffraction integral (18) of the lowest order $\nu+1$ should exhibit the smallest diameter of central bright disk in the diffraction pattern and hence the highest resolution on the basis of the Airy criterion. Sonine's integral formula is valid so long as $\nu>-1$, but $P(\rho)$ in Eq. (17) becomes infinite at the point $\rho=\rho_m$ when $\nu<0$. If it is required that $P(\rho)$ be finite everywhere, it follows that $\nu=0$ is the smallest permissible value of ν and that correspondingly, $J_1(z)/z$ will give the highest resolution when the exit pupil is coated so that $U(r)$ is given by a *single* Sonine diffraction integral. Stated in another way, the conclusion is that the application of Sonine diffraction integrals *singly* does not offer a means of increasing resolution beyond that already given by the Airy type objective.

It is possible, however, to increase this resolution by coating the exit pupil so that $U(r)$ is represented as a *series* of Sonine diffraction integrals. Let the exit pupil be coated so that

$$P(\rho)=\sum_\nu a_\nu[1-(\rho/\rho_m)^2]^\nu. \tag{19}$$

Then it is clear that

$$U(r)=\pi\rho_m{}^2\sum_\nu 2^{\nu+1}\times\Gamma(\nu+1)a_\nu J_{\nu+1}(2\pi r\rho_m)/(2\pi r\rho_m)^{\nu+1}. \tag{20}$$

When the constants a_ν have been assigned, both $P(\rho)$ and $U(r)$ are automatically determined. In Eqs. (19) and (20) the index ν is not restricted to integral values but may range over any finite or denumerably infinite set of non-negative real numbers.[8] By a proper choice of the coefficients a_ν, $U(r)$ can be made to vanish at any previously assigned value of r and, in particular, at a value of r less than that defining the Airy limit of resolution.

V. NUMERICAL RESULTS

In order to illustrate the theory we shall consider the simplest non-trivial example of a series (20), namely one which involves only two terms and we shall suppose that those terms involve Bessel functions of the first and second orders. It follows that

$$P(\rho)=a_0+a_1[1-(\rho/\rho_m)^2]; \tag{21}$$

$$U(r)=\pi\rho_m{}^2[2a_0J_1(z)/z+4a_1J_2(z)/z^2]; \tag{22}$$

where $z=2\pi r\rho_m$.

If we require that the limit of resolution is r_0, then $U(r_0)=0$, whence we see from Eq. (22) that

$$a_1=-a_0\pi\rho_m r_0 J_1(2\pi r_0\rho_m)/J_2(2\pi r_0\rho_m). \tag{23}$$

The coefficient a_0 is to be chosen as large as possible so that if

$$P(\rho)=a_0[1-\pi\rho_m r_0(1-\rho^2/\rho_m{}^2)J_1(2\pi r_0\rho_m)/J_2(2\pi r_0\rho_m)], \tag{24}$$

then,

$$|P(\rho)|\leqq|\psi(\rho)|. \tag{25}$$

For the Airy type objective which has $\psi(\rho)=1$, it is sufficient to choose $a_0=1$. Moreover, we can always normalize the function $\psi(\rho)$ so that we may choose

[7] G. N. Watson, *Bessel Functions* (Cambridge University Press, London, 1945), p. 508.

[8] In fact, if one were willing to introduce Stieltjes integrals, one could permit ν to be a continuous variable.

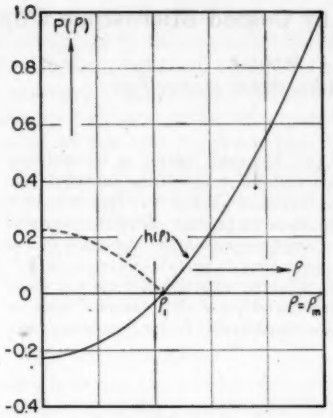

FIG. 4. Plot of the pupil function $P(\rho)$ for the case in which $2\pi r_0\rho_m=2.76$.

$a_0=1$ and this normalization does not affect the limit of resolution r_0 since $\psi(\rho)\neq 0$.

In this manner for each value of r_0 one obtains a uniquely determined pupil function $P(\rho)$ and an amplitude function $U(r)$ which vanishes at $r=r_0$. In the graph of Fig. 3 is plotted the normalized energy density $|U(r)/\pi\rho_m^2|^2$ as ordinate against the abscissa $z=2\pi r\rho_m$ for four different choices of r_0. The normalization factor is so chosen that the broken comparison curve, which corresponds to the case $P(\rho)\equiv 1$, has the ordinate unity when $r=0$. This comparison curve has its first zero at the usual Airy limit for which $z=3.831706$.

The family of four curves has been plotted for values of r_0 for which $2\pi r_0\rho_m$ falls between 2.59 and 2.95. As the radius r_0 of the central bright disk is reduced, the energy at the diffraction head $r=0$ falls rapidly while the energy content of the diffraction rings increases. This trend is well known from more general considerations. It will be noted that the successive diffraction rings in this particular family of diffraction patterns decreases in an orderly manner. Beyond $z=5$ the curves are indistinguishable.

In curve No. 1 the energy at the diffraction head is about 21 percent of that of the Airy type objective. The radius of the central bright disk is reduced to 77 percent of that of the Airy type objective. If the Airy criterion for the limit of resolution remains valid, this represents a significant gain in resolution. Objectives which are coated in this manner are worth further theoretical and experimental investigation. An as yet unpublished theoretical study of the resolution by such objectives of two microscopical particles against a bright field has been completed by H. Osterberg and Franklyn C. Wissler.

A plot of the pupil function $P(\rho)$ is given in Fig. 4 corresponding to the third diffraction curve of Fig. 3 for which $2\pi r_0\rho_m=2.76$. Suppose that a given objective is known to approximate the Airy type closely and that it is desired to find the coating function $c(\rho)$ of the material which must be applied to the exit pupil of the objective in order to realize the third diffraction curve of Fig. 3. Since the objective is of Airy type, $c(\rho)=P(\rho)$. With $a_0=1$, a_1 is now equal to -1.229 from Eq. (23). Therefore from Eq. (21) or (24)

$$c(\rho)=-0.229+1.229(\rho/\rho_m)^2\equiv h(\rho)e^{-i\delta(\rho)}, \quad (26)$$

in which $h(\rho)$ and $\delta(\rho)$ are respectively the amplitude transmission and the change in the optical path which must be introduced by the applied coating materials. Because $h(\rho)=|P(\rho)|$, the required amplitude transmission follows the broken curve of Fig. 4 from $\rho=0$ to $\rho=\rho_1$ and then the solid curve from ρ_1 to ρ_m. The applied coating is opaque at $\rho=\rho_1$. Since $P(\rho)$ is real, $\delta(\rho)=0$ or π. The change in optical path $\delta(\rho)$ is π or one-half wave-length in the interval $0\leqq\rho\leqq\rho_1$ and is zero in the interval $\rho_1\leqq\rho\leqq\rho_m$. This means that the exit pupil will be coated by a combination of absorbing and refracting materials whose composite amplitude transmission obeys the curve $h(\rho)$ and whose composite optical paths are distributed so as to change the optical path of the central zone extending from $\rho=0$ to $\rho=\rho_1$ by one-half wave-length with respect to the outer zone from ρ_1 to ρ_m. It is actually immaterial which of the two zones has the greater optical path so long as their optical path difference is one-half wave-length.

VI. CONCLUSIONS

It is clear that this method of using a series of Sonine diffraction integrals can lead to diffraction patterns having smaller central bright disks than is the case for uncoated objectives. By employing additional terms in the series, one can expect to reduce the radius of the central bright disk even further and at the same time control other important features of the diffraction pattern such as the maximum central energy density $|U(0)|^2$ and the fraction of the total transmitted energy which lies in the central bright disk. It is not possible to go far in this direction, however, because an arbitrary function $U(r)$ cannot be expanded into a series of the type (20). One necessary condition on $U(r)$ is that the integral

$$2\pi\int_0^\infty U(r)J_0(2\pi r\rho)rdr,$$

(which is equal to $P(\rho)$ when $\rho<\rho_m$ by virtue of the Hankel formula)[9] must vanish when $\rho>\rho_m$.

[9] R. Courant and D. Hilbert, *Methoden der Mathematischen Physik* (Verlag. Julius Springer, Berlin, 1931), Vol. I, p. 293.

The Resolution of Two Particles in a Bright Field by Coated Microscope Objectives

HAROLD OSTERBERG AND FRANKLYN C. WISSLER
American Optical Company, Scientific Instrument Division, Buffalo 15, New York

(Received April 25, 1949)

A theory is presented for determining the diffraction image of two, identical, opaque or transmitting, uniform, individually unresolved particles of finite area located in a uniform, transmitting surround. Numerical calculations are included for the classical Airy type objective, for center-blocked Airy type objectives and for simplified Sonine type objectives which have been coated so as to produce diffraction patterns having central disks of reduced diameter. It is shown that marked improvement in the resolution of two particles can be expected by such coated objectives. The resolving power for two particles increases rapidly with the area of the particles and has unexpectedly steep dependence upon the relative amplitude and phase transmission of particle and surround. The theory, subject to experimental verification, forms a basis for explaining why a microscope as used with transmitted light can resolve considerably better than is indicated by the Airy limit.

I. INTRODUCTION

WHEN the amplitude and phase transmission of the exit pupil of a microscope objective is suitably varied by coating the exit pupil with refracting and absorbing materials, it is possible to reduce the diameter of the Airy disk. Reduction of the diameter of the Airy disk below that of the central maximum in the classical, Airy type, diffraction image is necessarily accompanied by a marked drop in the energy density at the diffraction head and by a corresponding rise in the energy density of the diffraction rings. Therefore, the neighborhood of the geometrical image of two particles will be overlapped by an increasing amount of energy from the diffraction rings resulting from object points in the bright field as the object slide is viewed by objectives which have the same numerical aperture but which produce Airy disks of reduced diameter. The following theory will include the effects of the overlapping, diffracted energy from object points located in the bright field upon the image of two tranmitting or opaque particles. Each of the particles is assumed to be unresolvable and to have the area A. It is assumed for simplicity that the particles are identical, non-overlapping and have uniform phase and amplitude transmissions. The theory is readily extended to dissimilar, overlapping, unresolved particles. The total energy density in the image plane will be calculated upon the supposition that the source of light is uniform and is large enough to fill the exit pupil of the objective. The objectives may have numerical apertures ranging from low to intermediate values such as 0.7.

The X direction is chosen in the image plane along the line connecting the centers of the geometrical images of the two particles. The origin is located midway between these centers so that the centers are located at $x=\pm Ml$, where M is the magnification of the objective. The total energy density G is a function of both x and y. Consistent with the usual practice, the analysis will be confined to the energy distribution $G(x,0)\equiv G(x)$. The Airy limit of resolution is not a suitable limit for purposes of the following discussion. A more useful and *physical* limit of resolution is defined[1] as the separation $2l$ or $2Ml$ for which

$$\frac{d^2}{dx^2}G(x)=0 \qquad \text{when } x=0. \tag{1}$$

This physical limit is a function of the area and of the amplitude and phase transmission of the particles. It will be shown to decrease with the diameter of the Airy disk when the objective is coated for obtaining the simplest Sonine[2] type diffraction pattern or when the central zone of the objective is made opaque as in the classical method of the ink spot.

II. THE AMPLITUDE AND PHASE EQUATION

The conjugate object and image planes with magnification M are denoted, respectively, by X_0, Y_0 and X, Y. The object plane consists as in Fig. 1 of two, like, uniform particles of area A located at distances $x_0=\pm l$ from the optical axis and of a surround whose amplitude and phase transmission is chosen as reference and hence as the complex number unity. It is supposed that the surround is never opaque. The amplitude and phase transmission of the particles is represented by the complex number

$$f_0=ge^{-i\Delta}, \tag{2}$$

in which g is the ratio of the amplitude transmission of the particles to the amplitude transmission of the surround and in which Δ is the difference between the phase transmissions of the particles and surround considered as positive when the optical path of the particles exceeds that of the surround.

It is supposed that the microscope is adjusted for Köhler illumination and that the condenser diaphragm is adjacent to the first focal plane of the substage condenser. The object slide is then illuminated by substantially plane wave fronts which originate from each point in the condenser diaphragm. The normals to these wave

[1] Ramsay, Cleveland, and Koppius, J. Opt. Soc. Am. **31**, 28 (1941).
[2] Osterberg and Wilkins, J. Opt. Soc. Am. **39**, 553 (1949).

fronts have the optical direction cosines p_0, q_0. If the exit pupil is conjugate to the condenser diaphragm, an image of the source of light will be located at the exit pupil. It is supposed that the exit pupil is filled by the source. The amplitude and phase transmissions of the coating applied to the exit pupil are included in the pupil function $P(p, q)$ in which p, q are the optical direction cosines of the axial bundle in the image space. This pupil function includes the phase variation due to spherical aberration and also the amplitude variation on the spherical wave converging upon the axial point $x=y=0$. ϑ_m is the maximum angular aperture of the objective in its image space. The objective is assumed to obey the Abbe sine condition.

The relation between the condenser diaphragm and the plate for supporting the coating material at the exit pupil is similar to the relation between the condenser diaphragm and the diffraction plate in the phase microscope. Only the shape of the opening in the condenser diaphragm and the distribution of the coating materials upon the exit pupil are different. The general equations which appear in the theory of phase microscopy apply therefore to the amplitude and phase distribution $F_0(x, y, p_0, q_0)$ produced over the image plane from the incidence upon the object plane of a single wave front whose normal has the optical direction cosines p_0, q_0. Thus,[3]

$$F_0(x, y, p_0, q_0)=\int_{-\infty}^{\infty}\int_{-\infty}^{\infty} f(x_0, y_0, p_0, q_0) \times\exp[2\pi i(p_0x_0+q_0y_0)] \times U(x-Mx_0, y-My_0)dx_0dy_0, \quad (3)$$

in which $f(x_0, y_0, p_0, q_0)$ is the object function which specifies the modification of the amplitude and phase transmission of the object plane due to the presence of the object specimen. The object function is considered to vanish beyond the field of the optical system. $U(x, y)$ is the primary diffraction integral defined by

$$U(x, y)=\int\int P(p, q)\exp[2\pi i(px+qy)]dpdq; \quad (4)$$

$$p^2+q^2\leqq n^2\sin^2\vartheta_m\equiv n^2\rho_m{}^2=\rho_m{}^2. \quad (5)$$

All distances in Eqs. (3) and (4) are measured in wave-lengths.

As applied to the present problem of two particles in a bright field, the object function is taken as unity for all points x_0, y_0 of the surround and as f_0 over the area of the particles. It is natural to divide the function F_0 of Eq. (3) into two parts F_u and F_d which correspond, respectively, to the undeviated and deviated waves which arise from diffraction at the object plane. Thus,

$$F_0(x, y, p_0, q_0)=F_u(x, y, p_0, q_0)+F_d(x, y, p_0, q_0); \quad (6)$$

$$F_u(x, y, p_0, q_0)\equiv\int\int \exp[2\pi i(p_0x_0+q_0y_0)] \times U(x-Mx_0, y-My_0)dx_0dy_0, \quad (7)$$

in which the domain of integration extends over the entire field of view;

$$F_d(x, y, p_0, q_0)\equiv f\int\int \exp[2\pi i(p_0x_0+q_0y_0)] \times U(x-Mx_0, y-My_0)dx_0dy_0, \quad (8)$$

in which the domain of integration extends over the area of the two particles and in which

$$f\equiv f_0-1=g\exp(-i\Delta)-1. \quad (9)$$

The expression for F_u simplifies greatly whenever it can be assumed that the object field extends over a large number of wave-lengths. This assumption is usually satisfied by a microscope so that with negligible error,

$$F_u(x, y, p_0, q_0)=\int_{-\infty}^{\infty}\int_{-\infty}^{\infty}\exp[2\pi i(p_0x_0+q_0y_0)] \times U(x-Mx_0, y-My_0)dx_0dy_0. \quad (10)$$

When U from Eq. (4) is substituted into Eq. (10) and when the integration with respect to dx_0dy_0 is performed, it is found in a direct manner that

$$F_u(x, y, p_0, q_0)=\operatorname*{Limit}_{\substack{x_0=\infty\\ y_0=\infty}}\int\int P(p, q) \times\exp[2\pi i(px+qy)]\frac{\sin 2\pi x_0(p_0-Mp)}{\pi(p_0-Mp)} \times\frac{\sin 2\pi y_0(q_0-Mq)}{\pi(q_0-Mq)}\frac{d(Mp)d(Mq)}{M^2}. \quad (11)$$

When the integrations with respect to $d(Mp)$ and $d(Mq)$ are examined successively in view of the Dirichlet integral[4]

$$\int_{-a}^{a} f(x)\frac{\sin\alpha(x-t)}{\pi(x-t)}dx\to f(t) \text{ as } \alpha\to\infty, \quad (12)$$

it is seen that

$$F_u(x, y, p_0, q_0)=\frac{1}{M^2} \times\exp\left[\frac{2\pi i}{M}(p_0x+q_0y)\right]P\left(\frac{p_0}{M}, \frac{q_0}{M}\right). \quad (13)$$

[3] H. Osterberg, J. Opt. Soc. Am. 38, 686 (1948), Eq. (1).

[4] Churchill, *Fourier Series and Boundary Value Problems*, (McGraw-Hill Book Company, Inc., New York, 1941), p. 69, Eq. (6).

TABLE I. Separations $2L$ in number of Airy units of the two particles at the physical limit of resolution as a function of fk for Airy type objectives.

$-fk$	$2L$
0	0.7767
0.25	0.7610
0.50	0.7339
0.75	0.6780
0.9	0.5903
1.0	0

It has been assumed that each of the two object particles is unresolvable. The centers of the particles are located at $x_0=\pm l$. More specifically, it is assumed that the areas A of the particles are so small that the integral of Eq. (8) may be replaced by the sum

$$F_d(x, y, p_0, q_0)=fA[\exp(2\pi i p_0 l)U(x-Ml, y) + \exp(-2\pi i p_0 l)U(x+Ml, y)]. \quad (14)$$

This simplification of Eq. (8) can be shown to be valid when the effective radius of the particles does not exceed one-half of the Airy limit of resolution.

The amplitude and phase distribution $F_0(x, y, p_0, q_0)$ produced over the image plane by the incidence upon the object plane of a single wave front whose normal has the optical direction cosines p_0, q_0 is therefore given by

$$M^2F_0(x, y, p_0, q_0)=\exp\left[\frac{2\pi i}{M}(p_0x+q_0y)\right]P\left(\frac{p_0}{M}, \frac{q_0}{M}\right) + fM^2A\left[\exp(2\pi i p_0 l)U(x-Ml, y) + \exp(-2\pi i p_0 l)U(x+Ml, y)\right], \quad (15)$$

when the object plane contains two, uniform, unresolved particles of area A in a uniform, transmitting surround and when the particles are located about the points $x_0=\pm l$.

Considerations of the total energy distribution are limited in the following analysis to the line $y=0$. Accordingly,

$$M^2F_0(x, p_0, q_0)\equiv M^2F_0(x, 0, p_0, q_0) =\exp\left(\frac{2\pi i p_0 x}{M}\right)P\left(\frac{p_0}{M}, \frac{q_0}{M}\right) + \frac{fk}{\pi\rho_m{}^2}\left[\exp(2\pi i p_0 l)U(x-Ml) + \exp(-2\pi i p_0 l)U(x+Ml)\right], \quad (16)$$

in which

$$k\equiv\pi M^2\rho_m{}^2A=\pi(\text{N.A.})^2A. \quad (17)$$

The product fk represents the essential physical characteristic of the particles with reference to their effect upon the diffraction image. N.A. denotes the numerical aperture of the objective.

III. THE TOTAL ENERGY DENSITY

The total energy density in the image plane is the sum of the partial energy distributions $|F_0(x, y, p_0, q_0)|^2$ for all effective points in the source of light or, equivalently, for all incident wave fronts. Let $G(x, y)$ denote the total energy density. Then it can be shown[5] that

$$G(x, y)=\int\int\frac{S(p_0, q_0)}{n_0{}^2-p_0{}^2-q_0{}^2} \times|F_0(x, y, p_0, q_0)|^2dp_0dq_0, \quad (18)$$

in which the integration extends over the optical direction cosines p_0, q_0 of the family of rays incident upon the object plane and transmitted by the objective. n_0 is the refractive index in the object space.

It will be supposed that the energy density $S(p_0, q_0)$ of the source is uniform such that

$$S(p_0, q_0)=S=1. \quad (19)$$

If the variables of integration are transformed into their polar form in the image space in accordance with the relations,

$$p_0=n_0M\rho\cos\phi; \quad q_0=n_0M\rho\sin\phi; \quad \rho\equiv\sin\vartheta; \quad (20)$$

and if $F_0(x, 0, p_0, q_0)$ from Eq. (16) is substituted into Eq. (18), it is found that

$$G(x, 0)\equiv G(x)=\frac{1}{M^2}\int_0^{\rho_m}\int_0^{2\pi}|\exp(2\pi i\rho x\cos\phi)P(\rho) + \frac{fk}{\pi\rho_m{}^2}[\exp(2\pi i\rho Ml\cos\phi) \times U(x-Ml)+\exp(-2\pi i\rho Ml\cos\phi) \times U(x+Ml)]|^2\frac{\rho d\phi d\rho}{1-M^2\rho^2}. \quad (21)$$

The choice of limits of integration in Eq. (21) involves the supposition that the exit pupil of the objective is filled by the image of the source. The substitution $P(p_0/M, q_0/M)=P(\rho)$ involves the requirement that the optical system shall have axial symmetry. $\rho_m=\sin\vartheta_m$ where ϑ_m is the maximum angular aperture of the objective with respect to its image space as in Fig. 1.

Equation (21) shows that the essential physical characteristics of the two particles are contained in the product fk, where

$$fk=(ge^{-i\Delta}-1)\pi(\text{N.A.})^2A. \quad (22)$$

[5] H. Osterberg, J. Opt. Soc. Am. 38, 688 (1948), Eq. (19).

The total energy distribution $G(x)$ depends therefore upon the relative amplitude transmission g and the optical path difference Δ of the particles with respect to their surround and upon the unresolved area A of the particles.

The integral of Eq. (21) will be evaluated for the special cases in which fk is real, that is for optical path differences Δ equal to 0 or π. If $\Delta=0$,

$$fk=-(1-g)\pi(\text{N.A.})^2A. \tag{23}$$

If $\Delta=\pi$,

$$fk=-(1+g)\pi(\text{N.A.})^2A. \tag{24}$$

The integral will furthermore be evaluated under the simplifying approximation that the factor $1-M^2\rho^2$ in the denominator may be replaced by unity. Correspondingly, the energy density will be approximated with negligible error for objectives of numerical aperture of 0.25 or less. It is difficult to estimate the errors incurred by this approximation at higher numerical aperture, but it is expected that the degree of approximation will be satisfactory for many purposes when $M\rho_m=$N.A. is as large as 0.7.

In summary, the equations for calculating the total energy density become

$$M^2G(x)=\int_0^{\rho_m}\int_0^{2\pi}\Big|\exp(2\pi i\rho x\cos\phi)P(\rho)+\frac{fk}{\pi\rho_m{}^2}\Big[\exp(2\pi i\rho Ml\cos\phi)\times U(x-Ml)+\exp(-2\pi i\rho Ml\cos\phi)\times U(x+Ml)\Big]\Big|^2\rho d\phi d\rho, \tag{25}$$

with

$$U(r)=2\pi\int_0^{\rho_m}P(\rho)J_0(2\pi r\rho)\rho d\rho. \tag{26}$$

Equation (25) can be solved without approximation for the three pupil functions $P(\rho)$ of the following sections. For definiteness, fk is restricted to the special cases of Eqs. (23) and (24).

IV. THE AIRY TYPE OBJECTIVE

The Airy type objective has the simple pupil function

$$P(\rho)=1,\quad 0\leqq\rho\leqq\rho_m; \tag{27}$$

and produces the amplitude, phase distribution

$$U(r)=2\pi\rho_m{}^2\frac{J_1(Z)}{Z};\quad Z\equiv 2\pi r\rho_m. \tag{28}$$

If r_a denotes the distance from the diffraction head to the first zero of $J_1(Z)$,

$$2\pi\rho_m r_a=3.831706\equiv\beta. \tag{28.1}$$

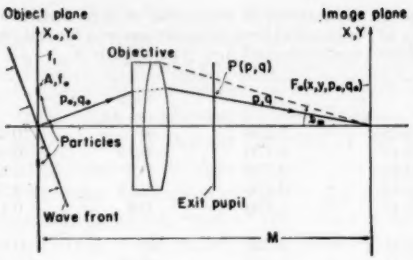

FIG. 1. The optical system and notation.

Let

$$r_a{}^0\equiv r_a/|M|; \tag{28.2}$$

$$L\equiv l/r_a{}^0. \tag{28.3}$$

$r_a{}^0$ or r_a is the Airy limit of resolution as measured in wave-lengths in the object or image space, respectively. $2L$ is the separation of the two particles as measured in Airy units. Corresponding to $r=x\mp Ml$ in Eqs. (28) it is convenient to set

$$Z_1\equiv 2\pi\rho_m(x-Ml)=\beta(x/r_a-L);$$
$$Z_2\equiv 2\pi\rho_m(x+Ml)=\beta(x/r_a+L). \tag{29}$$

Both x/r_a and L are therefore measured in Airy units.

When $U(x-Ml)$ and $U(x+Ml)$ are expressed with the aid of Eqs. (28) and (29) and are substituted into Eq. (25) on the supposition that fk is real, it is found that the total energy density $G(x)$ reduces to the

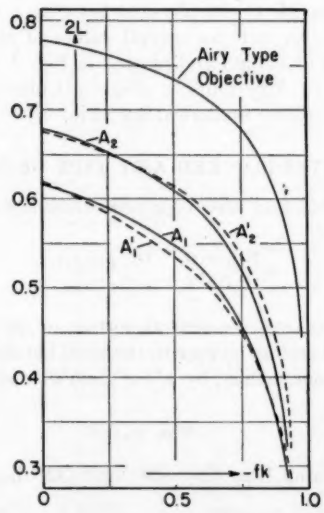

FIG. 2. Separations $2L$ at the physical limit of resolution of two particles. Curves A_1 and A_2 refer to the Sonine type objectives; A_1' and A_2', to the center-blocked Airy type objectives. Subscripts 1 and 2 refer to ratios r_0/r_a of 0.676 and 0.770, respectively.

TABLE II. Separations $2L$ in number of Airy units of the two particles at the physical limit of resolution as a function of fk for two different center-blocked Airy type objectives.

s	r_0/r_a	$-fk$	$2L$
0.6145	0.770	0	0.677
0.6145	0.770	0.25	0.652
0.6145	0.770	0.5	0.615
0.6145	0.770	0.75	0.538
0.6145	0.770	0.9	0.417
0.8551	0.676	0	0.620
0.8551	0.676	0.25	0.580
0.8551	0.676	0.5	0.535
0.8551	0.676	0.75	0.452
0.8551	0.676	0.9	0.355

expression

$$\frac{M^2G(x)}{\pi\rho_m^2}=1+4fk(2+fk)\left[\frac{J_1^2(Z_1)}{Z_1^2}+\frac{J_1^2(Z_2)}{Z_2^2}\right]+16f^2k^2\frac{J_1(2\beta L)}{2\beta L}\frac{J_1(Z_1)}{Z_1}\frac{J_1(Z_2)}{Z_2}. \quad (30)$$

It follows from Eqs. (1) and (30) that the condition for the physical limit of resolution of the two particles by Airy type objectives is equivalent to

$$2(2+fk)J_2^2(\beta L)=\left[2+fk\left(1+\frac{2J_1(2\beta L)}{2\beta L}\right)\right]\times\left[J_1^2(\beta L)+J_2^2(\beta L)-\frac{3J_1(\beta L)}{\beta L}J_2(\beta L)\right]. \quad (31)$$

Separations $2L$ at the physical limit have been calculated from Eq. (31) for several values of fk, and have been listed in Table I and plotted in Fig. 2. Since $2L$ is measured in Airy units, a single calculation includes objectives of any numerical aperture.

V. CENTER-BLOCKED AIRY TYPE OBJECTIVES

Center-blocked Airy type objectives have the pupil function

$$P(\rho)=0, \quad 0\leqq\rho\leqq\rho_1;$$
$$P(\rho)=1, \quad \rho_1\leqq\rho\leqq\rho_m. \quad (32)$$

The coating over the central portion of the exit pupil, Fig. 1, is therefore opaque to the axial bundle of rays in the axial cone defined by $p^2+q^2\leqq\sin^2\vartheta_1\equiv\rho_1^2$.

Let

$$s\equiv\rho_1/\rho_m. \quad (33)$$

It follows from Eqs. (26), (29), and (32) that

$$U(x-Ml)/\pi\rho_m^2\equiv u(Z_1)=2[-s^2J_1(sZ_1)/sZ_1+J_1(Z_1)/Z_1];$$
$$U(x+Ml)/\pi\rho_m^2\equiv u(Z_2)=2[-s^2J_1(sZ_2)/sZ_2+J_1(Z_2)/Z_2]. \quad (34)$$

Equation (25) can be integrated after the substitution of $P(\rho)$ and $U(x\mp Ml)$ from Eqs. (32) and (34) to obtain the total energy density $G(x)$ in the form

$$M^2G(x)/\pi\rho_m^2=1-s^2+fk(2+fk)[u^2(Z_1)+u^2(Z_2)]+4f^2k^2\frac{J_1(2\beta L)}{2\beta L}u(Z_1)u(Z_2). \quad (35)$$

The condition for the physical limit of resolution as determined from Eqs. (1) and (35) becomes

$$\left[2+fk+2fk\frac{J_1(2\beta L)}{2\beta L}\right]\left[-s^2\frac{J_1(s\beta L)}{s\beta L}+\frac{J_1(\beta L)}{\beta L}\right]\times\left[-3s^4\frac{J_2(s\beta L)}{(s\beta L)^2}+s^4\frac{J_1(s\beta L)}{s\beta L}+3\frac{J_2(\beta L)}{(\beta L)^2}-\frac{J_1(\beta L)}{\beta L}\right]=\left[2fk\frac{J_1(2\beta L)}{2\beta L}-(2+fk)\right]\times\left[-s^3\frac{J_2(s\beta L)}{s\beta L}+\frac{J_2(\beta L)}{\beta L}\right]^2. \quad (36)$$

If s is assigned a value in the range $0<s<1$, $U(r)=0$ at a corresponding distance $r=r_0$ from the diffraction head. This value of r_0 falls in the interval $0.6276<r_0/r_a<1$. As s approaches unity, r_0/r_a approaches 0.6276. This means physically that the radius of the Airy disk cannot be reduced below the fraction 0.6276 of its classical value by means of center-blocked objectives. Separations $2L$ at the physical limit of resolution have been computed from Eq. (36) for several values of fk at two fixed values of s and are listed in Table II.

VI. SONINE TYPE OBJECTIVES

The analysis of the diffraction images and physical limit of resolution for two particles viewed against a bright field will be made for the simple Sonine type of objective whose pupil function $P(\rho)$ obeys the law[2]

$$P(\rho)=1+a_1-a_1\rho^2/\rho_m^2; \quad (37)$$

$$-a_1=\frac{\beta}{2}\frac{r_0}{r_a}J_1(\beta r_0/r_a)/J_2(\beta r_0/r_a). \quad (38)$$

With this choice of pupil function, the radius of the Airy disk is reduced to the fraction r_0/r_a of its value for the Airy type objective.

From Eqs. (26), (29), and (37),

$$U(x-Ml)/\pi\rho_m^2 \equiv u(Z_1) = 2J_1(Z_1)/Z_1 + 4a_1 J_2(Z_1)/Z_1^2;$$
$$U(x+Ml)/\pi\rho_m^2 \equiv u(Z_2) = 2J_1(Z_2)/Z_2 + 4a_1 J_2(Z_2)/Z_2^2. \quad (39)$$

Let $P(\rho)$ and $U(x \pm Ml)$ from Eqs. (37) and (39) be introduced into Eq. (25). The result is

$$M^2 G(x)/\pi\rho_m^2 = 1 + a_1 + \frac{a_1^2}{3} + fk(2+fk)[u^2(Z_1)+u^2(Z_2)] + 4f^2k^2 \frac{J_1(2\beta L)}{2\beta L} u(Z_1)u(Z_2). \quad (40)$$

The physical limit of resolution has been calculated from Eqs. (1) and (40) for two values of a_1 from the formulation

$$\psi^2(r)\left[1 - \frac{2fk}{2+fk}\frac{J_1(2r)}{2r}\right] = -\phi(r)\alpha(r)\left[1 + \frac{2fk}{2+fk}\frac{J_1(2r)}{2r}\right]; \quad (41)$$

$$\phi(r) \equiv rJ_1(r) + 2a_1 J_2(r); \quad \psi(r) \equiv rJ_2(r) + 2a_1 J_3(r);$$
$$\alpha(r) \equiv (r + 10a_1/r)J_3(r) - (1+2a_1)J_2(r); \quad r \equiv \beta L.$$

The constants a_1 have been chosen so that the corresponding values of r_0/r_a are the same as in Table II. The resulting values of $2L$ as a function of fk are listed in Table III.

VII. COMPARISON OF THE PHYSICAL LIMITS OF RESOLUTION; INTERPRETATION

Separations $2L$ of the two particles at the physical limit of resolution are plotted in Fig. 2 for comparison of the three types of objectives. The two special cases of the Sonine type objective are represented by the curves A_1 and A_2 for which r_0/r_a are, respectively, 0.676 and 0.770. The two special cases of the center-blocked Airy type objective are represented by the curves A_1' and A_2' for which r_0/r_a are also 0.676 and 0.770, respectively. The ratio r_0/r_a may be considered as the actual radius of the Airy disk produced by a "coated" objective measured with the radius of the classical Airy disk at the given numerical aperture chosen as the unit of length. This length is called the Airy unit. The separations $2L$ are measured in Airy units. fk is given either by Eq. (23) or by Eq. (24). The curves of Fig. 2 apply therefore to two, identical, unresolved particles having optical paths which differ from that of their surround by zero or one-half wave-lengths. The area A and the amplitude transmission g of the particles may vary from one set of particles to another.

In the case of the Airy type objective the separation $2L$ is slightly less than 78 percent of the Airy limit when $fk=0$. This is a previously known property[6] which may be used in explaining why microscope objectives can resolve better than is indicated by the Airy limit. It will be noted from Fig. 2 that in the case of the center-blocked and Sonine type objectives the physical limits at $fk=0$ decrease approximately as the ratio r_0/r_a, that is approximately as the ratio of the radius of the contracted Airy disk to the radius of the classical Airy disk. This observation is interpreted to mean that the relative increase in the energy content of the rings in the diffraction image produced by objectives which have been coated so as to reduce the diameter of the Airy disk has but slight effect upon the physical limit of resolution of two infinitesimal particles. Since the curves of Fig. 2 drop at about the same rate with increasing $|fk|$ and hence with increasing area of the particles, this interpretation applies also to finite but unresolved particles.

The drop in $2L$ with increasing numerical value of fk is large. Consequently, microscope objectives may be expected to show markedly higher resolution for particles of increasing $|fk|$. This resolution is improved in so far as may be judged from Fig. 2 by coating the objective so as to reduce the diameter of the Airy disk. Reference to Eqs. (23) and (24) shows that the two particles should be more readily resolved as their area increases. The dependence of the physical limit of resolution upon the transmission of the particles is more complicated but can be ascertained from Eqs. (23) and (24) and the curves of Fig. 2.

The drop in the physical limits of Fig. 2 depends upon the maximum allowable values $|fk|_m$ of $|fk|$. It is important to distinguish three categories for $|fk|_m$. The first category is that which is consistent with the validity of replacing dx_0dy_0 in Eq. (8) by A as in Eq. (14). Let R denote the effective radius of the particles and let R_m be the maximum value of R for which Eq. (14) is a good approximation to Eq. (8). Since R_m may be taken as

TABLE III. Separations $2L$ in number of Airy units of the two particles at the physical limit of resolution as a function of fk for two different Sonine type objectives.

$-a_1$	r_0/r_a	$-fk$	$2L$
1.0872	0.770	0	0.6785
1.0872	0.770	0.25	0.6509
1.0872	0.770	0.5	0.6081
1.0872	0.770	0.75	0.5230
1.0872	0.770	0.9	0.3758
1.3397	0.676	0	0.6175
1.3397	0.676	0.25	0.5867
1.3397	0.676	0.5	0.5470
1.3397	0.676	0.75	0.4583
1.3397	0.676	0.9	0.3320

[6] R. K. Luneberg, *Mathematical Theory of Optics* (Brown University Press, Providence, 1944), pp. 389–90.

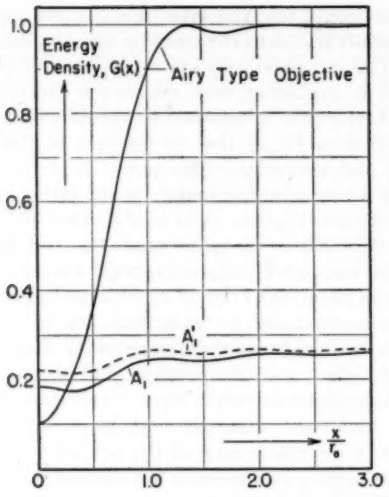

FIG. 3. Diffraction curves for the separation $2L=0.608$ Airy units and for $fk=-0.5$. Curves A_1 and A_1' belong to Sonine type and center-blocked objectives, respectively, whose ratio $r_0/r_a=0.676$.

large as one-half of the Airy limit,

$$R_m=0.61/2\text{N.A.} \tag{42}$$

The maximum allowable area A_m of the particles is correspondingly

$$A_m=\pi R_m^2=0.093\pi/(\text{N.A.})^2. \tag{43}$$

In Eqs. (23) and (24) let g' denote $-(1-g)$ or $-(1+g)$ according as $\Delta=0$ or π. Then, from Eqs. (23), (24), and (43),

$$|fk|_m=0.093\pi^2|g'|$$

or, approximately,

$$|fk|_m=|g'|. \tag{44}$$

Since $|g'|>1$ for particles whose optical path exceeds that of the surround by one-half wave-lengths, values $|fk|_m$ of the first category can readily exceed unity. Equations (14) and (25) contain the restriction that the particles shall not overlap. This restriction reduces $|fk|_m$. Let R_c denote the radii of two like particles which are in contact. Then,

$$R_c=Lr_a/|M|,$$

and

$$A_c=\pi L^2r_a^2/M^2=\pi L^2\beta^2/4\pi^2(\text{N.A.})^2. \tag{45}$$

From Eqs. (23), (24), and (45)

$$|fk|_{nom}=L^2\beta^2|g'|/4,$$

or, approximately,

$$|fk|_{nom}=|g'|(2L)^2, \tag{46}$$

in which the subscripts m, n, and o refer to the maximum allowable value of $|fk|$ in the second category for non-overlapping particles. Since $2L<1$ in Fig. 2, $|fk|_{nom}<|fk|_m$. As an example, the point $2L=0.5$, $-fk=0.9$ on the curve for the Airy type objective can be reached only with particles for which $|g'|=3.6$. Whereas such particles are possible, they are not common in microscopy. It can be expected for reasons beyond the scope of the present paper that the results predicted by Eq. (25) apply with at least fair approximation to the case of overlapping particles until the particles overlap to such an extent that the circumference of one particle passes through the center of the second particle. The extension of the equations to such particles constitutes an extrapolation which will be denoted by the subscript e. It follows that since $R_e=2R_c$,

$$|fk|_{em}=4|fk|_{nom}=4|g'|(2L)^2, \tag{47}$$

where $|fk|_{em}$ denotes the maximum value of $|fk|$ in the third category. The point $2L=0.5$, $-fk=0.9$ on the curve for the Airy type objective can be reached with particles for which $|g'|=0.9$. Particles for which $|g'|=1$ are not uncommon. For example, $|g'|=1$ with opaque particles. The range of fk in Fig. 2 can therefore be realized with observable particles.

It will be noted from Table I that with Airy type objectives the physical limit $2L$ approaches zero as fk approaches -1. Particles for which $fk\rightarrow-1$ as $2L\rightarrow0$ will have the optical path difference $\Delta=\pi$ and an increasingly great g value. This means that the surround becomes practically opaque. One can expect, accordingly, that transparent particles having an optical path difference of one-half wave-length with respect to an almost opaque surround will belong to the class of most

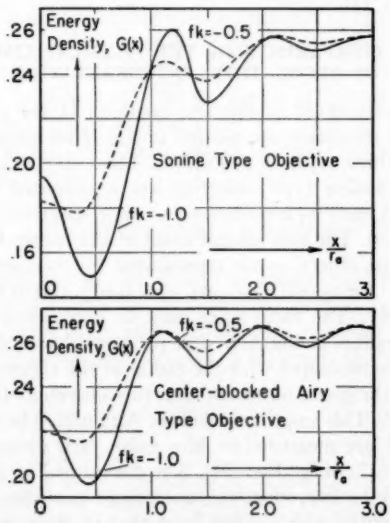

FIG. 4. Comparison of diffraction curves drawn for the two fk values of -0.5 and -1.0. The separation $2L$ is 0.608 and the ratio $r_0/r_a=0.676$ as with the Sonine type and center-blocked objectives of Fig. 3.

readily resolved particles. Small particles of this character are uncommon.

With particles whose optical path difference $\Delta=0$, $fk>0$ when $g>1$. The physical limits for such particles are not included in Fig. 2. The scope of this paper is limited to particles for which $fk<0$. An investigation by Dr. J. Ernest Wilkins, Jr., has shown that the physical limits become higher than 78 percent of the Airy limit when $fk>0$. This phenomenon which occurs with particles whose optical path difference $\Delta=0$ and whose amplitude transmission exceeds that of the surround will be described elsewhere.

At the selected ratios r_0/r_a of Fig. 2, the curves of the physical limits for center-blocked and Sonine type objectives do not differ significantly.

The possible theoretical variation of the physical limit of resolution in the direction of better resolution is impressive. It is emphasized, however, that the physical limit of resolution can only be approached whereas the Airy limit of resolution can be realized.

VIII. COMPARISON OF THE DIFFRACTION IMAGES

The diffraction curves of Figs. 3, 4, 5, and 6 represent the total energy densities computed from Eqs. (30), (35), or (40) with $M^2/\pi\rho_m^2$ set equal to unity. Since the curves are symmetrical about the origin, the abscissas are restricted to the positive values of x/r_a.

The diffraction curves of Fig. 3 are drawn for the case in which $fk=-0.5$ and in which the separation of the two particles is 0.6080 Airy units as measured in the object plane, that is $2l/r_a^0=0.6080$. Reference to Tables I, II, and III will show that at $fk=-0.5$ the separation 0.6080 exceeds the physical limit only for the center-blocked and Sonine type objectives for which $r_0/r_a=0.676$. The curves A_1' and A_1 for these objectives show a noticeable minimum between $x/r_a=0.3$ and $x/r_a=0.4$ Airy units, whereas the curve for the Airy type objective gives no direct indication for the presence of two particles. The curve A_1 for the Sonine type objective is considered to show slightly better contrast than the curve A_1' for the center-blocked objective. The gain in resolution of curves A_1 and A_1' is accompanied by great loss of contrast in the diffraction image with respect to the contrast displayed by the Airy type objective. When fk is decreased from -0.5 to -1.0, the diffraction curves for the separation $2L=0.6080$ show greater contrast and better evidence for the presence of two particles in the manner which is illustrated by Fig. 4 and which is consistent with the trends of Fig. 2.

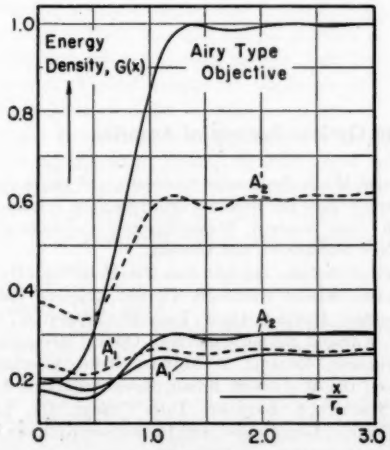

FIG. 5. Diffraction curves for the separation $2L=0.7338$ and $fk=-0.5$. Curves A_1 and A_2 refer to the Sonine type objectives; A_1' and A_2', to the center-blocked Airy type objectives. Subscripts 1 and 2 refer to the ratios r_0/r_a of 0.676 and 0.770, respectively.

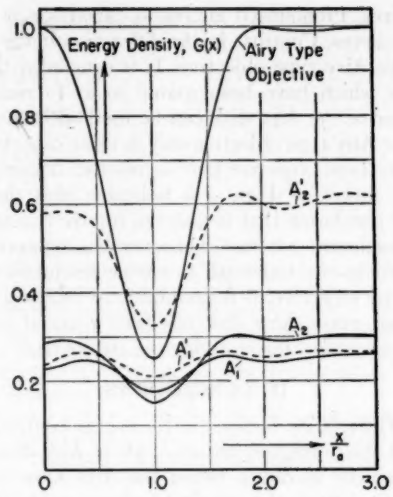

FIG. 6. Diffraction curves for the separation $2L=2$ and $fk=-0.5$. A_1, A_2, A_1', and A_2' have the same meanings as in Fig. 5.

Figure 5 has been drawn for the case in which $fk=-0.5$ and in which the separation $2l/r_a^0$ of the particles is equal to 0.7338, a distance large enough to enable resolution by both sets of Sonine and center-blocked objectives but too small to enable resolution by the Airy type objective. The Sonine and center-blocked objectives show pronounced minima near $x/r_a=0.4$ Airy units, whereas the Airy type objective gives no direct indication for the presence of a second particle. The set of curves A_2 and A_2' for which $r_0/r_a=0.770$ show more contrast than the set of curves A_1 and A_1' for which $r_0/r_a=0.676$. The curve A_2' for the center-blocked objective shows better contrast than the curve A_2 for the Sonine type objective. The best contrast in the diffraction image is shown again by the Airy type objective but this objective fails to resolve the two particles.

The curves of Fig. 6 have been drawn for the case in which $fk=-0.5$ and in which the separation $2l/r_a^0$ of the two particles is equal to 2 Airy units, a distance more than sufficient to enable resolution by all of the

objectives. Pronounced minima occur at $x/r_a=1$ in all of the curves. Contrast in the diffraction image is best with the Airy type objective. It is concluded that objectives which have been coated so as to reduce the diameter of the Airy disk can be used with advantage over the Airy type objective only in those cases in which the Airy type objective fails to resolve. A comparison of the curves of Figs. 3–6 indicates also the more general conclusion that in order to resolve two particles with maximum contrast whenever the separations of the particles are too small to enable resolution by the Airy type objective, it is preferable to choose a coated objective whose Airy disk has been reduced no more than is necessary for resolving the two particles.

IX. CONCLUSIONS

(1) The relative increase in the energy content of the rings in the diffraction patterns whose Airy disks have been reduced in radius below the Airy limit has but slight effect upon the physical limit of resolution of a microscope objective for two uniform, identical particles in a transmitting surround.

(2) Objectives which have been coated for reducing the radius of the Airy disk can be expected to show better resolution for two particles than the classical Airy type objective.

(3) With the center-blocked and the particular Sonine types of objectives which have been studied in this report, contrast in the diffraction image decreases steadily as the objective is coated to meet the demand of greater resolution.

(4) Contrast in the diffraction image deteriorates so rapidly with decreasing radii of the Airy disk at fixed numerical aperture that scattering by the optical system is expected to become a major difficulty in realizing the possible gains in resolution.

(5) The separation of the two particles at the physical limit of resolution decreases with unexpected rapidity as the unresolvable area of the particles is increased. This separation has a marked dependence also upon the relative amplitude and phase transmission of the particles with respect to the surround. With properly chosen particles the separation at the physical limit of resolution can drop to 50 percent of the separation at the Airy limit even with the classical Airy type objective.

(6) It is unfortunate that the usual particles of biological research have the least favorable amplitude and phase transmissions for taking advantage of the variation of the physical limit of resolution with the optical properties of the particles. For these particles, whose amplitude and phase transmission is not far different from that of the surround, the physical limit increases to 78 percent of the Airy limit. If the transmission of such particles is made different from that of the surround by staining either the particles or the surround, not only will the particles appear in better contrast but also their separation at the physical limit becomes smaller, that is the particles will be resolved more readily. It is emphasized, however, that the conclusions of this paragraph are not expected to apply without modification to the phase microscope.

(7) If the predicted variation of the physical limit of resolution with the properties of the particles proves to be in substantial agreement with carefully controlled experiments, there will exist a physical basis for explaining why a microscope can resolve considerably better than is indicated by the criterion of the Airy limit.

The authors are indebted to Miss Barbara R. Kloepfer for calculating the physical limits and diffraction patterns of the center-blocked objectives.

Installation of the New England Section of the Optical Society of America

THE New England Section of the Optical Society of America was officially installed at a meeting held in Boston on May 5, 1949. The brief ceremony was conducted by the Secretary for Local Sections, Dr. Stanley S. Ballard, with the assistance of two former presidents of the society, Professor Arthur C. Hardy and Dean George R. Harrison. The speech of the evening was given by Dr. Edwin H. Land of the Polaroid Corporation, who spoke on "Color Translation and Ultraviolet Microscopy." Dr. Land, a Director-at-Large of the Optical Society, is a member of the new section, as are the other three national officers just named.

This new section is the first one formed from a local group organized for the express purpose of petitioning for local section status. This group, the "New England Optical Society," had held three previous meetings, each of which was attended by well over 100 persons. While the charter membership of the new section is drawn largely from the Boston-Cambridge area, it includes representation from western Massachusetts, Connecticut, Rhode Island, New Hampshire, and Vermont.

Officers of the new section are: *President*, DR. DUNCAN E. MACDONALD, Boston University Optical Research Laboratory; *Vice President*, DAVID S. GREY, Polaroid Corporation; *Secretary*, JOHN T. WATSON, Boston University Optical Research Laboratory; *Treasurer*, RUSSELL P. MAHAN, Baird Associates, Inc.; *Councillors*, DR. WALTER S. BAIRD, Baird Associates, Inc., PROFESSOR STANLEY S. BALLARD, Tufts College, DR. ELKAN R. BLOUT, Polaroid Corporation, and PROFESSOR RICHARD C. LORD, Massachusetts Institute of Technology.

Some Variables Influencing Vernier Acuity

I. Illumination and Exposure Time

II. Wave-Length of Illumination*

KATHERINE ELEANOR BAKER**
Columbia University, New York

(Received June 25, 1948)

Since there is little experimental evidence on the influence of various stimulus factors on vernier acuity, functions relating vernier acuity to illumination have been obtained for two different exposure times and at three regions of the visible spectrum. An apparatus providing the necessary stimulus controls has been described in detail and the procedure is fully explained.

Vernier acuity, as measured by the reciprocal of the standard deviation of "alignment" settings, varies with illumination for both indefinitely long and for short exposures. At low brightness vernier acuity is low, rises rapidly with increase in illumination, and finally levels off at a constant level at high brightnesses.

Vernier acuity functions for short exposures are displaced downward and along the illumination axis relative to the function for long exposures. Thus maximum vernier acuity is never so high for short exposures and the maximum is reached at higher illuminations than with long exposures.

The relationship between vernier acuity and illumination for both long and short exposures is fitted by Hecht and Mintz's theoretical equation for visual acuity based on the brightness discrimination of the eye.

Variations in the functions with duration of exposure of the acuity object are interpreted in the light of the intensity-time relationship and the findings of Graham and Kemp on the effect of exposure time on brightness discrimination.

To investigate the influence of wave-length on vernier acuity, acuity *vs.* illumination functions have been found for red, yellow, blue, and white light. The experiments were carried out on two different apparatus.

The two sets of data obtained on the two apparatus show that all the functions are of the same shape, but that slightly different maximum acuities are reached with the different colored illuminations. Red gives the highest acuity, yellow next, white next, and blue least. When refractive correction is made to allow for sharp focusing in blue illumination, the highest acuities are found with this color.

It was concluded that wave-length of illumination is of some significance in vernier acuity, since higher acuities are found with nearly monochromatic light than with white. This improvement is perhaps caused by reduction of blurring of retinal images by restriction of the range of wave-lengths.

INTRODUCTION

VERNIER acuity, or coincidence acuity, is a particular type of visual acuity which involves the power of the eye to perceive a discontinuity or "break" in a stimulus object, usually a broken straight line or a broken circle. This type of acuity is measured in terms of the error in alignment of the two parts of the acuity object that just permits a discontinuity to be perceived. Such a measure may be made in two ways: (a) one may determine the average perceptible "offset" from perfect alignment, or (b) one may use the variability of "alignment" settings as a measure of the just perceptible misalignment. Visual acuity is taken to be the reciprocal of either measure in minutes of arc.

While our knowledge of other types of visual acuity has advanced in recent years, we still know relatively little about vernier acuity. Early workers were primarily interested in determining limiting values and speculating as to mechanisms which would permit the fine discriminations revealed by their data. The limiting values obtained range from 0.5 to 12 seconds of arc (for a review, see Walls[1]). Since the upper value of 12 seconds is only about one-third of the diameter of a foveal cone, such discriminations are not easily explainable in terms of the retinal mosaic, and a number of theories have been put forth to account for the delicacy of vernier acuity.

On the other hand, little attention has been paid to the stimulus factors which affect vernier acuity, the work of French[2] being the primary source of information on this aspect of the problem. French's study demonstrated the dependence of vernier acuity upon height and width of stimulus lines as well as the separation of two parts of the acuity object. In general, vernier acuity is better the narrower the separation between lines and the longer the stimulus lines. The width of the acuity lines affects the degree to which the above factors influence acuity. French states that vernier acuity is independent of the spectral characteristics of the illuminating light and that it holds up well under low illumination, a thousandfold change in illumination resulting in no change in acuity. No experimental evidence is presented for these latter statements.

It appears, then, that data on the effect of color and level of illumination on vernier acuity are lacking. Other types of visual acuity have been shown to depend upon illumination level in a characteristic manner, and

* Prepared under Project NR 142-404; Contract N6onr-271, Task Order II between Columbia University and the Office of Naval Research, U. S. Navy.

Submitted in partial fulfillment of the requirements for the degree of Doctor of Philosophy in the Faculty of Pure Science, Columbia University.

The author wishes to express her gratitude to Dr. Clarence H. Graham for his generous help in directing this research and to Dr. W. N. Schoenfeld for his helpful suggestions. Also the many hours of observation given by Conrad G. Mueller, Howard D. Baker, and Dorothy Yates are greatly appreciated. Special thanks go to Howard D. Baker in collaboration with whom the apparatus was designed and constructed.

** Now at Connecticut College for Women, New London, Connecticut.

[1] G. L. Walls, J. Opt. Soc. Am. **33**, 487 (1943).
[2] J. W. French, Trans. of the Opt. Soc. **21**, 127 (1919–1920).

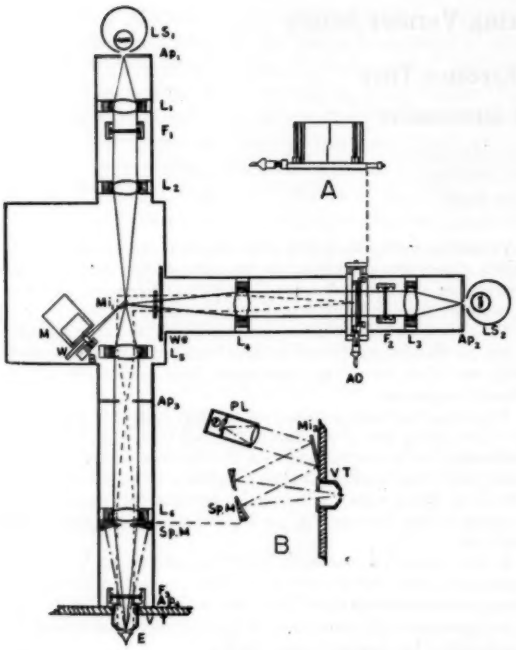

FIG. 1. A diagram of the apparatus used to measure vernier acuity at various levels of illumination and with long and short exposure durations. For explanation, see text.

it would be expected that vernier acuity, too, would depend upon illumination if a large enough range of illuminations were used. Since the degree of accommodation required for sharp focusing of objects varies with wave-length and since chromatic aberrations are reduced in nearly monochromatic light, experimental evidence on the influence of the color of illumination on vernier acuity is needed. In view of its influence on other visual functions, we might also expect duration of exposure to be a parameter which influences vernier acuity.

The present experiment represents a determination of the function relating vernier acuity to background brightness for two different durations of exposure. The data are interpreted in terms of Hecht's theory of brightness discrimination.[3] The second part of the paper deals with the relationship between vernier acuity and brightness for three regions of the visible spectrum.

I. ILLUMINATION AND EXPOSURE TIME

Apparatus

The apparatus provides a mechanism for presenting to the subject either of two 4°25′ diameter illuminated visual fields; one an adapting field, the other containing a vernier acuity object consisting of two black lines 7′ wide and 2°13′ long. One or the other of the two fields appears in the center of a larger illuminated surround field 12° in diameter, and the two visual fields are identical except for the presence of the acuity object in the one field. A mechanism is provided by means of which the field containing the acuity object is presented continuously or as a replacement for the adapting field for a duration of 0.019 second at intervals of about one second. The brightness of the fields and their surround may be varied separately or concomitantly by placing Wratten Neutral Filters in appropriate filter boxes. For purposes of the present experiments, the two fields were equal at brightnesses which were always 6 percent higher than the surround. The subject himself may adjust the alignment of the two acuity object lines from inside a dark room. All settings of the acuity object are measurable to one second of arc. The apparatus as described allows for the measurement of vernier acuity from the variability of alignment adjustments made by the subject over a wide range of background brightnesses and for short and long exposures.

Figure 1 shows a diagram of the apparatus. The two light sources (LS_1 and LS_2) are 100 and 150-watt bulbs, respectively, connected in parallel and operating at 120 volts d.c. throughout the experiments. Each bulb is enclosed in a lamphouse and light passes through a small aperture (Ap_1 and Ap_2) which makes the sources for the optical system nearly point sources.

Light from LS_1 forms the blank illuminated adapting field. Light from this source passes through a series of double convex lenses (L_1 and L_5, 11 diopters; L_2 and L_6, 4.6 diopters) and finally converges at the 2.4-mm diameter exit pupil (E) in the metal viewing tube (VT). Slotted metal filter boxes (F_1 and F_3), constructed to hold 2-inch Wratten filters, allow for variations in the brightness of the adapting field and a circular aperture (Ap_3) restricts its size to 4°25′.

Light from LS_2 illuminates the stimulus field. The optical system is identical with that of the adapting field except for the presence of an acuity object (AO), a photographic wedge and its balancer (We) for fine brightness variations and a small front surface mirror (Mi_1) which reflects the rays through 90°. Since the acuity object consists of black lines on transparent slides, the acuity object acts as a new source and, consequently, the path of the rays from the acuity object is different from that of the rays from the light source (LS_2). Light rays from the acuity object are shown as dotted lines in the diagram; rays from the sources are drawn in as solid lines. Rays from the acuity object are parallel at the exit pupil, thus the eye is not accommodated during observation of the object.

A front view of the mechanism of the acuity object is shown in insert A in the diagram. The object consists of two straight black lines, 7′ wide and 2°13′ long, placed one above the other in such a way that, when they are in alignment, there is neither a gap between the lines nor do they overlap. One line is photographed on a lantern slide which is held in a stationary position, while the other appears on a movable lantern slide.

[3] S. Hecht, J. Gen. Physiol. 18, 767 (1935).

The two emulsion sides of the slides face each other and are separated only by a strip of brass, 0.005 inch in thickness, thus preventing scratching of the two surfaces and producing only a subliminal degree of parallax.

The stationary slide is held in an upright position on a brass plate. The movable slide is held upright on a steel carrier which slides smoothly in a dove-tail slot in the brass plate to which the stationary slide is fastened. Movement is imparted to the sliding carrier by rotating a micrometer screw, and the movement is measurable to one ten thousandth of an inch, a distance which, in our optical system, represents a visual angle of one second of arc. A length of flexible speedometer cable connects the micrometer screw with the subject's knob inside the dark room.

The stimulus field containing the acuity object replaces the adapting field when the small mirror (Mi_1) interrupts the beam of light producing the adapting field. This mirror is fastened on the end of an aluminum wand (W) which turns with the shaft of a synchronous motor (M) operating on 115 volts a.c. and rotating 67 revolutions per minute. The shaft of the motor is kept from vibrating by rotating in a small ball bearing (B). When the motor is running, the stimulus field is exposed for 0.019 second for the conditions used: wand length, 19 cm; width of mirror, 2.5 cm; and speed of motor, 67 r.p.m. The stimulus field appears at maximum brightness during 80 percent of the duration of the exposure; 10 percent of the time is taken up by the onset of illumination and 10 percent by the cessation. This exposure mechanism provides for flashes of the acuity object for durations less than the critical duration (Graham and Cook[4]) at intervals slightly less than one second (1/67 minute). However, when long exposures are desired, the mirror is held in the position where the stimulus field is reflected into the eye.

Both the adapting and stimulus fields are seen through a hole in a spherical mirror used to provide an illuminated surround 12° in diameter. A side view of the mechanism used to produce the surround field is shown in insert B in the diagram. A projection lamp (PL), suspended from the wall, throws a beam of parallel rays on a plane mirror (Mi_2), which reflects the rays onto the front surface spherical mirror (Sp.M.). Rays reflected from the spherical mirror converge into the eye along with the rays from the adapting field. The aperture (Ap_4) restricts the surround field to 12°; and filters placed in the filter box (F_3) reduce its brightness along with the brightness of the fields seen through the hole in the center of the spherical mirror. A narrow dark ring exists between the small fields and the surround, thus providing a more restricted area within which the subject may fixate.

The outlines of Fig. 1 indicate steel plates onto which the various parts of the apparatus are fastened. All optical parts are enclosed in light-tight wooden boxes, the insides of which are painted flat black. Thus, stray light in the system is at a minimum. Except for the viewing tube, the apparatus is on the outside of a small light-tight cubicle. The subject, who observes from the inside of the cubicle, is provided with an adjustable chin rest to hold his head in a stationary position in front of the viewing tube.

At maximum, both the adapting and stimulus fields are 25,920 photons, while the surround is 94 percent of this value. The method of calibration of the apparatus involved a binocular match of the fields seen through the viewing tube and another field of the same size viewed through an artificial pupil of the same diameter as that in the viewing tube. The illumination of the matching field was measured with a Macbeth illuminometer and converted to the retinal illumination units, photons. Since the rays from the adapting and stimulus fields converge at the eye, the brightness of these fields must be expressed in apparent photons actually measured for the matching field. The brightness of the surround field was measured by reducing the brightness of the adapting field until the center of the visual field was equal in brightness to the surrounding portions.

Procedure

The subjects in the experiment were asked to make a number of settings of the movable half of the vernier acuity stimulus line at various background brightnesses with two different exposure durations. A measure of visual acuity was obtained from the reciprocal of the standard deviation of "alignment" settings in minutes of arc and could be plotted as a function of level of brightness. The same procedure was used with both indefinitely long exposure times and with short durations.

In the experimental sessions the subject was dark adapted for 10 to 15 minutes with red goggles (Miles[5]) and spent an additional 5 to 10 minutes in complete darkness before making settings. Since central fixation and relatively narrow stimulus lines were used, the experiment was concerned with cone vision and the amount of dark adaptation allowed was considered sufficient.

For the sessions with indefinitely long exposure times, the small front surface mirror (Mi_1) was held in position for continuous exposure of the stimulus field. Thus the subject saw an illuminated field 12° in diameter, in which the central 4°25′ had a slightly higher illumination than the rest (6 percent) and was separated from the outside portion by a narrow dark ring. The central area contained the two black lines of the vernier acuity object.

By placing neutral tint filters in the filter box nearest the subject's eye (F_3), a determination was made of the level of illumination where the subject reported that

[4] C. H. Graham and Carolyn Cook, Am. J. Psychol. 49, 654 (1937).

[5] W. R. Miles, Fed. Proc. Amer. Soc. Exp. Biol. 2, 109 (1943).

TABLE I. Experimental data on the effect of illumination and exposure time.*

Subject	Long exposures Log illumination in photons											
	$\bar{1}.51$	$\bar{1}.81$	0.11	0.41	0.81	1.41	1.81	2.41	2.81	3.41	3.81	4.41
H.B.	0.42	0.62	0.60	0.73	0.77	0.83	0.88	0.82	0.85	0.93	0.85	0.96
C.M.	0.34	0.48	0.69	0.75	0.78	0.92	0.89	0.91	0.82	0.91	0.84	0.91
Average	0.38	0.55	0.65	0.74	0.78	0.88	0.89	0.87	0.84	0.92	0.85	0.93

Subject	Short exposures Log illumination in photons											
	$\bar{1}.74$	0.11	0.41	0.81	1.11	1.41	1.81	2.41	2.81	3.41	3.81	4.41
H.B.		0.12	0.18			0.45	0.63	0.61		0.71		0.62
C.M.		0.11	0.27	0.39		0.37	0.41	0.49	0.46	0.50	0.45	0.46
Average (data for C.M. raised 0.15-log unit)		0.19	0.30			0.49	0.60	0.62		0.66		0.62

* Average log acuity is presented for each of two subjects for short and long exposure times at each illumination level. Averages for long exposures are based on four experimental sessions, while averages for short exposures represent six sessions. Averaged data for the two subjects appear at the bottom of each part of the table.

he could just see the stimulus lines while fixating the center of the field. Experimentation was started at this level and continued up to the limiting value of the apparatus (25,920 photons). In each experimental session with the indefinitely long exposure time acuity was measured at 12 levels covering a range of brightnesses (photons) from log $I=\bar{1}.51$ to log $I=4.41$.

In a given experimental session, the subject, using a bracketing method, made ten "alignment" settings of the vernier acuity object at each brightness level. Between settings, the experimenter set the acuity lines out of alignment, being careful to randomize the amount and direction of offset. After ten settings had been made, filters were adjusted to give the next highest brightness level, two minutes were allowed for light adaptation to the new level, and another ten settings were made. This procedure was repeated until acuity had been determined for all twelve brightness levels.

A preliminary experiment showed that ten alignment settings yielded a stable standard deviation. Since the standard deviation around the subjective mean setting is taken as the measure of vernier acuity, it is necessary that the measure of variability be a reliable one. The experiment showed a lack of orderly change in the standard deviation between 10 and 75 settings and the absolute amount of change represented a range of only 1.25 seconds of arc. In other words, the maximum error that could be made from calculating the standard deviation from 10 rather than 75 settings was about 10 percent. Since a quite reliable standard deviation could be made from 10 settings, it was possible to test for acuity at each of the twelve brightness levels in a single experimental session, thus avoiding problems of day to day variability.

For the experiments with short exposures, the rotating mirror was set in motion and kept running throughout the experimental session, thus providing flashes of the field containing the acuity object for 0.019-second durations at intervals of about 1 second. For the periods when the acuity object was not exposed, the adapting field appeared in the center of the whole visual field, and, since the adapting and stimulus fields were of the same brightness, the adaptation level of the eye was kept constant throughout the series of settings at any given brightness level. As before, the subject used a bracketing method to make "alignment" settings of the movable half of the stimulus line, and he was presented with as many exposures as he felt necessary to obtain a satisfactory setting. Since the exposures were short, the process of making a setting involved alternate adjustments and discriminations by the subject until he felt satisfied with the setting. The experimenter again set the lines out of alignment between settings.

The lowest level at which settings could be made was determined, and experimentation was carried out at each successive brightness level between this level and the limiting value of 25,920 photons. In the case of one subject (C.M.), ten levels were used, ranging from log $I=0.41$ to log $I=4.41$, while for the other subject (H.B.) experimentation was begun at log $I=0.11$ and progressed in eight steps to log $I=4.41$.

Another preliminary experiment was performed to determine the number of settings necessary to obtain a stable standard deviation under the short exposure conditions. In the case of one subject (C.M.) it was decided that 10 settings were sufficient for the calculation of the standard deviation. However, for the other subject, H.B., when the first five settings were ignored, the standard deviation for the next 10 settings was essentially the same as that obtained for the next 70 settings. Consequently, for subject H.B., 15 settings were required for each brightness level, the first five of which were discarded and the standard deviations were

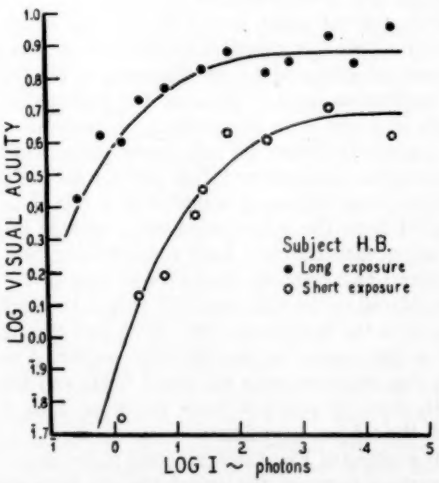

FIG. 2. Curves relating the logarithm of visual acuity to the logarithm of retinal illumination for subject H.B. The solid dots are data obtained with indefinitely long exposures, while the data shown as open dots were found with short exposures. All data are taken from Table I.

then calculated on the basis of the remaining 10 settings. As with long exposures, a complete function covering all intensity levels was determined during each experimental session.

Two trained subjects were used for the experiments, each repeating the settings in four experimental sessions with long exposures and six sessions with short exposures. Two practice sessions with each exposure duration were given prior to the experimental sessions. The experimental sessions with short exposures were randomly mixed with those for the indefinitely long exposures in order that practice effects would not differ for the two conditions. Both subjects were graduate students and both possessed 20/20 vision, one wearing glasses which corrected his vision to this level.

Results

Table I presents the experimental data obtained in the experiments on short and indefinitely long exposure times for the range of background brightnesses used. The average log acuity is shown for each of the two subjects for various values of log retinal illumination measured in photons, and the average data for the two subjects are shown at the bottom of each part of the table. It was found that the data for subject C.M. were on the average 0.15-log unit lower for short exposures than those obtained with subject H.B. All the data for C.M. with short exposures were raised by this amount before being averaged with H.B.'s data, a procedure which does not affect the shape of the function which is our primary interest in this experiment.

The data from Table I are shown graphically in Figs. 2–4. Figures 2 and 3 show both the long and short exposure curves for the subjects individually, while the average data are plotted in Fig. 4. All curves show average log visual acuity as a function of the logarithm of the retinal illumination.

The most striking feature of all the curves is the change in vernier acuity with change in background brightness. At low brightnesses, acuity is low, improves rapidly with increase in illumination and finally levels off at a constant level for high brightnesses.

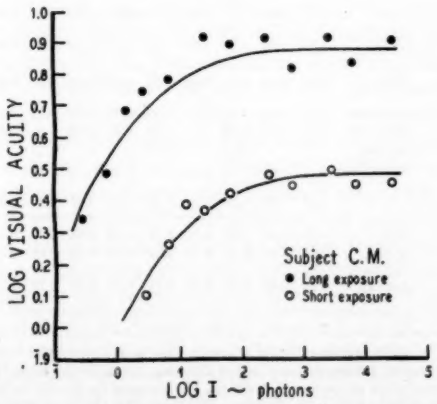

FIG. 3. Curves relating the logarithm of visual acuity to the logarithm of retinal illumination for subject C.M. The solid dots are data obtained with indefinitely long exposures, while the data shown as open dots were found with short exposures. All data are taken from Table I.

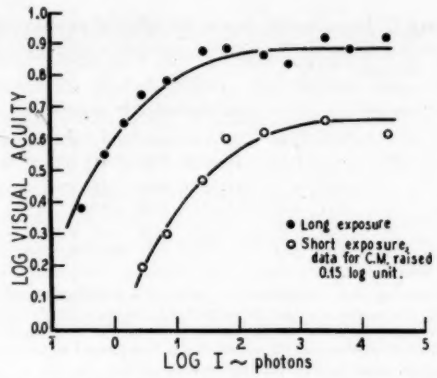

FIG. 4. The logarithm of visual acuity as a function of the logarithm of retinal illumination based on averaged data for two subjects. Data obtained with long exposures are shown as solid dots and the open dots represent data found with short exposures. The data for subject C.M. with short exposures were raised 0.15-log unit before averaging. All data are from Table I.

In the cases of both subjects, the curves for short exposures of the acuity object are displaced downward and to the right of the long exposure curves. For long exposures, vernier acuity reaches its maximum at about 1000 photons, and the maximum value for both subjects is about 7.6 (=1/0.132 minutes of arc). For short exposures, the curve for C.M. appears to level off at a brightness level about 0.5-log unit higher than that for the corresponding part of his long exposure curve, while the curve for H.B. becomes flat only after a corresponding 1 log unit change. In the case of C.M., the maximum acuity reached with short exposures is only approximately half that obtained with the long exposure conditions, while H.B. attained acuity values of about two-thirds of his maximum for long exposures.

The average curves in Fig. 4 show essentially the same feature as the individual curves. For long exposures, vernier acuity appears to change by a factor of a little more than three over a five log unit change in brightness. A constant value of vernier acuity may be expected for brightnesses of about 1000 photons and above under the long exposure conditions. For short exposures, the total acuity change is a little less than three for a change in brightness of four log units. Constant values of acuity are attained at about 3500 photons. The maximum acuity shown with long exposures is about 1.6 times as high as that found under short exposure conditions.

Discussion

These experiments have demonstrated the dependence of vernier acuity on background brightness below 1000 photons for long exposures and below 3500 photons for short exposures. The constancy of acuity above

TABLE II. Experimental data on the effect of wave-length.*

Color	Wratten filter number	Log illumination in photons								
		$\bar{2}.81$	$\bar{1}.41$	$\bar{1}.81$	0.11	0.41	0.81	1.41	1.81	2.41
Red	70	0.07	0.42	0.58	0.74	0.83	0.88	0.89	0.96	0.91
		$\bar{1}.21$	$\bar{1}.51$	$\bar{1}.81$	0.21	0.81	1.21	1.81	2.21	2.81
Yellow	73	0.22	0.33	0.64	0.79	0.94	0.95	0.85	0.92	0.87
		$\bar{2}.91$	$\bar{1}.21$	$\bar{1}.61$	$\bar{1}.91$	0.21	0.61	1.21	1.61	2.21
Blue	75	$\bar{1}$.93	0.13	0.42	0.49	0.51	0.69	0.75	0.78	0.88

* Average log acuity is presented for each of the illumination levels used with red, yellow, and blue light for subject H.B. on the original apparatus. Each average is based on 20 settings, 10 from each of two experimental sessions. The brightness of the colored lights is expressed in terms of the brightness of white light which is subjectively equal.

these brightness levels makes it understandable why French[2], who probably worked with a restricted range of brightnesses, reported that vernier acuity does not vary with illumination.

It is of considerable interest to apply Hecht's theory of brightness discrimination to the present data. According to Hecht[3], the discrimination ratio, $\Delta I/I$, for brightness discrimination of the cones is predicted by the relation

$$\Delta I/I = c'[1+1/(KI)^{\frac{1}{2}}]^2 \qquad (1)$$

where c' and K are constants and I is adapting intensity. Hecht and Mintz[6] state that the critical visual angle, α, for the resolution of fine lines is directly proportional to $\Delta I/I$, making visual acuity $(=1/\alpha)$ inversely proportional to the discrimination ratio. A similar assumption applied to the present data would state that our measure of visual acuity, v, is inversely proportional to $\Delta I/I$, i.e., $v \propto I/\Delta I$; and Eq. (1) becomes

$$v = c''KI/[1+(KI)^{\frac{1}{2}}]^2, \qquad (2)$$

where c'' contains c' and an additional proportionality constant. The curves drawn through the data of Fig. 2, 3, and 4 are computed from Eq. (2), and it may be seen that they fit the results in a satifsactory manner. Therefore, the data of vernier acuity fit into a descriptive theoretical framework which has been successful in accounting for brightness discrimination (Hecht[3]) and other forms of acuity (Hecht and Mintz[6]). Although Shlaer[7] denies the dependence of acuity for gratings and for a C upon brightness discrimination, the form of the equation used by him to fit data for these types of acuity may be derived from our Eq. (2).

Not only does the same expression that describes the relationship between background brightness and acuity for fine lines fit the vernier acuity data, but also the brightness level at which maximum acuity is attained is of the same order of magnitude for both. The same may be said for a comparison of Shlaer's grating and C type acuities[7] with the present results. Acuities as high as 20 were found with thin lines, while acuities of the order of magnitude of 2 were found with the C and, in our experiment, vernier acuity reached a maximum of about 8. Thus, vernier acuity is a type which results in the resolution of very fine details, details which are well within the limits of the visual angle of a single cone.

Following Hartline's[8] demonstration of the reciprocal relation between the duration of exposure and level of illumination for visual responses, the effect of exposure time has been studied for several visual functions. Graham and Cook[4] and Niven and Brown[9] have shown the dependence of visual acuity upon the duration of exposure of the acuity object, and, at least in the case of the grating, visual acuity exhibits a critical duration beyond which exposure time becomes a greatly diminished factor.

In our experiment, we have used two different exposure times, one below what might be expected to be the critical durations for the brightnesses used and one long enough to show a failure of the reciprocal relation. Our data show that for the short exposure time the curves are displaced on the abscissa toward higher brightness values and on the ordinate toward lower acuities.

From a consideration of the reciprocal relation known

TABLE III. Experimental data on the effect of wave-length.*

Color	Subject	Log illumination in photons									
		$\bar{2}.80$	$\bar{1}.40$	0.40	1.40	1.80	2.40	2.80	3.40	3.80	4.40
Red (Wratten No. 70)	D.Y.	$\bar{1}$.90	0.23	0.53	0.69	0.70	0.75	0.90	0.76	0.78	0.79
	K.B.	0.02	0.32	0.37	0.72	0.61	0.53	0.70	0.83	0.76	0.86
	Average	1.96	0.28	0.45	0.71	0.66	0.64	0.80	0.80	0.77	0.83
		$\bar{2}.65$	$\bar{1}.65$	0.65	1.65	2.05	2.65	3.05	3.65	4.05	4.65
Yellow (Wratten No. 73)	D.Y.	$\bar{1}$.95	0.43	0.66	0.80	0.94	0.67	0.81	0.63	0.84	0.70
	K.B.	$\bar{1}$.92	0.43	0.64	0.68	0.67	0.62	0.71	0.70	0.73	0.84
	Average	$\bar{1}$.94	0.43	0.65	0.74	0.81	0.65	0.76	0.67	0.79	0.77
		$\bar{2}.30$	$\bar{1}.30$	0.30	1.30	1.70	2.30	2.70	3.30	3.70	4.30
Blue (Wratten No. 75)	D.Y.	$\bar{1}$.94	0.24	0.52	0.60	0.76	0.77	0.79	0.86	0.81	0.79
	K.B.	$\bar{1}$.65	0.01	0.36	0.50	0.50	0.62	0.62	0.58	0.60	0.64
	Average	$\bar{1}$.80	0.12	0.44	0.55	0.63	0.69	0.70	0.72	0.71	0.72
	D.Y. with =1.5-diopter lens	0.04	0.40	0.78	0.87	0.98	0.79	0.72	1.01	0.83	0.96
		$\bar{2}.45$	$\bar{1}.45$	0.45	1.45	2.45	3.05	3.45	4.05	4.45	5.05
White	D.Y.	$\bar{1}$.80	0.44	0.51	0.71	0.75	0.76	0.68	0.77	0.71	0.77
	K.B.	$\bar{1}$.95	0.40	0.67	0.63	0.67	0.70	0.82	0.68	0.70	0.75
	Average	$\bar{1}$.88	0.42	0.59	0.67	0.71	0.73	0.75	0.73	0.71	0.76

* Average log acuity is presented for each of two subjects for various levels of illumination by red, yellow, and blue light, as well as for white light. Each average is based on two experimental sessions making a total of 20 settings, except for the values for D.Y. for blue light which are averages of 40 settings. The average of the data for the two subjects appears in the last row of each section of the table. The brightness of the colored lights is expressed in terms of the brightness of white light which is subjectively equal.

[6] S. Hecht and Esther V. Mintz, J. Gen. Physiol. **22**, 593 (1939).
[7] S. Shlaer, J. Gen. Physiol. **21**, 165 (1937).
[8] H. K. Hartline, J. Cell. and Comp. Physiol. **5**, 229 (1934).
[9] J. T. Niven and R. H. Brown, J. Opt. Soc. Am. **34**, 738 (1944).

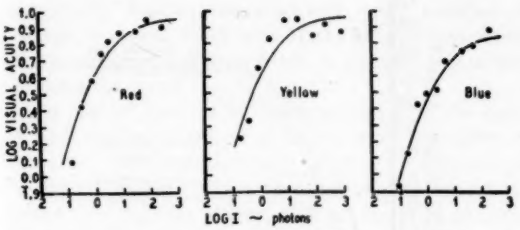

FIG. 5. Curves relating the logarithm of visual acuity to the logarithm of illumination for red, yellow, and blue illumination. The data are taken from Table II and were obtained with one subject with the original apparatus.

to hold between duration of exposure of the acuity object and illumination (Graham and Cook[4]), we should expect the function relating acuity to brightness for short exposures to be displaced toward higher brightnesses compared to the function for long exposures when the short exposures are of critical duration or below. This expectation is consistent with our findings, but such a reciprocal relationship alone cannot explain the downward displacement also seen in our data. Therefore, it is necessary to consider another parameter.

Graham and Kemp[10] have shown for intensity discrimination that the critical duration of exposure of ΔI is a function of intensity, the higher the intensity, the shorter the critical duration. According to their treatment, $\Delta I/I$ for any given level of illumination is a minimum at the critical duration for that level. For durations below critical duration, $\Delta I/I$ is inversely proportional to duration. Insofar as visual acuity may be thought to be limited by the intensity discrimination of the eye, the findings of Graham and Kemp should apply to functions relating visual acuity to illumination.

If the 0.019-second exposure of our experiment is below critical duration for all brightnesses used, we should expect the maximum values for acuity shown with short exposures to be less than those found for long exposures, i.e., maximum visual acuity, being inversely proportional to limiting $\Delta I/I$ values, should be directly proportional to exposure duration. This difference was actually found in our experiment, and, presumably, if the obtained values for short exposures were multiplied by the exposure duration, they would fall on the same curve as the one given by values for acuity found with long exposures when each of these values has been multiplied by the critical duration that exists for the particular brightness level at which they were obtained. The curves for the two exposure conditions used would be expected to meet only when and if the exposure of 0.019 second were no longer below critical duration and evidently we have not used high enough brightnesses for such a situation to obtain, if it ever does.

Averill and Weymouth[11] have argued that, if eye movements are important in vernier acuity, decreasing exposure time and thereby restricting the use of eye movements, should reduce the values obtained for vernier acuity. They used exposure times of 3.0, 1.54 seconds, and 0.03 second and found that acuities attained with the shortest exposure time were only about half those obtained with the longer durations. Since the shortest exposures were less than they considered the minimum duration for eye movements, it was assumed that most eye movements were eliminated and their absence as aids to discrimination resulted in a reduction of vernier acuity. Our results point to the fact that Averill and Weymouth's results may be interpreted as due to the dependence of vernier acuity on duration of stimulation and not to restriction of eye movements. Data on critical durations for the brightness levels used by Averill and Weymouth[11] are required before such an interpretation may be advanced unequivocally.

II. WAVE-LENGTH OF ILLUMINATION

Apparatus and Procedure

One part of the experiment on wave length of illumination made use of the apparatus of the previous experiments and employed a procedure identical with that used for indefinitely long exposure times except in one detail: Wratten color filters were provided to control wave length of the stimulating light. Wratten filters Numbers 70, 73, and 75, giving red, yellow, and blue light, respectively, were placed in the filter box nearest the subject's eye thus making the 4°25′ adapting and stimulus field as well as the 12° diameter surround the same color. The central wave-lengths of these filters are approximately as follows: No. 70, 690 mμ; No. 73, 575 mμ; and No. 75, 490 mμ.

In order to obtain comparable results with the various filters, the apparent brightnesses of the fields were determined with each filter in place. By heterochromatic

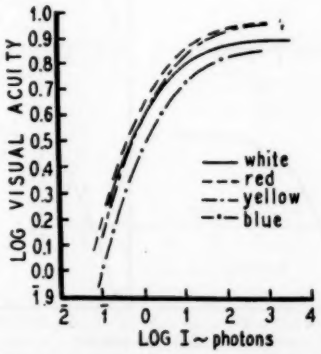

FIG. 6. Curves relating the logarithm of visual acuity to the logarithm of illumination for red, yellow, blue, and white light. These are the curves shown separately in Fig. 5, together with the curve obtained for the same subject with white light in a previous experiment.

[10] C. H. Graham and E. H. Kemp, J. Gen. Physiol. 21, 635 (1938).

[11] H. L. Averill and F. W. Weymouth, J. Comp. Psychol. 5, 147 (1925).

matches made by each of the subjects, both in the apparatus and by independent means, a determination was made of the density of neutral filter necessary to reduce white light of known brightness to the same brightness as each of the colored lights. The average density was calculated for each colored filter, and this value was taken as the "effective density" of the color filter. The "effective densities" of the filters as measured with a densitometer were very similar to the measurements in the apparatus itself. Consequently, the averaged results of both methods were used in the final brightness calculations.

One of the subjects who served in the previous experiments (H.B.) provided the data for the first part of the experiment. In six experimental sessions, he made two sets of 10 vernier settings at each brightness level with each of the colors, red, yellow, and blue. Each session involved the determination of a brightness function for a given color. The order in which the sessions with the different colors were run was random.

For the second part of the experiment, a somewhat different apparatus was employed. The original acuity object, together with its adjustment mechanism was set up in a beam of parallel light and was viewed through a 5.5-diopter double convex lens and a 2.8-mm diameter exit pupil. As before, rays from the acuity object were parallel, and accommodation was for infinity. A filter box was provided between the acuity object and the last lens in the system to allow for brightness variation and for the placement of colored filters. The characteristics of this optical system allowed for the measurement of acuity to the nearest 2.9 seconds of arc.

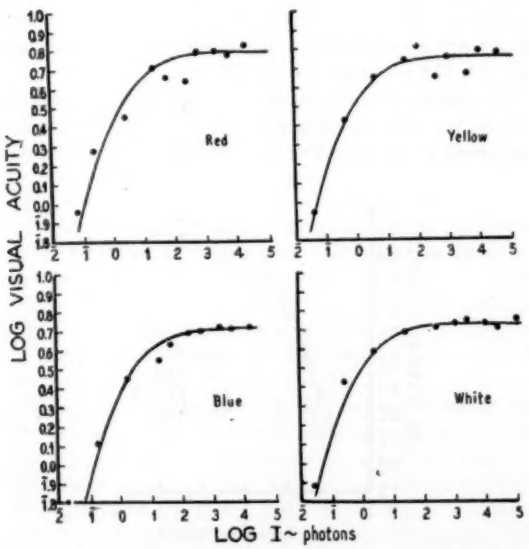

FIG. 7. Curves relating the logarithm of visual acuity to the logarithm of illumination for red, yellow, blue, and white light. These curves are based on averaged data obtained for two subjects on the new apparatus and the data are from Table III.

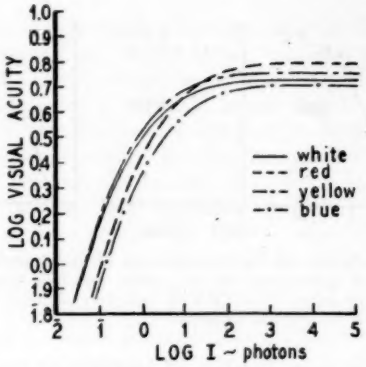

FIG. 8. Curves relating the logarithm of visual acuity to the logarithm of illumination for red, yellow, blue, and white light. These are the curves of Fig. 7 shown together.

Under these experimental conditions, two subjects (K.B. and D.Y.) made twenty settings of the acuity object at each brightness level in red, yellow, blue, and white light. Subject D.Y. made an additional twenty settings in blue light at each brightness level as well as twenty acuity settings at each level with blue light through a −1.5-diopter lens placed 2 cm from the exit pupil inside the viewing tube. As in the first part of this experiment, an experimental session involved making ten settings at each brightness and the values obtained in the different days' sessions were averaged for the final acuity values.

Since the sensitivity of the measurements with the new apparatus was only about one-third as fine as with the original apparatus, Sheppard's correction was applied to the standard deviations taken as the measure of vernier acuity. This correction is applicable when it is desireable to compare data obtained by coarse grouping with data obtained by fine grouping.

Results

The experimental data obtained with the original apparatus appear in Table II, and Table III contains the results of the experiments with the new apparatus. The data from Table II are plotted in Figs. 5 and 6. Figure 5 shows log visual acuity as a function of log apparent brightness for each of the colors used, while Fig. 6 shows these curves, together with the curve obtained for the same subject with white light. Figures 7 and 8 from the data of Table III, are comparable to Figs. 5 and 6 and show the averaged data for the two subjects examined in the new apparatus. The curves plotted in Fig. 9 show the effect of viewing the acuity object in blue light with and without a negative lens. Both curves were obtained with subject D.Y. and the actual experimental values, not shown in the interest of clarity, may be found in Table III.

It will be noted from the graphs in which the actual data appear that the data show considerable variability,

presumably due to the relatively small number of settings. However, Hecht and Mintz's theoretical curve[6] for visual acuity has been fitted to all sets of data and indicates the trend.

Our special interest in this experiment is the comparison of the functions obtained with the different colors; such a comparison may be made by reference to the figures in which the different functions appear together. The data for subject H.B. on the original apparatus indicates that different maximum values of acuity are obtained with different colors. The curves for red and yellow level off at about the same acuity value, a value slightly higher than the maximum found for white light and still higher than that found for blue light. The difference between the final constant level reached with red or yellow and that obtained with white light is small, about 0.05-log unit, and a difference of the same order of magnitude is found between the maximum acuities attained for blue and white light, white giving the higher values. Although differences in maximum acuities seem to exist for different colors, all of the curves of acuity *vs.* log *I* reach their maxima at about the same brightness level.

The measurements made with the new apparatus with subjects K.B. and D.Y., indicate the continued presence of slight differences among the final acuity values reached with different colors. The maximum value for red is slightly greater than that for yellow; yellow in turn gives a somewhat higher maximum than white; and white gives a greater maximum than blue.

Since blue light is focused nearer the lens than yellow light, it is impossible for an eye which is accommodated for infinity in order to focus an object in yellow light to be accommodated for the same object in blue light. A negative lens must be provided in order for the blue rays to be focused on the retina, while for red light, the eye itself can provide the positive lens necessary for sharp focusing. Our experimental conditions, involving accommodation for infinity in yellow light, might produce inferior acuity in blue light merely due to the inability of the eye to obtain a sharp focus for blue light. To test this notion, a -1.5-diopter lens was placed in the system, thus allowing the eye to accommodate for objects in blue illumination. Figure 9 shows the functions obtained with subject D.Y. under the two conditions, and it may be seen that a considerable increase in maximum acuity results under the conditions of using a negative lens. This increase amounts to about 0.15-log unit, an increase sufficient to make acuity with the lens superior to the vernier acuity shown with either of the other colors or with white.

Discussion

The fact that Hecht and Mintz's[6] formulation of visual acuity as limited by brightness discrimination fits our data for colors and white light probably indicates that the process represented by the acuity *vs.* log *I* plot is similar in all cases. Not only are the functions of the same shape, but they reach their final constant levels, whatever they may be, at about the same brightness level.

Our data show that, from greatest to least, the order of superiority for maximum vernier acuity is: red, yellow, white, and blue. This order has been demonstrated for three subjects and two different apparatuses. Although the data show considerable variability and the differences in maximum acuities are small, the fact that the same order was obtained in repeated tests probably means that the differences are real. When the myopia of the eye for blue light was corrected by interposing a negative lens, the maximum acuity attainable with blue light increased to such a marked degree that it became greater than the maximum acuities for the other colors.

These findings are not consistent with those of Ferree and Rand[12] who found that acuity for all colors except yellow was worse than the acuity for white. Ferree and Rand report an order of superiority of yellow, white, red, and blue. Their explanation given for the obtained differences involves the assumption that the eye tends to accommodate for the yellow region of the spectrum, and any deviation from this wave-length region results in focussing errors. On their assumption, one would expect that a greater error would occur for an object viewed in blue light and with accommodation adjusted for yellow than would occur when an object is viewed in red light with accommodation for yellow. Wald and Griffin[13] have shown that an accommodation of about 0.5 diopter relative to the accommodation for yellow is required to bring objects in extreme red into sharp focus, while for objects in violet light, a change in accommodation of about -2.75 diopters is required. The

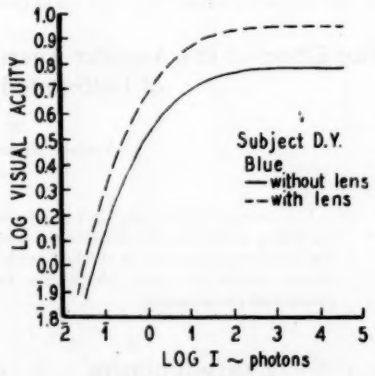

FIG. 9. Curves relating the logarithm of visual acuity to the logarithm of illumination for blue light when the acuity object is viewed through a -1.5-diopter lens and without the use of the lens. The curves were obtained with subject D.Y. and the actual data may be found in Table III.

[12] E. Ferree and G. Rand, J. Aviat. Med. **13**, 193 (1942).
[13] G. Wald and D. R. Griffin, J. Opt. Soc. Am. **37**, 321 (1947).

method used by Wald and Griffin in measuring the refractive changes necessary for sharp focussing requires that the eye actually accommodate to the particular wave-length being used.

With due regard to the need for providing a refractive correction for blue light, our results seem to mean that acuity is better for nearly monochromatic light than for white light. Such a finding indicates that the effects of chromatic aberration in the eye may be significant for vernier acuity, but, since the superiority of acuity in colored light over acuity in white light is slight, the significance of this factor does not appear to be great.

Possibly, the improvement in acuity obtained with a restricted range of wave-length is caused by the reduction in blur of the retinal image, which is at a maximum in white light. Such an assumption, however, does not explain the order of superiority of the colors as reported here.

SUMMARY

In order to extend information on the variables which influence vernier acuity, experiments have been carried out to yield information about the effect of three variables: illumination, exposure time, and wave-length of illumination.

An apparatus providing the necessary stimulus controls has been described in detail.

The results of an experiment on the effect of illumination show that vernier acuity varies with illumination level. Acuity is low at low brightnesses, rises rapidly with increase in brightness, and finally reaches a constant value for 1000 photons and above. An adequate fit of the data is provided by Hecht and Mintz' formulation[6] of visual acuity in terms of the brightness discrimination of the eye.

The curves relating vernier acuity to level of illumination for short exposures (0.019 second) are displaced downward and along the abscissa toward higher brightness levels relative to the long exposure curves. These shifts are interpreted in terms of the data on intensity-time relationships in the retina and the findings of Graham and Kemp[10] on the effects of exposure time on brightness discrimination.

To determine the effect of wave-length of illumination, functions relating vernier acuity to brightness level were obtained for red, yellow, and blue, as well as white light.

The results of the experiment indicate that red and yellow illumination allow for the attainment of higher maximum vernier acuities than white or blue light, although the shapes of the curves relating acuity to brightness are similar and the brightness level at which maximum acuities are reached is constant. Of the colors examined, red gives the highest maximum acuity; yellow next; white next; and blue, least.

Since the conditions of the experiment did not allow for optimum accommodation of the eye for blue light, additional settings were made with this color with a -1.5-diopter lens. When this refractive correction was provided, blue light provided the highest acuity of any color. Thus, when account is taken of necessary refractive corrections, vernier acuity in nearly monochromatic light seems to be superior to that obtained with white light.

It is possible that the superiority of acuity in colored light over that obtained with white light may be caused by the reduction of blurring of the retinal image due to chromatic aberration of the eye. However, no explanation can be given for the order of superiority of the colors found in the present experiment.

JOURNAL OF THE OPTICAL SOCIETY OF AMERICA VOLUME 39, NUMBER 7 JULY, 1949

The Effect of the Angular Aperture of a Telephotometer on the Telephotometry of Collimated and Non-Collimated Beams*

W. E. KNOWLES MIDDLETON
National Research Council of Canada, Ottawa, Ontario

(Received April 29, 1949)

It is shown theoretically that in telephotometry in a foggy atmosphere, large errors may arise from the scattering of light by the fog into the telephotometer. These errors depend both on the angular aperture of the telephotometer and on the half-angle of the cone of air illuminated by the distant lamp. Some experimental results are given, which show even larger errors than the hypothetical atmospheres chosen for theoretical investigation.

1. INTRODUCTION

THE results of telephotometry in a turbid atmosphere at night will obviously be somewhat affected by light scattered into the receiver (eye, photocell, etc.,) of the telephotometer by the atmosphere in the vicinity of the light-source being measured, and indeed by all parts of the atmosphere that are "looked at" by the telephotometer and illuminated in any way. This was mentioned by Collier[1] in the discussion of his

* Contribution from the Division of Physics, National Research Council, Ottawa. Issued as N.R.C. No. 1958.

[1] L. J. Collier, Trans. Illum. Eng. Soc. London 43, 141 (1938).

FIG. 1. Illustrating the derivation of Eq. (8).

excellent general paper on visual telephotometry, but the idea was not developed further. There has been some doubt[2, 3] whether transmission measurements with a collimated beam give the same results as would be obtained by measurements on a lamp illuminating the entire atmosphere, and a good deal of speculation as to whether the difference is important.

This paper is an attempt to investigate the effect of two variables: the angular aperture of the instrument, and what may be called the angular aperture of the distant light source, i.e., the half-angle of the cone into which it radiates. An elementary treatment has been given by Foitzik,[4] but it is restricted to apertures of a degree or so for both the lamp and the telephotometer.

Suppose a source of light having intensity I_0, radiating into a cone of half-angle Θ, and let this source be looked at (as in Fig. 1) by a telephotometer having an angular aperture defined by the half-angle Ψ. Light from the source can reach the telephotometer in three ways:

(*a*) directly;

(*b*) after one scattering in that portion of the atmosphere at which the instrument is able to "look" (Fig. 1);

(*c*) after two or more scatterings. This will not be considered in this paper.

To simplify the calculation we shall make the following assumptions:

(*i*) The atmosphere is homogeneous over the entire region and has an extinction coefficient σ.

(*ii*) Absorption may be neglected.

(*iii*) Both the source and the entrance pupil of the telephotometer are very small compared to the distance between them.

(*iv*) The entire system is axially symmetrical about the axis of the telephotometer.

(*v*) There are no solid surfaces in a position to reflect light from the source into any part of the beam, either before or after scattering. In practice this means that the proximity of the ground is not taken into account.

(*vi*) The light is monochromatic, of wave-length λ.

(*vii*) There are no other sources illuminating the portion of the atmosphere in question.

2. DIRECT LIGHT

The light reaching the telephotometer directly from the source produces an illuminance E_a in the plane of its entrance pupil.

$$E_a = I_0 r_0^{-2} e^{-\sigma r_0}, \tag{1}$$

where r_0 is the distance from the source to the instrument.

3. LIGHT SCATTERED ONCE

In that part of the atmosphere illuminated by the lamp and also viewed by the telephotometer, let us consider a toroidal element of volume dv (Fig. 1), defined by its cross-section $r_2 dr_2 d\psi$ and its radius $r_2 \sin\psi$. The volume of this is

$$dv = 2\pi r_2^2 \sin\psi dr_2 d\psi. \tag{2}$$

Since no useful telephotometer will have an angular aperture Ψ as great as 3°, we may, to an accuracy of 0.1 percent, substitute r for r_2, and elsewhere in the argument ψ for $\sin\psi$ and $\tan\psi$, and unity for $\cos\psi$. Collier's conclusions (1) on the accuracy of telephotometry will amply justify such an approximation. We may write, then

$$dv = 2\pi r^2 \psi dr d\psi. \tag{3}$$

The illuminance at dv due to I_0 is

$$E_1 = I_0 e^{-\sigma r_1} \cdot r_1^{-2} = I_0 e^{-\sigma r_1} / [(r_0 - r)^2 + r^2\psi^2]. \tag{4}$$

The total intensity of the element of volume dv in the direction of the telephotometer is the product of this illuminance (lumens/m^2), the volume (m^3), and a scattering function $\beta(\varphi)$(m^{-1}) which expresses the dependence of the intensity on the angle φ through which the

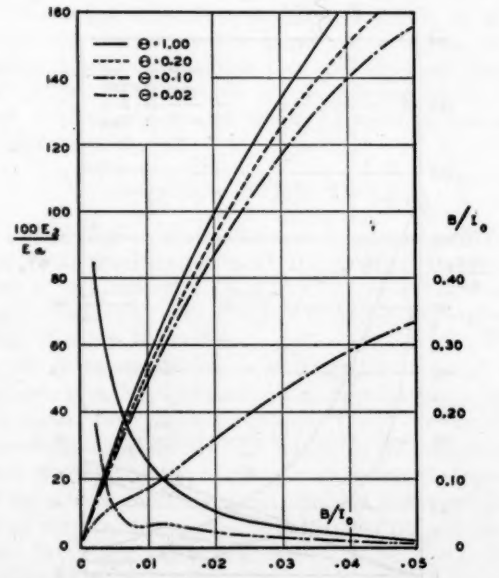

FIG. 2. Percentage error, $100E_2/E_a$, Case I; also distribution of luminance across the field, $B(\psi)/I_0$.

[2] S. Q. Duntley, J. Opt. Soc. Am. 38, 179 (1948).

[3] C. A. Douglas and L. L. Young, C.A.A. Tech. Development Report No. 47, U. S. Department of Commerce, Washington.

[4] L. Foitzik, *D. R., Reichsamt für Wetterdienst, Wiss. Abh.* (Berlin, 1938), Vol. 4, No. 5.

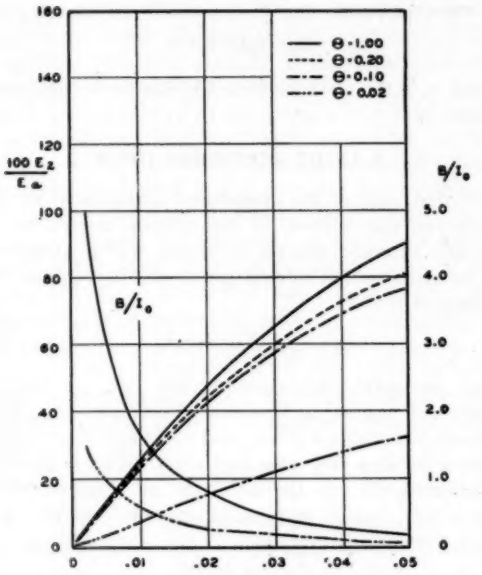

FIG. 3. Percentage error and distribution of luminance, Case II.

light is deviated by the scattering. We may write

$$dI_1 = E_1\beta(\varphi)dv = 2\pi r^2 I_0 \frac{e^{-\sigma r_1}}{(r_0-r)^2+r^2\psi^2}\cdot\beta(\varphi)\psi dr d\psi. \quad (5)$$

The illuminance at the telephotometer due to this volume element is now found by division by r_2^2 (or by r^2 to a sufficient approximation), and multiplication by the transmittance of the atmosphere along the path r_2:

$$dE_2 = 2\pi I_0 e^{-\sigma(r_1+r_2)} \frac{\psi}{(r_0-r)^2+r^2\psi^2}\beta(\varphi)dr d\psi. \quad (6)$$

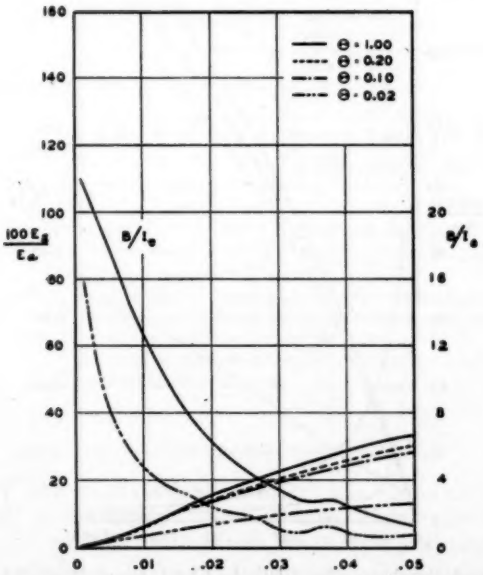

FIG. 4. Percentage error and distribution of luminance, Case III.

We must now consider the terms $\beta(\varphi)$ and $e^{-\sigma(r_1+r_2)}$. The scattering function $\beta(\varphi)$ has received an immense amount of theoretical attention, especially in the case of spherical particles. These are important, because the particles of haze and fog are chiefly small droplets of water, more or less pure, while many of the smokes used for tactical purposes are also composed of liquid droplets. Recent theoretical work, of which an excellent summary is given by Sinclair[5] has in general followed the lines of the theory of Mie.[6] The calculations and experiments of LaMer and Sinclair[7] have established the essential correctness of the Mie theory, which is based on the electromagnetic theory of light, and is particularly applicable to particles of radii between 0.1 and 10 wave-lengths of light. For larger droplets, computations on the Mie theory become very lengthy, but it has been shown by Bricard in two very interesting papers[8] that for drops more than about 5 wave-lengths in radius, the Mie theory can be approximated by combining the purely geometrical theory of reflection and refraction given by Wiener[9] and the classical diffraction theory due to Airy.[10] From both these approaches there emerges the interesting fact, for some time rather mysterious, that a large droplet acts on an area of a plane wave front twice that of the cross section of the droplet. Bricard[8] following Mecke[11] has shown that a droplet of radius R (meters) scatters by reflection an amount of flux πER^2 (lumens) when illuminated by E lumens/m^2; that is to say, all the flux that strikes it; and that it scatters by diffraction a further flux πER^2 lumens, making a total of $2\pi ER^2$ lumens. Almost all of the second of these amounts is scattered in a small solid angle about the direction of the incident beam, and contributes to the formation of the well-known corona.

While an analytical expression can in this way be found for $\beta(\varphi)$, it will be very complicated, and it is preferable to substitute numerical values in Eq. (6), and integrate mechanically. Bricard[8] has furnished separate tables for the two parts of the function in units of ER^2, so that they may be used for computation with little trouble.** The function representing the result of diffrac-

[5] D. Sinclair, J. Opt. Soc. Am. **37**, 475 (1947).
[6] G. Mie, Ann. d. Physik (4)**25**, 377 (1908).
[7] V. K. LaMer and D. Sinclair, O.S.R.D. No. 1857, Department of Commerce Office of Publication Board, Report No. 944.
[8] J. Bricard, J. de phys. et rad. **4**, 57–66 (1943); Ann. de Geophys. **2**, 231–248 (1946).
[9] C. Wiener, Nova Acta Kaiser Leopold Deutsche Akad. d. Naturf. Halle **73 iii**, 3 (1907); **91 iii**, 81 (1910).
[10] G. Airy, Cambridge Phil. Trans. **5**, 183 (1834). See also J. M. Pernter and F. M. Exner, *Meteorologische Optik* (Leipzig, 1922), second edition, p. 476.
[11] R. Mecke, Ann. d. Physik **65**, 257 (1921).
** The two parts of the light are not completely incoherent; but for large droplets the neglect of this does not produce a very serious error, and greatly simplifies the calculations.

tion is actually as follows:

$$I_d=\tfrac{1}{4}\alpha^2\left[\frac{2J_1(u)}{u}\right]^2, \tag{7}$$

where I_d is the intensity (lumens/steradian) in the direction φ, due to diffraction by a droplet of radius R,

$$\alpha=2\pi R/\lambda, \quad u=\alpha\sin\varphi,$$

and $J_1(u)$ is the Bessel function of the first order. It is of interest that for $\varphi=0°$ and $\alpha=30$, $I_d=55.98I_r$, where I_r is the intensity due to reflection and refraction. This means that these large droplets give a very great preponderance of forward scattering.

In view of this we shall neglect that part of the atmosphere behind the lamp; then because of the small values of Ψ involved we may write r_0 for (r_1+r_2) in the expression $e^{-\sigma(r_1+r_2)}$ without much error. Numerical estimates indicate that this should not increase the value of E_2 by as much as one percent. Then, integrating Eq. (6),

$$E_2=2\pi I_0 e^{-\sigma r_0}$$

$$\times\int_0^{\Psi}\int_0^{r_0/(1+\psi\cot\Theta)}\frac{\psi}{(r_0-r)^2+r^2\psi^2}\beta(\varphi)dr d\psi, \tag{8}$$

where φ is a function of r and ψ defined by

$$\sin\varphi=\frac{r_0\psi}{[(r_0-r)^2+r^2\psi^2]^{\frac{1}{2}}}. \tag{9}$$

Numerical integration is necessary.

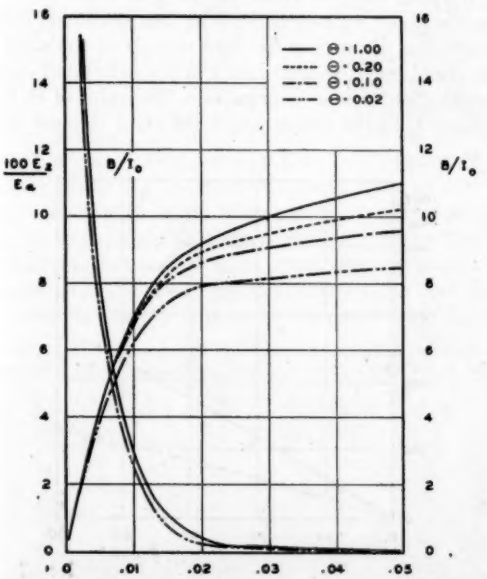

FIG. 5. Percentage error and distribution of luminance, Case IV.

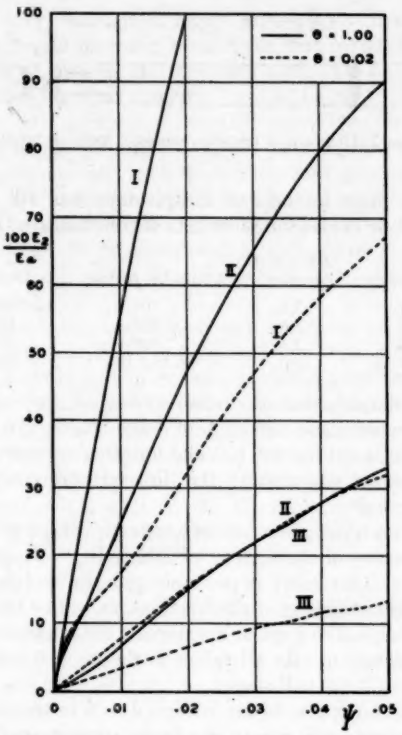

FIG. 6. Percentage error, Cases I to III, for two values of Θ.

4. CALCULATIONS FROM EQUATION (8)

The sort of atmosphere envisaged in this paper is a foggy one, characterized by droplets of several microns radius, in such numbers that they limit the visual range in daylight to 1000 meters or less. A concentration of 10^6 droplets/m^3, each of radius 2.5 microns, has an extinction coefficient

$$\sigma=2\pi NR^2=3.93\times10^{-3}[m^{-1}],$$

corresponding to a visual range of just under 1000m under the usual assumptions.[12] If the radii of the droplets is 5μ, a concentration of $2.5\times10^{-7}/m^3$ will have the same effect, or we may substitute 6.25×10^6 droplets/m^3, each of radius 10 microns.

While the visual range is unchanged by this sort of reciprocal variation of number and cross section, it will be evident from inspection of Eqs. (7) and (8) that the phenomenon in which we are interested will be a function of the size of the droplets. It also seems likely that if we observe the source from distances somewhat less than the visual range the ratio between the scattered and direct light will be different.

[12] S. Q. Duntley, J. Opt. Soc. Am. 38, 237 (1948). "The meteorological range—is—that distance for which the contrast transmittance of the atmosphere is two percent."

FIG. 7. Diagram of telephotometer of variable aperture.

The main features of the phenomenon will be displayed by considering four sets of conditions, as follows:

Case	Radius of droplets	Number per m³	Distance
I	2.5μ	10^8	1000 m
II	2.5	10^8	500
III	2.5	10^8	200
IV	10.0	6.25×10^6	500

To simplify the calculation somewhat, the computations were made for light of wave-length $\pi/6=0.524$ microns, but they will be valid for other wave-lengths if the droplet size and all the distances are changed in proportion.

For each case, four values were adopted for the angular opening of the light: $\Theta=0.02$, 0.10, 0.20, and 1.00 radians. This latter is probably practically equivalent to a light radiating in all directions, as will be seen from the results. The angular aperture of the telephotometer was allowed to take all values in the range $0\leqslant\Psi\leqslant0.05$ radians (2° 52′ half-angle).

The results are shown in Figs. 2 to 5 in terms of the percentage error due to the finite angular aperture of the telephotometer, assuming that the correct result should be E_a, given by Eq. (1). In Fig. 6 we have collected the results for three distances and for $\Theta=0.02$ and $\Theta=1.00$ radians. In Figs. 2 to 5 we have also indicated the luminance $B(\psi)$ of the field of view at an angle ψ from the light source, obtained from the relation

$$B(\psi)=(1/2\pi\sin\psi)dE_2/d\psi. \qquad (10)$$

This is shown only for $\Theta=0.02$ and $\Theta=1.00$ to avoid crowding, and is given as $B(\psi)/I_0$ m^{-2}.

5. EXPERIMENTAL CHECK

The results for $100E_2/E_a$ are surprisingly large, so large in fact that they started a most thorough search for a major error in computation. No such mistake could be discovered, but it was decided nevertheless to check the general magnitude of the effect by direct experiment. Accordingly a telephotometer of variable angular aperture was constructed, using a very large and excellent old transit as a starting point. The telescope of this instrument has a focal length of 76.5 cm.

The optical arrangements are shown in Fig. 7. The objective L_1, which was bloomed, forms an image of the distant light in the plane of the iris diaphragm I. Just behind this is a field lens L_2, which forms an image of L_1 on the cathode of a photo-multiplier tube P. This ensures that no matter what the angular aperture of the photometer as defined by the opening of the iris, the same area of the photo-multiplier cathode will be illuminated. Filters may be inserted at F.

The iris was provided with arbitrary graduations, and these were calibrated by pointing the instrument at a small lamp in the laboratory, focusing it after removing L_2, F, and P and replacing them by an eye-piece, then replacing these parts and making flux readings as the telescope was traversed across the field. The edges of the field of view were taken arbitrarily as the points where the flux had fallen to 90 percent of its maximum. This arbitrary choice is not important, since the flux invariably fell to 10 percent in a further 0.0005 radian (1.7′) on each side. Scattered light appeared to be negligible, since with the lamp outside the field by 0.005 radian, only about 1/1000 of the flux remained. Calibrating the iris in this way, a highly satisfactory straight line relation was found between the angular aperture of the telephotometer and the graduation on the iris.

This instrument, with a cathode-follower circuit of standard type and a high-speed recording potentiometer, was installed 114 meters from a 100-watt pointolite lamp. This was in a housing which permitted the illumination of a cone of air having a half-angle of 0.30 radians. The lamp was run on regulated voltage. The path of sight was across the flat roof of a very large building, which screened it entirely from other sources. The telephotometer was in a very warm room, which precludes the possibility of condensation on the optical parts.

On March 27, 1949, a suitable fog occurred. No information is available about the particle sizes in this fog, but from visual observations an extinction coefficient $\sigma=31$ Km^{-1} was deduced, corresponding to a daylight visual range of about 125 meters. Thus while the fog was about 8 times as dense as that envisaged in the theory, the distance of the light was about the same as the visual range, so that case I in the calculated values should afford the best comparison. The value of Θ, 0.30 radians, is in the region where the error changes little

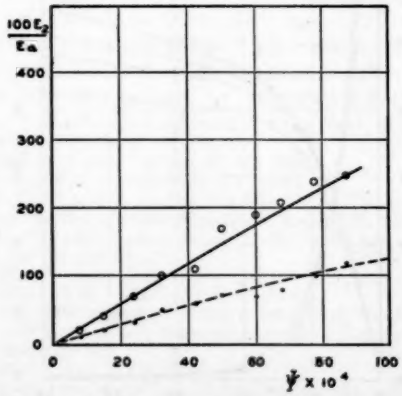

FIG. 8. Experimental values of $100E_2/E_a$, at two periods in a fog, March 27, 1949.

with Θ. An interference filter passing a narrow band at 0.54μ was placed at F.

Observations were made as follows: after a zero had been taken by capping the telescope, the iris was set at ten successive angular apertures increasing from $\psi=0.0008$ to 0.0087 radians (half-angle), following each other as rapidly as the recording potentiometer would take up a reading (about 2 seconds) and then at decreasing apertures back to 0.0008 radians again, after which another zero was taken. Fogs are very far from uniform, and only eight out of twelve sets of observations were usable. These were evaluated by taking the mean of the ascending and descending readings for each value of ψ, plotting these means, and extrapolating to $\psi=0$. The result of this extrapolation was then taken as E_a, and the error $100E_2/E_a$ plotted against ψ as shown in Fig. 8. The two curves in this figure refer to two sets of observations taken at different periods, the fog having become denser during the interval between the run shown by dots and that shown by open circles. The other six runs gave similar results.

Three nights later, advantage was taken of an exceptionally clear atmosphere to repeat the experiment. On this occasion, opening the iris from its smallest to its largest setting made less than 1 percent difference in the reading given by the lamp. We may conclude that the entire effect in fog is actually due to scattered light.

6. DISCUSSION

It will be seen that the error due to the finite opening of the telephotometer is even more serious than that indicated by the theory. Since the fog developed from a fairly dense haze, it is probable that a good many rather small droplets were present, which would certainly increase the effect. The theory could only be checked accurately if measurements of the size distribution of the fog particles and the total water-content of the fog were made at the same time, as for instance by the method of Houghton and Radford.[13] Every fog will be different from the last, and the theory above is therefore of no use for predicting the errors that will occur on a given occasion. The elaborate instrumentation that would be necessary to check the theory could only be justified in a foggy region and if other researches were contemplated. It is, however, felt that enough has been done to show the very serious errors that may occur in telephotometry through a foggy atmosphere. Few projectors have a narrower beam than that corresponding to $\Theta=0.02$ radians, and at such a spread the half-angle of the telephotometer would have to be kept down to about 0.001 radian (3.4′) to keep the error down to 5 percent on the assumptions of our Case I, which, as we have seen, are not extreme. An obvious cure for this state of affairs at night would be to have a large uniform source, subtending an angle at the telephotometer greater than the angular opening of the latter; but this could be used in the daytime only if this source were modulated.

There will be an additional error due to light scattered more than once, but it will probably be small. Attempts to calculate it lead to extremely complicated integrals.

These experiments do not settle the question raised by Duntley[2] and mentioned at the beginning of this paper, but in the opinion of the writer they strengthen the probability that the extinction coefficient for contrast is identical with that for a collimated beam. This is not the place to discuss fully the evidence for this identity; but, it should be noted that the percentage error of the telephotometer is independent of I_0, and also approaches zero when either Θ or Ψ approach zero. This permits the interpretation of the discrepancy between experiment and theory[3,14] as an experimental error of this type.

The source of error here considered is probably of some importance in the photometry of searchlights by the method[15] of comparison with a standard lamp placed beside the searchlight, unless very clear nights are used.

We shall close with a remark on the distribution of luminance $B(\psi)$ near the light-source. It is generally assumed that the normal absence of a well-defined corona around a lamp in a fog is due to the inhomogeneity of the fog. Our calculations, which refer to monodisperse fogs, show no distribution of luminance that would be appreciated as definite rings, even in monochromatic light. The absence of a corona, then, is adequately accounted for by the fact that a large range of values of ϕ (see Fig. 1) is associated with each value of ψ. The best coronas are seen in plane distributions of droplets, as on a window.

Thanks are due to Miss Marian Holmes and Mr. P. A. Tate for checking some of the work.

[13] H. G. Houghton and W. H. Radford, Papers in Phys. Oceanography & Met. (Cambridge, Massachusetts, 1938) Vol. 6, No. 4.

[14] J. R. Bibby, Air Ministry, Met. Res. Comm. Rep. MRP 236, London (April 21, 1945).

[15] Cameron, Rayner, Thomas, and Winch, in "Symposium on searchlights," Illum. Eng. Soc. London, pp. 50–74 (1948).

The Apparent Colors of Surfaces of Small Subtense—A Preliminary Report*

W. E. KNOWLES MIDDLETON AND MARIAN C. HOLMES
National Research Council of Canada, Ottawa

(Received March 28, 1949)

The early observations of König on the apparent tritanopia of the central fovea were confirmed by Willmer and Wright. Hartridge showed that the small size of the test field, rather than the location of its image on the retina, leads to the tritanopia. In the present work, twenty colors around the Munsell 5-plane were observed against a dark grey background at an angular subtense of 2 minutes and 1 minute of arc, under Macbeth (6800°K) daylight. They were matched with a complete chart of the 5-plane on a similar background and under the same illumination, a mask being provided for the isolation of one color. The phenomenon is somewhat personal but its main features are beyond question. The locus of the "reduced" colors approximates an ellipse with its long axis in the general direction red to blue-green but differing in eccentricity for different observers. The displacement of most of the colors is approximately towards or away from the blue end of the spectrum. There is evidence that the phenomenon cannot be explained by the effect of the macular pigment, but the "dominator-modulator" theory of Granit would seem to offer an explanation for it.

1. INTRODUCTION

THE investigation reported in this paper was suggested by the observations of Willmer,[1] Willmer and Wright,[2] Wright,[3] and Hartridge,[4] on the apparent tritanopia of the central fovea, and especially by the work of Hartridge, whose observations indicate that the small size of the test field, rather than the location of its image on the retina, leads to the tritanopia. It occurred to one of us that if this is so, a number of colors of fairly high chroma should be investigated to determine quantitatively how they appear when subtending angles of only a few minutes at the eye of the observer, since such information might be of practical, as well as theoretical, importance.

FIG. 1. General view of the apparatus.

It may be well to summarize briefly the characteristics of tritanopia, as observed by König.[5] Tritanopes:

(1) match yellow-green (0.556–0.570μ) with an unsaturated complementary blue
(2) confuse greenish-yellow with grey and rose-purple
(3) confuse blue-green with blue
(4) confuse yellowish green with bluish violet
(5) confuse orange with reddish purple
(6) have a neutral band in the yellow (0.562–0.570μ)
(7) see the violet end of the spectrum as very dark green
(8) match yellow and blue with grey;

but

(9) there is no confusion between reds and greens.

We may state immediately that the present experiments demonstrate quite clearly that the eye tends toward trianopia when small areas of color are observed against a dark grey background. The above items 2 to 5 inclusive, and 9, are apparent in

TABLE I.

	First Group		Second Group
0	5*R* 5/6	10	10*R* 5/6
1	5*YR* 5/8	11	10*YR* 5/8
2	5*Y* 5/6	12	2.5*GY* 5/6
3	5*GY* 5/8	13	10*GY* 5/6
4	2.5*G* 5/8	14	10*G* 5/6
5	5*BG* 5/6	15	10*BG* 5/6
6	10*B* 5/6	16	5*PB* 5/10
7	10*PB* 5/10	17	5*P* 5/10
8	7.5*P* 5/8	18	2.5*RP* 5/10
9	5*RP* 5/10	19	10*RP* 5/10

* Contribution from the Division of Physics, National Research Council, Ottawa, Canada, as N.R.C. No. 1947.
[1] E. N. Willmer, Nature **153**, 774 (1944).
[2] E. N. Willmer and W. D. Wright, Nature **156**, 119 (1945).
[3] W. D. Wright, *Researches on Normal and Defective Color Vision*, (Henry Kimpton, London, 1946).
[4] H. Hartridge, Phil. Trans. Royal Soc. **B232**, 419 (1947).
[5] A. König, *Physiologische Optik* (Johann Ambrosius Barth, Leipzig, 1903), p. 396.

the results, but of course the conditions of the experiments do not permit the evaluation of items 1, 6, and 7. Item 8 does not seem to be confirmed in any way.

2. PLAN OF THE EXPERIMENTS

The experiments were designed to determine the appearance of small circular disks of Munsell papers when viewed from such a distance that they subtended either 2 minutes or 1 minute of arc. The diameter chosen was 3 mm, the corresponding distances being 5.15 m and 10.30 m, respectively. Obviously the possible combinations of background, color of illuminant, and illuminance are without number, and since our purpose was to make a preliminary investigation, we confined our study to dark grey backgrounds (reflectance about 2.5 percent), and artificial daylight having a color temperature of about 6800°K, produced by means of incandescent lamps and Macbeth filters.

Most of the observations were taken by two women, H. and R., aged 22. Additional observations, but not as complete, were made by observer M., male, aged 46. All these observers had normal color vision as determined by the A.O. test and the Farnsworth dichotomous test, and better than average color discrimination as indicated by the Farnsworth-Munsell 100-hue test. All had acuity

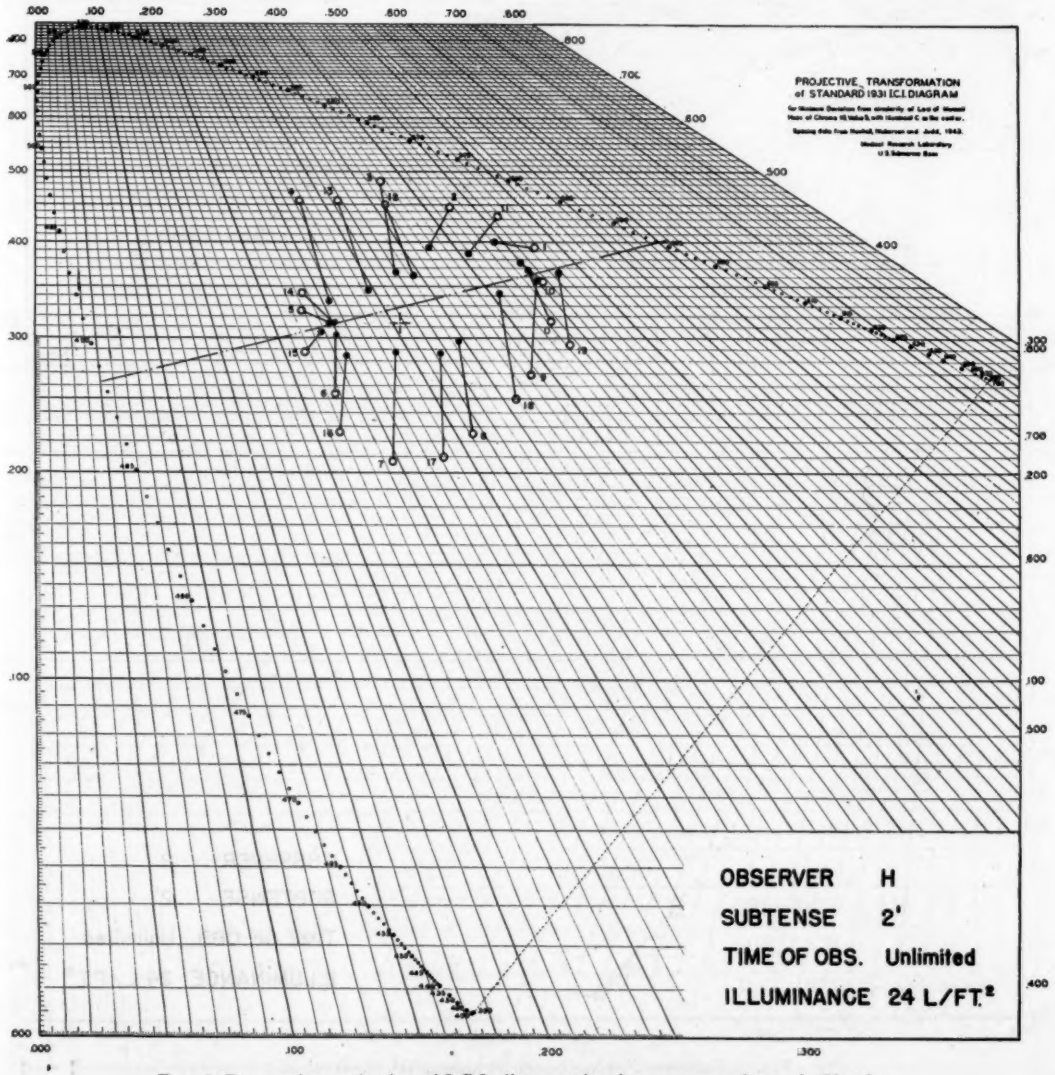

FIG. 2. Perspective projection of I.C.I. diagram showing apparent change in 20 colors. Subtense 2'. Illuminance 24 lumens/ft². Observer H.

about 20/15 (observer R. with glasses), and good muscle balance. Observer M. has about 0.38 diopter of astigmatism in each eye at 90°, but was not conscious of any effects due to this during the experiments.

The most distinct difference between the eyes of the three observers is in Y/B ratio.[6] This was measured at about the time the observations were discontinued, and it was found that observers R. and M. had Y/B ratios of about 1.06, observer H., on the contrary, 0.92, indicating large differences in macular pigmentation. This will be referred to below.

Much study was given to the question of a suitable experimental method. It is not claimed that the method finally adopted is free from all objections on psychological grounds, but only that it led to the description of a visual phenomenon that is quite distinct, if somewhat personal in its details. Briefly stated, the method is as follows: Individual small colors are presented to the observer in a completely random order against the chosen background and illuminated by the chosen lighting. The observer, seated at the proper distance, is provided with a chart containing a large number of colors, systematically arranged, mounted

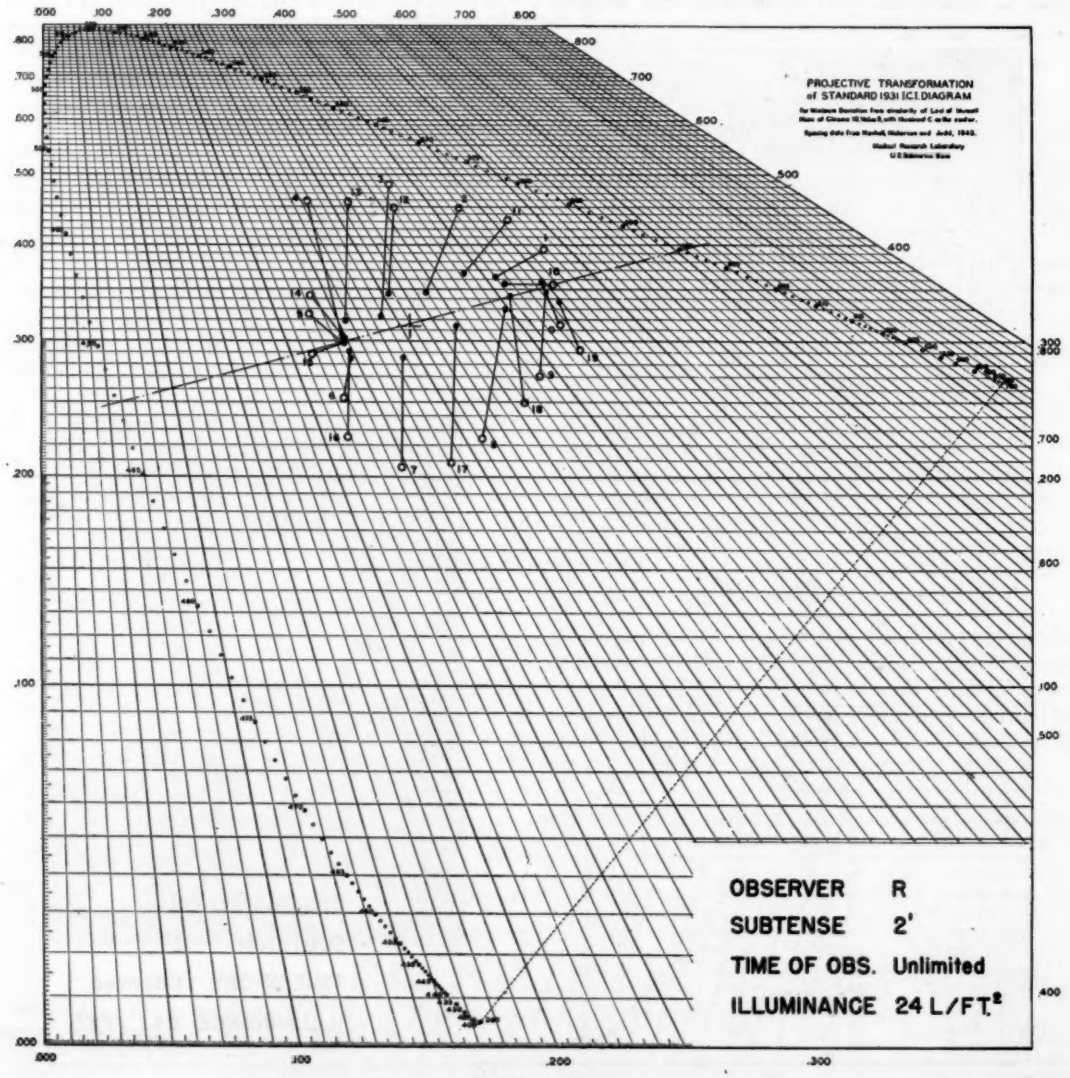

FIG. 3. Subtense 2'. Illuminance 24 lumens/ft². Observer R.

[6] J. W. T. Walsh, *Photometry* (Constable & Company, London, 1926), p. 263.

on a similar background, and illuminated in as nearly as possible the same way as the small colors. He is also given a mask of color and reflectance similar to the background, with which any one color may be isolated. The colors of the chart are provided with code numbers (read through another aperture in the mask). When the observer is satisfied with the match, he calls out the proper code number, which is recorded by the experimenter, who then removes the small color from the field of view and substitutes another. An obvious variation is to display the small color for only a short interval, and then remove it, so that the observer has to make the match from memory.

It should be remarked that the colors of the comparison chart are large enough to avoid the phenomenon of induced tritanopia.

The advantages of this way of making the experiment are:

(a) It is simple mechanically.

(b) It gives the observer a simple decision of equality to make, or at most an interpolation in one attribute only (chroma) between two neighboring colors.

(c) When a number of small colors are presented to the observer in completely random order, he is unlikely to try to memorize his previous responses.

(d) The results are easy to evaluate statistically.

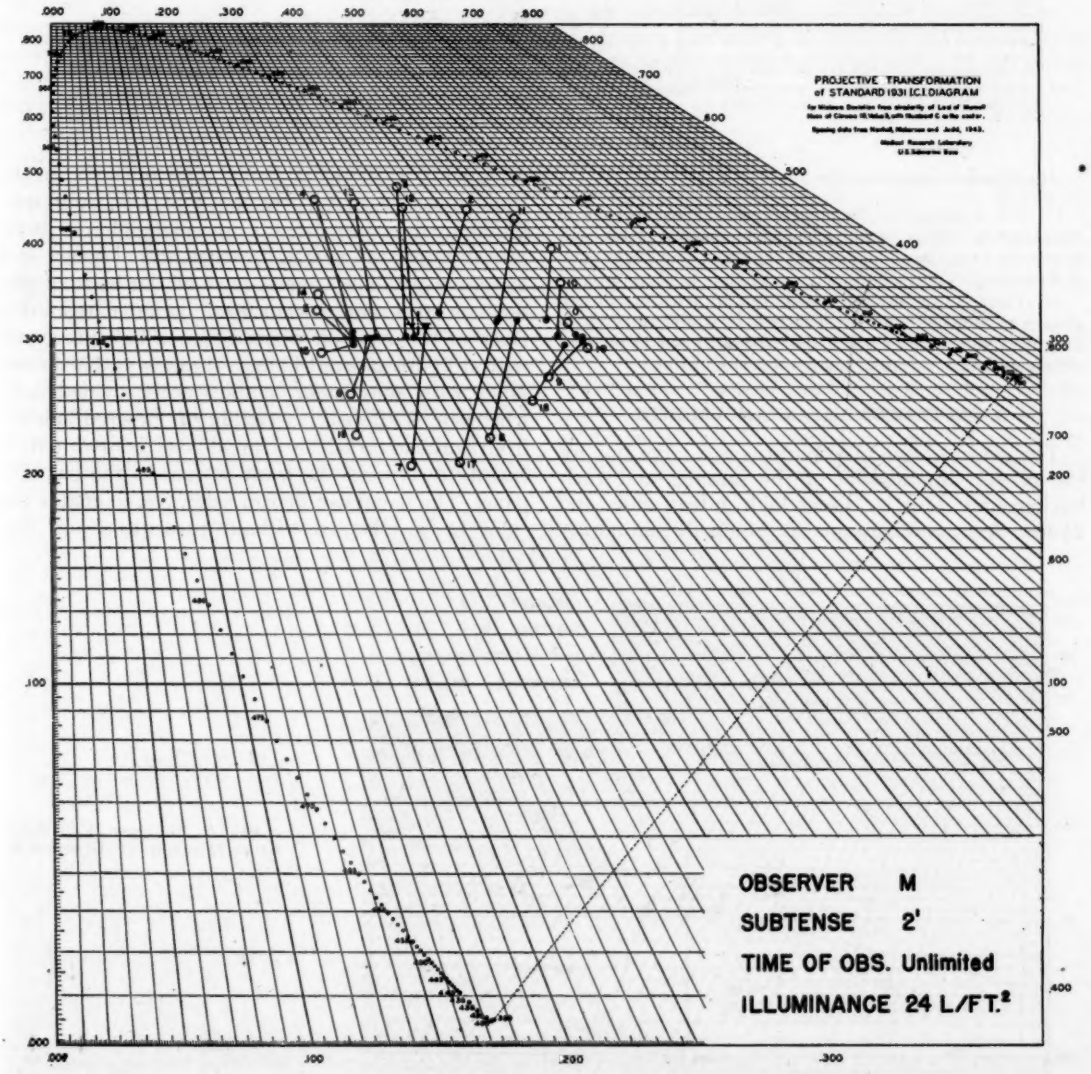

FIG. 4. Subtense 2′. Illuminance 24 lumens/ft². Observer M.

about 20/15 (observer R. with glasses), and good muscle balance. Observer M. has about 0.38 diopter of astigmatism in each eye at 90°, but was not conscious of any effects due to this during the experiments.

The most distinct difference between the eyes of the three observers is in Y/B ratio.[6] This was measured at about the time the observations were discontinued, and it was found that observers R. and M. had Y/B ratios of about 1.06, observer H., on the contrary, 0.92, indicating large differences in macular pigmentation. This will be referred to below.

Much study was given to the question of a suitable experimental method. It is not claimed that the method finally adopted is free from all objections on psychological grounds, but only that it led to the description of a visual phenomenon that is quite distinct, if somewhat personal in its details. Briefly stated, the method is as follows: Individual small colors are presented to the observer in a completely random order against the chosen background and illuminated by the chosen lighting. The observer, seated at the proper distance, is provided with a chart containing a large number of colors, systematically arranged, mounted

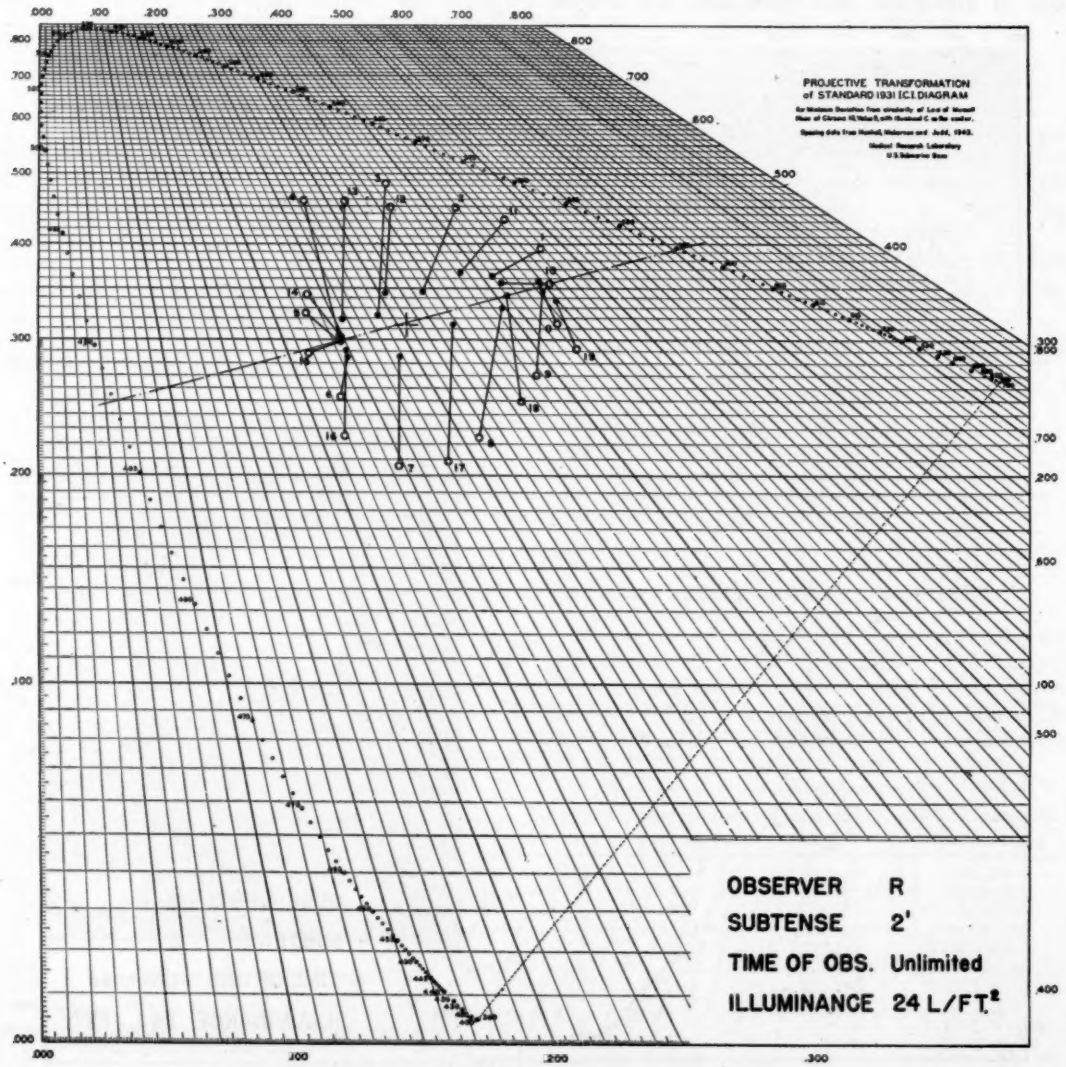

FIG. 3. Subtense 2'. Illuminance 24 lumens/ft². Observer R.

[6] J. W. T. Walsh, *Photometry* (Constable & Company, London, 1926), p. 263.

on a similar background, and illuminated in as nearly as possible the same way as the small colors. He is also given a mask of color and reflectance similar to the background, with which any one color may be isolated. The colors of the chart are provided with code numbers (read through another aperture in the mask). When the observer is satisfied with the match, he calls out the proper code number, which is recorded by the experimenter, who then removes the small color from the field of view and substitutes another. An obvious variation is to display the small color for only a short interval, and then remove it, so that the observer has to make the match from memory.

It should be remarked that the colors of the comparison chart are large enough to avoid the phenomenon of induced tritanopia.

The advantages of this way of making the experiment are:

(a) It is simple mechanically.

(b) It gives the observer a simple decision of equality to make, or at most an interpolation in one attribute only (chroma) between two neighboring colors.

(c) When a number of small colors are presented to the observer in completely random order, he is unlikely to try to memorize his previous responses.

(d) The results are easy to evaluate statistically.

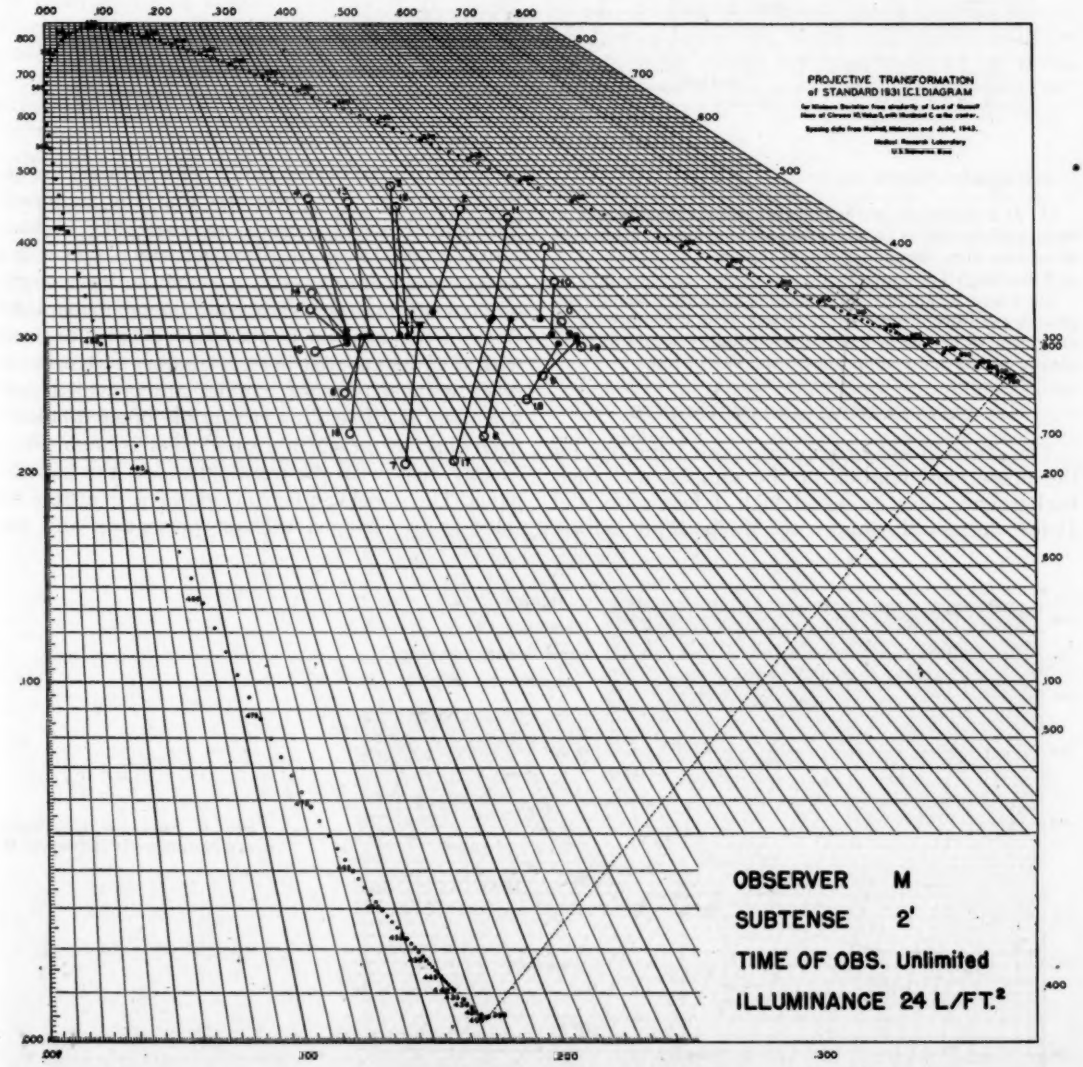

FIG. 4. Subtense 2'. Illuminance 24 lumens/ft². Observer M.

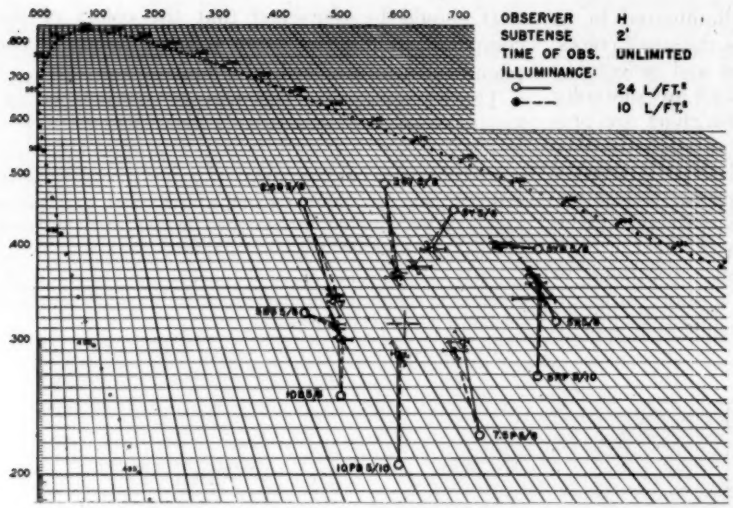

FIG. 5. Subtense 2'. Comparison of 24 and 10 lumens/ft². Observer H.

Its disadvantages are:

(a) It is necessary for the observer to shift his direction of view, and to change the state of accommodation of his eyes, in passing from the small color to the chart and back again (1.8 diopters). This undoubtedly contributes to visual fatigue.

(b) There is an obvious possibility of after-images, although these have not been detected. It is difficult even to imagine a technique in which this possibility would be completely excluded, except at a great sacrifice of time.

3. EXPERIMENTAL ARRANGEMENTS

The central piece of apparatus is a large box for the proper illumination of the samples and their background. This is 7½-feet high, 6-feet wide, and 2½-feet deep, and contains six Macbeth luminaries, each with a 500-watt lamp. The opening in the front measures 3×4 feet, so that the uniformly illuminated area subtends an angle of 11° horizontally and 14° vertically when the observer is 5 meters away. The central part of the back of the box is a steel plate with a 9-in. diameter hole in it. Back of this runs on wooden rails a bakelite panel with a 2½-in. tapered hole; a number of hardwood plugs with convenient handles are provided, and when one of these is inserted in the tapered hole its front surface, on which a small color is mounted, is exactly flush with the front surface of the bakelite panel. The panel can be run sideways, to enable the color to be changed without presenting any dis-

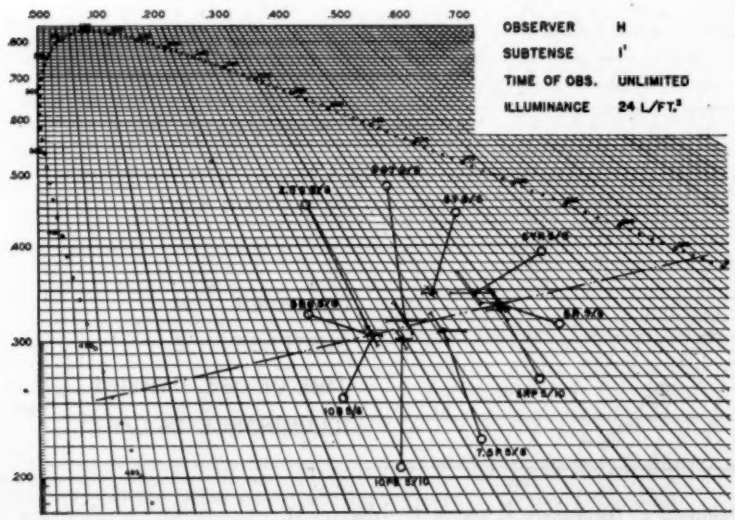

FIG. 6. Subtense 1'. Illuminance 24 lumens/ft². Observer H.

turbing patterns to the observer.** The front of the steel plate, the bakelite panel, and the wooden plugs, are all painted with the same color—a matte "black," actually a fairly neutral grey having a reflectance of about 2.5 percent.

The upper and lower parts of the back of the box were painted a color approximating Munsell *N*5/, in order to provide an adaptation field of about the same luminance as the sample colors. The observers were encouraged to look at this while colors were being changed. The entire outside of the box was painted in this neutral grey.

The comparison colors were arranged on a specially built stand of which Fig. 1 will give an adequate idea. This figure also shows the mask which the observer can manipulate to isolate any color desired, and the two Macbeth luminaires on pipe stands which illuminate the comparison colors. Equality of illumination between these and the sample colors was established before each series of experiments, using a photoelectric photometer. The mask was prevented from touching the comparison colors by the cut-out surround, as shown in Fig. 1.

Two people generally worked alternately as observer and experimenter, changing over after 40 observations. Ten colors were used concurrently, randomized by means of a list of numbers prepared beforehand by shuffling and dealing a double deck of playing cards with the court cards removed. In this way eight complete sets were obtained for each 80 observations, and it is believed that the order was quite sufficiently random for the purpose. For most of the experiments a second group of ten colors was also employed, lying between the colors of the first group when plotted on the (x, y) plane. The actual colors used are shown in Table I.

Each of these groups gave a rough circle when plotted on the Farnsworth perspective transformation of the I.C.I. mixture diagram,*** shown in Figs. 2 to 4. This chart was designed to present the colors of the Munsell 5-plane with a uniform chromaticity scale, and is therefore particularly suitable for our purpose.

4. SCOPE OF THE EXPERIMENTS

In the time available after the experimental procedure had been stabilized, only a limited number of conditions could be tested. As noted above, the background was dark grey throughout, the illumination artificial daylight. The following experiments were performed, always with 50 observations of each color except for experiment *D*, in which 100 sets were made:

Experiment

- A Twenty colors in 2 sets of 10 each, for three observers. (Comparison of observers). Subtense 2′, illuminance 24 lumens/ft², time of observation unlimited.
- B Ten colors, two observers, subtense 2′, illuminance 10 lumens/ft², time of observation unlimited.
- C Ten colors, two observers, subtense 1′, illuminance 24 lumens/ft², time of observation unlimited.
- D Ten colors, two observers, subtense 2′, illuminance 24 lumens/ft², time of observation 5 sec.

These observations enable us to compare three observers under similar conditions, to establish the equivalence of two interlocking sets of colors, to compare the 2′ and the 1′ subtense, to compare two

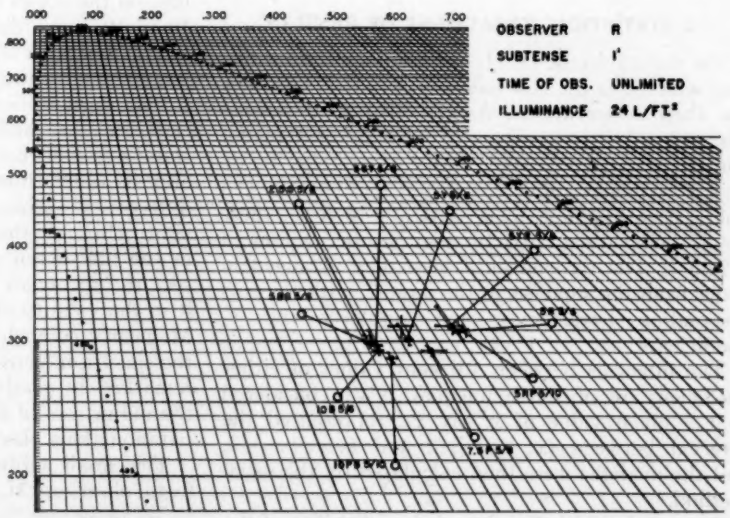

FIG. 7. Subtense 1′. Illuminance 24 lumens/ft². Observer R.

** There were other mechanical features for use with an alternative experiment which was tried and found unsatisfactory.
*** Published by the Medical Research Laboratory, U. S. Submarine Base, as Diagram No. 38.

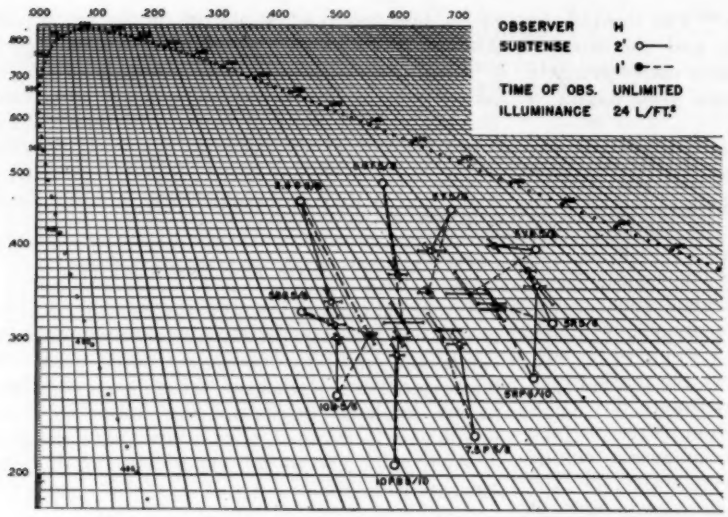

FIG. 8. Comparison of subtense 2′ and 1′. Observer H.

values of illuminance (unfortunately in rather a narrow range), and to compare matching by looking alternately at the sample and comparison colors with matching by memory. An estimate of the effect of practice could also be derived from the results, especially those of experiment *D*.

A control experiment was also tried, in which large (30 mm) disks of a number of colors were exhibited. No evidence of any systematic shift appeared, though errors of one hue step or one chroma step were often made. No evidence of an apparent change in value was found as long as the illuminance of the sample color was the same as that of the comparison chart.

5. STATISTICAL TREATMENT OF RESULTS

On the advice of Dr. J. W. Hopkins the median was selected as the best measure of central tendency for these observations. As the dispersion is two-dimensional, it is necessary to calculate medians for the trilinear coefficients x and y separately. To do this a frequency table was scored for the observed colors corresponding to a particular sample, these colors being designated by their proper values of x and y. The x-coefficients were then arranged in order from the smallest to the largest, with the corresponding frequencies, and similarly the y-coefficients.

The intervals between adjacent values of either coefficient are, of course, unequal. It was considered that a given value of x, say x_n, represented the interval between $(x_n+x_{n-1})/2$ and $(x_{n+1}+x_n)/2$, and the medians were then calculated by the usual method.[7]

As a statistical indication of the reliability of the observations, a method of confidence ranges due to W. R. Thompson[8] was applied, using tables by Nair.[9] These are indicated in Figs. 5 to 9 by crosses, which indicate the interval in which the medians of 99 percent of an infinite number of such sets of observations might be expected to lie. We may make the general remark that there is a good deal of difference in the certainty of matching the various colors.

6. RESULTS AND DISCUSSION

The results of experiment *A* are shown in Figs. 2 to 4 for the three observers. Each original color is joined to the corresponding reduced color by a line. In each instance 50 sets of observations were made first on the colors 0 to 9, and then 50 sets on colors 10 to 19, more than a month later. The increased familiarity with the observations does not seem to be reflected in the results.

The most noticeable feature of these results is that they are highly personal. There is a general similarity between the results for observers H. and R., but those for observer M. are entirely different. A broken line has been drawn in each figure through the concentrations of observations in the blue-green and red, and produced to intersect the spectrum locus. Those for H. and R. cut it in the vicinity of 488 and 595 mμ, while that for M. nearly coincides with the line $y=.300$, cutting the spectrum locus near 490 and 625 mμ. It may be remarked in passing that this direction is that of the major axis of the reduced ellipse of colors for a tritanomalous observer, as given by Farnsworth.[10]

The small subtense of the colors obviously affects observer M. much more than the others.

[7] J. P. Guilford, *Psychometric Methods*, (McGraw-Hill Book Company, Inc., New York, 1936), p. 41.

[8] W. R. Thompson, Ann. Math. Stat. **7**, 122–128 (1936). (Quoted by Nair.)

[9] K. R. Nair, Indian J. Statistics **4**, 551–558 (1939).

[10] Dean Farnsworth, J. Opt. Soc. Am. **33**, 568 (1943), p. 574, Fig. 11.

Similar differences probably occur between E. N. Willmer and H. Hartridge, since Hartridge reports[11] that he is unable to repeat Willmer's experiment[1] with a small circle made up of four quadrants of colored paper. Willmer's experiment was set up and observed by H. and M.; the effects described by Willmer appeared quite clearly to M., but H. was not satisfied with the description. (Observer R. was not available for this experiment.)

It was mentioned above that H. has a Y/B ratio less than unity, R. and M. greater than one. Since the results of these experiments for R. and H. greatly resemble one another, M.'s being much different, it seems unlikely that macular pigmentation has anything to do with the differences. On the other hand the relative sensitivity to red and green is different for M. and H., as measured on a visual trichromatic colorimeter, H. being less red-sensitive. It is regretted that this instrument was not available when observer R. was employed on these experiments; but H. and R. obtained similar readings on an Eastman color-temperature meter, used in place of an anomaloscope, and thus there is a little evidence to relate anomaloscope readings to the slope of the "red to blue-green axis" and possibly also to the degree of tritanomaly induced by the small subtense, though it is difficult to see why there should be a connection.

Coming now to the details of these figures, it will be seen that all the colors except those in the red and blue-green tended to move towards or away from the general direction of the violet end of the spectrum. Observers H. and R., it is true, find an exception to this rule in the yellow, but still the changes in this can be considered as an addition of blue. We do not think it wise to lay too much stress on the actual color changes at this stage, partly because the phenomenon is obviously highly personal, and also because the manner of experimenting may lead to artifacts, although we have not been able to devise a better.† Nevertheless it is quite clear that the color changes support and amplify the description given by Hartridge of this induced tritanomaly (ref. 11, p. 391). He says:

> "...it will be found that the following changes occur: red and orange remain unchanged; yellow, yellow-green and green have blue added to them; blue-green remains unchanged; blue, violet, mauve and crimson have blue subtracted from them."

If we interpret "remain unchanged" as meaning "remain of the same general hue," this is a good description of the phenomenon as we have found it.

Experiment B was similar to experiment A except that the illuminance was reduced, and only the colors 0 to 9 were employed. The results were negative for both observers (H. and R.). The comparison of experiments A and B for observer H. is shown in Fig. 5, in which the 99 percent confidence intervals have been indicated by short lines with crossed ends, parallel to the co-ordinate network. Except for the color $5Y$ 5/6, the difference between the two sets is not significant; but it must be remembered that the ratio of the two values of illuminance is only $2\frac{1}{2}$ to 1. We made some attempts to observe out of doors in full daylight, but these were handicapped by unsuitable weather, and all that can be said is that the phenomenon is qualitatively the same even under several hundred lumens/ft^2.

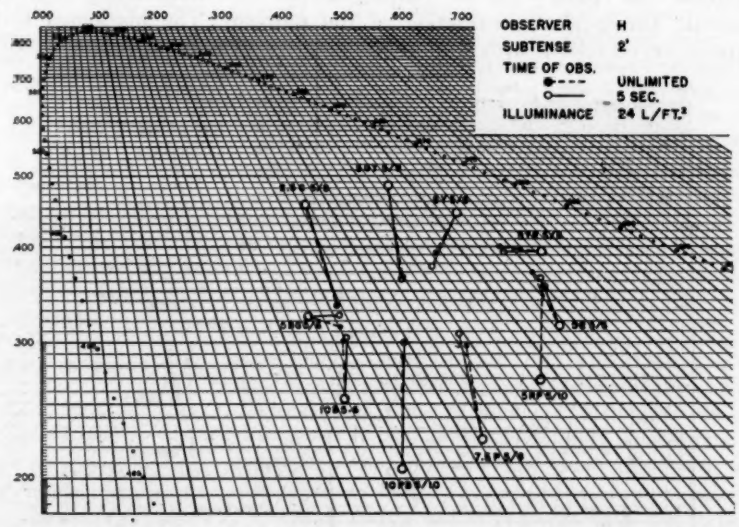

FIG. 9. Comparison of unlimited time of observation with 5-second time of observation. Subtense 2'. Observer H.

[11] H. Hartridge, Nature **155**, 391–392 (1945).

† Some overlap ought to have been provided in the chart of comparison colors. It is possible that the omission of this may have affected the position of colors 17 and 8 for observer M.

It is possible that the peculiar behavior of the yellow may be connected with the fact that yellow, alone among the hues, completely changes its character with reduced illumination, becoming brown; but actually the color 5*Y* 5/6 does not appear a true yellow to begin with, even against a dark background, so that the explanation loses much of its plausibility.

Experiment *C* differed from experiment *A* in that the colors were observed at twice the distance. It would have been preferable to have made them half the size (diam. 1.5 mm.) but this was thought to be inadvisable because of the difficulty of producing neat enough circles of such a small diameter in Munsell papers. The original colors were not made larger because insufficient space was available when the experiment was started, but before experiment *C* the apparatus was transferred to a larger room.

The results for observers H. and R. appear in Figs. 6 and 7, and in Fig. 8 we have plotted a comparison of the 2′ and 1′ subtense for observer H. It will be noticed that at 1′, the red and blue-green colors begin to close in towards the neutral point ($x=.308$, $y=.314$), and for both observers the widely separated colors 2.5*G* 5/8, 5*BG* 5/6, and 10*B* 5/6 become virtually the same, and certainly indistinguishable. Now, however, and certainly for observer R., the changes in yellows and purples can no longer be described as a mere addition or subtraction of blue, but tend to the entire loss of chromatic sensation. There is a further interesting circumstance, for which we have no explanation, that the rough ellipse formed by R.'s colors at this subtense lies entirely on the purple side of the neutral. The general contraction of the pattern agrees, nevertheless, with Hartridge's statement (4, p. 576) that "the different colours lose colour at different visual angles; red and blue-green at small angles; yellow and blue at larger ones."

Experiment *D* limited to 5 seconds the time for which the colors were exposed, not with any thought that the phenomenon would not be completely developed in this interval, but to ensure that the comparison would be performed chiefly from memory. Figure 9 shows for observer H. how the results compare with those of experiment *A*, and the differences are scarcely significant. They suggest a slightly greater degree of induced tritanomaly. The scatter of these judgments was greater, and Fig. 10 shows the result of comparing two series of 50 sets of observations under such conditions.

As a general result of all these experiments, one might conclude that while the phenomenon of induced tritanomaly is highly personal, it varies little for a given observer with luminance or between memory and unlimited comparison. It must be remembered, however, that the range of conditions under which we have had time to work is very narrow, and that the effect of background color (in particular) remains to be investigated. As far as they go, our results do not conflict with Hartridge's theory (4, p. 575) of the "antichromatic responses," the four nervous mechanisms that he believes responsible for the reduction of color vision with angular subtense, and thus for the high acuity displayed by the eye in spite of chromatic aberration.

7. SUBSIDIARY EXPERIMENTS

The effect of very brief exposure was investigated, though scarcely more than qualitatively, by mounting a large camera shutter in the apparatus. The blackened leaves of this happened to have about the same reflectance as the background used

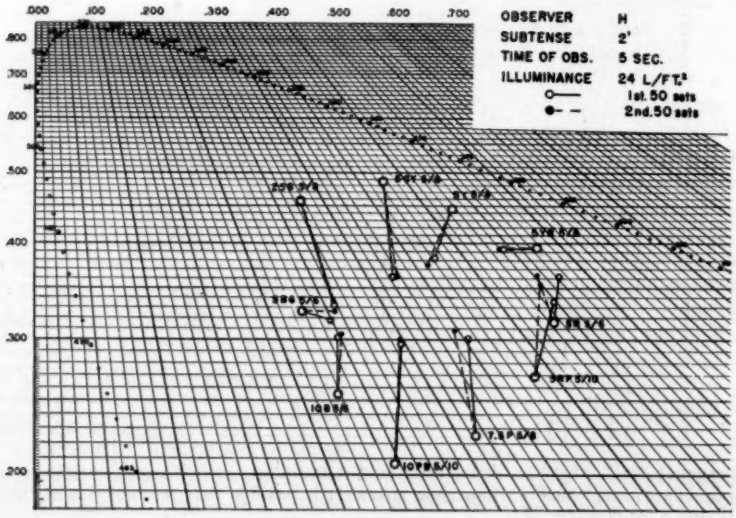

FIG. 10. Comparison of 2 groups of 50 observations of each color. Subtense 2′. Observer H. Time 5 seconds.

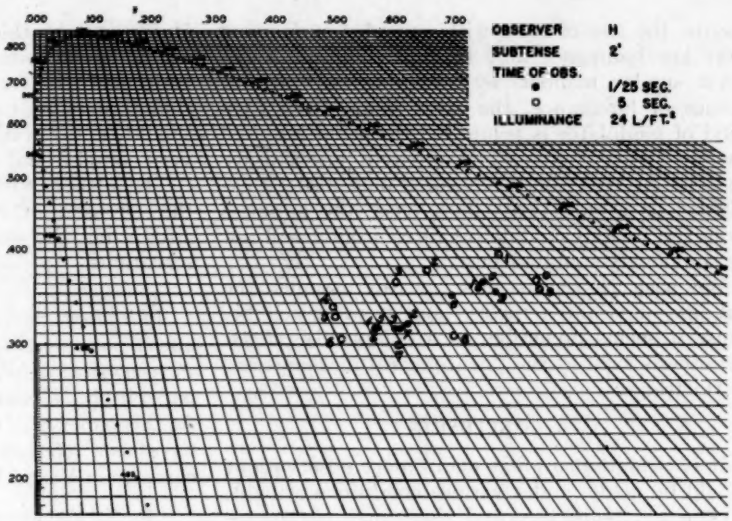

FIG. 11. Subtense 2'. Comparison of 5 sec. and 1/25-sec. exposure, 24 lumens/ft². Observer H.

in our other experiments, and enabled us to display the various small colors in random order for intervals as short as 1/25 second, (The shutter was calibrated with a photocell and oscillograph just before the experiments.) Observers H. and M. each made 25 sets of observations on colors 0 to 9 with 24-lumens/ft² illuminance at exposures of 1/25 and 1/7 sec. The scatter of these observations is large, but nevertheless it may be worthwhile to present Fig. 11, showing how the results for 1/25 sec. exposure compare with those for 5 seconds. Perhaps all we should say about this is that the tritanomaly is much more pronounced. This agrees with Hartridge's idea (4, p. 576) that the four nervous mechanisms "are adjusted for the production of colourless vision, when the fovea is not being stimulated."

Another qualitative experiment was made with the well-known *Glenn Colorule* published by Sidney Blumenthal & Co., which consists of two series of dyed textile samples appearing (in daylight) brown to blue and yellow-green to purple, respectively. After a metameric match had been obtained on the rule in the usual way, the observer looked at it (not the entire rule) from a distance of about 30 feet. Observers M. and H. agreed that their own matches were in no way disturbed by this reduction in angular subtense; an observation which merely suggests that it may be the actual color, not its spectral composition, which determines its appearance when small.

8. THEORETICAL CONSIDERATIONS

The "neurological hypothesis" of Hartridge[4] assumes a complicated "switching" mechanism in the connections between retina and brain, and independent evidence for such a mechanism is entirely lacking. It is therefore important to investigate other possible explanations for the phenomena we have studied. Such an explanation may be found in the recent "dominator-modulator" theory of Granit,[12] which is at least based on numerous electro-physiological experiments on lower animals. We do not feel competent to express an opinion on the validity of Granit's conclusions, but wish only to suggest a way in which our observations may be explained on the basis of the dominator-modulator theory, supposing the latter to be correct.

A stimulus consisting of light falling on an extended area of the fovea will excite a large number of the various modulators, each according to its own response to the distribution of wave-lengths present in the stimulus. These will send signals to the brain which determine the perceived color. At the same time a large number of dominators will be affected, and these will send signals which determine the brightness perceived.

If now the area of the fovea exposed to the stimulus is reduced, fewer dominators and modulators will be excited. In order to explain the reduction in color-sensation with very small fields, it is necessary to assume only that the brain, in order to perceive color, has to receive responses from a certain minimum number of modulators, a number that is least in the case of the red modulators, somewhat greater for the blue-green, and a good deal greater for those modulators producing the remaining sensations of color. The dominators, on the other hand, continue to give sensations of brightness no matter how few of them are stimulated.

Though it has nothing to do with our experi-

[12] R. Granit, *Sensory Mechanisms of the Retina* (Oxford University Press, London, 1947).

ments, the loss of color with extended surfaces at very low luminance may be explained in a somewhat similar manner, by assuming that at low values of luminance, the total signal from each kind of modulator is below the threshold required by the higher centers. The apparent insensitivity to color in very short exposures may also be explained as a statistical effect, since the impulses from the various modulators of each kind will not be completely simultaneous.

We wish to repeat that all this assumes the validity of Granit's theory, and is presented because it seems preferable to a completely *ad hoc* hypothesis such as the "neurological mechanisms" of Hartridge.

9. CONCLUSION

It is clear that a great many more observations should be made, under various conditions of light, background, subtense, and time, and not necessarily confined to the Munsell 5-plane, which was chosen because of its range of available papers. Unfortunately this sort of experimentation does not fit in well with the program of this laboratory, and cannot be continued. It is possible, however, that it may be carried on elsewhere. This report should be taken as an elementary description of a very complex and interesting phenomenon.

The authors wish to thank Dr. J. W. Hopkins of the Division of Applied Biology for invaluable advice on the statistical treatment of the observations.

Addendum: Shortly after passing the proof of the above paper, we happened to notice a reference in *Psychological Abstracts* for January 1949 to the paper by B. N. Kompaneisky†† with the above title. As this paper is in the same field it should certainly have been referred to. It is not listed in the Bibliography of Visual Literature 1939–1944.†††

†† B. N. Kompaneisky, Prob. Fiziol. Optiki **2**, 187–197 (1944), (in Russian with English summary).

††† Publication No. 11, Historical Library, Yale Medical Library, 1945.

JOURNAL OF THE OPTICAL SOCIETY OF AMERICA VOLUME 39, NUMBER 7 JULY, 1949

The Ridgway Color Standards with a Munsell Notation Key

D. H. HAMLY
Department of Botany, University of Toronto, Toronto, Canada

(Received March 28, 1949)

A correlation of a copy of Ridgway's *Color Standards and Nomenclature* with the Munsell *Book of Color* is presented. This key will prolong the usefulness of data already recorded in Ridgway terms, but is not recommended for making new observations in terms of specific color names.

INTRODUCTION

WHILE Ridgway's *Color Standards and Nomenclature*[1] has been widely useful in biological work,[2] it is unfortunate that physical means did not exist at the time of publication of this work that would have permitted its precise duplication and republication, or a precise description of its colors in terms of some permanent system.

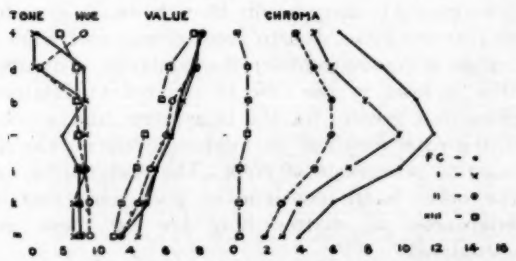

FIG. 1. Ridgway Hue 15—Yellow-Orange.

In 1938, during the course of work in which color descriptions were required, it was noted that irregularities existed in the Ridgway book which could be explained as resulting from aging and wear. These changes shifted the colors of certain chips from their original positions in the color solid. When a key correlating Ridgway to a more permanent set of Ridgway standards could not be found, one was compiled using the Munsell notation. While it was felt that the usefulness of this key was limited because of the non-permanent state of the Ridgway color chips for which it was con-

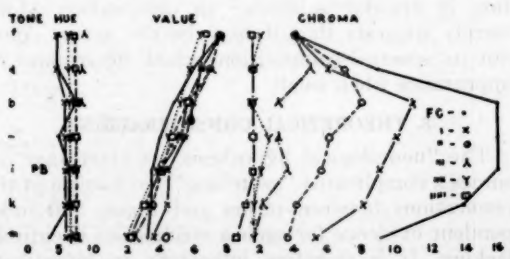

FIG. 2. Ridgway Hue 49—Blue.

[1] R. Ridgway, *Color Standards and Nomenclature* (Washington, D. C., 1912).

[2] D. H. Hamly, Science **109**, 605–608 (1949).

TABLE I. Ridgway color names and Munsell equivalents with supplementary notes.

Color name	Plate	Hue and tone number	Munsell notation	Notes
Absinthe Green	XXXI	29″	5GY 6.6/5.5	
Acajou Red	XIII	1′i	2.5R 4.0/5.5	
Acetin Blue	XXXV	49″k	7.5PB 3.5/4.0	
Ackermann's Green	XVIII	35′k	3.5G 4.5/4.0	
Aconite Violet	XXXVII	63″	7.5P 4.5/7.0	
Ageratum Violet	XXXVII	63″b	7.5P 5.4/6.0	
Alice Blue	XXXIV	45″b	10B 6.5/4.0	
Alizarine Blue	XXI	51′m	6PB 3.5/6.0	
Alizarine Pink	XIII	1′d	2.5R 6.5/7.5	MF
Amaranth Pink	XII	69d	2.5RP 6.0/11.0	
Amaranth Purple	XII	69i	8.5RP 3.2/10.0	
Amber Brown	III	13k	5YR 3.8/8.0	
Amber Yellow	XVI	21′b	5Y 8.0/8.0	SF
American Green	XLI	33‴i	10GY 5.2/3.0	
Amethyst Violet	XI	61	3.5P 5.0/14.0	2.5P 3.4/15.0
Amparo Blue	IX	51b	7.5PB 5.8/12.0	
Amparo Purple	XI	63b	5P 5.5/10.0	
Andover Green	XLVII	25⁗i	5GY 4.8/2.0	
Aniline Black	L	69⁗m	7.5P 2.5/1.0	
Aniline Lilac	XXXV	53″d	10.0PB 7.0/8.0	
Aniline Yellow	IV	19i	2.5Y 6.0/9.0	
Anthracene Green	VII	39m	5BG 3.5/4.5	
Anthracene Purple	XLIV	69⁗k	5RP 2.6/3.0	
Anthracene Violet	XXV	61′k	2.5P 3.5/6.0	
Antimony Yellow	XV	17′b	1YR 7.4/7.5	SF
Antique Brown	III	17k	7.5YR 4.4/5.0	
Antique Green	VI	35m	2.5G 3.5/2.0	
Antwerp Blue	VIII	45k	10B 3.0/5.0	
Apple Green	XVII	29′	7.5GY 6.5/8.0	
Apricot Buff	XIV	11′b	5YR 7.0/7.5	
Apricot Orange	XIV	11′	2.5YR 6.0/9.0	
Apricot Yellow	IV	19b	2.5Y 7.8/9.5	SF
Argus Brown	III	13m	6YR 3.8/4.0	
Argyle Purple	XXXVII	65″b	2.5RP 5.2/8.0	
Army Brown	XL	13‴i	5YR 4.4/2.5	
Artemisia Green	XLVII	33⁗	2.5BG 5.6/1.0	
Asphodel Green	XLI	29‴	5GY 5.8/3.5	
Aster Purple	XII	67i	1P 3.4/10.0	
Auburn	II	11m	2.5YR 3.4/4.0	
Auricula Purple	XXVI	69′k	3.5RP 3.2/8.0	
Avellaneous	XL	17‴b	10YR 7.0/3.0	
Azurite Blue	IX	53m	8.5PB 2.5/6.0	
Barium Yellow	XVI	23′d	7.5Y 8.0/7.5	SF
Baryta Yellow	IV	21f	5Y 8.4/6.0	SF
Bay	II	7m	10R 2.6/6.0	
Begonia Rose	I	1b	5R 5.6/11.5	SF
Benzo Brown	XLVI	13‴i	5YR 4.5/2.0	
Benzol Green	VII	41	7.5BG 5.0/8.0	8.0BG 5.2/10.5
Berlin Blue	VIII	47m	5PB 2.6/5.0	
Beryl Blue	VIII	43f	5B 8.0/6.0	
Beryl Green	XIX	41′b	7.5BG 6.4/8.0	
Bice Green	XVII	29′k	7.5GY 5.0/4.0	
Biscay Green	XVII	27′i	6GY 5.2/4.5	
Bishop's Purple	XXXVII	65″	2.5RP 4.0/7.2	
Bister	XXIX	15″m	9YR 3.5/2.0	
Bittersweet Orange	II	9b	1YR 6.0/10.0	SF
Bittersweet Pink	II	9d	2.5YR 7.0/8.5	SF
Black	LIII	NG00	N2.2/	
Blackish Brown (1)	XLV	1⁗m	10RP 1.0/3.0	
Blackish Brown (2)	XLV	5⁗m	2.5R 2.8/1.0	
Blackish Brown (3)	XLV	9⁗m	5YR 2.5/1.0	
Blackish Green-Blue	VIII	43m	5B 3.2/5.0	
Blackish Green-Gray	LII	35⁗⁗m	5G 2.4/0.2	
Blackish Mouse Gray	LI	15⁗⁗m	7.5YR 3.0/0.5	
Blackish Plumbeous	LII	49⁗⁗k	7.5PB 3.0/1.0	
Blackish Purple	XI	65m	10P 2.0/3.5	
Blackish Red-Purple	XII	67m	5RP 2.4/5.0	
Blackish Slate	LIII	CGm	N2.6/	
Blackish Violet	X	59m	1P 2.5/5.0	
Blackish Violet-Gray	LII	59⁗⁗m	2.5P 3.2/0.5	
Blanc's Blue	XX	47′k	2.5PB 4.0/7.0	
Blanc's Violet	XXIII	59′k	1.5P 3.5/3.0	
Blue-Violet	X	55	9PB 3.5/16.0	
Blue-Violet Black	XLIX	57⁗⁗m	2.5P 3.0/0.5	
Bluish Black	XLIX	49⁗⁗m	6.5PB 2.0/1.5	
Bluish Glaucous	XLII	37⁗⁗f	7.5BG 8.0/2.5	
Bluish Gray-Green	XLII	41‴	2.5BG 5.5/2.0	
Bluish Lavender	XXXVI	57″d	2.5P 6.2/6.0	
Bluish Slate-Black	XLVIII	45⁗⁗m	5PB 2.5/2.0	
Bluish Violet	X	57	9PB 3.8/16.0	
Bone Brown	XL	13⁗⁗m	5YR 2.6/1.5	
Bordeaux	XII	71k	5RP 3.4/6.0	
Bottle Green	XIX	37′m	3.5G 3.4/3.0	
Bradley's Blue	IX	51	6PB 4.2/16.0	
Bradley's Violet	XXIII	59′	2.5P 4.5/9.0	
Brasil Red	I	5i	7.5R 4.0/10.5	
Bremen Blue	XX	43′b	2.5B 6.5/6.0	
Brick Red	XIII	5′k	10R 3.6/5.0	
Bright Chalcedony Yellow	XVII	25′	2.5GY 8.0/7.0	
Bright Green-Yellow	V	27	4GY 7.0/12.0	
Brownish Drab	XLV	9⁗⁗	5YR 4.6/2.0	
Brownish Olive	XXX	19″m	2.5Y 3.8/3.0	
Brownish Vinaceous	XXXIX	5‴b	5R 6.0/3.0	
Brussels Brown	III	15m	7.5YR 3.5/4.0	
Buckthorn Brown	XV	17′i	10YR 5.0/7.0	

Color name	Plate	Hue and tone number	Munsell notation	Notes
Buff-Pink	XXVIII	11″d	5YR 7.0/5.0	
Buffy Brown	XL	17⁗i	10YR 5.5/4.0	
Buffy Citrine	XVI	19′k	2.5Y 5.0/5.0	
Buffy Olive	XXX	21″k	5Y 5.0/4.0	
Buff-Yellow	IV	19d	2.5Y 8.0/7.0	SF
Burn Blue	XXXIV	47″f	5PB 7.5/7.0	
Burnt Lake	XII	71m	2.5RP 3.4/4.0	
Burnt Sienna	II	9k	10R 3.4/8.0	
Burnt Umber	XXVIII	9″m	2.5YR 3.0/2.0	
Cacao Brown	XXVIII	9″i	2.5YR 4.6/4.0	
Cadet Blue	XXI	49′i	6PB 4.5/9.0	
Cadet Gray	XLII	45‴b	2.5PB 6.5/3.0	
Cadmium Orange	III	13	5YR 6.0/14.0	
Cadmium Yellow	III	17	7YR 6.6/12.0	0.5Y 7.2/13.0
Calamine Blue	VIII	43d	5B 7.5/6.0	
Calla Green	V	25m	1GY 4.0/4.5	
Calliste Green	VI	31i	5GY 6.5/8.0	
Cameo Brown	XXVIII	7″k	2.5YR 4.0/3.0	
Cameo Pink	XXVI	71′f	5RP 8.0/9.0	
Campanula Blue	XXIV	55″b	9PB 6.0/10.0	
Capri Blue	XX	43′i	2.5B 4.4/5.5	
Capucine Buff	III	13f	9YR 8.0/6.0	BF
Capucine Orange	III	13d	6YR 7.0/8.5	SF
Capucine Yellow	III	15b	8.5YR 7.0/11.0	
Carmine	I	1i	5R 3.4/12.5	
Carnelian Red	XIV	7′	10R 6.0/11.5	
Carob Brown	XIV	9′m	2.5YR 2.0/4.0	
Carrot Red	XIV	7′b	10R 8.5/6.0	SF
Cartridge Buff	XXX	19″f	2.5Y 8.5/3.5	SF
Castor Gray	LII	35⁗⁗i	5G 4.8/0.5	
Cedar Green	VI	31m	5GY 4.5/4.0	
Celandine Green	XLVII	33⁗⁗b	2.5BG 6.5/1.0	
Cendre Blue	VIII	43b	7.5B 6.5/8.0	
Cendre Green	VI	35b	1G 7.5/8.0	
Cerro Green	V	27m	5GY 4.2/3.5	
Cerulean Blue	VIII	45	10B 5.0/10.0	9.5B 4.7/11.0
Chaetura Black	XLVI	17⁗⁗m	10YR 2.4/1.0	
Chaetura Drab	XLVI	17⁗⁗k	10YR 3.6/1.0	
Chalcedony Yellow	XVII	25′b	10Y 8.2/6.5	
Chamois	XXX	19″b	2.5Y 7.5/6.0	
Chapman's Blue	XXII	49*i	6.5PB 4.5/8.0	
Chartreuse Yellow	XXXI	25″d	10Y 8.2/6.0	
Chatenay Pink	XIII	3′f	6R 7.5/6.0	MF
Chessylite Blue	XX	45′k	9B 3.5/5.0	
Chestnut	II	9m	10R 3.0/5.0	
Chestnut-Brown	XIV	11′m	2.5YR 3.4/3.0	
Chicory Blue	XXIV	57*d	9PB 6.4/8.0	
China Blue	XX	45′i	10B 5.0/5.5	
Chinese Violet	XXV	65′b	5P 5.4/8.0	
Chocolate	XXVIII	7″m	2.5YR 2.6/2.5	
Chromium Green	XXXII	31″i	7.5GY 5.5/5.0	
Chrysolite Green	XXXI	27″b	2.5GY 7.0/5.0	
Chrysopraise Green	VII	37b	10GY 7.0/6.5	
Cinereous	LII	49⁗⁗d	7.5PB 6.5/1.5	
Cinnamon	XXIX	15″	7.5YR 6.2/6.0	
Cinnamon-Brown	XV	15′k	7.5YR 3.8/4.0	
Cinnamon-Buff	XXIX	17″b	1Y 7.2/6.0	
Cinnamon-Drab	XLVI	13⁗	5YR 5.5/2.5	
Cinnamon-Rufous	XIV	11′i	2.5YR 5.0/8.0	
Citrine	IV	21k	5Y 4.5/5.0	
Citrine-Drab	XL	21‴i	5Y 5.2/4.0	
Citron Green	XXXI	25″b	10Y 7.0/5.0	
Citron Yellow	XVI	23′b	7.5Y 8.0/8.0	SF
Civette Green	XVIII	31′k	9GY 4.8/4.0	
Claret Brown	I	5m	7.5R 3.0/5.0	
Clay Color	XXIX	17″	1Y 5.4/5.0	
Clear Cadet Blue	XXI	49′	6PB 5.5/10.0	
Clear Dull Green Yellow	XVII	27′b	5GY 7.5/7.0	
Clear Fluorite Green	XXXII	33″b	10GY 7.0/5.0	
Clear Green-Blue Gray	XLVIII	45⁗⁗d	10B 6.0/1.5	
Clear Payne's Gray	XLIX	49⁗⁗b	6.5PB 5.2/1.5	
Clear Windsor Blue	XXXV	49″	7.5PB 4.6/6.0	
Clear Yellow-Green	VI	31b	3.5GY 8.0/7.5	
Clove Brown	XL	17⁗⁗m	10YR 2.8/1.5	
Cobalt Green	XIX	37′b	3.5G 7.0/5.0	
Colonial Buff	XXX	21″d	5Y 8.4/6.0	
Columbia Blue	XXXIV	47″b	3.5PB 5.5/8.0	
Commelina Blue	XXI	51′	7.5PB 5.0/15.0	
Congo Pink	XXVIII	7″b	1YR 7.0/7.0	
Coral Pink	XIII	5′d	10R 7.0/7.5	SF
Coral Red	XIII	5′	7.5R 5.2/9.5	
Corinthian Pink	XXVII	3″d	5R 7.2/4.5	SF
Corinthian Purple	XXXVIII	69″k	7.5RP 3.4/6.0	
Corinthian Red	XXVII	3″	3.5R 5.2/6.0	
Cornflower Blue	XXI	53′	8.5PB 4.8/15.0	
Corydalis Green	XLI	29″d	7.5GY 8.0/3.0	
Cossack Green	VI	33m	7.5GY 4.4/3.0	
Cosse Green	V	29i	5GY 5.8/9.0	
Cotinga Purple	XI	63k	7.5P 3.5/8.0	
Courge Green	XVII	25′i	2.5GY 5.8/4.5	
Court Gray	XLVII	29⁗⁗f	7.5G 8.0/1.5	
Cream-Buff	XXX	19″d	2.5Y 8.0/6.5	
Cream Color	XVI	19′f	3.5Y 8.5/5.5	SF
Cress Green	XXXI	29″k	5GY 4.5/4.0	
Cyanine Blue	IX	51m	7.5PB 3.0/6.0	

TABLE I.—*Continued.*

Color name	Plate	Hue and tone number	Munsell notation	Notes
Dahlia Carmine	XXVI	71′k	7.5RP 3.2/6.0	
Dahlia Purple	XII	67k	1P 2.8/7.0	
Danube Green	XXXII	35″m	3.5G 3.5/2.5	
Daphne Pink	XXXVIII	60″b	5RP 6.0/9.0	
Daphne Red	XXXVIII	60″	5RP 5.0/9.0	
Dark American Green	XLI	33‴k	2.5G 3.5/2.5	
Dark Aniline Blue	X	55m	9PB 2.6/2.0	
Dark Anthracene Violet	XXV	61′m	5P 2.5/3.0	
Dark Bluish Glaucous	XLII	37‴b	5G 7.0/2.5	
Dark Bluish Gray-Green	XLII	41‴k	7.5BG 3.5/2.5	
Dark Bluish Violet	X	57m	10PB 2.5/5.0	
Dark Cadet Blue	XXI	49′m	6PB 3.5/5.0	
Dark Chrysolite Blue	XX	45′m	9B 3.0/5.0	
Dark Cinnabar Green	XIX	39′k	10G 4.0/3.0	
Dark Citrine	IV	21m	5Y 4.2/4.0	
Dark Corinthian Purple	XXXVIII	60″m	10RP 3.2/4.0	
Dark Cress Green	XXXI	29″m	5GY 3.5/3.5	
Dark Delft Blue	XLII	45‴m	2.5PB 2.6/3.0	
Dark Diva Blue	XXI	51′k	7.5PB 3.8/9.0	
Dark Dull Blue-Violet	XXXVI	53″k	10PB 3.2/4.0	
Dark Dull Bluish Violet (1)	XXIV	57′k	10PB 3.0/5.0	
Dark Dull Bluish Violet (2)	XXXV	51″k	10PB 3.8/4.0	
Dark Dull Bluish Violet (3)	XXXVI	57″k	5P 3.0/5.0	
Dark Dull Violet-Blue	XXIV	53′k	9PB 3.6/4.0	
Dark Dull Violet-Blue	XXXV	55′k	10PB 3.2/4.0	
Dark Dull Yellow-Green	XXXII	31″m	7.5GY 3.5/3.0	
Dark Glaucous-Gray	XLVIII	37‴b	7.5BG 5.0/1.5	
Dark Gobelin Blue	XXXIV	43′k	2.5B 3.8/3.0	
Dark Grayish Blue-Green	XLVIII	37‴k	7.5BG 3.0/0.5	
Dark Grayish Blue-Violet	XXIV	55′k	10PB 3.4/4.0	
Dark Grayish Brown	XLV	5‴k	2.5R 3.8/1.5	
Dark Grayish Lavender	XLIII	57″b	2.5P 6.0/3.5	
Dark Grayish Olive	XLVI	21‴k	5Y 3.5/1.0	
Dark Green	XVIII	35′m	2.5G 3.5/2.5	
Dark Green-Blue Gray	XLVIII	45‴	10B 4.2/3.5	
Dark Green-Blue Slate	XLVIII	45‴k	5PB 2.5/3.0	
Dark Greenish Glaucous	XLI	33‴b	10GY 6.5/4.0	
Dark Greenish Olive	XXX	23″m	7.5Y 3.8/3.0	
Dark Gull Gray	LIII	CG	N4.3/	
Dark Heliotrope Gray	L	65‴	5P 4.5/2.5	
Dark Heliotrope Slate	L	65‴k	5P 3.0/1.5	
Dark Hyssop Violet	XXXVI	59″k	7.5P 3.5/4.0	
Dark Indian Red	XXVII	3″m	5R 3.5/2.5	
Dark Ivy Green	XLVII	25‴k	5GY 3.6/2.0	
Dark Lavender	XLIV	61‴b	6P 6.5/6.0	
Dark Livid Brown	XXXIX	1‴k	2.5R 3.6/2.0	
Dark Livid Purple	XXXVII	63″m	5RP 2.5/3.0	
Dark Livid Red	Apparently a synonym for Dark Livid Brown			
Dark Madder Blue	XLIII	53‴k	8.5PB 3.2/3.0	
Dark Madder Violet	XXV	63′m	5P 2.5/3.0	
Dark Maroon Purple	XXVI	71′m	2.5RP 3.4/4.0	
Dark Medici Blue	XLVIII	41‴i	7.5B 4.0/1.0	
Dark Mineral Red	XXVII	1″m	2.5R 3.5/2.0	
Dark Mouse Gray	LI	15‴k	7.5YR 3.5/0.5	
Dark Naphthalene Violet	XXXVII	61″m	10P 3.0/3.0	
Dark Neutral Gray	LIII	NGk	N3.1/	
Dark Nigrosin Violet	XXV	65′m	5P 2.2/3.0	
Dark Olive	XL	21‴m	5Y 3.5/2.0	
Dark Olive-Buff	XL	21‴	5Y 6.2/4.5	
Dark Olive-Gray	LI	23‴i	7.5Y 4.0/1.5	
Dark Orient Blue	XXXIV	45″k	10B 4.0/3.0	
Dark Payne's Gray	XLIX	49‴k	6.5PB 2.8/1.5	
Dark Perilla Purple	XXXVII	65″m	7.5RP 3.0/3.5	
Dark Plumbago Blue	XLIII	53″b	10PB 5.6/3.0	
Dark Plumbago Gray	L	61‴	7.5P 4.5/1.5	
Dark Plumbago Slate	L	61‴k	7.5P 3.5/1.0	
Dark Plumbeous	LII	49‴i	7.5PB 4.2/1.0	
Dark Porcelain Green	XXXIII	39″k	2.5PG 3.8/2.0	
Dark Purple-Drab	XLV	1‴i	8RP 3.6/2.0	
Dark Purplish Gray	LIII	67‴k	10P 3.5/0.5	
Dark Quaker Drab	LI	1‴k	5RP 3.5/1.0	
Dark Russian Green	XLII	37″k	7.5G 3.5/2.0	
Dark Slate-Purple	XLIV	65″k	2.5RP 3.4/3.5	
Dark Slate-Violet (1)	XLIII	57‴k	1P 2.6/1.0	
Dark Slate-Violet (2)	XLIV	61‴k	7.5P 3.8/2.5	
Dark Soft Blue-Violet	XXIII	55′k	9PB 3.8/6.0	
Dark Soft Bluish Violet	XXIII	57′k	10PB 3.0/8.5	
Dark Sulphate Green	XIX	39′i	10G 4.6/4.0	
Dark Terre Verte	XXXIII	41″k	2.5BG 3.8/2.0	
Dark Tyrian Blue	XXXIV	47″k	5PB 3.8/3.0	
Dark Varley's Gray	XLIX	57‴k	2.5P 3.4/1.0	
Dark Vinaceous	XXVII	1″	2.5R 4.6/5.0	
Dark Vinaceous-Brown	XXXIX	5‴k	7.5R 3.8/2.0	
Dark Vinaceous-Drab	XLV	5‴i	2.5R 3.8/1.5	
Dark Vinaceous-Gray	L	69‴	7.5P 4.6/2.0	
Dark Vinaceous-Purple	XXXVIII	67″k	3.5RP 3.4/5.0	
Dark Violet	X	59k	1P 3.2/7.0	
Dark Violet-Gray	LII	50‴k	2.5P 3.4/0.5	
Dark Violet-Slate	XLIX	53‴k	8.5PB 3.4/2.0	
Dark Viridian Green	VII	37k	6G 4.4/5.5	
Dark Yellowish Green	XVIII	33′m	10GY 2.5/3.0	
Dark Yvette Violet	XXXVI	55″m	1P 2.8/2.0	
Dark Zinc Green	XIX	37′k	5G 4.5/3.0	
Dauphin's Violet	XXIII	59′i	2.5P 3.8/8.0	
Dawn Gray	LII	35‴‴d	2.5B 6.8/0.5	

Color name	Plate	Hue and tone number	Munsell notation	Notes
Deep Aniline Lilac	XXXV	53″b	10B 6.0/10.0	
Deep Blue-Violet	X	55i	9PB 2.8/14.0	
Deep Bluish Glaucous	XLII	37‴d	7.5BG 7.8/3.0	
Deep Bluish Gray-Green	XLII	41‴i	5BG 4.2/2.5	
Deep Brownish Drab	XLV	9‴i	5YR 3.5/2.0	
Deep Brownish Vinaceous	XXXIX	5‴	5R 5.2/3.5	
Deep Cadet Blue	XXI	49′k	6PB 4.4/8.0	
Deep Chicory Blue	XXIV	57″b	10PB 5.4/10.0	
Deep Chrome	III	17b	9YR 6.8/12.0	SF
Deep Chrysolite Green	XXXI	27″	2.5GY 6.0/4.5	
Deep Colonial Buff	XXX	21″b	5Y 7.8/6.5	
Deep Corinthian Red	XXVII	3″i	6.5R 4.4/4.0	
Deep Delft Blue	XLII	45‴k	2.5PB 3.5/3.0	
Deep Dull Bluish Violet (1)	XXIV	57′i	10PB 3.8/9.0	
Deep Dull Bluish Violet (2)	XXXV	51″i	9PB 4.5/4.5	
Deep Dull Bluish Violet (3)	XXXVI	57″i	2.5P 3.8/6.0	
Deep Dull Lavender	XLIV	61‴d	7.5P 6.6/3.5	
Deep Dull Violaceous Blue	XXII	51′k	7.5PB 3.6/8.0	
Deep Dull Violet-Blue	XXXV	53″i	10PB 4.2/6.5	
Deep Dull Yellow-Green (1)	XXXII	31‴k	7.5GY 4.5/4.0	
Deep Dull Yellow-Green (2)	XXXII	33‴k	1G 4.4/3.0	
Deep Dutch Blue	XLIII	49‴	6.5PB 5.0/3.0	
Deep Glaucous-Gray	XLVIII	37‴‴d	2.5B 6.4/1.0	
Deep Glaucous-Green	XXXIII	39″b	5G 6.8/4.0	
Deep Grape Green	XLI	25‴i	2.5GY 5.0/3.0	
Deep Grayish Blue-Green	XLVIII	37‴i	7.5BG 3.8/1.5	
Deep Grayish Lavender	XLIII	57‴d	2.5P 6.2/3.0	
Deep Grayish Olive	XLVI	21‴i	5Y 4.0/1.0	
Deep Green-Blue Gray	XLVIII	45‴‴b	10B 4.5/3.0	
Deep Greenish Glaucous	XLI	33‴d	5G 8.0/3.0	
Deep Gull Gray	LIII	CGb	N5.7/	
Deep Heliotrope Gray	L	65‴‴b	5P 5.2/2.5	
Deep Hellebore Red	XXXVIII	71″i	7.5RP 4.2/6.0	
Deep Hyssop Violet	XXXVI	59′i	5P 3.8/7.0	
Deep Lavender	XXXVI	59″d	2.5P 6.5/6.0	
Deep Lavender-Blue	XXI	53′b	8.5PB 5.8/10.0	
Deep Lichen Green	XXXIII	37″d	1G 7.5/3.0	
Deep Livid Brown	XXXIX	1‴i	2.5R 4.5/2.5	
Deep Livid Purple	XXXVII	63″k	5RP 3.0/5.0	
Deep Madder Blue	XLIII	53‴i	8.5PB 3.6/4.0	
Deep Malachite Green	XXXII	35″	10GY 5.6/5.0	
Deep Medici Blue	XLVIII	41‴‴	7.5B 4.8/1.0	
Deep Mouse Gray	LI	15‴‴i	7.5YR 4.5/0.5	
Deep Neutral Gray	LIII	NGi	N3.7/	
Deep Olive	XL	21‴k	5Y 4.4/3.0	
Deep Olive-Buff	XL	21‴b	5Y 7.6/4.0	
Deep Olive-Gray	LI	23‴‴	7.5Y 5.0/1.0	
Deep Orient Blue	XXXIV	45′i	10B 4.5/3.0	
Deep Payne's Gray	XLIX	49‴i	6.5PB 3.8/2.0	
Deep Plumbago Blue	XLIII	53‴d	10PB 6.4/2.5	
Deep Plumbago Gray	L	61‴b	10P 5.2/1.0	
Deep Plumbeous	LII	49‴‴	7.5PB 5.0/1.5	
Deep Purplish Gray	LIII	67‴‴i	10P 3.8/1.0	
Deep Purplish Vinaceous	XLIV	69‴	7.5RP 4.8/5.0	
Deep Quaker Drab	LI	1‴‴i	5RP 4.0/1.0	MF
Deep Rose-Pink	XII	71d	5RP 6.6/12.0	
Deep Seafoam Green	XXXI	27″d	2.5GY 8.0/5.0	
Deep Slate-Blue	XLIII	49‴k	6.5PB 3.4/2.0	
Deep Slate-Green	XLVII	33‴k	10G 3.8/1.0	
Deep Slate-Olive	XLVI	29‴k	3.5G 4.0/1.0	
Deep Slate-Violet	XLIV	61‴i	7.5P 4.2/3.0	
Deep Slaty Brown	L	69‴k	7.5P 3.2/2.0	
Deep Soft Blue-Violet	XXIII	55′i	9PB 4.0/8.0	
Deep Soft Bluish Violet	XXIII	57′i	10PB 4.2/10.0	
Deep Turtle Green	XXXII	31″	8.5GY 6.0/7.0	
Deep Varley's Gray	XLIX	57‴i	2.5P 4.0/1.5	
Deep Vinaceous	XXVII	1″b	2.5R 5.6/6.5	
Deep Vinaceous-Gray	L	69‴b	7.5P 5.2/2.0	
Deep Vinaceous-Lavender	XLIV	65‴d	2.5RP 6.5/4.0	
Deep Violet-Gray	LII	50‴‴i	2.5P 4.5/0.5	
Deep Violet-Plumbeous	XLIX	53‴	8.5PB 4.0/4.0	
Deep Wedgewood Blue	XXI	51′d	7.5PB 7.0/10.0	
Delft Blue	XLII	45‴i	2.5PB 4.5/3.0	
Diamin-Azo Blue	XXXV	51″m	10PB 3.0/3.0	
Diamine Brown	XIII	3′m	7.5R 3.2/2.5	
Diamine Green	VII	37m	7.5G 3.5/3.0	
Diva Blue	XXI	51′i	7.5PB 4.5/11.0	
Drab	XLVI	17‴	10YR 5.5/3.0	
Drab-Gray	XLVI	17‴‴d	10YR 6.6/2.0	
Dragons-blood Red	XIII	5′i	7.5R 4.2/7.5	
Dresden Brown	XV	17′k	10YR 3.8/4.0	
Duck Green	XIX	39′m	10G 3.2/2.0	
Dull Blackish Green	XLI	33‴m	2.5G 2.5/1.5	
Dull Blue-Green Black	XLVIII	41‴‴m	7.5B 2.0/1.0	
Dull Blue-Violet (1)	XXIV	55•	9PB 4.5/12.0	
Dull Blue-Violet (2)	XXXVI	55″i	1P 3.6/6.0	
Dull Bluish Violet (1)	XXIV	57•	10PB 4.5/12.0	
Dull Bluish Violet (2)	XXXV	51″	10B 4.5/6.0	
Dull Bluish Violet (3)	XXXVI	57″	2.5P 4.2/9.0	
Dull Citrine	XVI	21′k	5Y 4.5/4.5	
Dull Dark Purple	XXVI	67′k	10P 3.5/9.0	
Dull Dusky Purple	XXVI	67′m	10P 2.6/3.0	
Dull Greenish Black (1)	XLVII	29‴‴m	3.5G 3.5/0.5	
Dull Greenish Black (2)	XLVII	33‴‴m	10G 3.0/0.5	
Dull Green-Yellow	XVII	27″	5GY 6.8/9.0	

TABLE I.—*Continued.*

Color name	Plate	Hue and tone number	Munsell notation	Notes
Dull Indian Purple	XLIV	69″″i	5RP 3.8/3.5	
Dull Lavender	XLIV	61″″f	10P 7.4/3.0	
Dull Magenta Purple	XXVI	67′i	10P 4.5/10.5	
Dull Opaline Green	XIX	37′f	3.5G 8.0/2.0	
Dull Purplish Black	L	65″″m	5P 2.6/1.0	
Dull Slate-Violet	Apparently a synonym for Dull Violet-Black			
Dull Violet-Black (1)	XLIV	61″″m	7.5P 3.0/1.0	
Dull Violet-Black (2)	XLIX	53″″m	8.5PB 2.8/1.5	
Dull Violet-Black	L	61″″m	7.5P 2.5/0.5	
Dull Violaceous Blue	XXII	51•	7.5PB 4.8/12.5	
Dull Violet-Blue	XXIV	53•	8.5PB 4.6/12.0	
Dull Violet-Blue	XXXV	53″	10PB 4.2/8.0	
Dusky Auricula Purple	XXVI	69′m	2.5RP 2.2/3.0	
Dusky Blue	XXII	49•m	6.5PB 4.4/4.0	
Dusky Blue-Green	XXXIII	39″m	5BG 3.4/1.5	
Dusky Bluish Green	XXXIII	41″m	2.5BG 3.2/1.0	
Dusky Blue-Violet (1)	XXIII	57′m	10PB 2.8/4.0	
Dusky Blue-Violet (2)	XXIV	55•m	10PB 2.4/2.0	
Dusky Brown	XLV	1″″k	8RP 3.2/1.5	
Dusky Drab	XLV	9″″k	5YR 3.5/1.0	
Dusky Dull Bluish Green	XLII	41″″m	7.5BG 2.6/2.0	
Dusky Dull Green	XLII	37″″m	7.5G 2.5/1.0	
Dusky Dull Violet (1)	XXXVI	57″m	5P 3.0/4.0	
Dusky Dull Violet (2)	XXXVI	56″m	7.5P 3.5/5.0	
Dusky Dull Violet-Blue	XXXV	53″m	10PB 3.2/3.0	
Dusky Green	XXXIII	37″m	5G 3.5/1.5	
Dusky Green-Blue (1)	XX	43′m	10BG 3.4/3.0	
Dusky Green-Blue (2)	XXXIV	43″m	5B 3.0/2.5	
Dusky Green-Gray	LII	35″″″k	5G 3.0/0.2	
Dusky Greenish Blue	XX	47′m	5PB 3.0/7.0	
Dusky Neutral Gray	LIII	NGm	N2.8/	
Dusky Olive-Green	XLI	25″″m	2.5GY 3.4/2.0	
Dusky Orient Blue	XXXIV	45″m	10B 3.5/3.0	
Dusky Purplish Gray	LIII	67″″″m	10P 2.5/0.5	
Dusky Slate-Blue	XLIII	49″″m	7.5PB 2.4/1.5	
Dusky Slate-Violet	XLIII	57″″m	2.5P 2.5/1.0	
Dusky Violet	XXIII	59′m	2.5P 3.4/2.0	
Dusky Violet-Blue (1)	XXIII	55′m	9PB 3.0/3.5	
Dusky Violet-Blue (2)	XLIII	53″″m	8.5PB 2.4/1.5	
Dusky Yellowish Green	XLI	29″″m	5GY 3.4/2.5	
Dutch Blue	XLIII	49″″b	8.5PB 6.0/3.0	
Ecru-Drab	XLVI	13″″d	6YR 6.6/2.0	
Ecru-Olive	XXX	21″i	5Y 5.8/5.0	
Elm Green	XVII	27′m	5GY 3.8/3.0	
Emerald Green	VI	35	10GY 7.5/9.0	2.0G 6.7/10.0
Empire Green	XXXII	33″m	1G 3.5/2.0	
Empire Yellow	IV	21b	4Y 8.2/10.0	SF
Endive Blue	XLIII	49″″d	8.5PB 7.0/5.0	
English Red	II	7i	10R 4.2/10.0	
Eosine Pink	I	1d	2.5R 6.0/12.0	MF
Etain Blue	XX	43′f	10BG 7.8/2.5	
Ethyl Green	VII	41i	7.5BG 4.0/7.0	
Eton Blue	XXII	49•k	6.5PB 3.5/8.0	
Etruscan Red	XXVII	5″	7.5R 5.0/4.5	
Eugenia Red	XIII	1′	2.5R 4.8/8.0	
Eupatorium Purple	XXXVIII	67″	2.5RP 5.5/8.0	
Fawn Color	XL	13″″	5YR 4.6/3.0	
Ferruginous	XIV	9′i	1YR 4.5/8.0	
Flame Scarlet	II	9	10R 6.0/14.0	
Flax-flower Blue	XXI	51′b	7.5PB 6.0/11.0	
Flesh Color	XIV	7′d	2.5R 7.0/6.5	SF
Flesh Ocher	XIV	9′b	2.5YR 6.6/8.0	SF
Flesh Pink	XIII	5′f	10R 8.0/5.5	MF
Fluorite Green	XXXII	33″	1G 6.4/6.0	
Fluorite Violet	XI	61m	5P 2.5/5.0	
Forest Green	XVII	29′m	7.5GY 4.5/3.5	
Forget-me-not Blue	XXII	51•b	7.5PB 6.2/10.0	
French Gray	LII	49″″″f	7.5PB 6.8/1.5	
French Green	XXXII	35″i	3.5G 4.6/3.5	
Fuscous	XLVI	13″″″k	5YR 3.5/1.0	
Fuscous-Black	XLVI	13″″″m	5YR 2.6/0.5	
Garnet Brown	I	3k	6R 3.0/10.0	
Gendarme Blue	XXII	47•k	5PB 4.0/6.0	
Gentian Blue	XXI	53′i	8.5PB 4.0/10.0	
Geranium Pink	I	3d	4R 6.4/11.0	
Glass Green	XXXI	29″d	5GY 8.0/4.5	
Glaucous	XLI	29″″f	7.5GY 8.0/2.0	
Glaucous-Blue	XXXIV	43″b	2.5B 6.4/4.0	
Glaucous-Gray	XLVIII	37″″″f	2.5B 7.5/1.0	
Glaucous-Green	XXXIII	39″d	5G 7.4/2.0	
Gnaphalium Green	XLVII	29″″″d	5G 7.5/1.5	
Gobelin Blue	XXXIV	43″i	5B 3.8/3.0	
Grape Green	XLI	25″″	2.5GY 5.8/4.5	
Grass Green	VI	33k	7.5GY 5.2/4.0	
Grayish Blue-Green	XLVIII	37″″″	7.5BG 4.5/1.5	
Grayish Blue-Violet (1)	XXIV	55•i	9PB 4.0/9.0	
Grayish Blue-Violet (2)	XXXV	51″b	7.5PB 5.5/8.0	
Grayish Lavender	XLIII	57″″f	5P 7.2/2.0	
Grayish Olive	XLVI	21″″	5Y 4.8/2.5	
Grayish Violaceous Blue	XXII	51•i	7.5PB 4.6/8.0	
Grayish Violet-Blue	XXIV	53•i	10PB 4.5/6.0	
Green-Blue Slate	XLVIII	45″″i	10B 3.8/2.0	
Green-Yellow	V	27b	1GY 8.2/9.0	
Greenish Glaucous	XLI	33″″f	10GY 8.2/2.0	
Greenish Glaucous-Blue	XLII	41″″b	6.5BG 6.0/3.0	
Greenish Slate-Black	XLVIII	37″″″m	7.5BG 2.5/0.5	

Color name	Plate	Hue and tone number	Munsell notation	Notes
Greenish Yellow	V	25	10Y 7.8/10.0	1.8GY 8.2/11.0
Grenadine	II	7b	9R 6.0/12.0	MF
Grenadine Pink	II	7d	9R 7.0/10.0	MF
Grenadine Red	II	7	8.5R 5.4/13.0	10.0R 5.5/17.5
Guinea Green	VII	39i	2.5BG 4.2/8.0	
Gull Gray	LIII	CGd	N6.1/	
Haematite Red	XXVII	5″m	7.5R 3.4/2.0	
Haematoxylin Violet	XXV	61′i	3.5P 3.6/7.0	
Hair Brown	XLVI	17″″″i	10YR 4.4/1.0	
Hathi Gray	LII	35″″″″b	5G 6.5/0.5	
Hay's Blue	IX	53k	7.5PB 3.2/10.5	
Hay's Brown	XXXIX	9″″k	10R 4.5/2.0	
Hay's Green	XVIII	33′k	10GY 4.5/4.0	
Hay's Lilac	XXXVII	63″d	5P 6.4/7.0	
Hay's Maroon	XIII	1′m	2.5R 2.5/2.0	
Hay's Russet	XIV	7′k	10R 4.0/5.0	
Hazel	XIV	11′k	2.5YR 4.4/5.5	
Heliotrope Gray	L	65″″d	5P 5.5/2.0	
Heliotrope Slate	L	65″″″i	5P 3.8/2.0	
Hellebore Green	XVII	25′m	2.5GY 4.5/3.0	
Hellebore Red	XXXVIII	71″	7.5RP 4.8/9.0	
Helvetia Blue	IX	51k	7.5PB 3.2/10.0	
Hermosa Pink	I	1f	2.5R 7.8/8.0	BF
Hessian Brown	XIII	5′m	10R 2.5/2.5	
Honey Yellow	XXX	19″	2.5Y 6.5/7.0	
Hortense Blue	XXII	47•m	5PB 3.5/5.0	
Hortense Violet	XI	61b	5P 6.0/12.0	
Hyacinth Blue	X	55k	9PB 2.6/8.0	
Hyacinth Violet	XI	61i	5P 3.0/10.0	
Hydrangea Pink	XXVII	5″f	7.5R 8.0/5.0	SF
Hydrangea Red	XXVII	1″i	2.5R 4.2/5.0	
Hyssop Violet	XXXVI	59″	5P 5.0/5.5	
Indian Lake	XXVI	71′i	7.5RP 3.8/7.0	
Indian Purple	XXXVIII	67″m	7.5RP 3.0/3.0	
Indian Red	XXVII	3″k	5R 4.0/4.0	
Indigo Blue	XXXIV	47″m	5PB 3.0/3.0	
Indulin Blue	XXII	51•m	7.5PB 3.0/3.5	
Invisible Green	XIX	41′m	7.5BG 3.0/2.5	
Iron Gray	LI	23″″″k	7.5Y 3.8/1.0	
Isabella Color	XXX	19″i	2.5Y 5.8/4.5	
Italian Blue	VIII	43	5B 5.0/10.0	3.5B 5.2/11.0
Ivory Yellow	XXX	21″f	5Y 8.5/3.0	SF
Ivy Green	XXXI	25″m	10Y 3.5/3.0	
Jade Green	XXXI	27″k	2.5GY 4.2/3.0	
Japan Rose	XXVIII	9″b	5YR 6.6/4.5	
Jasper Green	XXXIII	37″i	7.5G 5.0/3.0	
Jasper Pink	XIII	3′d	6R 6.5/8.5	MF
Jasper Red	XIII	3′	5R 4.8/10.5	
Javel Green	V	27i	1GY 6.8/6.0	
Jay Blue	XXII	47•i	5PB 4.5/7.0	
Jovence Blue	XX	43′k	10BG 4.0/4.0	
Kaiser Brown	XIV	9′k	2.5YR 3.8/6.0	
Kildare Green	XXXI	29″b	5GY 7.2/5.0	
Killarney Green	XVIII	35′i	2.5G 5.0/5.0	
King's Blue	XXII	47•b	2.5PB 5.8/8.0	
Kronberg's Green	XXXI	25″k	10Y 4.5/4.0	
Laelia Pink	XXXVIII	67″d	2.5RP 6.4/9.0	
La France Pink	I	3f	2.5R 7.5/12.0	BF
Lavender	XXXVI	59″f	2.5P 7.6/5.0	
Lavender-Blue	XXI	53′d	8.5PB 6.5/9.0	
Lavender-Gray	XLIII	49″″f	9PB 7.5/4.0	
Lavender-Violet	XXV	61′b	2.5P 6.0/10.0	
Leaf Green	XLI	29″″k	5GY 4.0/2.5	
Leitch's Blue	VIII	47i	2.5B 4.0/10.0	
Lemon Chrome	IV	21	4Y 7.8/10.0	5.2Y 8.0/11 0
Lemon Yellow	IV	23	7.5Y 8.0/10.5	
Lettuce Green	V	29k	4GY 5.8/5.5	
Lichen Green	XXXIII	37″f	5.5G 8.2/2.0	
Light Alice Blue	XXXIV	45″d	2.5PB 7?0/5.0	
Light Amparo Blue	IX	51d	6PB 7.0/10.0	
Light Amparo Purple	XI	63d	5P 7.0/10.0	
Light Bice Green	XVII	29′i	7.5GY 5.6/4.5	
Light Blue-Green	VII	39d	7.5G 7.0/7.0	
Light Blue-Violet	X	55b	8.5PB 5.4/14.0	
Light Bluish Violet	X	57b	9PB 5.5/11.0	
Light Brownish Drab	XLV	9″″b	6YR 5.4/2.0	
Light Brownish Olive	XXX	19″k	2.5Y 4.6/3.5	
Light Brownish Vinaceous	XXXIX	5″″d	2.5R 7.0/2.0	SF
Light Buff	XV	17′f	1Y 8.5/4.5	MF
Light Cadet Blue	XXI	49′b	6PB 6.0/11.0	
Light Cadmium	IV	19	2.5Y 7.5/12.0	
Light Campanula Blue	XXIV	55•d	8.5PB 6.6/10.0	
Light Celandine Green	XLVII	33″″d	5BG 6.5/1.0	
Light Cendre Green	VI	35d	10GY 8.0/7.0	
Light Cerulean Blue	VIII	45b	10B 6.0/8.0	
Light Chalcedony Yellow	XVII	25′d	10Y 8.4/6.0	
Light Chicory Blue	XXIV	57•f	10PB 7.4/6.0	
Light Cinnamon-Drab	XLVI	13″″b	5YR 5.8/2.5	
Light Columbia Blue	XXXIV	47″d	3.5PB 6.5/6.0	
Light Congo Pink	XXVIII	7″d	2.5YR 8.0/5.0	
Light Coral Red	XIII	5′b	7.5R 6.0/10.0	SF
Light Corinthian Red	XXVII	3″b	5R 6.2/6.5	
Light Cress Green	XXXI	29″i	5GY 5.2/4.0	
Light Danube Green	XXXII	35″k	5G 4.0/3.0	
Light Drab	XLVI	17″″b	10YR 5.8/2.0	
Light Dull Bluish Violet	XXXVI	57″b	1P 5.6/8.0	

TABLE I.—*Continued.*

Color name	Plate	Hue and tone number	Munsell notation	Notes
Light Dull Glaucous-Blue	XLII	41‴d	2.5B 6.8/3.0	
Light Dull Green-Yellow	XVII	27″d	3.5GY 7.5/4.5	
Light Elm Green	XVII	27″k	6GY 4.8/4.0	
Light Fluorite Green	XXXII	33″d	7.5GY 8.0/4.0	
Light Forget-me-not Blue	XXII	51*d	5PB 6.8/8.0	
Light Glaucous-Blue	XXXIV	43″d	5B 7.6/4.0	
Light Grape Green	XLI	25‴b	2.5GY 7.0/4.5	
Light Grayish Blue-Violet	XXXV	51″d	6.5PB 7.2/7.0	
Light Grayish Olive	XLVI	21⁗b	5Y 5.8/2.0	
Light Grayish Vinaceous	XXXIX	9‴d	10R 6.8/2.0	SF
Light Grayish Violet-Blue	XXIV	53*b	8.5PB 5.8/10.0	
Light Greenish Yellow	V	25b	10Y 8.0/9.0	
Light Green-Yellow	V	27d	1GY 8.4/7.0	
Light Gull Gray	LIII	CGf	N6.5/	
Light Heliotrope-Gray	L	65⁗f	2.5RP 6.4/2.0	
Light Hellebore Green	XVII	25″k	2.5GY 5.0/3.0	
Light Hortense Violet	XI	61d	5P 6.0/10.0	
Light Hyssop Violet	XXXVI	59″b	2.5P 5.6/7.0	
Light Jasper Red	XIII	3″b	5R 5.5/10.5	
Light King's Blue	XXII	47*d	1PB 7.5/4.0	
Light Lavender-Blue	XXI	53″f	8.5PB 7.4/8.0	
Light Lavender-Violet	XXV	61″d	1.5P 6.0/7.0	
Light Lobelia Violet	XXXVII	61″d	6P 6.5/7.0	
Light Lumiere Green	XVII	29″d	7.5GY 8.0/4.5	
Light Mallow Purple	XII	67d	1P 6.0/12.0	
Light Mauve	XXV	63″d	2.5P 7.0/8.0	
Light Medici Blue	XLVIII	41⁗d	10B 5.4/2.0	
Light Methyl Blue	VIII	47b	2.5PB 5.5/10.0	
Light Mineral Gray	XLVII	25⁗f	5GY 8.4/1.0	
Light Mouse Gray	LI	15⁗⁗b	7.5YR 6.0/1.0	
Light Neropalin Blue	XXII	49*d	3.5PB 7.0/4.0	
Light Neutral Gray	LIII	NGb	N5.2/	
Light Niagara Green	XXXIII	41″d	5BG 7.0/5.0	
Light Ochraceous-Buff	XV	15′d	8.5YR 7.2/8.0	SF
Light Ochraceous-Salmon	XV	13′d	8YR 8.0/5.5	SF
Light Olive-Gray	LI	23⁗⁗d	7.5Y 7.0/1.0	
Light Orange-Yellow	III	17d	1Y 7.5/9.0	SF
Light Oriental Green	XVIII	33″b	2.5G 6.6/6.0	
Light Paris Green	XVIII	35′d	1G 7.5/4.0	
Light Payne's Gray	XLIX	49‴d	6.5PB 5.8/1.5	
Light Perilla Purple	XXXVII	65″i	2.5RP 4.0/5.0	
Light Phlox Purple	XI	65d	10P 6.0/9.5	
Light Pinkish Cinnamon	XXIX	15″d	1YR 8.0/5.0	
Light Pinkish Lilac	XXXVII	65″f	2.5RP 7.8/5.5	
Light Plumbago Gray	L	61⁗f	10P 6.4/1.0	
Light Porcelain Green	XXXIII	39″	5BG 5.5/4.0	
Light Purple-Drab	XLV	1⁗b	7.5RP 5.4/2.0	
Light Purplish Gray	LIII	67⁗⁗b	10P 4.8/0.5	
Light Purplish Vinaceous	XXXIX	1‴d	10RP 7.0/3.5	MF
Light Quaker Drab	LI	1⁗⁗b	5RP 5.4/1.0	SF
Light Rosolane Purple	XXVI	69′b	3.5RP 5.8/13.0	
Light Russet-Vinaceous	XXXIX	9‴b	1YR 6.4/4.0	
Light Salmon-Orange	II	11d	5YR 7.0/7.0	BF
Light Seal Brown	XXXIX	9‴m	10R 2.6/1.0	
Light Sky Blue	XX	47″f	2.5PB 7.4/4.0	
Light Soft Blue-Violet	XXIII	55′b	9PB 6.0/10.0	
Light Squill Blue	XX	45′d	2.5PB 6.8/6.0	
Light Sulphate Green	XIX	39′b	2.5BG 6.2/6.0	
Light Terre Verte	XXXIII	41″	6BG 5.2/3.4	
Light Turtle Green	XXXII	31″d	4GY 8.0/4.5	
Light Tyrian Blue	XXXIV	47″	5PB 4.5/3.0	
Light Varley's Gray	XLIX	57⁗⁗b	2.5P 5.8/2.0	
Light Vinaceous-Cinnamon	XXIX	13″d	7.5YR 8.0/5.0	
Light Vinaceous-Drab	XLV	5⁗⁗b	2.5R 5.4/2.0	
Light Vinaceous-Fawn	XL	13‴d	5YR 7.4/2.5	SF
Light Vinaceous-Gray	L	69⁗⁗f	2.5RP 6.5/1.5	
Light Vinaceous-Lilac	XLIV	69‴d	2.5RP 6.5/5.0	
Light Vinaceous-Purple	XLIV	65″b	2.5RP 5.2/4.5	
Light Violet	X	59b	9PB 6.0/12.0	
Light Violet-Blue	IX	53b	8.5PB 5.0/12.0	
Light Violet-Gray	LII	59⁗⁗b	2.5P 5.6/0.5	
Light Violet-Plumbeous	XLIX	53‴d	8.5PB 5.5/3.0	
Light Viridine Green	VI	33f	3.5GY 8.5/5.0	
Light Viridine Yellow	V	29d	1.5GY 8.2/7.0	BF
Light Windsor Blue	XXXV	49″b	7.5PB 5.6/8.0	
Light Wistaria Blue	XXIII	57′d	9PB 7.0/8.0	
Light Wistaria Violet	XXIII	59′d	10PB 7.0/8.0	
Light Yellow-Green	VI	31d	5GY 8.0/7.0	
Light Yellowish Olive	XXX	23″i	7.5Y 5.8/6.0	
Lilac	XXV	65′d	5P 7.0/5.0	
Lilac-Gray	LII	59⁗⁗⁗f	2.5P 7.0/1.0	
Lily Green	XLVII	33‴i	2.5BG 5.0/1.0	
Lime Green	XXXI	25″	10Y 6.5/5.0	
Lincoln Green	XLI	25‴k	2.5GY 4.0/2.0	
Liseran Purple	XXVI	67′b	10P 5.5/9.0	
Litho Purple	XXV	63′i	5P 3.5/9.0	
Liver Brown	XIV	7″m	10R 3.0/3.5	
Livid Brown	XXXIX	1‴	3R 5.0/3.0	
Livid Pink	XXVII	3″f	5R 8.0/3.0	SF
Livid Purple	XXXVII	63″i	10P 3.6/6.0	
Livid Violet	XXXVII	61″i	7.5P 3.8/5.0	
Lobelia Violet	XXXVII	61″b	6.5P 5.8/7.0	
Lumiere Blue	XX	43′d	10BG 6.5/4.0	
Lumiere Green	XVII	29′b	7.5GY 7.5/6.0	
Lyons Blue	IX	51i	6PB 3.4/12.0	
Madder Blue	XLIII	53‴	10PB 5.0/3.0	

Color name	Plate	Hue and tone number	Munsell notation	Notes
Madder Brown	XIII	3″k	7.5R 3.6/4.0	
Madder Violet	XXV	63″k	5.0P 2.8/4.5	
Magenta	XXVI	67′	10P 5.0/12.0	
Mahogany Red	II	7k	10R 3.5/6.0	
Maize Yellow	IV	19f	2.5Y 8.5/6.0	SF
Malachite Green	XXXII	35″b	10GY 6.8/5.0	
Mallow Pink	XII	67f	1P 7.0/10.0	
Mallow Purple	XII	67b	1P 5.5/14.0	
Manganese Violet	XXV	63′	5P 4.5/11.0	
Marguerite Yellow	XXX	23″f	6.5Y 8.4/3.0	
Marine Blue	VIII	45m	10B 3.2/6.0	
Maroon	I	3m	7.5R 2.4/4.0	
Mars Brown	XV	13′m	5YR 3.4/3.5	
Mars Orange	II	9i	10R 4.5/10.0	
Mars Violet	XXXVIII	71″m	10RP 3.0/2.5	
Mars Yellow	III	15i	7.5YR 5.6/10.0	
Martius Yellow	IV	23f	7.5Y 8.5/7.0	
Massicot Yellow	XVI	21′f	6Y 8.4/5.0	SF
Mathews' Blue	XX	45′	2.5PB 4.8/10.0	
Mathews' Purple	XXV	65′	5P 4.0/9.0	
Mauve	XXV	63″b	2.5P 6.0/10.0	
Mauvette	XXV	65′f	10P 8.0/6.0	
Mazarine Blue	IX	49d	5PB 6.0/9.0	
Meadow Green	VI	35k	2.5G 4.6/4.0	
Medal Bronze	IV	19m	2.5Y 3.8/4.0	
Medici Blue	XLVIII	41⁗⁗b	7B 5.0/1.0	
Methyl Blue	VIII	47	2.5PB 5.0/14.0	
Methyl Green	XIX	41′	5BG 5.4/7.0	
Microcline Green	XIX	39″f	2.5BG 8.0/4.0	
Mignonette Green	XXXI	25″i	10Y 3.5/5.0	
Mikado Brown	XXIX	13″i	5YR 5.0/5.0	
Mikado Orange	III	13b	5YR 7.0/12.0	SF
Mineral Gray	XLVII	25⁗⁗d	5GY 7.4/2.0	
Mineral Green	XVIII	31′	6.5GY 6.5/8.0	
Mineral Red	XXVII	1″k	2.5R 3.6/4.0	
Montpellier Green	XXXIII	37″	7.5G 5.5/4.0	
Morocco Red	I	5k	7.5R 3.4/6.0	
Motmot Blue	XX	43′	2.5B 5.2/6.5	
Motmot Green	XVIII	35′	2.5G 5.8/7.0	
Mouse Gray	LI	15⁗⁗	7.5YR 5.0/1.0	
Mummy Brown	XV	17′m	10YR 3.4/3.0	
Mulberry Purple	XI	61k	5P 3.0/7.0	
Mustard Yellow	XVI	19′b	3.5Y 7.8/9.0	SF
Mytho Green	XLI	29″b	7.5GY 7.0/3.0	
Myrtle Green	VII	41m	9BG 3.2/4.0	
Naphthalene Violet	XXXVII	61″k	10P 3.2/5.0	
Naphthalene Yellow	XVI	23′f	7.5Y 8.5/5.0	SF
Naples Yellow	XVI	19′d	3.5Y 8.2/7.0	SF
Natal Brown	XL	13‴k	5YR 3.8/2.0	
Navy Blue	XXI	53′m	8.6PB 2.8/5.0	
Neropalin Blue	XXII	49*b	3.5PB 6.0/8.5	
Neutral Gray	LIII	NG	N4.7/	
Neutral Red	XXXVIII	71″k	7.5RP 3.5/5.5	
Neuvider Green	VII	37d	10GY 8.2/6.0	
Neva Green	V	29	5GY 7.6/10.0	
Niagara Green	XXXIII	41″b	2.5BG 6.2/2.5	
Nickel Green	XXXIII	37″k	5.0G 4.0/2.5	
Night Green	VI	33	6.5GY 7.2/12.0	
Nigrosin Blue	XXXV	49″m	7.5PB 4.2/3.5	
Nigrosin Violet	XXV	65′k	5P 2.8/6.0	
Nile Blue	XIX	41′d	5BG 7.0/6.0	
Nopal Red	I	3i	4R 4.0/12.0	
Ochraceous-Buff	XV	15′b	1YR 8.0/6.0	SF
Ochraceous-Orange	XV	15′	8.5YR 6.5/12.0	
Ochraceous-Salmon	XV	13′b	5YR 7.4/7.0	
Ochraceous-Tawny	XV	15′i	8.5YR 5.5/7.0	
Ocher Red	XXVII	5″i	7.5R 4.4/4.0	
Oil Green	V	27k	4GY 5.0/4.5	
Oil Yellow	V	25i	10Y 6.0/6.0	
Old Gold	XVI	19′i	3.5Y 5.5/6.0	
Old Rose	XIII	1′b	2.5R 5.2/7.5	
Olivaceous Black (1)	XLVI	21⁗⁗m	5Y 3.0/1.0	
Olivaceous Black (2)	XLVII	25⁗⁗m	5GY 2.5/1.5	
Olivaceous Black (3)	LI	23⁗⁗⁗m	7.5Y 3.0/0.5	
Olive	XXX	21″m	5Y 3.8/3.0	
Olive-Brown	XL	17‴k	10YR 3.8/2.0	
Olive-Buff	XL	21‴d	5Y 8.0/3.5	SF
Olive-Citrine	XVI	21′m	5Y 3.8/3.5	
Olive-Gray	LI	23⁗⁗b	7.5Y 5.8/2.0	
Olive-Green	IV	23m	7.5Y 4.0/3.5	
Olive Lake	XVI	21′i	5Y 5.5/4.5	
Olive-Ocher	XXX	21″	5Y 6.5/6.5	
Olive-Yellow	XXX	23″	7.5Y 6.8/7.0	
Olivine	XXXII	35″d	10G 7.5/4.0	
Olympic Blue	XX	47′	3.5PB 5.0/11.0	
Onion-skin Pink	XXVIII	11″b	5YR 7.0/6.0	
Ontario Violet	XXXVI	55″b	10PB 5.2/8.0	
Opaline Green	VII	37f	6.5GY 8.4/3.0	
Orange	III	15	5YR 6.6/12.0	5.2YR 6.7/14.0
Orange-Buff	III	15d	8.5YR 7.2/9.0	
Orange Chrome	II	11	2.5YR 6.0/15.0	
Orange-Cinnamon	XXIX	13″	5YR 5.8/7.0	
Orange-Citrine	IV	19k	2.5Y 4.8/6.0	
Orange-Pink	II	11f	2.5YR 8.0/10.0	SF
Orange Rufous	II	11i	2.5R 5.0/10.0	
Orange-Vinaceous	XXVII	5″b	5R 6.5/9.5	

TABLE I.—*Continued.*

Color name	Plate	Hue and tone number	Munsell notation	Notes
Oriental Green	XVIII	33′	2.5G 5.6/6.0	
Orient Blue	XXXIV	45″	10B 5.0/5.0	
Orient Pink	II	9f	10R 8.0/8.0	BF
Oural Green	XVIII	33′f	8.5GY 8.5/3.0	
Ox-blood Red	I	1k	5R 2.4/10.0	
Oxide Blue	VIII	45i	10B 3.5/9.0	
Pale Amaranth Pink	XII	69f	2.5RP 7.0/10.0	
Pale Amparo Blue	IX	51f	4PB 7.5/4.0	
Pale Amparo Purple	XI	63f	7.5P 7.0/8.0	
Pale Aniline Lilac	XXXV	53″f	10B 7.5/6.0	
Pale Blue (Ethyl Blue)	VIII	45f	3.5B 8.0/3.0	
Pale Blue-Green	VII	39f	2.5G 8.4/2.0	
Pale Blue-Violet	X	55d	8.5PB 6.4/10.0	
Pale Bluish Lavender	XXXVI	57″″f	2.5P 8.4/3.0	
Pale Bluish Violet	X	57d	8.5PB 7.0/10.0	
Pale Brownish Drab	XLV	9″″d	6YR 7.0/1.0	
Pale Brownish Vinaceous	XXXIX	5″″f	2.5R 8.0/2.5	SF
Pale Cadet Blue	XXI	49′d	5PB 6.5/5.0	
Pale Campanula Blue	XXIV	55″f	8.5PB 7.5/6.0	
Pale Cendre Green	VI	35f	7.5GY 8.8/3.0	
Pale Cerulean Blue	VIII	45d	10B 7.5/6.0	
Pale Chalcedony Yellow	XVII	25′f	7.5Y 8.5/4.0	
Pale Cinnamon-Pink	XXIX	13″f	6.5YR 8.0/3.0	SF
Pale Congo Pink	XXVIII	7″″f	10R 8.0/3.0	SF
Pale Drab-Gray	XLVI	17″″″f	10YR 8.5/0.5	SF
Pale Dull Glaucous-Blue	XLII	41″″f	2.5B 7.5/2.0	
Pale Dull Green-Yellow	XVII	27′f	2.5GY 8.2/4.0	
Pale Ecru-Drab	XLVI	13″″″f	5YR 8.0/1.0	SF
Pale Flesh Color	XIV	7″f	2.5YR 8.0/3.5	MF
Pale Fluorite Green	XXXII	33″f	10GY 8.6/2.0	
Pale Forget-me-not Blue	XXII	51″f	5PB 7.4/4.0	
Pale Glass Green	XXXI	29″f	2.5GY 8.4/3.0	
Pale Glaucous-Blue	XXXIV	43″f	5B 8.0/3.0	
Pale Glaucous-Green	XXXIII	39″f	4G 8.4/2.0	
Pale Grayish Blue	XXI	49′f	5PB 7.6/4.0	
Pale Grayish Blue-Violet	XXXV	51″f	8.5PB 7.6/4.0	
Pale Grayish Vinaceous	XXXIX	9″″f	2.5YR 8.0/1.5	SF
Pale Grayish Violet-Blue	XXIV	53″d	8.5PB 7.0/8.0	
Pale Greenish Yellow	V	25d	10Y 8.0/7.0	
Pale Green-Blue Gray	XLVIII	45″″″f	10B 6.5/2.0	
Pale Green-Yellow	V	27f	1GY 8.5/5.0	
Pale Gull Gray	LIII	CG0	N7.8/	
Pale Hortense Violet	XI	61f	5P 7.5/6.0	
Pale King's Blue	XXII	47″f	10PB 8.5/4.0	
Pale Laelia Pink	XXXVIII	67″″f	2.5RP 7.5/6.0	
Pale Lavender-Violet	XXV	61′f	5P 7.4/5.0	
Pale Lemon Yellow	IV	23b	8.5Y 8.5/10.0	
Pale Lilac	XXXVII	63″f	10P 7.8/4.0	
Pale Lobelia Violet	XXXVII	61″″f	7.5P 7.5/3.0	
Pale Lumiere Green	XVII	29′f	2.5GY 8.0/4.5	
Pale Mauve	XXV	63′f	6P 8.5/4.0	
Pale Mazarine Blue	IX	49f	5PB 7.5/4.0	
Pale Medici Blue	XLVIII	41″″″f	10B 6.5/1.5	
Pale Methyl Blue	VIII	47d	10B 7.2/6.0	
Pale Mouse Gray	LI	15″″″d	7.5YR 6.5/1.0	SF
Pale Neropalin Blue	XXII	49″f	2.5PB 8.0/3.5	
Pale Neutral Gray	LIII	NGd	N8.9/	
Pale Niagara Green	XXXIII	41″f	7.5BG 7.8/2.0	
Pale Nile Blue	XIX	41′f	7.5BG 8.4/4.0	
Pale Ochraceous-Buff	XV	15′f	1YR 8.2/5.0	SF
Pale Ochraceous-Salmon	XV	13′f	1Y 8.5/4.0	SF
Pale Olive-Buff	XL	21″″f	5Y 8.4/2.5	SF
Pale Olive-Gray	LI	23″″″f	7.5Y 8.5/1.0	
Pale Olivine	XXXII	35″f	10GY 8.2/2.0	
Pale Orange-Yellow	III	17f	1Y 8.0/8.0	BF
Pale Payne's Gray	XLIX	49″″″f	6.5PB 6.4/2.0	
Pale Persian Lilac	XXXVIII	69″f	5RP 7.4/8.0	
Pale Pinkish Buff	XXIX	17″f	10YR 8.2/2.5	SF
Pale Pinkish Cinnamon	XXIX	15′f	8.5YR 8.4/4.0	SF
Pale Purple-Drab	XLV	1″″d	7.5RP 6.6/2.0	
Pale Purplish Gray	LIII	67″″″d	10P 5.8/1.0	
Pale Purplish Vinaceous	XXXIX	1″″f	10RP 8.0/4.5	MF
Pale Quaker Drab	LI	1″″″d	7.5RP 6.5/1.0	SF
Pale Rhodonite Pink	XXXVIII	71″f	6.5RP 7.6/7.0	
Pale Rose-Purple	XXVI	67′f	8.5P 6.5/7.0	
Pale Rosolane Purple	XXVI	69′d	3.5RP 6.4/12.0	
Pale Russian Blue	XLII	45″″f	2.5PB 8.5/4.0	
Pale Salmon Color	XIV	9′f	7.5YR 8.0/3.5	SF
Pale Smoke Gray	XLVI	21″″″f	5Y 7.5/1.5	
Pale Soft Blue-Violet	XXIII	55′d	9PB 7.0/8.0	
Pale Sulphate Green	XIX	39′d	2.5BG 7.0/4.0	
Pale Tiber Green	XVIII	33′f	7.5GY 8.5/4.0	
Pale Turquoise Green	VII	41f	5BG 8.0/4.0	
Pale Turtle Green	XXXII	31″f	6.5GY 8.2/3.0	
Pale Varley's Gray	XLIX	57″″d	2.5P 6.0/3.0	
Pale Verbena Violet	XXXVI	55″f	10PB 7.6/6.0	
Pale Veronese Green	XVIII	31′f	8GY 8.2/3.0	
Pale Vinaceous	XXVII	1″f	2.5R 7.8/5.0	SF
Pale Vinaceous-Drab	XLV	5″″″d	2.5R 6.5/1.5	
Pale Vinaceous-Fawn	XL	13″″f	5YR 8.0/1.5	SF
Pale Vinaceous-Lilac	XLIV	69″″f	2.5RP 7.8/5.0	
Pale Vinaceous-Pink	XXVIII	9″f	2.5YR 8.0/2.5	SF
Pale Violet	X	59d	9PB 6.5/8.0	
Pale Violet-Blue	IX	53d	6.5PB 7.0/10.0	
Pale Violet-Gray	LII	59″″″d	2.5P 6.4/0.5	
Pale Violet-Plumbeous	XLIX	53″″″f	8.5PB 7.0/3.0	
Pale Viridine Yellow	V	29f	1.5GY 8.4/5.0	BF
Pale Windsor Blue	XXXV	49″′d	7PB 7.0/7.0	
Pale Wisteria Blue	XXIII	57″f	10PB 7.5/6.0	
Pale Wistaria Violet	XXIII	59′f	2.5P 7.2/5.0	
Pale Yellow-Green	VI	31f	5GY 8.4/5.0	
Pale Yellow-Orange	III	15f	1.5YR 8.4/6.5	BF
Pallid Blue-Violet	X	55f	8.5PB 7.5/6.0	
Pallid Bluish Violet	X	57f	9PB 7.5/6.0	
Pallid Brownish Drab	XLV	9″″″f	5YR 8.0/1.0	SF
Pallid Grayish Violet-Blue	XXIV	53″f	7.5PB 7.2/5.0	
Pallid Methyl Blue	VIII	47f	2.5PB 8.0/6.0	
Pallid Mouse Gray	LI	15″″″f	5YR 8.0/0.5	SF
Pallid Neutral Gray	LIII	NGf	N7.4/	
Pallid Purple-Drab	XLV	1″″″f	7.5RP 7.2/1.5	
Pallid Purplish Gray	LIII	67″″″″f	10P 8.0/1.0	
Pallid Quaker Drab	LI	1″″″f	7.5RP 8.0/1.0	SF
Pallid Soft Blue-Violet	XXIII	55′f	9PB 7.5/6.0	
Pallid Vinaceous-Drab	XLV	5″″″f	7.5RP 8.0/1.5	SF
Pallid Violet	X	59f	9PB 7.5/5.0	
Pallid Violet-Blue	IX	53f	6.5PB 7.5/6.0	
Pansy Purple	XII	69k	7.5RP 3.2/6.0	
Pansy Violet	XI	63i	7.5P 4.0/12.0	
Paris Blue	VIII	47k	5PB 3.0/10.0	
Paris Green	XVIII	35′b	2.5G 6.8/6.5	
Parrot Green	VI	31k	5GY 5.5/5.5	
Parula Blue	XLII	45″	2.5PB 5.5/4.0	
Patent Blue	VIII	43k	7.5B 3.0/6.0	
Payne's Gray	XLIX	49″″	6.5PB 4.4/2.5	
Peach Red	I	5b	7.5R 5.5/9.4	SF
Peacock Blue	VIII	43i	5B 3.6/8.5	
Peacock Green	VI	35i	7.5GY 6.2/5.0	
Pea Green	XLVII	29″″b	10GY 6.4/1.0	
Pearl Blue	XXXV	49″f	7.5PB 7.5/4.0	
Pearl Gray	LII	35″″″f	2.5B 8.0/0.2	
Pecan Brown	XXVIII	11″i	5YR 5.0/4.5	
Perilla Purple	XXXVII	65″k	7.5RP 3.4/4.5	
Persian Blue	XX	45′f	2.5PB 7.5/4.0	
Persian Lilac	XXXVIII	69″d	5RP 6.2/7.0	
Petunia Violet	XXV	65′i	5.0P 3.4/8.0	
Phenyl Blue	IX	53	7.5PB 3.5/16.0	8.0PB 3.5/17.0
Phlox Pink	XI	65f	7.5P 7.0/6.0	
Phlox Purple	XI	65b	10P 5.0/11.0	
Picric Yellow	IV	23d	8.5Y 8.5/9.5	
Pinard Yellow	IV	21d	5.0Y 8.4/8.0	SF
Pinkish Buff	XXIX	17″d	1YR 8.0/4.0	
Pinkish Cinnamon	XXIX	15″b	7.5YR 6.6/6.0	
Pinkish Vinaceous	XXVII	5″d	7.5R 7.5/5.5	SF
Pistachio Green	XLI	33″″	10GY 5.5/3.0	
Pteroma Violet	XXV	61′	2.5P 4.5/11.0	
Plumbago Blue	XLIII	53″″f	10PB 7.2/3.0	
Plumbago Gray	L	61″″″d	10P 5.4/1.0	
Plumbago Slate	L	61″″″i	7.5P 4.0/1.0	
Plumbeous	LII	49″″″b	7.5PB 5.6/1.5	
Plumbeous-Black	LII	49″″″m	7.5PB 2.2/0.5	
Plum Purple	XXIV	57″m	10PB 2.4/4.0	
Pois Green	XLI	29″″i	5GY 5.0/2.5	
Pomegranate Purple	XII	71i	5RP 3.8/7.0	
Porcelain Blue	XXXIV	43″	2.5B 5.6/3.5	
Porcelain Green	XXXIII	39″i	2.5BG 4.8/3.0	
Pompeian Red	XIII	3′i	5R 4.2/8.0	
Primrose Yellow	XXX	23″d	7.5Y 8.2/6.5	
Primuline Yellow	XVI	19′	3.5Y 7.5/10.0	
Prout's Brown	XV	15′m	7.5YR 3.5/3.0	
Prune Purple	XI	63m	7.5P 2.2/6.0	
Prussian Blue	IX	49m	3.5PB 3.2/9.0	
Prussian Green	XIX	41′k	7.5BG 3.4/4.0	
Prussian Red	XXVII	5″k	7.5R 4.0/3.5	
Puritan Gray	XLVII	33″″″f	7.5G 7.0/1.5	
Purple (true)	XI	65	10P 4.0/14.0	9.5P 4.2/17.0
Purple-Drab	XLV	1″″	8RP 4.6/2.0	
Purplish Gray	LIII	67″″″	10P 4.0/1.5	
Purplish Lilac	XXXVII	65″d	2.5RP 6.5/8.0	
Purplish Vinaceous	XXXIX	1″″b	2.5R 6.2/4.5	
Pyrite Yellow	IV	23i	7.5Y 6.0/7.0	
Quaker Drab	LI	1″″″	5RP 4.6/0.5	
Rainette Green	XXXI	27″i	2.5GY 5.5/4.0	
Ramier Blue	XLIII	57″″	2.5P 4.5/3.0	
Raisin Black	XLIV	65″″m	2.5RP 2.6/2.0	
Raisin Purple	XI	65k	10P 2.8/6.0	
Raw Sienna	III	17i	7.5YR 5.5/9.0	
Raw Umber	III	17m	7.5YR 3.5/3.0	
Reed Yellow	XXX	23″b	7.5Y 7.8/6.0	
Rejane Green	XXXIII	37″b	2.5G 6.5/4.5	
Rhodamine Purple	XII	67	1P 4.5/14.0	2.0RP 4.3/17.5
Rhodonite Pink	XXXVIII	71″d	7.5RP 6.0/7.0	
Rinnemann's Green	XVIII	31′i	7.5GY 5.5/4.5	
Rivage Green	XVIII	31′b	6.5GY 7.5/6.5	
Rocellin Purple	XXXVIII	71″b	7.5RP 5.8/9.0	
Roman Green	XVI	23′m	7.5Y 4.0/3.5	
Rood's Blue	IX	49k	6.5PB 3.5/14.0	
Rood's Brown	XXVIII	11″k	4YR 4.5/3.0	
Rood's Lavender	XLIX	57″″″f	2.5P 6.5/2.0	
Rood's Violet	XI	65i	10P 3.0/9.0	
Rose Color	XII	71b	5RP 5.5/14.0	
Rose Doree	I	3b	6R 6.0/12.0	SF
Rose Pink	XII	71f	5RP 8.0/8.0	

TABLE I.—*Continued.*

Color name	Plate	Hue and tone number	Munsell notation	Notes
Rose-Purple	XXVI	67′d	8.5P 6.5/10.0	
Rose Red	XII	7i	7.5RP 4.8/14.0	
Rosolane Pink	XXVI	69′f	5RP 8.0/9.0	
Rosolane Purple	XXVI	69′	5RP 4.4/12.0	
Roslyn Blue	X	57k	9PB 3.0/8.0	
Royal Purple	X	59i	1P 3.5/8.0	
Rufous	XIV	9′	10R 5.2/10.0	
Russet	XV	13′k	5YR 3.8/4.0	
Russet-Vinaceous	XXXIX	9‴	10R 5.0/3.0	
Russian Blue	XLII	45‴′d	2.5PB 7.5/3.0	
Russian Green	XLII	37‴′i	2.5G 4.0/1.5	
Saccardo's Olive	XVI	19′m	2.5Y 4.5/4.0	
Saccardo's Slate	XLVIII	41‴′k	7.5B 2.8/1.0	
Saccardo's Umber	XXIX	17″k	1Y 4.0/2.0	
Saccardo's Violet	XXXVII	61″	6P 4.8/9.0	
Safrano Pink	II	7f	10R 8.0/8.0	BF
Sage Green	XLVII	29′′′′	10GY 5.6/1.5	
Sailor Blue	XXI	53′k	8.5PB 3.5/10.0	
Salmon-Buff	XIV	11′d	7.5YR 7.8/6.0	
Salmon Color	XIV	9′d	5YR 7.5/6.0	SF
Salmon-Orange	II	11b	2.5YR 7.0/11.0	MF
Salvia Blue	IX	49b	7.5PB 5.0/16.0	
Sanford's Brown	II	11k	2.5YR 4.2/8.0	
Sayal Brown	XXIX	15″i	8.5YR 5.2/5.0	
Scarlet	I	5	7.5R 5.0/12.0	
Scarlet-Red	I	3	5R 4.4/16.0	
Scheele's Green	VI	33i	7.5GY 6.5/7.0	
Schoenfeld's Purple	XXVI	69′i	5RP 3.2/10.0	
Seafoam Green	XXXI	27‴f	1GY 8.2/4.0	
Seafoam Yellow	XXXI	25‴f	7.5Y 8.4/5.0	SF
Sea Green	XIX	41′i	7.5BG 4.5/6.0	
Seal Brown	XXXIX	3‴m	7.5R 3.2/1.5	
Seashell Pink	XIV	11′f	7.5YR 8.0/3.0	SF
Sepia	XXIX	17‴m	1Y 3.4/2.0	
Serpentine Green	XVI	23′k	7.5Y 4.8/4.0	
Shamrock Green	XXXII	33″i	1G 5.4/4.0	
Shell Pink	XXVIII	11″f	2.5YR 8.0/2.5	SF
Shrimp Pink	I	5f	10R 8.0/6.0	
Skobeloff Green	VII	39	2.5BG 4.8/10.0	
Sky Blue	XX	47′d	2.5PB 7.0/7.0	
Sky Gray	XXXIV	45″f	2.5P B8.5/2.0	
Slate-Black	LIII	CGOO	N2.4/	
Slate-Blue	XLIII	49‴i	7.5PB 4.0/3.5	
Slate Color	LIII	CGk	N3.4/	
Slate-Gray	LIII	CGi	N3.5/	
Slate-Olive	XLVII	29′′′′i	3.5G 5.0/1.0	
Slate-Purple	XLIV	65‴i	2.5RP 4.0/3.0	
Slate-Violet (1)	XLIII	57′′′′i	1P 3.4/1.5	
Slate-Violet (2)	XLIV	61‴	7.5P 4.5/3.0	
Smalt Blue	IX	53i	8.5PB 3.2/14.0	
Smoke Gray	XLVI	21′′′′d	5Y 6.8/2.0	
Snuff Brown	XXIX	15″k	9.0YR 4.5/3.0	
Soft Blue-Violet	XXIII	55′	10PB 4.8/12.0	
Soft Bluish Violet	XXIII	57′	1P 4.2/12.0	
Sooty Black	LI	1′′′′m	5RP 3.0/0.5	
Sorghum Brown	XXXIX	9‴i	10R 3.5/2.0	
Sorrento Green	VII	41k	9BG 3.8/6.5	
Spectrum Blue	IX	49	5PB 4.0/16.0	
Spectrum Red	I	1	5R 4.0/15.0	SF
Spectrum Violet	X	59	10PB 3.5/10.0	10.0PB 3.3/14.0
Spinach Green	V	29m	5GY 4.6/4.0	
Spinel Pink	XXVI	71′b	5RP 5.2/12.0	
Spinel Red	XXVI	71′	8.5RP 5.0/12.0	
Squill Blue	XX	45′b	2.5PB 6.2/8.0	
Stone Green	XLII	37‴′	2.5G 5.5/3.0	
Storm Gray	LII	35′′′′	5G 5.4/1.0	
Strawberry Pink	I	5d	7.5R 6.4/10.0	SF
Straw Yellow	XVI	21′d	6Y 8.4/6.0	SF
Strontian Yellow	XVI	23′	7.5Y 7.5/9.0	
Sudan Brown	III	15k	7.5YR 4.5/6.0	
Sulphate Green	XIX	39′	10G 5.5/6.0	
Sulphine Yellow	IV	21i	5Y 5.8/6.0	
Sulphur Yellow	V	25f	7.5Y 8.4/5.0	
Taupe Brown	XLIV	69‴′m	5RP 2.6/2.0	
Tawny	XV	13′i	5YR 5.0/6.5	
Tawny-Olive	XXIX	17″i	1Y 5.2/4.5	
Tea Green	XLVII	25′′′′b	5GY 6.2/2.0	
Terra Cotta	XXVIII	7″	10R 5.4/6.5	
Terre Verte	XXXIII	41″i	4BG 4.5/2.0	
Testaceous	XXVIII	9″	2.5YR 5.0/5.0	
Thulite Pink	XXVI	71′d	5RP 6.6/11.0	
Tiber Green	XVIII	33′d	10GY 8.0/6.0	
Tilleul Buff	XL	17‴f	7.5YR 8.4/2.0	SF
Tourmaline Pink	XXXVIII	67″b	2.5RP 5.5/11.0	
Turquoise Green	VII	41d	5.0BG 7.0/6.0	
Turtle Green	XXXII	31″b	7.5GY 7.0/4.5	
Tyrian Blue	XXXIV	47″i	5PB 4.2/3.0	
Tyrian Pink	XII	69b	2.5RP 5.4/12.0	
Tyrian Rose	XII	69	5RP 4.5/14.0	8.0RP 4.3/15.0
Tyrolite Green	VII	39b	10G 5.6/6.0	
Ultramarine Ash	XXII	49*	6.5PB 5.0/12.0	
Ultramarine Blue	IX	49i	6.5PB 3.5/16.0	

Color name	Plate	Hue and tone number	Munsell notation	Notes
Urania Blue	XXIV	53*m	10PB 2.5/3.0	
Vanderpoel's Blue	XX	47′i	3.5PB 4.6/9.0	
Vanderpoel's Green	VI	33b	7.5GY 7.5/10.0	
Vanderpoel's Violet	XXXVI	55″	1P 4.8/6.0	
Vandyke Brown	XXVIII	11″m	5YR 3.5/2.5	
Vandyke Red	XIII	1′k	2.5R 3.8/5.0	
Variscite Green	XIX	37′d	3.5G 7.6/4.0	
Varley's Gray	XLIX	57′′′′	2.5P 4.6/2.5	
Varley's Green	XVIII	31′m	9GY 4.0/3.0	
Venetian Blue	XXII	47*	5PB 4.5/10.0	
Venetian Pink	XIII	1′f	7.5R 8.0/6.0	MF
Venice Green	VII	41b	4BG 6.0/8.0	
Verbena Violet	XXXVI	55″d	10PB 6.5/4.0	
Verdigris Green	XIX	37′	3.5G 6.0/5.0	
Vernonia Purple	XXXVIII	69″i	7.5RP 4.2/6.5	
Verona Brown	XXIX	13″k	5YR 4.2/3.0	
Veronese Green	XVIII	31′d	7.5GY 7.5/6.0	
Vetiver Green	XLVII	25′′′′	5GY 5.6/3.0	
Victoria Lake	I	1m	5R 2.0/4.0	
Vinaceous	XXVII	1″d	2.5R 6.5/7.0	SF
Vinaceous-Brown	XXXIX	5‴i	7.5R 4.8/2.5	
Vinaceous-Buff	XL	17′′′′d	6.5YR 8.0/3.0	
Vinaceous-Cinnamon	XXIX	13‴b	7YR 7.2/5.0	
Vinaceous-Drab	XLV	5′′′′	2.5R 5.0/2.0	
Vinaceous-Fawn	XL	13′′′b	2.5YR 6.8/3.0	
Vinaceous-Gray	L	69′′′′d	7.5P 5.5/2.0	
Vinaceous-Lavender	XLIV	65‴f	10RP 7.6/6.0	
Vinaceous-Lilac	XLIV	69′′′b	5RP 5.5/6.0	
Vinaceous-Pink	XXVIII	9″d	2.5YR 6.0/5.0	
Vinaceous-Purple	XXXVIII	67‴i	3.5RP 4.5/7.0	
Vinaceous-Purple	XLIV	65‴	10P 3.8/3.5	
Vinaceous-Rufous	XIV	7′i	10R 4.5/9.0	
Vinaceous-Russet	XXVIII	7″i	2.5YR 4.5/4.0	
Vinaceous-Slate	L	69′′′′i	7.5P 3.8/2.0	
Vinaceous-Tawny	XXVIII	11″	2.5YR 5.6/6.0	
Violet Carmine	XII	69m	7.5RP 3.0/4.0	
Violet-Gray	LII	59′′′′	2.5P 5.4/1.0	
Violet-Plumbeous	XLIX	53′′′′b	8.5PB 5.2/4.0	
Violet-Purple	XI	63	6.5P 5.0/14.0	5.0P 4.1/15.0
Violet-Slate	XLIX	53′′′′i	8.5PB 3.6/2.5	
Violet Ultramarine	X	57i	9PB 3.4/12.0	
Viridian Green	VII	37i	5G 5.5/8.0	
Viridine Green	VI	33d	6.5GY 8.0/8.0	
Viridine Yellow	V	29b	1GY 7.8/8.0	5.5G 5.4/9.5
Vivid Green	VII	37	4G 6.0/10.0	
Wall Green	VII	39k	5BG 3.8/6.0	
Walnut Brown	XXVIII	9″k	2.5YR 4.0/3.0	
Warbler Green	IV	23k	7.5Y 5.0/5.0	
Warm Blackish Brown	XXXIX	1‴m	2.5R 3.4/1.5	
Warm Buff	XV	17′d	1Y 7.8/6.0	MF
Warm Sepia	XXIX	13″m	5YR 3.8/2.0	
Water Green	XLI	25‴d	2.5GY 7.6/2.0	
Wax Yellow	XVI	21′	5Y 7.0/9.0	
Wedgewood Blue	XXI	51′f	7PB 7.5/8.0	
White	LIII	NGo	N9.5/	
Windsor Blue	XXXV	49″i	8.0PB 4.0/5.5	
Winter Green	XVIII	33′i	2.5G 4.8/4.0	
Wistaria Blue	XXIII	57′b	9PB 5.8/10.0	
Wistaria Violet	XXIII	59′b	2.5P 6.0/12.0	
Wood Brown	XL	17′′′′	9YR 6.0/3.0	
Xanthine Orange	III	13i	5YR 5.2/12.0	
Yale Blue	XX	47′b	3.5PB 6.0/8.0	
Yellow-Green	VI	31	5GY 8.0/10.0	4.5GY 7.2/11.0
Yellowish Citrine	XVI	23′i	7.5Y 6.0/6.0	
Yellowish Glaucous	XLI	25‴f	2.5GY 8.4/2.0	
Yellowish Oil Green	V	25k	10Y 5.0/6.0	
Yellowish Olive	XXX	23″k	7.5Y 4.5/4.0	
Yellow Ocher	XV	17′	10YR 5.8/7.0	
Yew Green	XXXI	27″m	5GY 3.4/3.5	
Yvette Violet	XXXVI	55″k	1P 3.5/4.0	
Zinc Green	XIX	37′i	5G 5.4/4.0	
Zinc Orange	XV	13′	5YR 6.5/10.0	
White, Grays, and Blacks.				
* 1. Black	LIII		NGOO	N2.2/
2. Slate-Black	LIII		CGOO	N2.4/
3. Blackish Slate	LIII		CGm	N2.6/
4. Slate Color	LIII		CGk	N3.4/
5. Slate-Gray	LIII		CGi	N3.5/
6. Gray (Dark Gull Gray)	LIII		CG	N4.3/
7. Gray (Deep Gull Gray)	LIII		CGb	N5.7/
8. Gray (Gull Gray)	LIII		CGd	N6.1/
9. Gray (Light Gull Gray)	LIII		CGf	N5.7/
10. Gray (Pale Gull Gray)	LIII		CGo	N7.8/
White	LIII		NGo	N9.5/
Pallid Neutral Gray	LIII		NGf	N7.4/
Pale Neutral Gray	LIII		NGd	N5.9/
Light Neutral Gray	LIII		NGb	N5.2/
Neutral Gray	LIII		NG	N4.7/
Deep Neutral Gray	LIII		NGi	N3.7/
Dark Neutral Gray	LIII		NGk	N3.1/
Dusky Neutral Gray	LIII		NGm	N2.8/

The Munsell notation equivalents reported here are for colors found in a good copy of the Ridgway Standards known as copy T, in possession of the Department of Botany, University of Toronto. It is considered to be similar to other copies of the standards in good condition.

The notes give alternative notations for certain colors which are thought to be closer to the original color, and, also refer to the color chips that fluoresce; BF refers to bright fluorescence; MF to medium fluorescence; SF to slight fluorescence.

Fluorescence was produced by a strong irradiation from a quarts mercury arc lamp filtered through a Corning 9863 filter. It is thought that the notations of the colors marked BF should be used very cautiously.

* The descriptions given are as found under the chips on Plate LIII.

structed, it was deposited in the library of the University of Toronto in 1942 as a possible aid to others. At that time the author urged that biologists consider the use of a more permanent means of color description.[3]

The subject was reopened in 1946 when Nobles[4] consulted the Toronto key and found marked differences between its notations and those derived from a comparison of chips in her copy of Ridgway with the Munsell *Book of Color*.[5] Checking showed that the discrepancies might be explained by *real* differences between chips of the same name in different copies of the Ridgway standards. These differences were verified and a report concerning them was published by Illman and Hamly.[6]

The presence of these differences makes impossible the preparation of a key which would be applicable to all copies of Ridgway. It was considered, however, that data derived from a single, well-preserved volume of Ridgway would provide useful approximations of colors referred to in the literature by Ridgway names. It is not offered for use as a substitute for physically standardized color systems.

Experimental Work and Results

The methods used in making the notations were similar to those described by Judd and Kelly[7] and by Illman and Hamly.[6] Natural daylight, however, was entirely replaced by light from two Spencer Daylight lamps. While no precise calibration of the color of the lamps was available, repeated checks showed that notations obtained with them and with illumination from north sky light were very similar. Daylight was avoided because of its variable content of ultraviolet radiations which caused many of the white chips and some of the green-yellow, green, and purple chips to fluoresce.

The Ridgway volume used was that referred to as copy T_b in a previous report.[6] It was in good condition as a result of rare and careful use. Though purchased in 1940 it resembled another copy which had been obtained from Ridgway early in 1913. The only marked difference observed between these two copies was in the kind of tissue used as interleafing.

The key was recorded on filing cards and grouped according to the several Ridgway hue series. Charts were then drawn so that the relations of the colors to one another in the same and in neighboring hue series were evident.

Notations presented in Table I were obtained by two observers and checked by the author for errors. Deviations from systematic trends were noted by charting the notations according to hue, value and chroma. Certain hue series showed greater variations than did others (Figs. 1 and 2). When marked deviation patterns occurred, the divergent colors were checked visually in five available copies of Ridgway. As they were found to be similar in most cases, it was concluded that the anomalies were present when originally published. It is probable that they represented differences between the published work and the original material prepared by Ridgway. Color chips that fluoresced in ultraviolet light have been noted in Table I, and it is suggested that the notations of these colors be applied with caution.

Discussion

Biologists repeatedly state that Ridgway's book *Color Standards and Nomenclature* is most useful for their work because it contains many colors that are absent from other color standards. A check of the notations in Table I showed that of the 1044 colors of the Ridgway Standards arranged in 36-hue series, 450 are outside the range of the 40-hue *Munsell Book of Color*. In making this check the notations of each Ridgway hue series were compared with the nearest corresponding Munsell hue series. It was found that 221-Ridgway colors are higher in value and/or chroma, 136 colors found in 18 hues possess a lower chroma, and 97 colors are marginal. The large number of low chroma colors in Ridgway is noteworthy, for they are especially useful in ornithology, mammalogy, and mycology. An example of the biologist's need for low chroma colors is the work of Snyder in which he relates small variations in plumage color to geographic distribution.[8]

On the basis of these facts it is urged that any new system of color description for biological use should adequately cover the range of colors found in the Ridgway standards.

ACKNOWLEDGMENT

This work has been completed due to encouragement by members of the Inter-Society Color Council and has been assisted by a grant from the President's fund in aid of research at the University of Toronto.

[3] D. H. Hamly, Science **94**, 586 (1941).
[4] Mildred K. Nobles, Can. J. Research, Section C **26**, 281–431 (1948).
[5] Munsell, *Book of Color* (Munsell Color Company, Baltimore 2, Md., 1929).
[6] W. I. Illman, and D. H. Hamly, Science **107**, 626–628 (1948).
[7] D. B. Judd and K. L. Kelly, U. S. National Bur. Stand. J. Res. (RP1239) **23**, 355–385 (1939).
[8] L. L. Snyder and T. M. Shortt. Can. J. Research, Section D **24**, 118–133 (1946).

Index of Refraction and Coefficients of Expansion of Optical Glasses at Low Temperatures

FRED A. MOLBY
Department of Physics, West Virginia University, Morgantown, West Virginia
(Received October 18, 1948)

It is found that the absolute refractive index of any optical glass studied attains a minimum value at some temperature, and that the minimum refractive index is attained at decidedly higher temperatures with long wave-lengths than with short wave-lengths. Absorption bands in the ultraviolet are known to advance toward longer wave-lengths when an absorbing glass is warmed from liquid air temperature. Because of its closer proximity, the absorption band's advance would be accompanied by a more rapid increase of absolute refractive index N in the short wave end than in the long wave end of the spectrum, with rising temperature. At the same time expansion decreases the physical density and so tends to diminish N with rising temperature. At some particular temperature the two effects of temperature change may cancel each other. At lower temperatures than this, the density effect may prevail and N *fall with rising temperature*, while at higher temperatures than that for minimum N, the absorption effect may exceed the density effect, and the N *must rise with rising temperature*.

THIS paper deals with the changes in the absolute index of refraction, N, of some twenty optical glasses from the Glass Works of Schott and Genossen, of the Bausch and Lomb Optical Company, and of the Eastman Kodak Company. Expansion coefficients were incidental to the method used. Four or more wave-lengths of light were used with each glass. The change in N was found from ice to steam and from ice to liquid nitrogen, fixed temperatures at six points being used. Observations were made on the changes of optical thickness with temperature by aid of an interferometer of Pulfrich type, made by the writer especially for this work.

A method of interpolation was used to find from the data for fixed points, other data for any temperature between the fixed temperatures, and for slight extrapolations. It was found that for any given glass and wave-length, N attains a minimum value in this range of temperatures, and that the minimum N is attained at decidedly higher temperatures with *long wave-lengths than with short wave-lengths.*

The writer requested specimens of Schott's glasses to correspond with those studied by J. O. Reed[1] (1898), but in a number obtained, only one corresponded to any listed by Reed. Some reports on Schott's glasses were made by the writer[2] in 1911. Unexpectedly, the workman preparing samples at the factory must have lost the identity of the samples and supplied optical data, as for Table IV, not corresponding to the sample markings, and one or two sets foreign to any of the samples. In 1940 it was suspected that this had happened, and specific gravity tests and approximate measurements of N were made to find the samples that corresponded to data given. The conclusions stated in the preceding paragraph then became evident.

[1] J. O. Reed, Ann. d. Physik **65** (1898).
[2] F. A. Molby, Phys. Rev. **34**, 232 (1912); **35**, 77 (1912).

APPARATUS

The apparatus was designed to be rigid, free from shocks and vibrations, and, as far as possible, free from relative displacement of parts. A large-sized monochromator and a homemade interferometer of Pulfrich type were assembled on a masonry pier with slate top, in a basement room. A large tub was placed on a corner of the pier top and filled eight inches deep with dry sand. Castings designed and made for the purpose included a thick disk of 18-inch diameter to which was clamped, with large U bolts, a heavy box-shaped casting long enough to be equally divided over the sand base for balance, with one end projecting over the pier's edge to leave free space between the attached interferometer and the floor. Sand and castings weighed about 500 pounds. Mercury, mercury-cadmium amalgam, and sodium vapor arc lamps were used with the monochromator. (High pressure arcs may not be used.)

Figure 1 is a sketch of the apparatus, without the monochromator. The monochromator focused spectral lines at F, which was made coincident with the principal focus of the lens L, as modified by the prism P. The lens was a plano convex achromatic, 15-mm diameter and 10-cm focal length. An adjustable support from the barrel B held a metal screen with a variable four-slide aperture to admit a small part of a spectrum line to the prism P. The lens collimated the light and focused light reflected from the interferometer surfaces to form images of interference bands in the field of the micrometer eyepiece. The part B was a thick-walled brass tube clamped to an angle iron which in turn was bolted to the heavy casting which extended over the top of the pier about six inches to one side. Q was a support for the specimen S. It was made from a thermometer stem made fast below L in the tube, and formed like a duck's foot at its lower end.

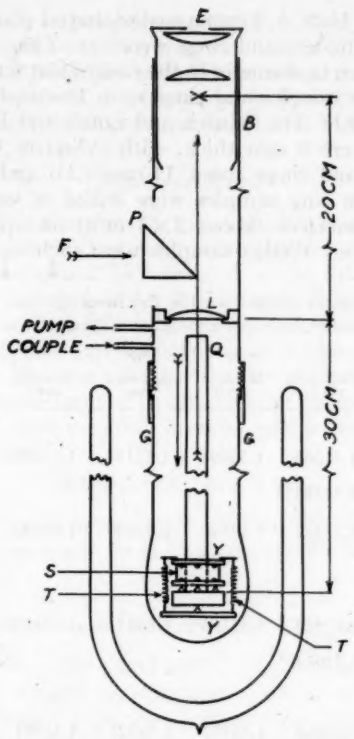

FIG. 1. Drawing of apparatus (interferometer).

Three glass points were fused into the foot, to support specimens on three-point bearing. A plano convex glass bed plate, for orienting specimens, was placed on the three bearing points.

The ring specimens were secured to the duck's foot by small springs *TT* and a yoke and equalizer bar *YY*. Use of the springs and all glass assembly largely obviates the faults of the interferometer method pointed out by Saunders.[3] Expansion measurements were made with ring specimens in a vacuum of 0.5 mm or lower pressure. The exhaust tube and a tube of small-sized glass to hold a thermal junction entered the barrel just below the lens. The tube extended far enough down to hold the junction close to but not touching the specimen. Solid specimens were observed at atmospheric pressure with the pump ready to remove frost on occasions when it collected on the specimen. (Optical thickness seemed unaffected by one atmosphere pressure.) For solids, the bed plate was weighted with a lead ring. The chamber *GG* was medium weight tubing, blown thinner at the lower end, about 30-mm I.D., held firmly by the ferule threaded into a collar on the brass tube. The Dewar cylinder represents quickly exchangeable heat environs. Screen wells were used in solids when suitable, and a well made from 2-inch I.D. iron tubing closed at the bottom, when using freezing mercury. The chamber *GG* was immersed from 5 to 9 inches in stationary temperature environments until change stopped.

[3] J. B. Saunders. Bur. Stand. J. Research 23, 179–195 (1939).

Fixed Temperature and Temperature Measurement

A four-quart Dewar jar with a two-inch screen wire *well* at the center was filled with cracked ice to immerse the chamber full depth. For the most part it was allowed to stand for several hours or overnight before any optical measurement was started. A supersensitive electrically controlled device at 41 degrees was used. Also a conventional double-walled and wrapped hypsometer, heated by steam through rubber tubing from a boiler; an iron well in a jar of mercury, (18 lb.), melting or freezing in dry ice in a Dewar; dry ice in a ten-inch Dewar; also liquid nitrogen with six- to eight-inch immersion, from 2 to 3 hours.

A Standard Leeds and Northrup potentiometer with sensitive galvanometer, a copper constantan junction of No. 40 insulated copper wound closely around a No. 28 constantan to eliminate conduction in the copper, with 1×1-cm vane of thin copper radiator at the junction, a few mm from the specimen at its level in the chamber (the chamber wall touched neither the specimen support nor the junction). Standard methods were used to find the

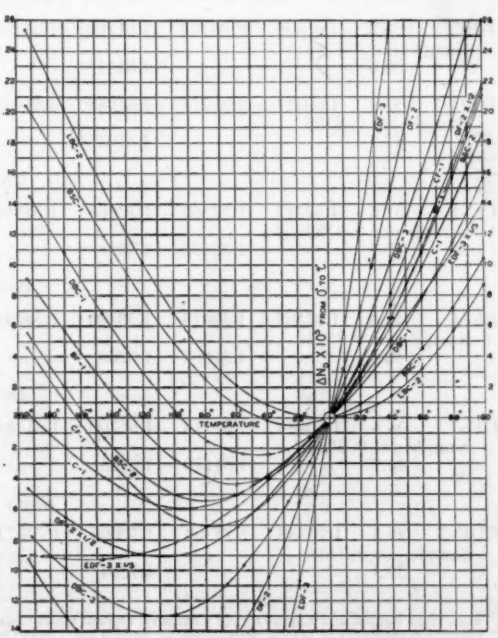

FIG. 2. Curves for N_D only, ten Bausch and Lomb glasses.

deviations of E from values compiled by Adams[4] (International Critical Tables). The nitrogen point was found by comparison with a couple tested for the purpose by the National Bureau of Standards.

Temperatures stated in tabulations are thought to be correct at the stationary temperatures listed above, with an error of $\pm 0.05°$, and somewhat less certain at the intermediate temperatures and the very low ones.

Glass samples were prepared by Optical Companies in U. S. A. From a wedge-shaped plate 8-mm thick, cylinders and rings were cut. The cylinders were 8-mm in diameter in the case of the Schott and Genossen samples and rings were 10-mm I.D. and 16-mm O.D. The Bausch and Lomb and Eastman glasses were 8 mm thick, with cylinders 1-cm diameter, and rings about 11-mm I.D. and 18-mm O.D. The ring samples were *milled to leave three* bearing surfaces (about 2×3 mm) on upper and lower faces. Wedge samples were such as to pro-

TABLE I. Characteristics of Bausch and Lomb Optical Company glass samples used in this investigation.

Type	$\frac{V}{n_D-1}$	$n_{A'}$ Potassium 766.5	n_C Hydrogen 656.3	n_D Sodium 589.3	n_d Helium 587.6	n_e Mercury 546.1	n_F Hydrogen 486.1	n_g Mercury 435.9	$n_{G'}$ Hydrogen 434.1	n_h Mercury 404.7	Specific gravity
Borosilicate Crown											
BSC–1	63.5	1.50578	1.50860	1.51100	1.51107	1.51300	1.51665	1.52096	1.52114	1.52454	2.48*
Sample pot 0–9793	63.6		1.50781	1.5102			1.51583**				
BSC–2	64.5	1.51179	1.51461	1.51700	1.51707	1.51899	1.52262	1.52690	1.52709	1.53043	2.53*
Sample pot 0–6670	64.4			1.5166**							
Crown											
C–1	58.6	1.51729	1.52036	1.52300	1.52307	1.52520	1.52929	1.53415	1.53435	1.53819	2.53*
Sample pot 0–4571	58.6		1.52069	1.5233			1.52962**				
Light Barium Crown											
LBC–2	57.4	1.56619	1.56956	1.57250	1.57259	1.57497	1.57953	1.58497	1.58521	1.58951	3.21*
Sample pot 0–1569	57.3		1.56909	1.5721			1.57908**				
Dense Barium Crown											
DBC–1	58.8	1.60439	1.60793	1.61100	1.61109	1.61357	1.61832	1.62396	1.62421	1.62867	3.58*
Sample pot 0–5195	58.6			1.6111**							
DBC–3	57.2	1.60411	1.60773	1.61088	1.61097	1.61352	1.61841	1.62426	1.62450	1.62911	3.57*
Sample pot 0–8305	57.2			1.6103**							
Crown Flint											
CF–1	51.6	1.52217	1.52560	1.52860	1.52869	1.53112	1.53584	1.54153	1.54178	1.54633	2.73*
Sample pot 0–9766	51.3		1.52578	1.5288			1.53608**				
Barium Flint											
BF–1	46.0	1.57598	1.58013	1.58380	1.58391	1.58693	1.59282	1.60002	1.60033	1.60615	3.31*
Sample pot 0–2594	46.0		1.58005	1.5838			1.59274**				
Dense Flint											
DF–2	36.6	1.60684	1.61218	1.61700	1.61715	1.62115	1.62904	1.63887	1.63929	1.64740	3.64*
Sample pot 0–2636	36.7		1.61170	1.6165			1.62848**				
Extra Dense Flint											
EDF–3	29.3	1.70555	1.71309	1.72000	1.72022	1.72602	1.73766	1.75239	1.75304	1.76542	4.51*
Sample pot 0–3428	29.3			1.7204**							

* Taken from Bausch and Lomb Optical Company, Optical Glass Catalog current in 1940.
** Refraction constants of sample determined by Bausch and Lomb Optical Company.

[4] L. H. Adams, Int. Crit. Tab. 1, 58 (1926).

duce about 12 bands per cm of glass face. Samples were placed on the "duck foot" with an adapter base glass to facilitate the orientation of samples, and always in a manner to make the direction of interference band *shift* parallel to the edges of the prism P.

Equations Used

Let N be the absolute index of glass at 0°C for a wave-length λ. The path difference for the interfering beams is $2NX$, where X is the thickness of glass in cm. Let δn be the number of bands that travel past the fiducial mark on the solid sample, and δm be the number of bands shift past a fiducial mark on the ring assembly for any given change of temperature from 0°C, the *ring* to be *observed in vacuum*. Now $n=2NX/\lambda$, or $n\lambda=2NX$. It is easily shown that

$$\Delta N=(\lambda/2X)(\delta n-N\delta m) \qquad (1)$$

for any given wave-length. When different wave-lengths are used, δm is to be multiplied by a ratio factor.

Interpolations for Intermediate Temperatures

Between −80°C and 100°C temperature changes produce δn and δm changes, each of which are, within about 1 percent, proportional to the corresponding changes in thermocouple indications in microvolts, with ice as reference point. To minimize errors of approximation, the following equations were assumed to hold.

$$\delta n=\alpha' E+\beta' E^2, \quad \delta m=a' E+b' E^2 \qquad (2)$$

from ice to steam.

$$\delta n=\alpha E+\beta E^2+\gamma E^3, \quad \delta m=aE+bE^2+cE^3 \qquad (3)$$

from ice to liquid nitrogen, where E is the *corrected e.m.f.* found from the thermocouple indications, and I.C.T. tabulations.

The constants for Eqs. (2) and (3) were computed from data observed (and corrected with respect to E) at the fixed points, for given wave-lengths and glasses in the Bausch and Lomb set of glasses and Eastman Kodak series. Making use of these constants, desired temperatures were expressed in E values given in the I.C.T. tabulations, and Eqs. (2) and (3) were computed to find the values of δn and δm which would obtain at those values of E. Computations of ΔN-values were then made by use of Eq. (1). *All computations* were made by the use of logarithms with the approximations of computation held to *small fractions* of the experimental errors in data. They have been systematically tabulated and verified, and finally tested by plotting results on large scale graphs.

Table I gives data from the Bausch and Lomb catalog of use in 1942, and other data supplied with the list of samples which Messrs. Rayton and Turner[5] thought would fairly represent the Company's glasses. The sample BSC–2 was too prismatic for good use and errors of experiment with it may be larger than usual.

Table II is of interest for comparison with Tables I and III and in connection with the usual explanation for a minimum point in an index temperature curve, and for the fact that it falls to a

TABLE II. Transmission of optical glass.* Thickness 10 mm, reflection deducted.

	BSC-1	BSC-2	C-1	LBC-2	DBC-1	DBC-3	CF-1	BF-1	DF-2	EDF-3
Cut-off in mμ	300	296	301	306	328	320	310	316	326	350
T at 300 mμ	0.0	0.8	0.0	0.0	0.0	0.0	0.0	0.0	0.0	0.0
320 mμ	25.0	30.0	19.5	5.0	0.0	0.0	10.5	1.0	0.0	0.0
340 mμ	64.5	53.0	55.5	25.0	2.0	9.5	87.5	59.0	20.0	0.0
360 mμ	90.0	76.0	84.0	47.5	22.0	82.5	97.0	94.0	72.5	6.5
380 mμ	98.0	95.0	97.2	92.5	96.8	98.5	99.0	98.0	84.5	47.0
400 mμ	99.5	99.5	99.3	99.5	99.5	99.4	99.5	99.5	90.5	70.0
420 mμ	99.5	99.5	99.3	99.5	99.5	99.4	99.5	99.5	93.5	85.5
440 mμ	99.5	99.5	99.3	99.5	99.5	99.4	99.5	99.5	95.5	92.0
460 mμ	99.5	99.5	99.3	99.5	99.5	99.4	99.5	99.5	97.0	96.2
480 mμ	99.5	99.5	99.3	99.5	99.5	99.4	99.5	99.5	98.0	98.5
500 mμ	99.5	99.5	99.3	99.5	99.5	99.4	99.5	99.5	98.9	99.3
600 mμ	99.5	99.5	99.3	99.5	99.5	99.4	99.5	99.5	99.5	99.5
700 mμ	99.5	99.5	99.3	99.5	99.5	99.4	99.5	99.5	99.5	99.5
800 mμ	99.5	98.5	99.3	99.2	99.4	99.4	99.5	99.5	99.5	99.5
1000 mμ	99.5	94.5	99.3	97.2	96.6	99.4	99.5	99.5	99.5	99.5
2000 mμ	88.8	85.0	95.0	90.5	65.0	80.5	70.0	88.5	99.5	99.5
3000 mμ	0.5	0.0	17.5	0.6	0.0	0.0	0.9	0.9	6.0	3.0
4000 mμ	0.0	0.0	0.0	0.0	0.0	0.0	0.0	0.0	0.0	1.2
Cut-off in mμ	3200	3000	4000	3200	2900	2850	3350	3250	3500	4100

* This tabulation of transmission of the ten Bausch and Lomb Optical Company glasses was prepared in that Company's laboratory, using freshly polished samples from the pots with which it supplied the interferometer samples.

[5] A. Francis Turner, J. Opt. Soc. Am. 30, 654 (1940).

lower temperature in violet than in red end of the spectrum. (See the paragraph following "Remarks on Figs. 3, etc." which follow Fig. 8.) Tilton[6] recently showed eight curves which he obtained with eight widely separated spectrum lines of the visible spectrum with Fluor Crown glass at temperatures 15 to 55. The minima for some of his curves would evidently fall at temperatures some degrees higher than 55°. His curves conform to the generalizations stated in this paper, and cause this writer to question whether some untried glass may not have its minimum index of refraction at much higher temperatures. See Fig. 6.

All the values of ΔN in Table III were computed as explained in connection with Eq. (1). Eight decimal places were found by the use of logarithms, the seventh place actually represented by tenths of $\frac{1}{10}$ inch in some of the graphs. The writer thinks that at their worst, some points may be in error by an amount of 5 in the sixth place, but from experience in making repeat measurements, plotting and searching out errors, *the relative values* of tabulated quantities seem in much better agreement, say ± 2 in the sixth decimal.

Figure 2 shows changes in N with temperature for D lines in ten Bausch and Lomb glasses over range of 294°. (Original 30×40 inches.)

Figure 3 is a reduction from a 20×43-inch sheet

TABLE III. Changes in absolute index of refraction from 0° to t°, (ΔN), for Bausch and Lomb Company glasses.

$t°$ / λ	−194	−170	−145	−120	−100	−80	−60	−40	−20	0	20	40	60	80	100	$\Delta N/1°$ at 20°
Borosilicate Crown BSC-1																
4801A	+15.9	+11.8	+ 7.6	+ 3.95	+ 1.60	− 0.11	− 1.10	− 1.37	− 0.96	0	+ 1.73	+ 4.0	+ 7.0	+10.4	+14.3	0.101
5087A	+17.5	+13.4	+ 9.2	+ 5.34	+ 2.81	+ 0.87	− 0.38	− 0.93	− 0.77	0	+ 1.46	+ 3.53	+ 6.2	+ 9.4	+13.1	0.087
5894A	+20.4	+16.4	+11.9	+ 7.8	+ 4.92	+ 2.56	+ 0.84	− 0.18	− 0.45	0	+ 0.89	+ 2.38	+ 4.51	+ 7.2	+10.4	0.059
6440A	+21.8	+17.7	+13.3	+ 9.1	+ 6.1	+ 3.51	+ 1.53	+ 0.23	− 0.30	0	+ 0.70	+ 1.99	+ 3.89	+ 6.3	+ 9.2	0.050
Borosilicate Crown BSC-2																
4801A	+ 1.0	− 2.0	− 4.7	− 6.7	− 7.57	− 7.64	− 6.9	− 5.3	− 2.9	0	+ 3.6	+ 8.0	+13.0	+18.7	+25.1	0.200
5087A	+ 2.63	− 0.41	− 3.22	− 5.3	− 6.3	− 6.6	− 6.0	− 4.7	− 2.6	0	+ 3.4	+ 7.5	+12.4	+17.9	+24.0	0.189
5462A	+ 4.53	+ 1.05	− 2.17	− 4.6	− 5.8	− 6.1	− 5.6	− 4.3	− 2.4	0	+ 3.2	+ 7.2	+11.8	+16.7	+22.4	0.180
5894A	+ 5.6	+ 2.0	− 1.32	− 3.8	− 5.0	− 5.4	− 5.0	− 3.8	− 2.1	0	+ 3.0	+ 6.5	+10.8	+15.6	+21.1	0.160
6440A	+ 6.9	+ 3.6	+ 0.5	− 2.1	− 3.6	− 4.4	− 4.44	− 3.7	− 2.2	0	+ 2.8	+ 6.1	+10.2	+14.9	+20.3	0.152
Crown C-1																
4801A	− 5.8	− 7.7	− 9.2	− 9.9	− 9.9	− 9.0	− 7.5	− 5.5	− 2.9	0	+ 3.6	+ 7.9	+12.7	+17.9	+23.5	0.199
5087A	− 3.7	− 5.7	− 7.3	− 8.3	− 8.5	− 7.9	− 6.7	− 4.9	− 2.7	0	+ 3.1	+ 6.8	+11.3	+16.4	+22.1	0.171
5462A	− 1.6	− 3.7	− 5.5	− 6.7	− 7.1	− 6.7	− 5.8	− 4.3	− 2.3	0	+ 2.9	+ 6.4	+10.5	+15.2	+20.4	0.159
5894A	+ 0.3	− 2.0	− 3.9	− 5.3	− 5.9	− 5.8	− 5.1	− 3.8	− 2.1	0	+ 2.7	+ 6.0	+ 9.8	+14.0	+18.6	0.150
6440A	+ 2.2	− 0.16	− 2.3	− 3.8	− 4.5	− 4.5	− 4.1	− 3.1	− 1.7	0	+ 2.3	+ 5.2	+ 8.7	+12.4	+16.7	0.131
Light Barium Crown LBC-2																
4801A	+20.2	+15.3	+10.3	+ 6.0	+ 3.1	+ 1.1	− 0.25	− 0.8	− 0.62	0	+ 1.4	+ 3.4	6.2	9.6	13.6	0.085
5087A	+22.1	+17.0	+11.9	+ 7.3	+ 4.3	+ 1.9	+ 0.5	− 0.4	− 0.6	0	+ 1.1	+ 2.9	5.3	8.3	11.8	0.072
5894A	+25.4	+20.3	+15.0	+10.2	+ 6.8	+ 4.1	+ 2.1	+ 0.9	+ 0.19	0	+ 0.4	+ 1.4	3.2	5.7	8.7	0.036
6440A	+28.4	+23.1	+17.5	+12.3	+ 8.5	+ 5.6	+ 3.1	+ 1.5	+ 0.4	0	+ 0.14	+ 0.9	2.3	4.1	6.4	0.025
Dense Barium Crown DBC-1																
4801A	+ 9.6	+ 5.4	+ 1.3	− 1.9	− 3.7	− 4.6	− 4.4	− 3.6	− 2.1	0	+ 3.0	+ 6.5	10.6	15.1	20.1	0.162
5087A	+11.8	+ 7.6	+ 3.3	0.0	− 2.0	− 3.3	− 3.7	− 3.3	− 2.1	0	+ 2.8	+ 5.7	9.4	13.7	18.4	0.143
5462A	+13.7	+ 9.3	+ 5.1	+ 1.4	− 1.0	− 2.2	− 2.9	− 2.6	− 1.8	0	+ 2.3	+ 5.2	8.6	12.4	16.6	0.131
5894A	+14.8	+10.8	+ 6.5	+ 3.0	+ 0.5	− 1.3	− 2.3	− 2.4	− 1.7	0	+ 2.1	+ 4.6	7.8	11.5	15.7	0.116
6440A	+16.6	+12.2	+ 7.8	+ 3.9	+ 1.4	− 0.4	− 1.3	− 1.6	− 1.2	0	+ 1.8	+ 4.1	6.9	10.1	13.7	0.103
Dense Barium Crown DBC-3																
4801A	−14.3	−15.7	−16.8	−17.1	−16.6	−15.2	−13.0	− 9.8	− 5.3	0	+ 5.9	+12.2	19.0	26.2	33.8	0.305
5087A	−11.7	−13.9	−15.5	−16.1	−15.7	−14.3	−11.9	− 8.7	− 4.7	0	+ 5.5	+11.5	18.0	24.8	32.0	0.276
5894A	− 7.5	− 9.9	−11.8	−12.9	−12.9	−12.0	−10.1	− 7.6	− 4.3	0	+ 4.9	+10.3	16.0	22.1	28.4	0.256
6440A	− 5.2	− 7.9	−10.1	−11.4	−11.5	−10.9	− 9.2	− 6.8	− 3.8	0	+ 4.5	+ 9.5	14.9	20.7	26.7	0.237
Crown Flint CF-1																
4801A	− 2.6	− 5.7	− 8.5	−10.5	−11.2	−11.0	− 9.8	− 7.5	− 4.2	0	+ 4.8	+10.4	16.9	24.1	32.0	0.261
5087A	− 0.1	− 3.2	− 6.1	− 8.3	− 9.3	− 9.5	− 8.8	− 6.9	− 4.0	0	+ 4.5	+ 9.7	15.9	22.8	30.4	0.244
5894A	+ 4.6	+ 1.0	− 2.4	− 5.1	− 6.5	− 7.1	− 6.8	− 5.4	− 3.1	0	+ 3.7	+ 8.1	13.4	19.4	26.0	0.205
6440A	+ 7.4	+ 3.6	0.0	− 3.1	− 4.8	− 5.7	− 5.8	− 4.8	− 2.9	0	+ 3.3	+ 7.3	12.1	17.7	23.9	0.184
Barium Flint BF-1																
4801A	− 0.4	− 3.7	− 6.7	− 8.9	− 9.9	− 9.9	− 8.9	− 6.9	− 3.9	0	4.5	9.8	15.9	22.7	30.1	0.246
5087A	+ 3.6	+ 0.1	− 3.3	− 5.9	− 7.3	− 7.7	− 7.3	− 5.8	− 3.3	0	3.9	8.7	14.3	20.4	27.3	0.218
5894A	+ 9.3	+ 5.8	+ 2.2	− 0.8	− 2.8	− 4.0	− 4.5	− 4.0	− 2.5	0	2.8	6.3	10.9	16.1	21.5	0.162
6440A	+13.6	+ 9.2	+ 4.7	+ 1.0	− 1.3	− 2.7	− 3.3	− 3.0	− 1.8	0	2.4	5.6	9.5	14.1	19.2	0.140
Dense Flint DF-2																
4360A	−40.4	−42.0	−42.4	−40.8	−37.8	−33.1	−26.8	−19.0	− 9.9	0	11.2	23.4	36.8	51.3	66.9	0.586
4801A	−26.8	−29.1	−30.6	−30.5	−28.9	−26.0	−21.5	−15.6	− 8.3	0	9.3	19.7	31.1	43.5	57.0	0.492
5087A	−20.8	−23.3	−25.1	−25.5	−24.6	−22.5	−18.9	−13.9	− 7.5	0	8.5	18.0	28.4	39.8	52.1	0.450
5462A	−14.7	−18.3	−21.0	−22.3	−21.9	−20.1	−16.8	−12.2	− 6.5	0	7.6	16.2	25.7	36.1	47.4	0.405
5894A	− 9.2	−13.0	−16.2	−18.0	−18.1	−16.8	−14.3	−10.4	− 5.6	0	7.0	14.8	23.6	33.2	43.7	0.370
6440A	− 4.9	− 8.7	−12.0	−14.2	−15.0	−14.6	−12.9	− 9.9	− 5.6	0	6.3	13.4	21.3	30.1	39.7	0.334
Extra Dense Flint EDF-3																
	(−192.5°)		(−146°)													
4801A	−77.3	−75.6	−72.3	−66.4	−60.1	−51.9	−41.8	−29.8	−15.8	0	16.5	34.3	53.4	73.6	94.7	0.858
5087A	−65.5	−65.4	−63.6	−59.1	−53.6	−46.2	−36.9	−25.8	−13.8	0	15.1	31.4	48.7	66.8	85.9	0.784
5894A	−44.8	−46.2	−46.3	−44.2	−40.9	−35.8	−28.9	−20.5	−10.7	0	12.2	25.4	39.6	54.7	70.5	0.634
6440A	−36.0	−38.1	−39.1	−38.1	−35.5	−31.3	−25.4	−18.0	− 9.4	0	11.0	23.0	35.9	49.6	63.9	0.575

[6] L. W. Tilton, Bur. Stand. J. Research, **34**, 599–608 (1945).

ruled to 10 lines per inch. Figures 3 and 4 represent all the data listed in Table III. Some duplications were made in graphing, for the sake of comparisons.

Figure 3 displays two sets of curves with their respective axes through 0 and 0′, the ordinate value per inch in the set through 0′ being five

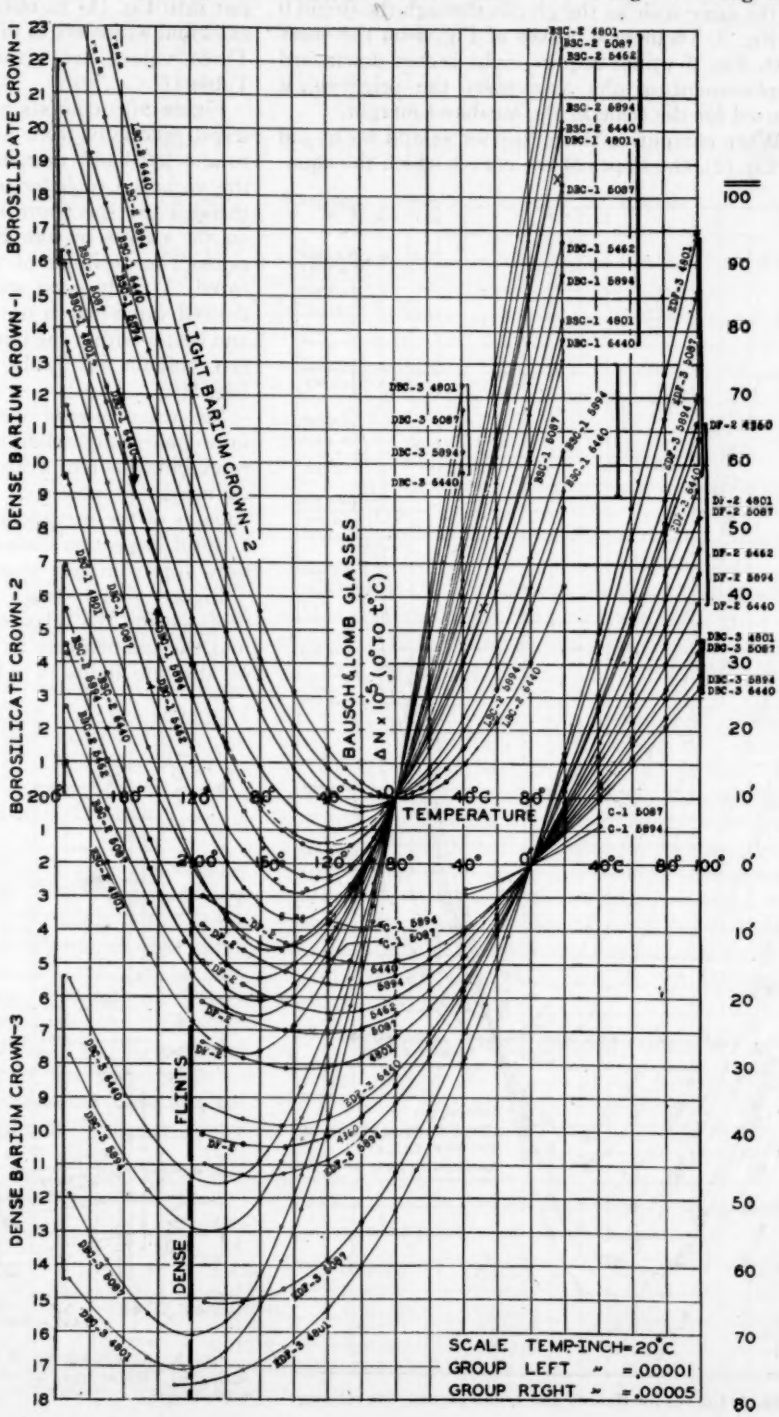

FIG. 3. Curves for Bausch and Lomb glasses, two sets in one.

times the ordinate value per inch in the set through 0.

Figure 4 includes graphs for four glasses drawn to the same scale as the graphs through the origin 0 of Fig. 3. To include curves of Fig. 4 on the sheet with Fig. 3 would require eight inches downward displacement of the axes from the origin 0, if plotted for the scale at the left-hand margin.

When computing the values for δn and δm by aid of Eq. (2), the slopes of the curves which the equations represent were computed analytically and used to find increments per degree at 20°C for the quantities δn and δm. These increments were then put into Eq. (1) to obtain $\Delta N/1°$ at 20° for each glass and wave-length of the Bausch and Lomb set. These values are given in the last column of Table III.

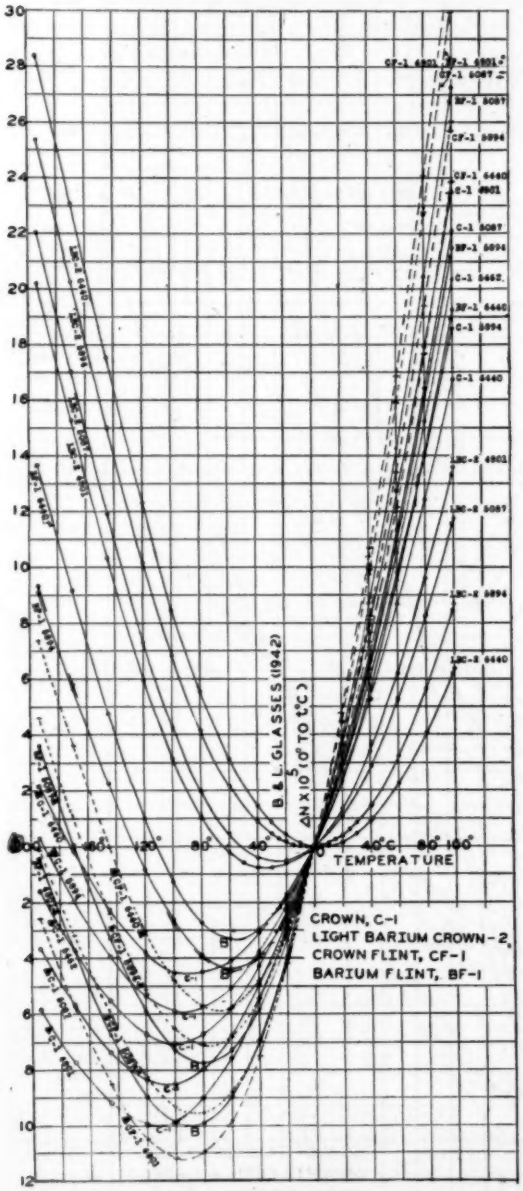

FIG. 4. Curves for Bausch and Lomb glasses, one set axes.

Figure 5(a) consists of the ten curves which descend gradually from left to right, to be referred to the left-hand margin scale. Each curve shows the variation of *index temperature coefficient at 20°* through the spectrum, for the glasses as indicated on the curves by the Bausch and Lomb designations. The positions of *F*, *D*, and *C* lines are indicated. A fairly good scaling can be made for any desired wave-length not too far beyond the limits and better within the limits of the observations. The last column in Table III includes the data of Fig. 5(a).

Six wave-lengths were used with DF–2. The unbroken straight line which rises from 3.3 to 5.8 represents the temperature index coefficients at 20° as nearly proportional to the reciprocals of the squares of the wave-lengths for which they obtain. Careful inspection shows that the linear relation is only approximately true, for DF–2 glass.

Figure 5(b) consists of ten broken line curves representing the relation between the wave-length and the temperature at which the minimum value of absolute index of refraction appeared for each

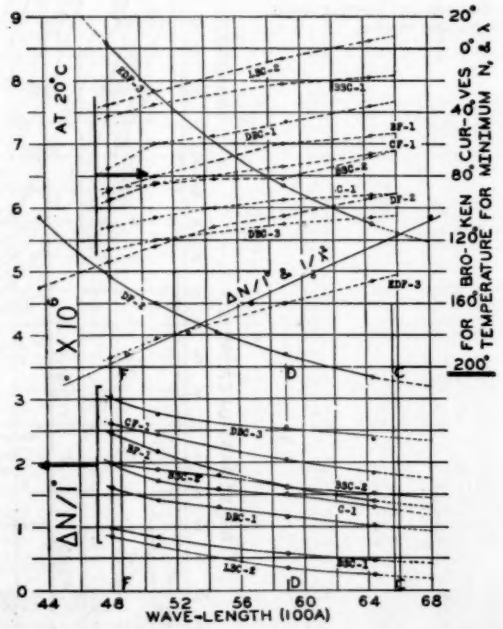

FIG. 5. (a) Curves for $\Delta N/1°$ at 20°, left-hand ordinate scale. (b) Temperature at which ΔN becomes a minimum vs. wave-length.

TABLE IV. Characteristics of samples from Schott and Genossen glasses (years 1910–1912).

Reference number	Name	Specific gravity at 21°C	n_D	$n_F - n_C$	$V = \left(\frac{n_D - 1}{n_F - n_C}\right)$	$n_D - n_C$	$n_F - n_D$	$n_G - n_F$
BSC	Borosilicate Crown	(2.47)	1.5093 (1.507)	0.00788	64.6	0.00236	0.00552	0.00449
2	Prism Crown (*R*) 0.3832	(2.46)	1.5156 (1.51)	0.00804	64.1	0.00240	0.00564	—
3	Ordinary Light Flint (0.276)?	(3.20)	1.57983 (1.580)	0.01381	42.0	0.00398	0.00983	0.00826
4	Ordinary Silicate Flint (*R*) 0.103	(3.71)	1.62161 (1.628)	0.01720	36.2	0.00492	0.01229	0.01054
5	Extra Dense Flint (0.41)	(4.47)	1.7180 (1.717)	0.02438 perhaps a duplication of No. 6	29.4	0.00685	0.01753	—
6	Extra Dense Flint 0.41	(4.48)	1.7180 (1.716)	0.02438	29.4	0.00685	0.01753	—
7	Heavy Silicate Flint (*R*) (0.165)	(4.78)	1.75453 (1.751)	0.02743	27.5	0.00768	0.01975	0.01646
1	Unknown	(3.48)	(1.610)	(0.0105)	(57.4)			
		(Wave-length	=4358A	4861A	5461A	5894A	6563A	
		n	=1.627	1.617	1.612	1.610	1.6065)	

Items marked (*R*) were identified by Messrs. Rayton and Turner.
Quantities in ( ) were determined by Molby.
All other names and quantities were furnished by the factory that made up the samples. The specific gravities of these agreed with those found by Molby.

of the Bausch and Lomb glasses, as designated by the lettering of each curve. The temperature scale is to be found at the right-hand margin for these curves.

Table IV gives the characteristics of the eight samples of glass from Schott and Genossen. As stated before, some difficulty resulted from mistaken identification in this set of samples. As given here they are thought to be correct. The glass sample number, and wave-length is on each curve, Fig. 6.

Figure 6 includes two sets of graphs which show the change in refractive index as computed from the steam point. The experimental data was taken more hurriedly than that for the Bausch and Lomb glasses, steam and liquid air points being the only stationary temperatures. Intermediate points were taken while the sample was held nearly at constant temperature in vapor above liquid air. As it turned out, sample 6 appears to be the same glass as sample 5. Two graphs representing these do not agree; subsequent to drawing these curves, work was done with wave-length 5462 with the result that is represented by the prominent circles plotted close to 5–λ5461A. In as much as glass No. 6 was the first sample on which the writer worked, he inclines to the belief that the findings for No. 5 are more reliable. There is an unexpected irregularity in the results for BSC in the two shorter wave-lengths. The sample should have been discarded because of bad preparation. A similar but less explainable error appears to have been made with glass 2–λ6438A. Experience with these glasses led to the adoption of the methods of temperature control described for the work on Bausch and Lomb glasses, where long periods of time could be had for the sample in a stationary temperature bath.

Data for the curves in Fig. 6 are justifiably omitted from this article.

Eastman Kodak Company Glasses

Upon request for glasses made without silica, the Eastman Kodak Company prepared samples of four glasses of its make. The general description as

TABLE V. Eastman Kodak Company optical glasses; characteristics determined by the Company (1947).

Sample mark	Melt No.	$N_D \pm$*	V	$F-C$ ±	$F-D$ ±	$g-F$ ±	$h-g$ ±	$D-A'$ ±
		0.0001		0.00002	0.00002	0.00002	0.00002	0.00002
11	110–5328	1.6973	56.0	0.01246	0.00877	0.00677	0.00562	0.00806
32	32–2641	1.7442	45.8	0.01624	0.01153	0.00913	0.00776	0.01018
33	33–2734*s*	1.7555	47.2	0.01602	0.01133	0.00890	0.00750	0.01014
45	45–29	1.8016	40.9	0.01959	0.01394	0.01118	0.00959	—

* N_D is the absolute index, ±0.0001, for the middle of the double line *D*.

to size, etc., of these is the same as for the Bausch and Lomb glasses. The experimental work done on these specimens by the writer was somewhat better because of the experience gained with the other makes of glasses.

The data for Table V were supplied with the

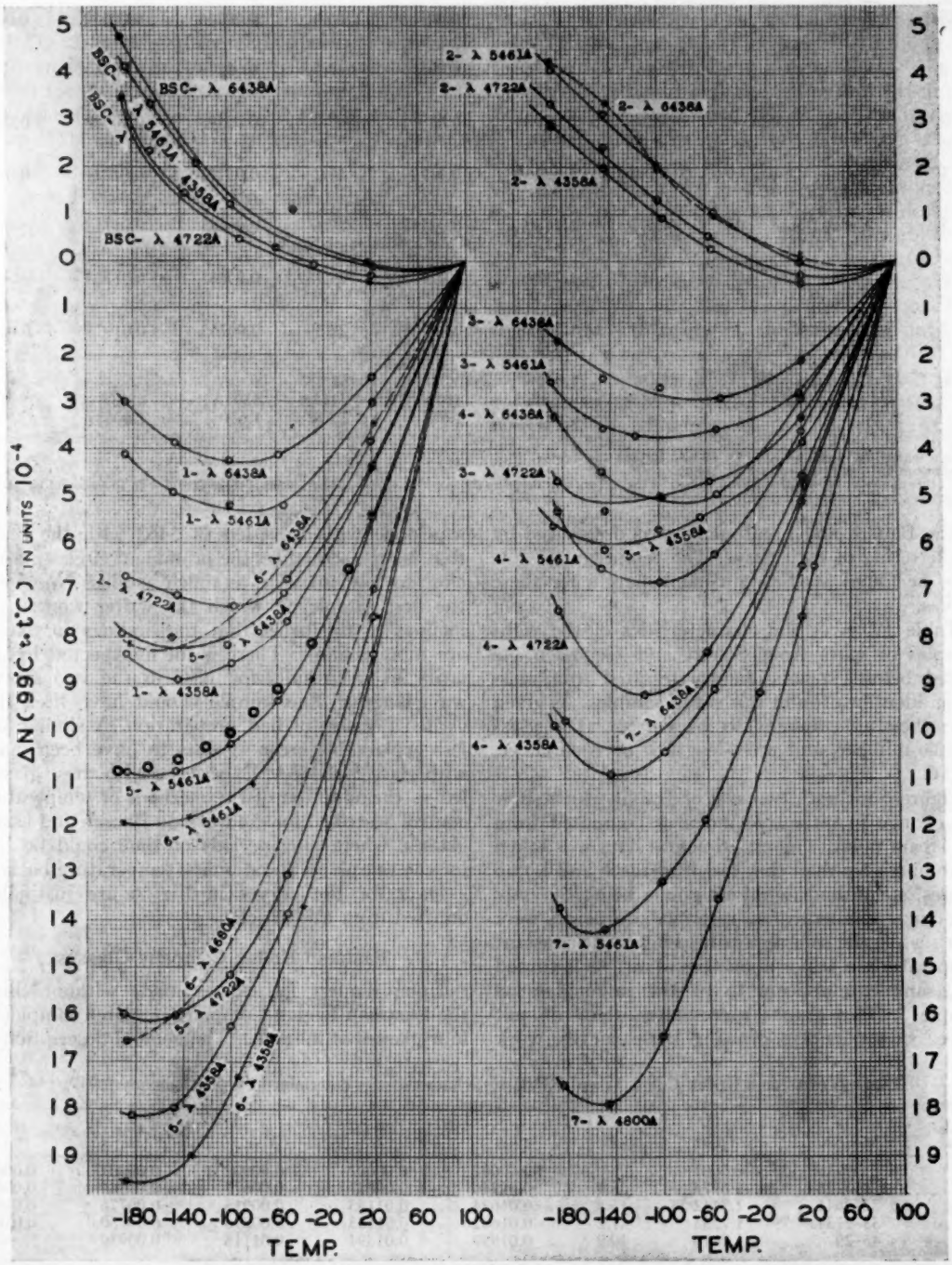

FIG. 6. Curves for eight Schott and Genossen glasses. ΔN 99° to −190° *vs.* wave-length and *t*.

samples. The "Mark numbers" have been used to designate the glasses in the tabulations of experimental results and in the graphs which represent the results.

TABLE VI. Eastman Kodak Company glasses, ΔN (units in 5th decimal place) from 0° to t°C.

	Glass Number 11				
t°C	λ4801 ΔN	λ5087 ΔN	λ5462 ΔN	λ5894 ΔN	λ6440 ΔN
100	16.6	15.0	13.2	11.8	10.2
80	11.8	10.5	9.2	8.0	6.5
60	7.7	6.8	5.8	5.0	3.7
40	4.5	3.9	3.2	2.7	1.8
20	1.9	1.6	1.3	1.1	0.6
0	0.0	0.0	0.0	0.0	0.0
− 20	− 0.9	− 0.5	− 0.3	− 0.5	+ 0.2
− 40	− 1.2	− 0.7	− 0.1	− 0.0	+ 0.9
− 60	− 0.9	− 0.3	+ 0.6	+ 1.2	+ 2.1
− 80	− 0.1	+ 0.6	+ 1.9	+ 3.0	+ 3.8
−100	+ 1.1	+ 2.0	+ 3.5	+ 5.2	+ 5.9
−120	+ 2.7	+ 3.8	+ 5.5	+ 7.5	+ 8.2
−145	+ 5.0	+ 6.4	+ 8.3	+10.5	+11.3
−170	+ 7.6	+ 9.2	+11.3	+13.3	+14.5
−194	+10.0	+12.0	+14.1	+15.7	+17.4
	Glass Number 32				
100		15.0	12.2	10.3	
80		10.7	8.6	7.0	
60		7.0	5.6	4.4	
40		4.1	3.2	2.4	
20		1.8	1.4	0.9	
0	0.0	0.0	0.0	0.0	0.0
− 20	− 1.7	− 1.2	− 0.4	+ 0.0	
− 40	− 2.2	− 1.3	− 0.1	+ 0.8	
− 60	− 1.7	− 0.5	+ 1.0	+ 2.1	
− 80	− 0.4	+ 1.1	+ 2.8	+ 4.2	
−100	+ 1.5	+ 3.3	+ 5.2	+ 6.8	
−120	+ 3.7	+ 6.0	+ 8.0	+ 9.8	
−145	+ 6.9	+ 9.9	+11.9	+14.2	
−170	+10.1	+14.1	+16.1	+18.7	
−194	+13.1	+18.0	+20.0	+22.9	+25.7
	Glass Number 33				
100	29.5	26.9	24.6	23.4	20.4
80	22.2	19.8	18.3	16.7	15.1
60	15.6	13.5	12.7	11.5	10.1
40	9.6	8.1	7.8	7.0	6.3
20	4.5	3.6	3.6	3.2	2.9
0	0.0	0.0	0.0	0.0	0.0
− 20	− 3.4	− 3.1	− 2.7	− 2.4	− 2.0
− 40	− 6.3	− 5.6	− 4.9	− 4.1	− 3.4
− 60	− 8.4	− 7.3	− 6.2	− 5.1	− 4.0
− 80	− 9.8	− 8.4	− 6.9	− 5.5	− 4.1
−100	−10.7	− 8.8	− 7.1	− 5.4	− 3.6
−120	−10.8	− 8.7	− 6.7	− 4.7	− 2.6
−145	−10.2	− 7.7	− 5.4	− 3.2	− 0.9
−170	− 8.8	− 6.1	− 3.6	− 1.2	+ 1.4
−194	− 7.1	− 4.2	− 1.5	+ 1.0	+ 3.7
	Glass Number 45				
100	44.0	40.2	36.4	33.3	30.3
80	33.8	30.8	27.8	25.2	23.0
60	24.3	22.1	19.9	17.5	16.3
40	15.5	14.1	12.6	11.2	10.3
20	7.4	6.7	6.0	5.3	4.9
0	0.0	0.0	0.0	0.0	0.0
− 20	− 6.6	− 5.9	− 5.5	− 4.8	− 4.1
− 40	−12.1	−10.7	− 9.6	− 8.5	− 7.3
− 60	−16.5	−14.5	−12.6	−11.2	− 9.7
− 80	−19.9	−17.3	−14.8	−13.1	−11.4
−100	−22.5	−19.4	−16.3	−14.4	−12.3
−120	−24.4	−20.8	−17.2	−15.1	−12.7
−145	−25.9	−21.9	−17.9	−15.4	−12.6
−170	−26.7	−22.3	−18.2	−15.3	−11.9
−194	−27.0	−22.3	−18.1	−14.9	−10.9

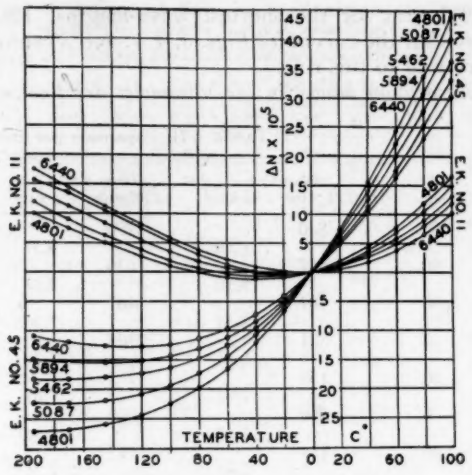

FIG. 7. Curves for Eastman Kodak No. 11 and No. 45. ΔN *vs.* wave-length and t, 100° to −194°.

Table VI gives the computed changes in refractive index referred to vacuum for the four Eastman Kodak Company glasses. Incomplete data are given for glass No. 32 because of a lamp failure when a suitable replacement was unobtainable. (High pressure vapor arcs broaden the lines to an unusable degree.)

Figure 7 shows curves representing the results for Eastman Kodak Company glasses Mark No. 11 and Mark No. 45. Please note that the temperature scale was made 20° per inch as in Figs. 3 and 4, but that the scale for ΔN corresponds with only that part of Fig. 3 where the curves pass through the origin 0′, namely, 5 units in the 5th decimal place, per inch.

Figure 8 shows the results as found in Table VI for Eastman Kodak Company glasses Mark No. 33 and Mark No. 32. Remarks on Fig. 7 apply to Fig. 8 also.

Remarks on Figs. 3, 4, 6, 7, 8. The curves in Fig. 6 give a fair indication that any glass will show a minimum index of refraction for any wave-length, at some temperature, and that this temperature will be highest for the longest wave-lengths

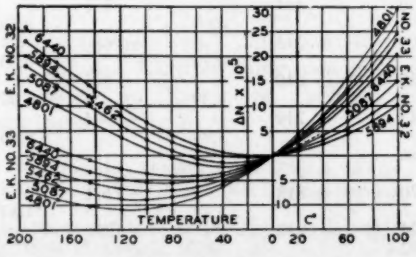

FIG. 8. Curves for Eastman Kodak No. 32 and 33. ΔN *vs.* wave-length and t. 100° to −194°.

and lowest for the shortest wave-lengths. Please note that the curves for Figs. 3, 4, 7, and 8 conform very well to this rule.

Absorption bands in the ultraviolet are known to progress toward the long wave end of the spectrum when an absorbing glass is warmed from liquid air temperature. Because of closer proximity, the absorption band's progress would be accompanied by

TABLE VII. Expansion per unit length, and the coefficient of expansion.

Temp.	Glass C-1 $\Delta L/L\times10^6$	$\alpha\times10^6$	Glass BSC-1 $\Delta L/L\times10^6$	$\alpha\times10^6$	Glass BSC-2 $\Delta L/L\times10^6$	$\alpha\times10^6$	Glass LBC-2 $\Delta L/L\times10^6$	$\alpha\times10^6$	Glass DBC-1 $\Delta L/L\times10^6$	$\alpha\times10^6$
100	830		796		675		800		669	
		8.69		8.31		7.03		8.28		7.05
80	657		630		534		635		528	
		8.50		8.13		6.89		8.15		6.87
60	487		467		396		472		390	
		8.31		7.96		6.75		8.00		6.69
40	321		308		261		312		256	
		8.11		7.78		6.61		7.86		6.50
20	158		152		129		154		126	
		7.92		7.61		6.46		7.72		6.32
0	000		000		000		000		000	
		7.69		7.36		6.30		7.51		6.18
− 20	− 154		− 147		− 126		− 150		− 124	
		7.47		7.21		6.12		7.36		5.99
− 40	− 303		− 292		− 248		− 297		− 243	
		7.16		7.00		5.91		7.15		5.81
− 60	− 446		− 431		− 367		− 440		− 359	
		6.80		6.72		5.66		6.90		5.57
− 80	− 582		− 566		− 480		− 578		− 471	
		6.39		6.41		5.39		6.60		5.32
−100	− 710		− 694		− 588		− 710		− 577	
		5.99		6.02		5.07		6.24		5.05
−120	− 830		− 814		− 689		− 835		− 678	
		5.44		5.55		4.67		5.77		4.68
−145	− 966		− 953		− 806		− 979			
		4.78		4.91		4.17		5.16		
−146									− 799	
										4.18
−170	−1086		−1076		− 910		−1108		− 900	
		4.10		4.25		3.61		4.49		3.67
−194	−1184		−1178		− 997		−1216			
−192									− 980	
At 20°		8.02		7.69		6.53		7.79		6.41

	Glass DBC-3		Glass DF-2		Glass EDF-3		Glass BF-1		Glass CF-1	
100	641		742		773		819		745	
		6.83		7.58		8.00		8.44		7.67
80	504		590		613		650		592	
		6.62		7.50		7.86		8.32		7.56
60	372		440		456		483		441	
		6.41		7.42		7.73		8.19		7.45
40	245		292		301		320		292	
		6.20		7.34		7.59		8.06		7.35
20	120		145		149		159		145	
		5.99		7.26		7.46		7.93		7.23
0	000		000		000		000		000	
		5.87		7.14		7.45		7.67		7.07
− 20	− 117		− 143		− 149		− 153		− 141	
		5.69		7.03		7.24		7.59		6.97
− 40	− 231		− 283		− 294		− 305		− 281	
		5.44		6.91		7.02		7.44		6.82
− 60	− 340		− 422		− 434		− 454		− 417	
		5.26		6.75		6.87		7.20		6.62
− 80	− 445		− 557		− 572		− 598		− 550	
		4.99		6.58		6.70		6.91		6.36
−100	− 545		− 688		− 706		− 736		− 677	
		4.73		6.33		6.47		6.54		6.03
−120	− 640		− 815		− 835		− 867		− 798	
		4.39		5.97		6.14		6.04		5.60
−145	− 749		− 964				−1018		− 938	
		3.94		5.46				5.41		5.02
−146					− 995					
						5.65				
−170	− 848		−1101		−1130		−1153		−1063	
		3.44		4.84		5.10		4.68		4.37
−194	− 930		−1216				−1266		−1168	
−192.4					−1244					
At 20°		6.09		7.30		7.52		7.99		7.29

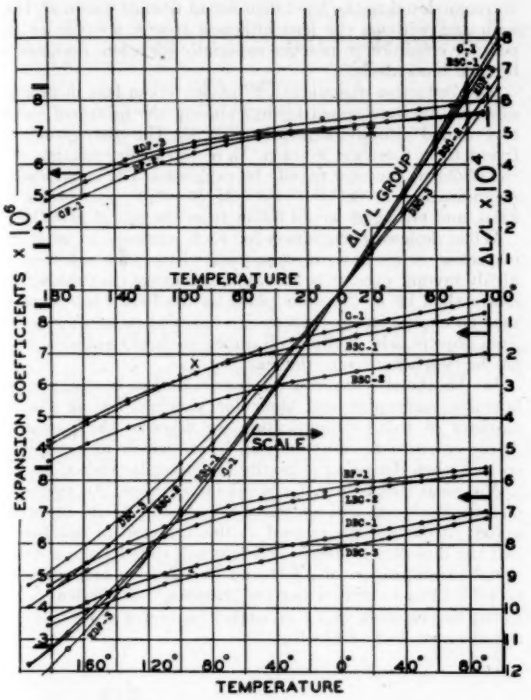

FIG. 9. (a) Expansion coefficients of ten Bausch and Lomb Company glasses. (b) $\Delta L/L$ of a few Bausch and Lomb glasses.

a more rapid increase of N in the short wave end than in the long wave end of the spectrum, with rising temperature. At the same time, expansion decreases the physical density and so tends to diminish the N with rising temperature. At some particular temperature the two effects of temperature change may cancel each other. At lower temperatures than this, the density effect may prevail and the N *fall* with *rising temperature*, while at higher temperatures than that for minimum N, the absorption effect may exceed the density effect, and the N must *rise with rising temperature.*

A part of these experimental results was analyzed a few years ago by a leading British manufacturer of optical glass. Like these results, the results of the analysis had very restricted unpublished circulation. It is the writer's hope that the results offered in this paper may be included in a further study by the British manufacturer, and that he will publish his analysis, and interpretation.

EXPANSION COEFFICIENTS

In connection with Eqs. (2) and (3), explanation was made of the method of finding quantities δm to correspond to any desired temperature change from 0°. (See Fig. 9(a) and (b).) Having such δm values computed by logarithms, a slight variation

TABLE VIII. Expansion per unit length and the coefficient of expansion Eastman Kodak Company glasses.

	Glass No. 11		Glass No. 32		Glass No. 33		Glass No. 45	
Temp.	$\Delta L/L$ ×10⁵	α ×10⁶	$\Delta L/L$ ×10⁵	α ×10⁶	$\Delta L/L$ ×10⁵	α ×10⁶	$\Delta L/L$ ×10⁵	α ×10⁶
100	635		639		594		634	
		6.61		6.74		6.27		6.70
80	503		505		469		500	
		6.50		6.59		6.11		6.54
60	373		373		347		369	
		6.38		6.42		5.95		6.36
40	245		245		228		242	
		6.21		6.22		5.78		6.15
20	121		120		112		119	
		6.04		6.01		5.60		5.94
0	0		0		0		0	
		5.90		5.83		5.44		5.76
− 20	−118		−117		−109		−115	
		5.73		5.70		5.24		5.62
− 40	−232		−231		−214		−228	
		5.49		5.50		5.05		5.37
− 60	−342		−341		−315		−335	
		5.17		5.23		4.72		5.04
− 80	−446		−445		−409		−436	
		4.82		4.91		4.39		4.66
−100	−542		−544		−497		−529	
		4.42		4.55		4.04		4.23
−120	−631		−635		−578		−614	
		3.95		4.11		3.64		3.73
−145	−729		−737		−669		−707	
		3.37		3.57		3.16		3.15
−170	−814		−826		−748		−786	
		2.84		3.01		2.68		2.60
−194	−882		−899		−812		−848	

was used to find values of $\Delta L/L$ corresponding to any temperature, where L represents length, elsewhere called X. Table VII gives the increments of length per unit of length, from 0°C to the tabulated temperatures, for the Bausch and Lomb glasses. The values of coefficient of expansion, α, given in the column under α, are the mean values between the two temperatures beside which the values appear in the table. The fairly regular way in which these values diminish from high to lower temperatures is somewhat reassuring for the whole general method of computing.

The last line in Table VII gives the value of α at 20° as found from tangents to curves computed analytically, (Eq. (2)) for δm, and evaluated for one C degree, at 20°. The values thus found at 20° usually do not differ from the mean values taken over the interval from 0° to 40°.

This table is similar to Table VII, except that the value for α at 20° was omitted.

For references on this topic see—Winkelmann's Handbuch der Physik;[7] Handbucher der Experimental Physik,[8] Vol. 19 (contains many references); Pulfrich's 56 pages Ueber den Einfluss der Temperatur auf die Lichtbrechung des glases;[9] and Peters' paper on Refractive Indices at High Temperatures.[10]

[7] A. Winkelmann, *Handbuch der Physik, zweite Auflage, Band* VI, (Johann Ambrosius Barth, Leipzig, Germany, 1906), p. 636.

[8] Wien-Harms, *Handbucher der Experimental Physik* (Akad. Verlag., m. b. H. Leipzig, 1928).

[9] C. Pulfrich, Ann. d. Physik **45**, 609–665 (1892).

[10] C. G. Peters, Sci. Pap. Bur. Stand. **20**, 521 (1926).

Letters to the Editor

Some Notes on the Designing of Aspherical Magnifiers for Binocular Vision

C. E. COULMAN AND G. R. PETRIE
Imperial Chemical Industries Limited, Plastics Division, Optical Development Department, The Hall, Welwyn, Herts, England

April 25, 1949

VARIOUS papers have appeared from time to time describing single lens magnifiers with aspheric surfaces, but to the best of the writers' knowledge no attempt has hitherto been made to design such lenses primarily for binocular vision. As a result of an extended investigation into this problem, considerable progress has been made, and it is proposed to publish a full account of the results elsewhere.

While engaged on this work, the Report on Survey of Optical Aids for Subnormal Vision[1] was brought to our notice, and we were interested to see that the specification for a proposed magnifier recommended therein (p. 58) closely resembled that of one we had already undertaken, namely 6-in. focus 6-in. diameter.

Unfortunately the focal length of the lens recommended was not explicitly stated, and, while endeavoring to infer its value, it was found that this otherwise excellent report did not satisfactorily deal with the magnification of low power magnifiers. As stated in the report this subject is fully discussed in Southall's "Mirrors, Prisms and Lenses," but a few remarks may not here be out of place.

When designing a reading lens (for monocular or binocular vision) two measures of its magnification may be used. These we call "conventional magnification" and "effective magnification." In Fig. 1 an object OA of height h is situated at distance l from a "thin" lens L of focal length f' and a virtual image of OA of height h' is formed at $O'A'$ when $O'L=l'$. An observer has his eye at E, where $LE=d$.

Assuming that the unaided eye would observe h at the least distance of distant vision D, then we can show effective magnification,

$$M=\frac{h'}{d-l'}\Big/\frac{h}{D}=\frac{D(1/f'-1/l')}{1-(d/l')}$$

From this formula we can deduce,

(1) If O' is at ∞ (i.e., when h is in the focal plane of the lens)

$$M=\frac{D}{f'}.$$

(2) If $d=0$, and $l'=-D$, $M=(1+D/f')$ *and is then a maximum* and this we call the "conventional magnification."

In the report[1] the magnification is given by $M=D/f'$ but herein we have conflicting conventions, i.e., we accommodate to D without the lens, but have the eye at rest when the lens is in use. We prefer to use the second expression $M=(1+D/f')$ as this contains the reasonable convention of the eye being accommodated to the least distance of distant vision D, both with and without the lens although clearly $d=0$ is an impossible condition in practice especially for a lens designed to be used binocularly.

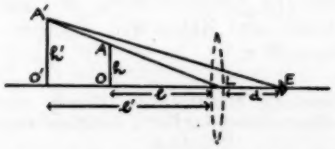

FIG. 1. Lengths to the left of the lens are measured negative, i.e., Conrady's Convention.

The "effective magnification" of any given lens in practice can only be determined by introducing the *measured* values of l' and d into the expression for M. The discrepancy referred to in footnote 36 on p. 37 of the report relating to a $+5.00D$ lens can now readily be explained. The conventional magnification is $(1+D/f')=1+25/20=2\frac{1}{4}\times$ as quoted by Zeiss, and not $1\frac{1}{4}$ as would follow from the use of $M=D/f'$.

When designing magnifiers for such purposes as industrial inspection or for cases of subnormal vision such as corrected highly myopic eyes, it is desirable to arrange that the virtual image shall be in the same plane as the bench top in order that no change in accommodation takes place when glancing from objects held in the hand under the lens to objects lying on the bench not under the lens.

In the above discussion no discrimination has been made between monocular and binocular viewing, but in the remainder of this communication we describe the particular defect common to most existing lenses which we set out to correct when designing primarily for binocular vision.

A typical lens is 6-in. focus, $4\frac{1}{2}$-in. aperture. An eye relief of 5 in. is chosen and an image distance of 13 in. (approximately) from the eye is used as this is found in practice to suit the majority of users. This lens will thus have a conventional magnification of $2.7\times$ and an effective magnification of $1.8\times$. For various reasons a "bending" of the lens is selected having radii of $7\frac{1}{2}$ in. and 5 in. and a section of the arrangement is shown in Fig. 2.

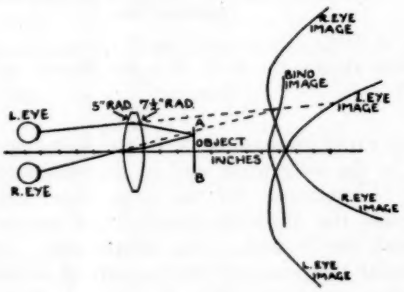

FIG. 2.

This section is so chosen as to contain both eyes of the observer and the axis of the lens both because in this section aberrations are, in general, a maximum, and furthermore the use of skew rays is largely avoided. We now consider the images of the section AB of a plane object as seen by each eye separately and by both eyes taken binocularly. It will be found that, in practice, a working distance of about three inches will automatically be assumed as by so doing the virtual image will be formed at approximately 13 in. from the eye, i.e., rather more than the least distance of distinct vision. The shapes and relative positions of these images may be determined either trigonometrically or by direct measurement and are also shown in Fig. 2. From these it will immediately be apparent that the two eyes are required to fuse two completely different images and that especially towards the edge of the field of view the normal relation[2] between accommodation and convergence is seriously disturbed. It should also be noted that the monocular fields extend considerably beyond the binocular field and this leads to a sharp discontinuity of viewing conditions. Needless to say distortion is also excessive.

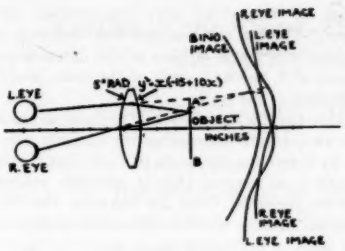

FIG. 3.

It has been our object primarily to remedy all these defects by aspherizing one or both surfaces of the lens and the extent to which we have succeeded will, we think, be clear from a study of Fig. 3.

This shows the effect of aspherizing the surface remote from the eyes and in this case the generator is a conic having the equation $y^2=x(-15+10x)$ using Cartesian coordinates with the usual sign conventions.

Needless to say the best results cannot be achieved by restricting the design to conics and details of lenses employing higher degree curves including the 6-in. focus, 6-in. aperture lens will be given elsewhere.

[1] V. J. Ellerbrook, J. Opt. Soc. Am. 36, 679 (1946).
[2] H. H. Emsley and Swaine, *Ophthalmic Lenses*, p. 260 (Hatton Press, London, 1947). H. H. Emsley, *Visual Optics* (Hatton Press, London, 1949) pp. 169, 427, 429.

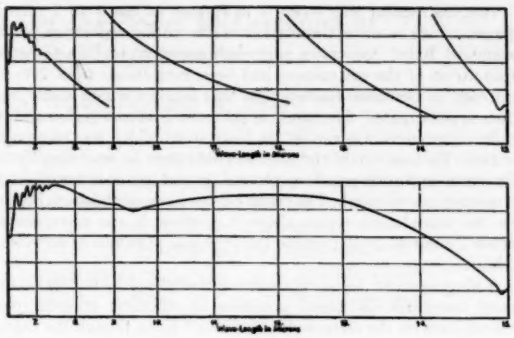

FIG. 1.

43 and 38 mm for the wave-length drive axis and slit-aperture axis.

The reproductibility is maintained by preventing the wires from slipping over the grooves. In order to do that, first of all, we lay rosin on the wire and turn it three times around each pulley.

Under those conditions, the right coupling slit-wave-length can stay on several days without any change from the operator.

This very simple modification is shown to be useful in control analysis because it permits the operator to calculate the previous results during the next run; in this way we increased the yield of the spectrometer and its reproductibility.

Improvement in Routine Analysis with the Beckman I.R. 2 Infra-Red Spectrophotometer by a Slight Mechanical Modification

A. F. CORNU AND P. A. TARDY
Compagnie Française de Raffinage, Paris, France
February 15, 1949

USING a Beckman I.R. 2 infra-red spectrophotometer for routine control analysis, we have noticed how disadvantageous the necessity was to stop the recording system several times at different wave-lengths to change the slit-width in order to keep the curve in the diagram; this modification during a run is not only a loss of time but mainly a failure of reproductibility.

While the slit-width meter can be read in tenths of a millimeter, a small difference of one-hundredth of a millimeter can make a pen deviation of several millimeters.

In order to prevent these discontinued slit-width changes, which cut the spectra into three or four pieces, giving also in the background curve an important and unnecessary slope, we move gradually at the same time the slit-width and the wave-length drive.

It has been noticed that this coupling is easily made on the I.R. 2 Beckman spectrophotometer by means of pulleys between the slit-width axis and the prism displacement axis. These two axes, parallel and 360 mm away from each other, are separated by the wave-length drive motor crankcase, which will be easily drilled through in order to make a path for the connection wires.

Figure 1 shows at the top the background spectrum commonly obtained with four slit-width changes between·15 and 7 microns, the record at the bottom represents the background spectrum between the same wave-lengths with automatic slit-width drive; the diameters of the pulleys are, respectively,

Infra-Red Interference Filter Used in Calibration

D. E. WILLIAMSON
Baird Associates, Inc., Cambridge, Massachusetts
May 16, 1949

THE newly developed Dennison-Hadley filters[1] have recently been put to use in the calibration of an infra-red spectrophotometer. Following procedures outlined by Fizeau, Foucault, and others, it is not only possible to check the over-all calibration of the wave-length scale, particularly at wave-lengths not typified by any convenient absorption band, but it is also possible to extend the range of the calibration into shorter wave-lengths where no convenient absorption bands exist.

The Dennison-Hadley filters are reflection filters which are typified by a series of reflection peaks whose width at the 50 percent reflectivity value is about half their separation. Over the wave-length region about which the filter is designed the reflectivity at peak is approximately 100 percent and drops to zero between peaks. The separation of peaks is approximately a constant in frequency units. Thus, in wave-length units the separation of peaks decreases going toward shorter wave-lengths. The bands are visible not only in the infra-red (for which the filters are designed) but also in the visible spectrum, although the efficiency of the filter in the visible is much reduced.

In the calibration of a spectrophotometer, it is of course desirable to have a filter whose absorption or transmission bands are known. However, in the absence of such a calibration it is still possible to check the consistency of the wave-length scale provided a few points on that scale have been established through the use of standard materials. The reflectivity curve of a Dennison-Hadley filter run on such an instrument should show the positions of the reflection minima spaced along the wave-length scale at regular intervals. Any departure of a single reflection minimum from its nominal position indicates anomaly in calibration at that point.

One instrument was recently calibrated in the 1 to 2 micron range, which is an extrapolation of the calibrated range of the standard Baird Associates spectrophotometer. In this case, the calibration of the instrument had been established from 2 to 16 microns. A Dennison-Hadley filter was selected which would produce approximately five bands in the 1- to 2-micron region and its reflectivity curve was run on the instrument which was to be calibrated. The position of the minima could then be read directly off the curve and their positions plotted on a graph of order of interference *vs.* wave-length. The curve having been established thereby for the wave-length region above 2 microns, it was extrapolated below 2 microns to determine the probable positions of reflection minima.

A more accurate means of extrapolation would be to plot on the same curve the calculated positions of reflection minima from known data on the dispersion of stibnite.[2] Even though the calculated and experimental curves might not coincide, the slopes of the two curves should be very similar from point to point and would serve as a guide for the extrapolation.

[1] L. N. Hadley and D. M. Dennison, Phys. Rev. **69**, 258 (1946); J. Opt. Soc. Am. **37**, 451 (1947); J. Opt. Soc. Am. **38**, 483 (1948).
[2] B. H. Billings and Mark Hyman, Jr., J. Opt. Soc. Am. **37**, 119 (1947).

Further Remarks on the Stiles-Crawford Effect

JOHN R. PLATT
Department of Physics, University of Chicago
May 20, 1949

TORALDO DI FRANCIA has emphasized quite properly the similarity between retinal cones and microwave dielectric antenna horns in accounting for the Stiles-Crawford effect.[1–3] It should be pointed out that the receiver angle-of-view equation,[4] which was applied to this effect earlier[5] using a geometrical ray determination of one quantity in the equation, remains valid even for the antenna horn situation. This is because the angle-of-view equation is derived from general thermodynamic considerations (conservation of flux = first law; conservation of brightness = second law).[4] The ray construction was used only to determine ω, the effective solid angle-of-view of the detector surface in the cone, in terms of θ, the half-angle of the cone, and θ', the angle of total reflection at the wall.

The effective angle ω may increase, perhaps as much as a factor of 2, as the wave-length approaches the detector size and diffraction begins to determine the angle of view; but the angle-of-view equation itself is so general that it probably remains valid by correspondence principle. Thus, for instance, the Abbe sine condition goes over into the familiar rule $\alpha D \sim$ constant (λ), where α is the mean angle of diffraction by an aperture or of reception by an "image," diffraction pattern or detector of diameter D. This rule would give a half-angle of about 6° for reception of green light by a 5-micron-diameter cone—close to the value given in reference 4 from the geometrical determination of ω. However, such diffraction arguments would predict in general a narrower Stiles-Crawford pattern for blue light than red. Since very little effect of this kind was found by Wright and Nelson, it follows that the ray picture is still a good approximation.

The only assumption involved in using the conservation laws of flux and brightness for this problem is that the system has efficient light utilization in at least one direction of view, which seems biologically plausible. (This in turn implies that the ratio of the two cone bases is near but not greater than about 9:1, as a geometrical ray construction will show. The values used by O'Brien[6] come very close to this ratio.)

The principal lobe in the radiation pattern as given by Toraldo di Francia[3] for a microwave dielectric horn should, therefore, also have its half-intensity-width given approximately by the angle-of-view equations in references 4 and 5 when its relative dielectric constant is replaced by the appropriate relative refractive index.

[1] G. Toraldo di Francia, Nuovo Cimento **5**, 110 (1948).
[2] G. Toraldo di Francia, Atti della Fondazione Giorgio Ronchi **5/6**, 137–144 (1948).
[3] G. Toraldo di Francia, J. Opt. Soc. Am. **39**, 324 (1949).
[4] H. S. Snyder and J. R. Platt, J. Opt. Soc. Am. **38**, 269 (1948), esp. pp. 275–6.
[5] John R. Platt, J. Opt. Soc. Am. **37**, 669 (1947).
[6] Brian O'Brien, J. Opt. Soc. Am. **37**, 275 (1947).

Minutes of the Thirty-Third Meeting of the Board of Directors of the Optical Society of America, Incorporated

HOTEL STATLER, NEW YORK, NEW YORK, MARCH 9, 1949

IN addition to the transaction of routine business, the following items of general interest to members of the Soceity were considered.

Announcements by Secretary

Under authority conferred by a previous Board, the President and Secretary had appointed George W. Moffitt and C. W. Keuffel proxies for the Optical Society of America at the annual meeting of the American Institute of Physics, held on February 19, 1949.

Results of letter ballots:

1. Approval of appointment of the following O.S.A. representatives to the U.S.N.C. of the I.C.I. for a term of three years, commencing in November, 1948:

Frank Benford, *Chairman*
L. A. Jones D. B. Judd

2. Approval of appointment of the following Ives Medal Committee:

G. S. Monk, *Chairman*
L. A. Jones W. R. Brode
K. S. Gibson G. H. Dieke

3. Approval of the following resolution:

Resolved, That Stanley S. Ballard be appointed a member-at-large of the Board of Directors to fill the unexpired term of the late Frank Benford.

4. Approval of the following resolution:

Resolved, That S. Q. Duntley be appointed to fill the unexpired term of the late Frank Benford as O.S.A. representative on the U.S.N.C. of the I.C.I.

5. Approval of the following resolution:

Resolved, That David L. MacAdam be appointed an O.S.A. representative on the U.S.N.C. of the I.C.I. to replace L. A. Jones, who was appointed by letter ballot of November 17, 1948, but who subsequently indicated that he prepfers not to serve in this capacity.

6. Approval of appointment of the following Nominating Committee for the 1949 elections:

G. R. Harrison, *Chairman*
Wallace R. Brode A. H. Pfund
Paul E. Klopsteg E. D. Tillyer

7. Approval of appointment of the following Program Committee for the annual meeting of the Society, to be held in Buffalo, New York, on October 27, 28, and 29, 1949:

Brian O'Brien, *Chairman*
R. H. Gillette, *Vice Chairman*
Stanley S. Ballard Allen B. Fuhr
Glenn A. Fry A. J. Kavanagh
Galen Porter

8. Approval of the following resolution:

Whereas, The late A. H. Pfund had been nominated to represent the Optical Society of America on the Governing Board of the American Institute of Physics for a term of three years to commence in February, 1949; therefore

Resolved, That the American Institute of Physics be advised that the Optical Society of America now submits the nomination of Wallace R. Brode.

Appointments

H. R. Condit was appointed alternate to B. H. Carroll and E. H. Greppin, Auditors for the accounts of the Optical Society of America, Inc.

C. C. Kiess was appointed to succeed himself as O.S.A. Representative to the American Association for the Advancement of Science for a term to expire in February, 1951.

Future Meetings of the Society

The annual meeting of the Optical Society will be held at the Hotel Statler, Buffalo, New York, on October 27, 28, and 29, 1949, and the next winter meeting will be held at the Hotel Statler, New York, New York, on March 9, 10, and 11, 1950.

Amendments to the By-Laws

By amendment of the By-Laws, the number of Directors-at-Large was reduced from five (5) to four (4), and the number of Officers was increased from six (6) to seven (7) by the addition of a Secretary for Local Sections. The By-Laws as amended appear elsewhere in this issue of the Journal.

ARTHUR C. HARDY, *Secretary*

Annual Report of the Editor of Publications

STATEMENT OF OPERATIONS OF THE JOURNAL OF THE OPTICAL SOCIETY OF AMERICA FOR THE YEAR ENDING DECEMBER 31, 1948

Income

Non-member subscriptions	$12,232.53
Net income from published articles	3,019.46
Net income from sale of back numbers	4,307.58
Total Income Exclusive of Member Subscriptions	$19,559.57

Expense

Printing and mailing		$20,949.22
Engraving		2,530.77
Editorial mechanics at A.I.P.:		
Salaries	$2,097.92	
Office expense	444.76	2,542.68
Subscription expense:		
Salaries	$2,224.85	
Office expense	457.27	2,682.12
Other expenses		65.04
Editorial office, Cambridge:		
Salaries	$1,250.00	
Office expense	142.67	1,392.67
Total Cost of Editing and Publishing Journal		$30,162.50
Net Cost of Operating Journal and Furnishing it to Members		$10,602.93

(Signed) GEORGE R. HARRISON, *Editor*

Annual Report of the Secretary of the Optical Society of America, Inc., For the Calendar Year 1948

MEMBERSHIP RECORD
JANUARY 1, 1948 TO JANUARY 1, 1949

	Honorary	Regular Emeritus	Associate Emeritus	Regular Life Payment	Associate Life Payment	Regular Annual Payment	Associate Individual Annual Payment	Associate Corporation	Student	Total
Membership as of record in the books of the Secretary 1/1/48	3	22	1	10	1	589	1028	31	19	1704
Gains during 1948										
By election as of 1/1/48							128	1	17	146
By election as of 1/1/49							28		6	34
By reinstatement		4				1	15		3	23
By transfer on 10/20/48						40				40
By transfer to Associate Membership							6			6
By transfer to Reg. Life Membership				1						1
	(0)	(4)	(0)	(1)	(0)	(41)	(177)	(1)	(26)	(250)
Losses during 1948										
By death		1				3	6			10
By resignation						10	30			40
By transfer on 10/20/48							40			40
By transfer to Associate Membership									6	6
By transfer to Reg. Life Membership						1				1
By separation for Non-Payment of Dues						7	41			48
By failure to renew student membership status									11	11
	(0)	(1)	(0)	(0)	(0)	(21)	(117)	(0)	(17)	(156)
Totals	3	25	1	11	1	609	1088	32	28	1798

New Members

Elected during 1948 as of January 1, 1948

Alpern, Mathew (2848 A)
Anthony, Romuald (2790 A)
Barry, F. M. (2772 A)
Been, Robert Belmont (2885 A)
Behner, H. C. (2872 A)
Bell, Mary F. (2802 A)
Benson, B. S., Jr. (2852 A)
Bing, Joseph M. (2870 A)
Boltz, David F. (2758 A)
Braden, William E. (2781 A)
Brands, Edwin R. (2800 A)
Brandstetter, F. X. (2835 A)
Brennan, J. S. (2850 A)
Brice, Arthur T. (2764 A)
Brophy, Vincent A. (2816 A)
Brown, W. R. J. (2746 A)
Burnham, Robert W. (2814 A)
Canada, Alfred H. (2834 A)
Carlson, Chester F. (2840 A)
Carnahan, Walter H. (2794 A)
Carpenter, Vance J. (2784 S)
Cerato, Charles C. (2857 A)
Clark, Melvin D. (2778 S)
Conrad, Anne L. (2881 A)
Cotton, C. F. (2862 A)
Devlin, James J., S.J. (2798 A)
Dyer, Clarence A. (2748 A)
Edge, James M. (2807 A)
Elarde, P. F. (2854 A)
Fagan, Herbert C. (2795 A)
Fentin, Arthur (2853 A)
Fink, George A. (2863 A)
Folsom, W. E. (2869 A)
Fonda, Gorton R. (2760 A)
Fontaine, Emile (2839 A)
Ford, Clinton B. (2782 A)
French, A. H. (2811 A)
Friel, Daniel D. (2780 A)
Gates, Peter Satterlee (2912 A)
Gee, Alan E. (2788 S)
General Electric Co. (2817 AC)
Gilkeson, David C. (2818 S)
Gordon, Donald A. (2832 A)
Gordon, Earl H. (2768 A)
Grey, David S. (2894 A)
Harmon, Duane D. (2837 A)
Harrigan, Robert F. (2855 S)
Hart, George G. (2858 A)
Hass, Georg H. (2815 A)
Heilprin, L. B. (2759 A)
Henry, William M. (2892 A)
Henthorn, D. W. (2886 A)
Herman, R. W. (2887 A)
Herrick, C. E., Jr. (2775 A)
Herscher, L. W. (2806 A)
Hesse, Ludwig F. (2750 A)
Hill, George C., Jr. (2884 A)
Hine, Sheldon H. (2777 A)
Holmes, Marian C. (2888 A)
Holter, Norman J. (2770 A)
Horn, H. W. (2868 A)
Howes, Walton L. (2819 S)
Hunter, Richard G. (2765 A)
Isakson, Frank B. (2820 A)
Johnson, C. Stanley (2827 A)
Jupnik, Helen (2846 A)
Kane, John (2809 A)
Kean, Lee (2812 A)
Keck, P. H. (2879 A)
Kline, John V. (2757 A)
Kolm, Henry H. (2833 S)
Krumrine, Elizabeth (2752 A)
Kuentzel, L. E. (2821 A)
Lamar, Edward S. (2838 A)
Larson, Daniel A. (2771 A)
Lee, Bernard S. (2907 A)
Leininger, R. K. (2859 A)
Leistner, Karl (2867 A)
Lipton, Sidney M. (2747 A)
Lit, Alfred (2883 A)
Lohse, John M. (2844 A)
Lowen, Herbert (2822 A)
Lutes, Olin S., Jr. (2825 A)
Marg, Elwin (2851 S)
Martz, E. P., Jr. (2754 A)
Matzka, L. H. (2803 A)
Mayo, Martha E. (2774 A)
McLean, Chas. H., Jr. (2831 A)
McNally, Frederick (2796 A)
Merchant, M. Eugene (2829 A)
Merrill, B. Darby (2856 A)
Merrill, Harrison J. (2767 A)
Michels, Walter C. (2799 A)
Miller, Foil A. (2749 A)
Mongello, Thomas (2743 A)
Morris, Charles A. (2843 A)
Nikkel, Henry (2804 A)
Nowicki, Edward R. (2842 A)
Ogle, Harlan V. (2773 S)
Olt, Richard G. (2896 A)
Orthwein, William C. (2766 S)
Pant, Banshidhar (2808 A)
Parke, Harry G. (2805 S)
Patrick, Francis B. (2789 A)
Peck, Edson R. (2895 A)
Perillo, F. J. (2763 A)
Pilston, Robert George (2745 S)
Pittman, M. A. (2861 A)
Potts, Charles R. (2792 A)
Power, John W., Jr. (2823 A)
Racine, F. L. (2776 A)
Radford, Richard D. (2915 A)
Ramanathan, Natesan (2810 S)
Ratoosh, Philburn (2882 A)
Robinson, Wm. J., Jr. (2791 A)
Sanford, Cecil E. (2866 S)
Schafstein, Nathan J. (2756 A)
Schottmiller, Gerard (2841 S)
Schwartz, Morris (2849 A)
Simi, Oliver R. (2769 A)
Smith, Buford, Jr. (2865 A)
Sponer, Hertha (2845 A)
Stansbrey, John J. (2761 A)
Steeb, E. S., Jr. (2873 A)
Stein, Anna (2793 A)
Stillman, Alan H. (2787 A)
Thielens, Emil H. (2785 A)
Todd, Edward P. (2826 A)
Troy, Daniel J., Jr. (2813 A)
Van Bergen, F. (2830 A)
Vance, C. F. (2875 A)
Verbinski, V. V. (2744 S)
Vogel, Roderick Q. (2779 A)
Weiss, Richard J. (2755 S)
Westfall, Oliver (2786 A)
Westheimer, Gerald (2900 A)
Wheat, J. Allen (2860 A)
White, Herbert H. (2762 A)
Widmyer, John H. (2783 A)
Wilkins, J. Ernest (2797 A)
Williams, Van Zandt (2801 A)
Wiseman, Robert S. (2864 A)
Woernley, D. L. (2836 A)
Woodford, D. E. (2751 A)
Yaseen, George (2824 A)
Yoder, Elwin C. (2753 A)

Elected during 1948 as of January 1, 1949

Alford, W. P. (2917 S)
Aneshansley, C. H. (2828 A)
Bastron, Harry (2918 A)
Besner, Aaron (2877 A)
Bluford, Benjamin L. (2901 A)
Blutman, E. (2878 A)
Chamberlain, K. (2898 A)
Cheesbrough, E. W. (2904 A)
Coleman, Eugene F. (2891 A)
Courmand, E. L. (2919 A)
Engelder, Theodore C. (2902 S)
Feinberg, L. M. (2911 A)

Fossum, Peter E. (2889 A)
Furlong, L. R. (2920 A)
Geary, Paul A. (2913 A)
Gibson, J. M. D. (2910 A)
Helz, Armin W. (2905 A)
Jalbert, Roland A. (2906 S)
Kessler, Karl G. (2829 A)
Mager, Robert G. (2903 A)
Montgomery, C. E. (2921 S)
Morgan, John H. (2922 S)
Murata, Kiguma J. (2871 A)
Nicholls, R. W. (2914 A)
Nobel, Robert H. (2893 A)
Palubinskas, Felix S. (2916 A)
Schweizer, Leslie R. (2847 A)
Signeur, Austin V. (2880 A)
Sihvonen, Y. T. (2874 S)
Smakula, Alexander (2909 A)
Tate, P. (2890 A)
Thies, Harry L. (2908 A)
Walters, S. H. (2876 A)
Whitney, Donald B. (2897 A)

Associate Members

Elected to Regular Membership by Action of the Board of Directors October 20, 1948, effective as of January 1, 1949

Benson, Nels C. (2674)
Blackwell, H. Richard (2234)
Blout, Elkan R. (2621)
Brice, Arthur T. (2764)
Bridgman, Charles S. (1940)
Chapanis, Alphonse (2719)
Coleman, Madeline F. (2677)
Corliss, C. H. (1574)
Davis, Faurest (2596)
Dunkelman, Lawrence (2515)
Enns, J. H. (2701)
Epstein, David W. (1952)
Fonda, Gorton R. (2760)
Friedel, Robert A. (2376)
Hardy, J. D. (2537)
Hawkes, John B. (1150)
Hendley, Charles D. (2516)
Hillyer, Curtis (2483)
Huxford, W. S. (2605)
Hyde, W. Lewis (2691)
Kaplan, Joseph (1992)
Lamar, Edward S. (2838)
Martz, E. P., Jr. (2754)
Meissner, K. W. (2734)
Michels, Walter C. (2799)
Rao, C. S. (2651)
Reimann, Genevieve B. (1224)
Saunders, Bernard (2209)
Seitz, Frederick (1863)
Sitterly, C. M. (2722)
Smith, Daniel (1676)
Sponer, Hertha (2845)
Tyler, John E. (1609)
Van Heel, A. C. S. (2399)
Verplanck, William S. (2671)
White, Harvey E. (1543)
Williams, Van Zandt (2801)
Woernley, D. L. (2836)
Woodford, Edward B. (2382)
Woodson, Robert A. (1925)

Student Members

Transferred to Associate Membership as of January 1, 1949

Clark, Melvin D. (2778)
Gilkeson, David C. (2818)
Gillis, Ronald C. (2598)
Howes, Walton L. (2819)
Minkler, Marcus W. (2697)
Nimeroff, Isadore (1691)

Losses by Death

Baldwin, H. Wallace (1505A)
Beck, William Henry (2441 A)
Benford, Frank (152 R)
Cooper, F. Leonard (1438 A)
Ellis, Frederick W. (50 R)
Hodge, Percy (475 RE)
Kelly, James H. (759 A)
Manahan, Paul R. (1326 A)
Organ, Thomas J. (2108 A)
Tolman, Richard C. (194 R)

ARTHUR C. HARDY, *Secretary*

Annual Report of the Treasurer of the Optical Society of America

Cash Transactions January 1, 1948 to December 31, 1948

Receipts

Dues	$6,926.98	
Dues in advance	7,578.55	
Income from unallocated securities	1,867.53	
Income from Ives Medal Fund	12.50	
Income from Adolph Lomb Fund	50.00	
Contribution by Rochester Section	100.00	
Sale of Addressograph	125.00	
Total Receipts		$16,660.56

Disbursements

Journal Publication Expense	9,369.72	
Journal Editorial Expense	1,350.00	
President's Expense	18.00	
Secretary's Expense	1,705.76	
Secretary Local Sections Expense	125.00	
Secretary's Travel Expense	116.41	
Treasurer's Expense	607.52	
Meetings & Programs	1,513.95	
Adolph Lomb Medal	24.47	
Contributions to the support of other organizations		
American Institute of Physics	1,522.97	
Inter-Society Color Council	25.00	
U.S.N.C. of the I.C.I.	100.00	
Total Normal Expenditures		16,478.80
Excess of Receipts over Normal Expenditures		$ 181.76
Special Appropriation		
Reprinting Journals	453.00	453.00
Excess of Total Disbursements over Receipts		$ 271.24

Balances December 31, 1947

Unallocated cash	$4,968.80	
Ives Medal Fund	128.93	
Adolph Lomb Fund	231.13	
Total		$ 5,328.86
Cash Balance December 31, 1948		$ 5,057.62

Ives Medal Fund

Income

Principal	$ 500.00	
Interest balance, January 1, 1948	128.93	
Interest accrued during 1948	12.50	
Total		$ 641.43

Disbursements

None	0.00	0.00
Balance December 31, 1948		$ 641.43

Note: The principal sum of $500.00 is invested in Series G War Bonds. They are included in the bonds reported in the accompanying Investment Statement.

Adolph Lomb Fund

Income

Principal	$2,000.00	
Interest balance January 1, 1948	231.13	
Interest accrued during 1948	50.00	
Total		$ 2,281.13

Disbursements

Medal for David S. Grey	24.47	24.47
Balance December 31, 1948		$ 2,256.66

Note: The principal sum of $2,000 is invested in Series G War Bonds. They are included in the bonds reported in the accompanying Investment Statement.

Investments

Investment portfolio with market value of securities as of December 31, 1949.

		Book Value	Market Value	Annual Income
9M	U. S. Treasury Bonds 2¼%	$ 9,088.14	$ 9,170	$ 202.50
11.6M	U. S. War Savings Bonds Series "G" 2½%	11,600.00	11,600*	290.00
5M	Atch. Top. & Santa Fe 4% Gen. Mtge. 1995	5,000.00	6,131	200.00
2M	Associated Electric Co. Deb. 4½%	1,959.00	1,930	90.00
3M	Consolidated Cigar Corp. S. F. Deb. 3½%	3,137.25	3,030	97.50
15 Shares	El Paso Natural Gas Co. Cum. Pfd. $4.10	1,636.50	1,402	61.50
30 Shares	20th Century Fox Film Corp. Pr. Pref. $4.50	3,077.80	2,955	135.00
20 Shares	Philip Morris & Co., Ltd. Cum. Pfd. 4%	2,173.70	1,870	80.00
75 Shares	Indianapolis Power & Light Co. Common	2,543.81	1,593	112.50
52½ Shares	National Lead Co. Common	1,605.79	1,575	65.50
50 Shares	Eastman Kodak Co. Common	1,718.19	2,194	90.00
65 Shares	General Electric Co. Common	2,544.23	2,527	130.00
35 Shares	Kennecott Copper Corp. Capital	1,729.53	1,942	140.00
42 Shares	Standard Oil Co. of N. J. Capital	2,262.72	2,885	84.00
		$50,076.66	$50,804	$1,778.50
	Average yield			3.5%

* Maturity value.

The undersigned, having been duly appointed to audit the books of the Treasurer of the Optical Society of America, Inc., from January 1, 1948 to December 31, 1948, hereby certify that the Treasurer's report of receipts and disbursements is correct as shown by records, vouchers, bank statement, etc., and that his accounts check accurately with vouchers and bank statements.

Signed L. T. STEADMAN, H. R. CONDIT, *Auditors*

By-Laws of the Optical Society of America, Inc.

ARTICLE I

MEMBERSHIP

Section 1. Classes of Membership: Membership in the society shall be regular, associate, student, corporation, emeritus, or honorary.

Section 2. Charter Members: The members of the unincorporated association, the Optical Society of America, at the time of the incorporation of said society shall be members in their respective classifications of the Optical Society of America, Inc. The charter members of the unincorporated society shall be known as the charter members of the incorporated society.

Section 3. Eligibility: Any person who has contributed materially to the advancement of optics is eligible for regular membership.

Any person who is interested in optics is eligible for associate membership.

Any *bona fide* student, undergraduate or graduate, of an educational institution of collegiate grade who is devoting more than half-time to activities within the institution is eligible for student membership.

Any corporation desirous of encouraging the work of the society is eligible for corporation membership.

Any person who has retired from active work, has reached the age of 65 years, and has been a member for at least 20 years is eligible for emeritus membership. Other members may, by a two-thirds (2/3) vote of the board of directors, be declared eligible for emeritus membership.

Any person who has rendered eminent service in the advancement of optics may be elected to honorary membership.

Section 4. Application for Membership: Applications for student membership must include a statement of the student's academic status and must be signed by one associate, regular, emeritus, or honorary member of the society. The correctness of the statements in the application must be certified by an officer or faculty member of the educational institution. Other applications for membership must state the candidate's name and qualifications for membership and must be signed by two associate, regular, emeritus, or honorary members of the society.

Section 5. Election to Membership: Applicants for student membership shall become members when their duly prepared applications have received the written approval of two members of the board of directors. All other applications from individuals for membership shall be considered first as applications for associate membership and shall be acted upon as such. Applicants shall become associate members when their duly prepared applications have received the written approval of three members of the board of directors.

Applicants for corporation membership shall become corporation members when their duly prepared applications have received the written approval of three members of the board of directors.

Associate members may be transferred to regular membership at any regular meeting of the board of directors by a two-thirds (2/3) vote of the members of the board present.

Any eligible member may, at his own request, be transferred to emeritus membership by the secretary.

Honorary members may be elected at any regularly called meeting of the board of directors by the unanimous vote of the entire board. In case any members of the board are not in attendance their ballots must be obtained by the secretary. The number of honorary members shall at no time exceed five (5).

Section 6. Duties and Privileges: Regular members shall have the right to vote, hold office, attend meetings, and receive the journal of the society and such other publications as the board of directors may direct.

Student and associate members shall have the same privileges as regular members except that they may not vote or hold office.

Corporation members shall receive the journal of the society and such other publications as the board of directors may direct. Their representatives may attend all meetings of the society.

Emeritus members shall have all of the privileges of their former membership status, except the right to receive the journal and other publications of the society.

Honorary members shall have all of the privileges of regular members.

Section 7. Termination of Membership: Membership in the society may be suspended or terminated by vote of the board of directors.

Failure to pay dues for one (1) year shall be deemed sufficient cause for suspension or termination of membership.

Student membership in the society shall terminate at the end of the calendar year unless the student requests continuation of his student membership. Such a request must include a statement of the student's eligibility, and the correctness of the statement must be certified by an officer or faculty member of the educational institution.

Section 8. Dues: The dues for the various classes of membership as outlined in Section 3 of this Article shall be as determined from time to time by the board of directors.

Section 9. Patrons: The payment, within any one year, of one thousand dollars ($1000.00) or more toward the expenses of the society by any corporation or individual shall entitle such corporation or individual to the rank of patron of the society, for a period of ten years in the case of a corporation, and for life in the case of an individual.

Section 10. Ownership of Corporation Property: The corporation shall not be operated for profit and its entire properties, assets, and facilities shall be devoted to the purposes for which it is organized as set forth in its certificate of incorporation as the same may be from time to time amended. No member shall have any right to or any share or interest in any of the property or assets of the corporation.

Section 11. Local Sections: Any regional group that accepts the aims and purposes of the Optical Society of America may be recognized by the board of directors as a local section.

Article II

Meetings of Members

Section 1. Annual Meeting of the Corporation: During October of each year at a time and place to be fixed by the board of directors, there shall be held the annual meeting of the members of the corporation for the election of directors and officers (if not previously elected by mailed ballot as hereinafter provided), and for the rendering to the membership of the annual report of the directors as required by law, and for the transaction of such other business as may properly come before the meeting.

At each annual meeting the directors shall present a report verified by the president and treasurer or by a majority of the directors, showing the whole amount of real and personal property owned by the corporation, where located and where and how invested, the amount and nature of the property acquired during the year immediately preceding the date of the report, and the manner of the acquisition; the amount applied, appropriated or expended during the year immediately preceding such date, and the purposes, objects, or persons to or for which such applications, appropriations or expenditures have been made; and the names and places of residence of the persons who have been admitted to membership in the corporation during such year, which report shall be filed with the records of the corporation and an abstract thereof entered in the minutes of the annual meeting.

Section 2. Notice of Annual Meeting: Notice of the annual meeting of members shall be given by mailing, not less than ten (10) days nor more than forty (40) days before the meeting, a copy of the notice of such meeting to every member of the corporation directed to him at his address as it appears upon the records of the corporation.

Section 3, Special Meetings: Special meetings of the members, except as otherwise provided by law or by these by-laws, may be called at any time by the board of directors or by the president, and shall be called by the president or by the secretary at the request in writing of a majority of the board of directors. Such request shall state the purpose or purposes of the proposed meeting.

Section 4. Notice of Special Meetings: Notice of each special meeting of the members shall be given by mailing, not less than ten (10) nor more than forty (40) days before the meeting, a copy of the notice of such meeting, stating the purpose or purposes for which the same is called, to each member directed to him at his address as it appears on the records of the corporation.

Section 5. Quorum: At any meeting of the members of the corporation a quorum shall consist of not less than twenty (20) voting members.

Section 6. Qualifications of Voters: Upon any question presented for vote to the membership, whether presented by mail or at a meeting of the members, each member entitled to vote pursuant to the provision of Section 6 of Article I shall be entitled to one (1) vote.

Section 7. Voting: Upon any question with respect to which a vote of the membership shall be required or deemed advisable, the board of directors may determine whether such vote shall

be taken by mail or by ballot at the next meeting of the membership. In case the directors shall determine to take such vote by mail, either upon any question of administration or policy or upon the election of officers, directors or others, forms for the casting of such vote or for the casting of a ballot for the election of any such officers, directors, or others, shall be forwarded to the entire membership entitled to vote thereon at least thirty (30) days prior to the date upon which the count of such votes or ballots shall be made by the directors or tellers appointed for the purpose (the date of which count shall be incorporated in the advice sent to the respective members) and the results of such vote or ballot shall be determined by the directors or tellers upon the date fixed for such purpose and shall be valid, binding and of full force and effect precisely as if such vote had been taken in open meeting of the membership regularly called and duly held, provided always, that in order to render valid such vote by mail, the number of votes cast shall be at least equal to the number of voting members required to constitute a quorum at any regular or special meeting of the membership.

Article III

Officers and Directors

Section 1. Officers Enumerated: The officers of the society shall be a president, a vice president, a secretary, a treasurer, a junior past president, an editor of publications, and a secretary for local sections.

Section 2. Directors Enumerated: The directors shall consist of the seven (7) officers mentioned in Section 1, all of whom shall be, ex-officio members of the board of directors, and four (4) directors-at-large.

Section 3. Eligibility and Election: Nine (9) directors and officers shall be elected by the voting members from among the regular, honorary, and emeritus members of the society. These directors shall consist of four (4) directors-at-large and the following officers of the society who shall be, ex-officio, members of the board of directors, to wit: president, vice president, secretary, treasurer, and secretary for local sections.

At the expiration of his term of office the president becomes the junior past president, one of the officers of the society, and ex-officio, a member of the board of directors.

The editor of publications shall be elected by the above-enumerated board of directors at an annual meeting of the board and shall upon such election become a voting member of such board.

Section 4. Terms of Office: The president, vice president, and secretary for local sections shall be elected for terms of two (2) years.

The secretary and the treasurer shall be elected for terms of four (4) years.

No officer elected by the membership shall be eligible for re-election except when such eligibility is established by special action of the board of directors. This shall require an affirmative vote of a majority of the entire board.

The junior past president shall serve until such time as his successor qualifies for the office by retiring from the office of president.

The editor of publications shall be elected for a term of four (4) years.

Members-at-large of the board of directors shall be elected for terms of four (4) years.

No member-at-large of the board of directors shall be eligible for re-election.

The term "re-election" as used in these by-laws shall be construed to mean only the election of an individual to succeed himself.

Section 5. Time of Election and Assumption of Duties: Election by the members of officers and members-at-large of the board of directors shall take place at an annual meeting of members in October, or by mailed ballot as provided in the following section.

The officers and directors elected shall assume their duties at the close of such annual meeting.

Section 6. Mode of Election: Elections shall be by ballot cast by mail as provided in Section 7 of Article II unless the board of directors shall, prior to the holding of any annual meeting of the membership, determine to hold such election at such annual meeting, in which case the members entitled to vote shall be notified of such determination. Nominations shall be made by a nominating committee appointed by the president and approved by the board of directors. This committee shall consist of five (5) regular members of the corporation, at least one (1) of whom shall be a past president.

Notices of the nominations made by the nominating committee shall be sent to all regular members at least thirty (30) days before the date on which the ballots are forwarded to the members. Additional nominations may be made by request of ten (10) members qualified to vote provided they are forwarded to the secretary within twenty (20) days after notices of the nominations are sent out.

Section 7. Vacancies: In the event of a vacancy occurring among the officers or the directors-at-large, the remaining directors, by an affirmative vote of a majority thereof, may fill such vacancies for the unexpired term of office.

Section 8. Organization of the Board of Directors: The president of the society shall be the chairman of the board of directors.

The secretary of the society shall be the secretary of the board of directors. He shall keep complete and precise records of the business transacted by the board of directors and shall send copies of the minutes to each member of the board and shall file copies of the minutes in a permanent record book provided for the purpose.

Section 9. Meetings of the Directors: The annual meeting of the board of directors shall be held in October. Meetings of the directors may be held at such other times as the chairman of the board may appoint. The directors may adopt rules and regulations governing their procedure, the notices to be given of meetings, the times and places of holding of regular meetings, and other matters with respect to the conduct of their business. The vote of directors upon any proposition, except as otherwise provided by these by-laws, may be obtained by mail during an interim between meetings.

Section 10. Quorum: At any meeting of the board of directors a majority of the entire membership of the board shall constitute a quorum and, except as otherwise provided by these by-laws, a majority of such a quorum shall decide any question that may come before the meeting.

Section 11. Duties of Officers: The duties of the president, vice president, secretary, treasurer, and secretary for local sections shall be the usual ones performed by such officers.

The treasurer shall be chargeable with the responsibility for the general funds of the corporation and for such special funds as may be from time to time placed in his custody or control by order of the board of directors, and he shall pay the bills of the corporation which have been approved by the board of directors either through adoption of an annual budget or by special action.

The custody of other special funds may be vested by the board of directors in agents other than the treasurer.

The treasurer and each other officer or agent having custody or control of any funds shall report periodically and at least once each year to the board of directors with respect to the management and disposition of the fund or funds with which he is chargeable, and the board of directors shall in turn incorporate such reports in their annual report to the members.

The editor of publications shall have general charge, under the supervision of the board of directors, of the publications of the society as set forth in Section 1 of Article V.

Section 12. Bonding: The treasurer and each other officer or agent having custody or control of any funds of the corporation shall be bonded for an amount to be fixed by the board of directors.

Section 13. Prohibitions on Officers: No director or other officer of the society shall receive, directly or indirectly, any salary, compensation or emolument from the corporation, either as such officer or director or in any other capacity, unless authorized by the by-laws of the society, or by the affirmative vote of two-thirds (2/3) of all the directors.

No director or other officer of the society shall be interested, directly or indirectly, in any contract relating to the operations conducted by the society, nor in any contract for furnishing supplies thereto, unless authorized by the by-laws of the society or by the affirmative vote of two-thirds (2/3) of the directors.

Article IV

Committees and Delegates

Section 1. Committees: The president may appoint, for a term not to exceed the remainder of his term of office and subject to the approval of the board of directors, such committees as may further the objects of the society, and such committees shall have such duties and responsibilities as shall be delegated to them by the president and the board of directors, but shall be subject at all times to the direction and control of the board of directors. Unless otherwise specifically provided in its appointment, each such committee shall serve until it has been discharged or its successor has been appointed.

Section 2. Representatives and Delegates: The president shall submit to the board of directors nominations for representatives and delegates to other organizations. Representatives and delegates shall be elected by the board of directors and for such terms as their respective offices may require. Unless otherwise specifically provided in his appointment each such representative or delegate shall serve until he has been discharged or his successor has been appointed.

Article V

Publications and Endowments

Section 1. Publications: The society shall publish a journal devoted to the advancement of optics and may publish such other scientific publications as may be deemed adivsable by the board of directors from time to time. In addition to the editor of publications, who shall be a member of the board of directors as hereinabove provided, the board of directors may appoint six or more associate editors whose terms of office shall be six (6) years, one-third (1/3) of them to be appointed biennially, but such appointments to be at all times subject to revocation by the board of directors. Every regular, associate, student, corporation, and honorary member of the society shall be entitled to receive the journal of the society.

Section 2. Endowments: The corporation may accept endowments for medals, scholarships, or for other purposes, and such endowments shall be maintained in accordance with the directions of the board of directors and the wishes of the donors.

Article VI

Finances

Section 1. Finances: The respective funds of the corporation shall be deposited with such bank or banks, trust company or trust companies as the board of directors may from time to time designate, and shall be subject to withdrawal by such officers or agents as may from time to time be designated by the board of directors.

Article VII

Corporate Seal

Section 1. Form of Seal: The seal of the corporation shall be circular in form with the words "Optical Society of America, Inc., New York" in the outer circle and "1932" together with the official emblem of the society within the inner circle. Such seal as is impressed on the margin hereof is hereby adopted as the corporate seal of the corporation.

Article VIII

Amendments

Section 1. Amendments by Directors: These by-laws may be amended, altered, or repealed in whole or in part by the affirmative vote of the majority of the entire board of directors expressed in writing or cast at any regular or special meeting of the board with or without mention thereof in the notice of the meeting at which the vote is taken. If, however, any such amendment is adopted at a meeting without mention thereof in the notice of such meeting, a copy of such amendment shall be mailed immediately after the meeting to each director not present at the meeting.

Section 2. Amendments by Members: These by-laws may be amended, altered, or repealed in whole or in part by the affirmative vote of a majority of the regular members of the society in good standing expressed in writing as provided in Section 7 of Article II or cast at any annual meeting of the members or at any special meeting of the members where such proposed action has been incorporated in the notice of the meeting. Amendments by the members may be made notwithstanding any previous action of the board of directors.

Proceedings of the Winter Meeting of the Optical Society of America

HOTEL STATLER, NEW YORK, NEW YORK, MARCH 10, 11, AND 12, 1949

THE winter meeting of the Optical Society of America was held at the Statler Hotel, New York, New York, on March 10, 11, and 12, 1949, with a total registration of 617.

The two sessions on March 10 were devoted to a Symposium on Luminescence consisting of two invited papers and fifteen contributed papers. The morning session was opened by an invited paper, "A Survey of Present Methods Used to Determine the Optical Properties of Phosphors" by Dr. Wayne B. Nottingham. The afternoon session commenced with the invited paper, "Review of the Interpretations of Luminescence Phenomena" by Dr. Ferd E. Williams.

Preceding the morning and afternoon sessions of contributed papers on Friday, invited papers were presented as follows: Friday morning—"The Ruling of Large Diffraction Gratings" by Dr. George R. Harrison; Friday afternoon—"Measurements of Size and Shape of Large Molecules by Light Scattering" by Dr. P. Debye. The simultaneous sessions of contributed papers following these were classified, respectively, under the subjects: Vision, General Optics, Color, and Infra-Red.

The dinner on Friday evening was attended by 297 members and guests. Immediately following the dinner a brief talk was given by Dr. George R. Harrison in commemoration of the centenary of the birth of Henry A. Rowland. The main part of the after-dinner program consisted of a demonstration talk by Mr. Alston Rodgers of the General Electric Company entitled "New Horizons in Lamp Research." The lecture was informative and well illustrated with novel and entertaining effects in lighting.

The Saturday morning meeting was opened with an invited paper, "A Color Translating Ultraviolet Microscope" by Dr. Edwin H. Land. A very effective demonstration of the microscope, together with the processing and projection equipment, was included. The two simultaneous sessions of contributed papers following the talk were devoted to ultraviolet microscopy and spectroscopy, respectively. The Saturday afternoon meeting consisted of a single session of contributed papers on the subject of general optics.

CONTRIBUTED PAPERS

The abstracts of the contributed papers are appended.

MEETING OF THE BOARD OF DIRECTORS

A meeting of the Board of Directors was held on Wednesday, March 9. The minutes of this meeting appear on page 617 of this issue.

J. H. WEBB, *Chairman*
Program Committee

Program of Sessions

1. Invited paper, entitled "A Survey of Present Methods Used to Determine the Optical Properties of Phosphors," BY WAYNE B. NOTTINGHAM, *Massachusetts Institute of Technology.*

2. Photometric Evaluation of Luminous Materials for Naval Use. W. S. PLYMALE, JR. AND L. H. DAWSON, *Naval Research Laboratory, D. C.*

Types of luminous materials being used by the Navy are given in brief outline with some mention of particular application to problems arising under dark or near dark conditions. The program for improving low brightness photometry at the Naval Research Laboratory is explained with special attention given to physical photometry, utilizing the photo-multiplier tubes. Also, brief mention is made of the efforts to revise brightness and color specifications to meet several specific needs.

3. The Measurement of the Luminescence of Fluoroscopic X-Ray Screens. R. H. PECKHAM, *Temple University School of Medicine, Philadelphia, Pennsylvania.*

The visual effectiveness of low brightness sources, such as roentgenoscopy screens, or discontinuous sources, such as

fluorescent lights and television screens, cannot always be adequately predicted from the computation of retinal luminosity or the measurement of apparent brightness. The estimate becomes particularly faulty when the brightness level approaches the rod-cone transition, owing to the Purkinje phenomenon. A statistical method of determining the probability of seeing a liminal stimulus at known levels of excitation and contrast has been developed. Stimuli varying logarithmically in diameter are presented at known levels of excitation and contrast. Using this method a series of screens of various ZnS to CdS ratios and thicknesses has been examined at clinical levels of roentgen intensity. The most visually effective screen was found to be yellower than would have been predicted at dominant wave-length of 567 millimicrons, instead of between 555 and 515 millimicrons. The improvement of the brightness of the screen by increasing the thickness is limited by the increased liminal value, due to the reduction of edge contrast. The selection of the best phosphor and thickness will permit clinical fluoroscopic examinations to be made just above the rod-cone transition, instead of mostly below as hithertofore.

4. A Vacuum Ultraviolet Monochromator for Absorption and Photo-Conductivity Measurements on Luminescent Solids. W. W. PARKINSON, JR. AND FERD E. WILLIAMS, *University of North Carolina.*

As part of a program of fundamental research on the mechanism of luminescence in inorganic solids, a vacuum ultraviolet monochromator covering the wave-length range 1200A to 3500A has been constructed for use in determining the excitation and conduction energy levels. The design is simplified by mounting the lightly ruled, one-meter, concave grating** and its rocking mechanism on one end plate and the source, slits, sample chamber, and detector on the other end plate. With 0.2-mm slit widths, a 5A wave-length interval over the entire wave-length range can be directed on the sample and the sample can be switched in and out of the optical path without disturbing the vacuum. An improved high voltage hydrogen discharge source and a phosphor-coated photo-multiplier detector are used. For photo-conductivity measurements, it is intended to eliminate dark current and polarization by modulating with the 120-cycle intermittant source the current produced by a 1000-cycle voltage on the sample and measuring the 120-cycle photo-current component. Representative applications such as the absorption spectra of evaporated deposits of the ZnF_2:Mn phosphor and its components will be presented.

* Supported by the Office of Naval Research through Contract N 7 onr-284, T.O. 1.
** Supplied by Mr. W. H. Perry of Johns Hopkins University.

5. Phosphorescent Response to Sinusoidal Excitation. D. T. WILBER, *Allen B. Du Mont Laboratories.*

A mathematical study of the variation of brightness of a phosphor with exponential type of decay excited by a cathode-ray beam of constant voltage and a beam current varying sinusoidally about a constant d.c. value. It is found that when the time of the phosphor to decay to $1/e$ of the initial brightness is one-fortieth a cycle of the applied current the lag is about 5°, but when the decay time is 2.5 cycles long the lag is 83°. For the short decay phosphor the positive or bright modulation is 32 percent of the applied signal and 96 percent for the negative or dark phase. For the long decay phosphor the modulation is 6 percent for the bright and 7 percent for the dark phase.

6. The Phosphorescence Decay of Halophosphates and Other Doubly Activated Phosphors. FRANK J. STUDER AND ALMA ROSENBAUM, *General Electric Research Laboratory.*

The decay rates of three doubly activated phosphors, namely, calcium halophosphate (Mn, Sb) calcium silicate (Mn, Pb) and zinc fluoride (Mn, Ti, or W) have been investigated under λ2537 excitation. Measurements were made using a mechanical phosphoroscope described by G. R. Fonda.[1] The halophosphates studied all showed initially a very rapid and abrupt decay, followed by a second stage of decay having a very slow rate. Both stages are of the exponential type. Investigation shows that the rapid rate (decay constant, 1500 sec.$^{-1}$) is to be ascribed to the antimony emission and the slow rate (k, 75 sec.$^{-1}$) to the manganese emission. Calcium silicate behaves in a similar fashion, the ultraviolet emission due to lead decaying rapidly (k, 570 sec.$^{-1}$) and the visible more slowly (k, 60 sec.$^{-1}$). The doubly activated zinc fluorides show similar behavior, though the great spectral width of the tungsten band makes separation of the two emission bands difficult. The fact that in all these cases the two activators each retain their characteristic decay rates in the presence of the other indicates that two types of centers exist in each of which the process of luminescence functions independently of the other.

[1] G. R. Fonda, J. App. Phys. 10, 408 (1939).

7. The Characteristics of Fluorescent Emission under Near Ultraviolet Radiation. C. E. BARNETT AND L. D. GRADY, *The New Jersey Zinc Company* (of Pa.).

The paper discusses the utilization of luminescent materials which respond to near ultraviolet radiation with special reference to applications in the forms of paints, plastics, ceramics, papers, and inks. Fluorescent pigments under excitation by near ultraviolet (3650A) emit colors which are more saturated than can be obtained by the normal reflectance process. Emission spectra are shown for five typical pigments which fluoresce in the following colors: blue, green, yellow, orange, and red. These are compared to reflectance spectra of paints tinted to approximate, in daylight, the fluorescent colors of the five pigments and to a series of standard artist's colors. The paper attempts to bring up to date practical information on the production of brightness with these phosphors. Following the general lines of development used by Kraehenbuehl and Chanon,[1] data are given showing the relation between ultraviolet intensity and fluorescent brightness and between the latter and the masking effect of ambient illumination. The efficiency of light production from fluorescence excited by different types of commercial sources of near ultraviolet is described.

[1] John O. Kraehenbuehl and H. J. Chanon, "The technology of brightness production by near-ultraviolet radiation," Trans. Illum. Eng. Soc. 36, 151 (1941).

8. Invited paper, entitled "Review of the Interpretations of Luminescence Phenomena," BY FERD E. WILLIAMS, *Research Laboratory, General Electric Company.*

9. Simplified Lenard-Phosphors. DONALD PEARLMAN, PLINY E. GODDARD, AND FRANZ URBACH, *Kodak Research Laboratories.*

Attempts were made to obtain well defined and simple singly activated strontium sulfide phosphors. Since it is apparently not possible to prepare oxide-free strontium sulfide,[1] the effect of strontium oxide was investigated. The amount of oxide required to affect materially the emission spectrum obtained with either copper or bismuth as activator was found to decrease with decreasing concentration of the strontium chloride flux used in these preparations. Thereupon, the investigation was extended to strontium oxide phosphors. Anionic impurities and flux can be avoided and at least some of these phosphors exhibit the essential characteristics of the complex Lenard phosphors. Copper was found to act as an activator of pure strontium oxide only if present in the univalent state; it produces an emission band with a maximum around 6200A.

[1] Kenneth F. Stripp and Roland Ward, J. Am. Chem. Soc. **70**, 401 (1948).

10. The Asymptotic Behavior of Spontaneous and Forced Decay. FRANZ URBACH, NELSON R. NAIL, AND DONALD PEARLMAN, *Kodak Research Laboratories.*

New experiments on the forced decay of infra-red-sensitive strontium sulfide (cerium-samarium) phosphors were carried out with the aims (a) of eliminating or minimizing the influence of absorption in thick layers, (b) of determining whether states of different stabilities toward infra-red light coexist in these phosphors, and (c) of extending the measurements to regions of very low intensity. Assuming that the precautions to insure (a) were sufficient, the answer to (b) is in the affirmative. In the later phases of the decay the curves seem to tend to $1/t^2$. These results will be discussed from the point of view of first- and second-order kinetics and with particular reference to the asymptotic behavior of complex second-order processes with a multiplicity of decay constants.

11. New Observations on Superlinear Luminescence. NELSON R. NAIL, FRANZ URBACH, AND DONALD PEARLMAN, *Kodak Research Laboratories.*

In earlier papers it was shown that a group of phosphors show an approximately linear increase of their efficiency with increasing intensity of excitation in certain ranges of that intensity. Tentatively, these observations and the interdependence of the effects of intensity, temperature, and "poisoning" found in the same phosphors were interpreted by the assumption that a non-radiative process of first-order kinetics competes with an emission process of the second order. This type of hypothesis, however, does not easily account for more than linear dependences of efficiency on intensity. Indications of such dependences had been found in our earlier work. In view of the possible theoretical significance of these results, a number of measures were taken to eliminate possible sources of errors. New measurements were carried out on a suitable series of poisoned zinc-cadmium sulfide phosphors. The existence of regions in which the intensity dependence of efficiency was even stronger than quadratic was ascertained. Furthermore, a remarkably strong dependence of the efficiency on the carefully controlled concentrations of the poison was found. The problems raised by these effects will be briefly discussed.

12. The Electrical and Optical Properties of Zinc Silicate Phosphors. ELEMÉR NAGY, *Research Laboratories of the United Incandescent and Electrical Company, Ltd. Ujpest near Budapest.*

The spectra of zinc silicates with varying concentrations of manganese were measured at several temperatures. It was found that these emission spectra could be separated into bands conforming to Gauss error curves and that the location of these bands is almost unaffected by temperature and composition changes. It is shown that the width of these bands increases linearly with temperature and that the bands become wider as the activator concentration departs from the optimum. The dielectric losses of these phosphors were also measured as a function of the temperature and the very close connection between luminescence and dielectric losses first reported by Szigeti and Nagy[1,2] for a zinc silicate sample was found valid for any zinc silicate. The electrical and luminescent constants all show maxima for the best fluorescing substances. These data make it very doubtful that activation is confined to divalent manganese. Consequently, a close analogy between the emission spectra of these silicates and the absorption spectra of permanganate and manganate compounds is worth studying.[3]

[1] G. Szigeti and E. Nagy, Nature **160**, 641.
[2] G. Szigeti and E. Nagy, publications of the University of Technical Sciences, Budapest, 1, 1948.
[3] G. Szigeti, E. Nagy, and E. Makai, J. Chem. Phys. **15**, 881 (1947).

13. A Correlation between Cathodoluminescence Efficiency and Decay.* RICHARD H. BUBE, *RCA Laboratories Division, Princeton, New Jersey.*

In the investigation of the temperature variation of the cathodoluminescence efficiency of a manganese-activated zinc fluoride phosphor (tetr.-ZnF_2:0.005 Mn), a pronounced increase in efficiency was found when the temperature was raised above 210° up to 300°C. This efficiency increase was shown to be accompanied by an intensity increase in the power-law decay "tail" through that temperature range. This indicates that emptying of traps at these temperatures is responsible for both observed results. Similar effects were found for a manganese-activated zinc sulfide phosphor (hex.-ZnS:0.018 Mn), the secondary efficiency maximum of which has been reported by P. Brauer,[1] and for a copper-activated zinc cadmium sulfide (hex.-ZnS·CdS:0.0001 Cu). All measurements were made on aluminum-backed phosphor screens in cathode-ray tubes specially designed by S. Lasof. Decays were measured for times from a fraction of a millisecond to one second by photographing the output of a multiplier photo-tube as recorded on a d.c. oscilloscope with a horizontal sweep synchronized with a timing signal, applied simultaneously to the oscilloscope's beam blanking amplifier.

* This work was done under Contract N6onr-236 between the ONR and the RCA.
[1] P. Brauer, P. B. 19206 (1944).

14. The Thermoluminescence of the ZnF_2:Mn Phosphor.* JAMES S. JOHNSON AND FERD E. WILLIAMS, *University of North Carolina.*

Thermoluminescence measurements at linear heating rates of 0.025 and 0.100K°/sec. on the ZnF_2:Mn phosphor with electron and ultraviolet excitation have been made as a function of activator concentration and previous heat treatment. At least six individual glow peaks between 100 and 700°K have been clearly resolved. Glow measurements using different excitation temperatures confirm the structure of the peaks. The relative intensities of the individual peaks depend on crystallization temperature and subsequent annealing. A detailed theoretical analysis of the data according to a refinement and extension of the method of Williams and Eyring[1] results in specific rate constants with frequency factors of about 10^{16} per sec. and trap depths of the order of magnitude of one electron volt. Evidence on the order of the kinetics dominating thermoluminescence and on the degree of retrapping have been obtained. Possibilities of the fundamental nature of the individual electron traps in ZnF_2:Mn will be discussed in the light of the thermoluminescence data.

* Supported by the ONR through Contract N7onr-284, T.O. 1.
[1] F. E. Williams and H. Eyring, J. Chem. Phys. **15**, 289 (1947).

15. Temperature Dependent Structure in Emission Spectra of Two Crystalline Forms of the Zinc Silicate:Mn Phosphor. ROSS E. SHRADER, *Radio Corporation of America, RCA Laboratories Division, Princeton, New Jersey.*

In studies of emission spectra of manganese-activated zinc silicate (Zn_2SiO_4:Mn) F. Kröger[1] and, more recently, F. J. Studer[2] have found differences at various operating temperatures. In the present experiments, some confirmations, some disagreements, and some new data have been obtained under conditions in which the same test sample was used over the whole temperature range (−196°C to 375°C) and in which essentially identical compositions were available in two crystalline forms. The rhombohedral form, which normally emits a green band (peak at 5275A) at room temperature, developes a yellow band (5665A) at higher temperatures. The high temperature-quenched form (nominally yellow-emitting, 5665A) develops two additional strong bands (5176A and 5420A) at −196°C. Comparing the various spectra obtained over the range of temperatures, it is apparent that the green-emitting form has a band at 5920A at the higher temperatures. Both forms develope an ultraviolet band (3950A) at high temperatures. At −196°C the green-emitting form exhibits a line approximately 10A wide at 5175A; the other form, at −196°C, has two very faint lines at 5350A and 5380A.

[1] F. Kröger, doctor's dissertation.
[2] F. J. Studer, *Cornell Symposium on Solid Luminescent Materials* (John Wiley & Sons, Inc., New York, 1946).

16. The Emission Spectrum of Manganese—Activated Magnesium Germanate.* STANLEY H. PATTEN AND FERD E. WILLIAMS, *University of North Carolina.*

An unusual fine structure of emission has been reported[1] for the manganese-activated magnesium germanate phosphor. In order to determine the precise nature of the transitions involved, the temperature-dependence of the actual intensities and half-widths and peak positions of the individual emission bands have been measured from −190°C to +100°C with ultraviolet excitation. The measurements were made in a constant temperature vacuum sample chamber and with a Littrow spectrograph containing calibrated photographic plates. Five emission bands were clearly resolved between 6200 and 6800A. The intensity of each band increases with temperature to a critical temperature above which the efficiency decreases rapidly. The short wave-length bands practically disappear at −190°C, and the individual bands shift slightly to shorter wave-lengths at low temperatures. The experimental results can be interpreted on the basis of a potential energy configuration diagram. The coupling of the excited electron to lattice vibrations has been estimated from the temperature dependence of the individual band widths, and correlations with atomic spectra are in progress.

* Supported by the ONR through Contract N7onr-284, T.O. 1.
[1] F. E. Williams, J. Opt. Soc. Am. **37**, 302 (1947).

17. Some Applications of Non-Linear Phosphors. FRANZ URBACH, NELSON R. NAIL, AND DONALD PEARLMAN, *Kodak Research Laboratories.*

Research on the behavior of superlinear phosphors suggested a variety of new applications, one of which will be described in some detail. The high temperature coefficients of efficiency encountered in many phosphors, the possibility of influencing these coefficients by suitable preparation without materially affecting the emission spectrum, the possibility, on the other hand, of obtaining different colors of emission with little variation of temperature characteristics, and, finally, the possibility of controlling these characteristics by variation of exciting intensities make certain groups of phosphors a useful tool for the determination of temperatures. This method is peculiarly suitable for qualitative visual observation of temperature distributions on various surfaces and for the photographic recording of such distributions. Some examples of different applications of this method will demonstrate its sensitivity, flexibility, and simplicity.

18. Invited paper, entitled "The Ruling of Large Diffraction Gratings," BY GEORGE R. HARRISON, *Massachusetts Institute of Technology.*

19. Experimental Studies of the Reduction of Apparent Contrast by Water. SEIBERT Q. DUNTLEY, *Massachusetts Institute of Technology.*

The reduction of apparent contrast by water for horizontal, inclined, and vertical paths of sight has been studied from underwater observing stations. Both black objects and white objects have been observed under natural daytime lighting conditions. When the path of sight is horizontal the apparent contrast of all objects is reduced by distance in accordance with the same laws which apply in the case of horizontal paths of sight through the atmosphere.[1] When the path of sight through water is inclined or vertical apparent contrast decreases exponentially with distance, but the attenuation coefficient varies with the

direction of the path of sight. These studies have been supported by the ONR.

[1] S. Q. Duntley, "Reduction of apparent contrast by the atmosphere," J. Opt. Soc. Am. 38, 179 (1948).

20. The Measurement of Meteorological Range in Water. SEIBERT Q. DUNTLEY, *Massachusetts Institute of Technology.*

Experimental studies of the reduction of apparent contrast by water have suggested that the vision-restricting properties of water can usefully be described in terms of meteorological range, i.e., in terms of that horizontal distance through optically homogeneous water for which the contrast transmittance is two percent. The measurement of meteorological range in water involves problems closely analogous to those encountered in measuring the meteorological range in air.[1] A new technique for measuring meteorological range by the space-light method[1] has been devised. Both visual and photoelectric instruments of the new type have been built and used in air, and the requirements for similar devices for use under water have been explored. This work has been supported by the ONR.

[1] Seibert Q. Duntley, "The measurement of meteorological range," J. Opt. Soc. Am. 37, 994A (1947).

21. The Steadiness of the Eye. LORRIN A. RIGGS AND FLOYD RATLIFF, *Brown University.*

Recent theories of visual acuity[1] have recognized the fact that the eye is never completely at rest.[2] The present experiments were designed to make photographic records of the involuntary eye movements which occur during steady monocular fixation of a stationary point. A first-surface plane mirror is sealed into a contact lens which has been fitted to the eye of the observer. Beams reflected from this mirror are used to trace the movements of the eye on a moving strip of film. By the use of dove prisms it has been possible to record simultaneously the horizontal and vertical components of these eye movements. Records on five observers reveal that "flutter" movements during optimal fixation have a median total excursion of 18 seconds (measured from peak to trough in units of visual angle) and frequencies of 30 to 70 cycles. There are slower waves of several minutes' total excursion and irregular frequency, and other phenomena including slow drifts and compensatory jumps. Horizontal and vertical components are quite similar. Control experiments have shown that none of the observed effects is an artifact of the recording apparatus or the contact lens.

[1] L. A. Jones and G. C. Higgins, "Photographic granularity and graininess. IV. Visual acuity thresholds; dynamic *vs.* static assumptions," J. Opt. Soc. Am. 38, 398 (1948).
[2] F. H. Adler and F. Fliegelman, "Influence of fixation on the visual acuity," Arch. Ophth. 12, 475 (1934).

22. The Threshold Gradient of Rods and Cones, in the Dark-Adapted and in the Partially Light-Adapted Eye. LOUISE L. SLOAN, *Wilmer Ophthalmological Institute, The Johns Hopkins University.*

The variation in sensitivity to light from center to periphery of the retina was studied in relation to anatomical factors which might be expected to affect the sensitivity gradient. The two factors considered were effective area of the pupil and density of the retinal receptors. Measurements were made for one normal subject of the threshold gradient of the rods and of the cones when the eye was adapted to darkness and when it was adapted to a brightness of 0.7 ml. The decrease in effective diameter of the subject's pupil from center to periphery was determined by photography.[1] The threshold gradients, corrected for effective area of pupil were then compared with the density gradients of the cones and of the rods, derived from Osterberg's data.[2] The rod threshold of the fully dark-adapted eye was found to be inversely proportional to the number of rods per unit area. In the light-adapted eye, however, the rod threshold did not show a similar relation to rod density. The cone threshold likewise was not closely related to cone density, either in the dark-adapted or in the light-adapted eye.

[1] K. H. Spring and W. S. Stiles, "Apparent shape and size of the pupil viewed obliquely," Brit. J. Ophth. 32, 347–352 (1948).
[2] J. Ten Doesschate, "Visual acuity and distribution of percipient elements on the retina," Ophthalmologica 112, 1–18 (1946).

23. A Functional Analysis of Regional Differences in the Human Fovea. WALTER R. MILES, *Yale University School of Medicine.*

Under suitable illumination the central fovea may be seen as an entoptic image. The yellow pigment absorbs blue light, but does not appreciably absorb red. The optimal filter, a purple dichroic, passing deep blue and deep red, was mounted beside a neutral filter. The filters were used alternately while viewing a fixation point on cross-ruled, light blue paper transilluminated with fluorescent daylight lamps. The borders of the subject's image were charted along two or more perimeters. Typical results for twenty men, ages 19 to 32, show: average diameter of the entoptic image equaling 2° 30′; charts for both eyes usually match or are complemental; the typical image shows three zones, two concentric annular rings surrounding a central disk averaging 33′ in diameter; the fixation point falls within the central disk but not always at its center. The central disk and outside ring show similar color responses which differ from those of the inside ring and visual field surrounding the total image. These color response differences within restricted zones in the central fovea still require explanation but have led to the prediction of experimental results with point color stimuli falling on pairs of charted zones.

24. The Colors of Natural Objects and Terrains and Their Relation to Visual Color Deficiency. CHARLES D. HENDLEY AND SELIG HECHT, *Laboratory of Biophysics, Columbia University.*

The colors of many natural objects and terrains were determined by visual matching with samples of known spectral reflectance (The Munsell Book of Color). There are only three important groups of colors. Foliage lies in a yellow-green region of dominant wave-length 557–574 millimicrons. Earths range between yellow and orange-red, 576–589 millimicrons. Water, sky, and distant objects are blue, 459–486 millimicrons. Colors of autumn foliage spread into the yellows and reds to the end of the spectrum. The outstanding characteristic of these terrain colors is their lack of saturation, most having an excitation purity of 40 percent or less. Furthermore, objects quickly lose saturation with increasing distance from the observer, so that even in the clearest weather encountered no object over 3½ miles

away had an excitation purity of over 11 percent. To the color-deficient observer these colors appear even less saturated than to the normal. In addition, the yellow to green region of the spectrum where the majority of discriminations must be made is one in which color blinds show poor hue discrimination. Thus, in both hue and saturation the color deficient is at a decided disadvantage in discriminating terrains.

25. Measurements of Influence of Local Adaptation on Color Matching. DAVID L. MACADAM, *Kodak Research Laboratories.*

A colorimeter was used in which the adjustable primaries can be separately extinguished and in which the comparison stimulus is synthesized by an equivalent optical system, assuring a physical as well as a visual match. After a few matches were obtained in the customary manner, two of the adjustable primaries were left undisturbed and the third was merely flashed intermittently, five seconds off, one-half second on. After observation of one or two cycles a great difference is apparent between the two halves of the field during the half-second when all three primaries are on. When the red primary is intermittent, the lower semicircle appears bluish-green for five seconds, and much too reddish to match the upper half during the brief flash. The observers readjusted the primaries until the two halves of the field appeared to match during the flash. Each primary was made intermittent, in turn, and also each pair of primaries, giving measurements of the effect for six different directions around each comparison color. Achromatic, and moderately saturated red, green, and purple comparison colors were investigated. The intermittent stimulus which appears to match the steady stimulus lies very nearly on the straight line in the chromaticity diagram connecting the latter with the adapting stimulus.

26. The Apparent Colors of Surfaces of Small Subtense —A Preliminary Report. W. E. KNOWLES MIDDLETON AND MARIAN C. HOLMES, *National Research Council of Canada, Ottawa.*

The early observations of König[1] on the apparent tritanopia of the central fovea were confirmed by Willmer and Wright.[2] Hartridge[3] showed that the small size of the test field, rather than the location of its image on the retina, leads to the tritanopia. In the present work, twenty colors around the Munsell 5-plane were observed against a dark grey background at an angular subtense of 2 minutes and 1 minute of arc, under Macbeth (6800°K) daylight. They were matched with a complete chart of the 5-plane on a similar background and under the same illumination, a mask being provided for the isolation of one color. The colors were presented in two sets of ten, one at a time in completely random order, and medians calculated for 25, 50, or 100 sets of observations. The phenomenon is somewhat personal but its main features are beyond question. The locus of the "reduced" colors approximates an ellipse with its long axis in the general direction red to blue green, but differing in eccentricity for different observers. The displacement of most of the colors is approximately towards or away from the blue end of the spectrum. There is evidence that the phenomenon cannot be explained by the effect of the macular pigment.

[1] A. König, *Physiologische Optik* (Barth, Leipzig, 1903), p. 396. Quoted by W. D. Wright, *Researches on Normal and Defective Color Vision* (Henry Kimpton, London, 1946), p. 333.
[2] E. N. Willmer and W. D. Wright, Nature **156**, 119 (1945).
[3] H. Hartridge, Phil. Trans. Roy. Soc. **B232**, 519 (1947).

27. A New Improved Refractometer. A. H. PFUND, *The Johns Hopkins University*, E. J. WEICHEL, AND B. H. BILLINGS, *Baird Associates, Inc.*

A new refractometer based on a method proposed by A. H. Pfund has been designed. A transparent hemisphere with a slightly curved lower surface makes point contact with the smooth surface of the sample to be measured. When viewed through the hemispherical surface, Newton's black spot is visible. At the critical angle, the light is totally reflected at the hemisphere boundary, and the black spot disappears. The critical angle at which the spot is no longer seen can be translated into the refractive index and measured with very simple equipment. Operation is unaffected by the index of the contact liquid and indices can be measured which are as high as the optical constants of the material available for the hemisphere. Using the polarized ω-image produced by a rutile hemisphere, refractive indices can be measured up to 2.6. Hemispheres of different refractive indices can be interchanged on the instrument so as to utilize the most accurate portion of the sine curve relating index and critical angle. Third-place accuracy should be attainable throughout the range of indices providing a simpler and more universal instrument than the present Abbé refractometer.

28. Coma of Slightly Decentered Wide-Aperture Systems. L. IVAN EPSTEIN, *Bausch and Lomb Optical Company.*

The diameter of the field of view, the decentrations and tilts of the elements of the system, and the spherical aberration of the system as a whole are taken to be infinitesimals. No limitation is placed on the aperture of the system or on the spherical aberration due to any portion of the system. Skew rays are traced with the aid of Lippich's theorem.[1] Any portion of the system adjacent to the aperture stop forms an astigmatic image of the plane of the aperture stop. The coma of the desired image is expressed in terms of the astigmatism and curvature of the pupil images.

[1] Cf., e.g., M. Herzberger, *Strahlenoptik* (Verlag Julius Springer, 1931), p. 78.

29. Analysis of Para-Elliptic Reflector. BENJAMIN GOLDBERG AND NELS C. BENSON, *Engineer Research and Development Laboratories, Fort Belvoir, Virginia.*

This paper presents an analysis of the para-elliptic reflector together with its possible applications when used as a searchlight mirror. The horizontal sections of a para-elliptic mirror are portions of ellipses and the vertical sections are parabolas. The mirror is so designed that each parabola lies in a vertical plane through the secondary focus of the horizontal ellipse which passes through the vertex of the mirror and each elliptical section lies in a plane parallel to that of the ellipse through the vertex of the mirror. A

beam of light projected from such a reflector converges in the horizontal planes to a line common to the intersection of the vertical planes and then diverges as a spread beam horizontally with minimum spread vertically.

30. Anodic Preparation of Oxide Films on Evaporated Aluminum Mirrors and Their Applications. GEORG HASS, *Radiation Branch, Engineer Research and Development Laboratories, Fort Belvoir, Virginia.*

By increasing the thickness of the natural oxide film on evaporated aluminum mirrors, a much better surface protection can be achieved. The oxide film thickness can be increased by heat treatment in air or by anodic oxidation. Heat treatment is not practical because the thermic oxidation of aluminum in air is slow at temperatures below 400°C[1] and the oxide film formed at higher temperatures is not uniform. Oxide films which have a precisely controllable uniform thickness can be formed by anodic oxidation in a suitable electrolytic bath. A 3-percent ammonium tartrate electrolyte is used for oxidizing vacuum-evaporated aluminum films. The thickness of the oxide layer formed in one minute by this treatment depends only on the applied voltage: thickness of Al_2O_3 (in A) = 12.5 × voltage. The resulting oxide films have an amorphous structure and are free of pores. They do not show any appreciable absorption in the ultraviolet, visible, and infra-red. Their refractive index between 3000 and 7000A varies from 1.65 to 1.60. To obtain highest reflectivity in the visible, the anodic oxidation should be performed with 120 volts. Anodized aluminum mirrors prepared by this method show excellent abrasion resistance. The precisely controlled uniform anodic films on opaque aluminum coatings are suitable for the preparation and investigation of reflection type interference filters. Protected, semitransparent aluminum films of any desired transmission can be produced by anodic oxidation of an opaque aluminum coating. The thickness of a pure aluminum film can be determined by the voltage required for complete oxidation.

G. Hass, Zeits. f. anorg. Chemie **254**, 96 (1947).

31. A 72-Inch High Vacuum Evaporator and Its Glow Discharge Equipment. NELS C. BENSON, GEORG HASS, AND NOEL W. SCOTT, *Engineer Research and Development Laboratories, Fort Belvoir, Virginia.*

This paper describes a 72-inch high vacuum evaporator designed to coat mirror forms up to 70-inch diameter with reflective and protective coatings. Data are presented on studies made to determine the optimum shape, size, and position of glow discharge cathode for obtaining uniform heating and consequent cleaning of mirror forms. The evaporator was constructed primarily for the reflective surfacing of 60-inch metal mirror forms used in the standard Army 60-inch searchlight. Satisfactory coatings of aluminum protected by SiO[1] have been made on the 60-inch forms.

[1] G. Hass and N. W. Scott, "Silicon monoxide protected front-surface mirrors," J. Opt. Soc. Am. **39**, 179 (1949).

32. Photogrammetric Errors from Camera Lens Decentering. P. D. CARMAN, *National Research Council of Canada, Ottawa, Ontario.*

A mathematical study has been made of the distortion introduced by a thin prism associated with a perfect lens of 6″ focal length covering a 9″×9″ negative. The position of the principal point for minimum distortion is found to lie away from the two currently used.

33. Physiological and Pharmacological Studies of Blood from X-Ray Personnel. DAVID I. MACHT, MARCUS OSTRO, AND STANLEY H. MACHT, *Departments of Pharmacology and Radiology of the Sinai Hospital, Baltimore, and the Department of Radiology, Baltimore City Hospitals.*

The senior author has called attention in many publications to the fact that certain seedlings grown in Hydroponic plant-physiological solutions under strictly controlled ecological conditions are able to detect abnormal or toxic constitutents in one percent solutions of blood serum, even though these are not detectable by ordinary pharmacological or biochemical methods. Thus it was shown that blood sera of various animals, including men, exposed to x-rays are definitely toxic for the growth of *Lupinus Albus* roots. In the present investigation, studies were made in two Baltimore hospitals of blood specimens taken from physicians, students, technicians, clerks, and other personnel employed in their radiological departments. Phytopharmacological tests were made on the one hand and morphological examinations on the other hand. It was discovered that almost all of the blood sera from x-ray personnel possessed Phytoxic properties, even before morphological changes could be discovered in the blood smears. A considerable number of the subjects also revealed changes in the blood cells, such as leucocytosis, etc. The findings point to the fact that stray radiations do occur in x-ray laboratories in spite of all the ordinary precautions taken to keep them out. This was corroborated by tests with supersensitive films. The hygienic implications of the above findings are obvious.

BIBLIOGRAPHY: David I. Macht, Science **71**, 3021 (1930). David I. Macht, Protoplasma **26**, 1 (1937). D. I. Macht, Am. J. Roentgen and Radium Therapy **41**, 769 (1939). D. I. Macht, Am. J. Roentgen and Radium Therapy **45**, 446 (1941).

34. Invited paper, entitled "Measurements of Size and Shape of Large Molecules by Light Scattering," BY P. DEBYE, *Cornell University.*

35. Metameric Colors and the Macular Pigment. WALTER C. GRANVILLE, *Container Corporation of America,* AND DEANE B. JUDD, *National Bureau of Standards.*

Two metameric pairs of gray paints have been prepared, one, nearly nonselective, from black and white pigments being common to each pair, the other two being spectrally selective mixtures of yellow, green, purple, and white pigments. One selective gray was formulated to match visually the non-selective gray when viewed at 20 feet (subtending about 2°). This pair becomes a serious mismatch[1] when viewed so as to stimulate extra-macular portions of the retina. The second selective gray was formulated to match the non-selective gray closely for observation at one foot. The spectral reflectance of the three paints was measured and the chromaticity coordinates computed for Macbeth 6800°K[2] by means of the 1931 ICI observer. The chromaticity differences so indicated were found to conform, as expected, to observations of these pairs by eight observers under Macbeth daylight at 20 feet. By dividing the tristimulus values of the spectrum by the spectral

transmittance of the macular pigment determined by Wald[3] a new basis for computations was set up that agreed with the colors perceived at a distance of 1 foot. Possible applications of this new basis to color matching and to the artist's distinction between "lively" and "dead" grays will be discussed.

[1] J. Scott Taylor, Preface to Part II, *Color Science*, by Wilhelm Ostwald, pp. ix and x (Winsor and Newton, London, 1933).
[2] Committee on Colorimetry, "Quantitative data and methods for colorimetry," J. Opt. Soc. Am. **34**, 647 (1944).
[3] G. Wald, "Human vision and the spectrum," Science **101**, 653 (1945).

36. The Ridgway Color Standards with a Munsell Notation Key. D. H. HAMLY, *Department of Botany, University of Toronto.*

The Ridgway Color Standards and Nomenclature published in 1912 satisfied a great want in biological color description for it contained a nomenclature of 1115 generally accepted color terms illustrated with colored chips. More than 25 years work had gone into the selection of a range of colors useful to biologists. This system contains a far larger number of colors useful to biologists than exist in other standard systems. Its success is shown by the practically complete acceptance of it by the biologists of the U. S., Canada, and Great Britain. The Ridgway standards, however, are now greatly limited in usefulness because pronounced differences in color are now being found on comparing chips of the same name in different books, further because no physical specifications exist for their reproduction. A key to Ridgway in terms of Munsell notations is presented and its usefulness is discussed. It is suggested that information obtained from the users of the Ridgway standards will provide useful data for the production of a set of modern color standards suitable for use by biologists in making records for publication.

BIBLIOGRAPHY: W. I. Illman and D. H. Hamly, "A report on the Ridgway Color Standards," Science **107**, 626–628 (1948).

37. The Plochere Color System: A Descriptive Analysis. W. E. KNOWLES MIDDLETON, *National Research Council of Canada.*

The Plochere Color System is a collection of 1248 painted papers, the colors being produced by systematic pigment mixtures. These were matched under Macbeth daylight illumination with the chips in The Munsell Book of Color. Certain regularities and singularities in the system will be discussed.

38. The Design of a Daylight Filter for Color Film Sensitometry. R. H. BINGHAM, *Ansco Research Laboratories.*

In the sensitometric testing of daylight type color film, the light source must have a spectral energy distribution which matches as accurately as possible that of natural daylight. The theoretical and experimental details of the design of such a filter are discussed. A solution is given of the least squares problem of adjusting the components of a filter in order that the energy distribution obtained in combination with a given light source shall most closely fit a desired curve. Using the least squares formulas obtained from this analysis, a filter was designed which, when used with a tungsten 2800 K light source, yields a spectral energy distribution closely matching that of average photographic (sunny) daylight. It consists of two colored glasses between which is cemented a gelatin layer containing four dyes. Spectral characteristics and fading characteristics are discussed.

[1] R. Davis and K. S. Gibson, Nat. Bur. Stds. MP. No. 114 (1931).
[2] A. H. Taylor and G. P. Kerr, J. Opt. Soc. Am. **31**, 3 (1941).
[3] P. Moon, J. Franklin Inst. **230**, 583 (1940).

39. An Automatic, Continuous Tristimulus Integrator. H. R. DAVIDSON AND L. W. IMM, *Central Research Laboratory, General Aniline & Film Corporation and Librascope, Inc.*

An automatic tristimulus integrator has been developed for use with the General Electric Recording Spectrophotometer. Selsyn transmitters mounted on the spectrophotometer relay the wave-length and reflectance to the computer where integration is carried out by means of mechanical analog techniques developed during the war. The integrations are performed continuously while the curve is being drawn at either fast or slow speed. Tristimulus values for any curve may, therefore, be obtained by the spectrophotometer operator with no additional expenditure of time other than that required to record the values and return the counters to zero. The precision of the prototype computer is about ± 0.0005 when the tristimulus values are so normalized that $Y = 1.0000$ for a sample whose reflectance is 100 percent. Also, we have found that the combination of spectrophotometer and integrator is at least as sensitive and usually more sensitive than the eye for the detection and evaluation of small color differences. The absolute accuracy of the tristimulus values obtained is approximately ± 0.001. Examples will be given to indicate that this high speed computer, which will be available commercially, makes practical the application of numerical methods to the solution of color problems.

40. Tristimulus Computation in the Dyestuff and Textile Field. I. H. GODLOVE, *General Aniline & Film Corporation.*

The Tristimulus Integrator[1] described on this program by H. R. Davidson and L. W. Imm has been found, because of its high precision and saving of time, to yield many results of interest to the textile-dyeing field not conveniently obtained previously. It permits statistical analyses; for example, obtaining a measure of "unevelness" (nonuniformity) of dyeings. The average differences between the trichromatic coefficients x and y for A.M. and P.M. repeats on six red wool dyeings was 0.0004. This includes the overall errors due to the spectrophotometer itself, the positioning of samples and those of the integrator. Other work indicates that the precision is adequate for small-difference colorimetry. Work has been done on liquid and film filters to yield analyses for night lighting as well as daylight, "change of shade in artificial light" being of much interest to dyers. Results contrasting additive mixing on a "union" (cotton and wool) dyeing and the subtractive mixture of dye solutions, will be shown; also studies on "dyer's brightness," which is related to saturation. The Computer has also been used to follow the striking changes of color due to aggregation of dye molecules in solution; this and other dye phenomena will be illustrated.

[1] Preceding paper on this program by H. R. Davidson and L. W. Imm.

41. Colorimetry by Abridged Spectrophotometry. ARTHUR C. HARDY AND F. MANSFIELD YOUNG, *Massachusetts Institute of Technology.*

It seems to be generally conceded that the results obtained with a photoelectric colorimeter are significant only when the spectral characteristics of the sample and standard are similar. When this is the case, the selected ordinate method of integrating spectrophotometric data can be greatly abridged, a single selected ordinate being adequate under many circumstances. This means that an abridged spectrophotometer can be used for the dual purpose of production control and, when necessary, the determination of tristimulus values.

42. Performance of a New Double Beam Infra-Red Spectrophotometer. JOHN U. WHITE AND MAX D. LISTON, *The Perkin-Elmer Corporation.*

A new recording infra-red spectrophotometer[1,2] has been constructed and tested under a variety of operating conditions. Resolution has been observed approaching the theoretical limit for the rock salt prism used. Stability corresponds to 1.5 times the Johnson noise of the thermocouple used as detector, or to an r.m.s. equivalent noise input of 1.5×10^{-10} to 0.5×10^{-10} watt, depending on the speed of response. The variation of I_0 with wave-length is small, and the scattered light is kept to less than 1 percent throughout the useful range. The instrument's performance will be illustrated with spectra measured under conditions showing its versatility in such variables as resolution, speed, stability, etc.

[1] John U. White and Max D. Liston, J. Opt. Soc. Am. **38**, 1098A (1948).
[2] Max D. Liston and John U. White, J. Opt. Soc. Am. **38**, 1098A (1948).

43. A Rapid-Scanning Spectrometer for the Near Infra-Red.* B. W. BULLOCK AND S. SILVERMAN, *Applied Physics Laboratory, The Johns Hopkins University.*

A scanning spectrometer[1-4] has been built for use in the lead sulphide region. Suitable spectra in emission as well as in absorption have been obtained at scanning rates up to 120 spectra per second in the region 360 millimicrons to 3 mu. Scanning time per cycle is approximately 20 percent of the total cycle. Scanning is achieved by oscillating the Littrow mirror the spectrometer, using a torque motor and direct link as the driving mechanism. This results in an approximate sine wave oscillation with a maximum usable amplitude of 1.5°. With LiF optics, the region 1–3 microns can be covered in a single range. Preliminary results have also been obtained with a rocking grating as the dispersive element. Resolving power limitations are set by the time constant (approximately 30 microseconds) of the Pb-S cell and amplifier. A liquid-air cooled Pb-Te cell was tried in the instrument; however, the long time constant (1–2 milliseconds) required a decrease in scanning speed to a few cycles per second.

* The work described in this paper was supported by the Bureau of Ordnance, U. S. Navy, under Contract NOrd-7386.
[1] Feldt and Berkley, Nat'l Electronics Conference, Chicago, 1946.
[2] F. F. Daly and G. B. B. M. Sutherland, Proc. Phys. Soc. (London) **59**, 77 (1947).
[3] W. E. Deal, W. Bradshaw, and F. A. Matsen, J. Chem. Phys. **16**, 638 (1948).
[4] S. Silverman, J. Opt. Soc. of Am. **38**, 664A (1948).

44. An Experimental Study of Dennison-Hadley Infra-Red Reflection Filters. E. E. BARR, *Research Laboratory, Baird Associates, Inc.*

Dennison-Hadley[1,2] filters consist of a dielectric layer sandwiched between a highly reflecting metallic backing and a semi-conducting metallic front layer. The spectral curve obtained by reflection gives alternate maxima and minima values practically equal to 100 percent and 0 percent respectively. Experimental curves will be shown in the 2 to 16 micron spectral region to demonstrate the dependence of band width and band position on the optical thickness of the dielectric layer. A method of producing very narrow bands by the use of a number of filters in series will also be discussed with accompanying curves.

[1] L. N. Hadley and D. N. Dennison, J. Opt. Soc. Am. **37**, 451–465 (1947).
[2] L. N. Hadley and D. N. Dennison, J. Opt. Soc. Am. **38**, 483–496 (1948).

45. An Experimental Study of Turner Frustrated Total Reflection Filters in the Infra-Red. B. H. BILLINGS, *Research Laboratory, Baird Associates, Inc.*

In contrast to the solid Fabry-Perot interference filter the Turner Frustrated Total Reflection filter contains no metallic surfaces and depends for its operation solely on index differences. It is thus possible to make these filters for any part of the spectrum for which there are transparent materials of different indices. As a result of theoretical calculations, filters have been designed to operate in the 250 micron region with a band width of approximately 0.25 micron. Measurements will be shown of a filter built for the 5 micron region which has a passband approximately $\frac{1}{10}$ of a micron wide.

46. Infra-Red Transmitting Filters.* E. R. BLOUT, R. S. CORLEY, AND P. L. SNOW, *Research Laboratory, Polaroid Corporation.*

Transmission filters which absorb substantially all ultraviolet, visible, and near-infra-red radiation to wave-lengths around 1 micron have been made from plastic materials without the use of dyes. The filters, which have visual transmittances for tungsten light of 3×10^{-8} and lower, have two pass bands in the infra-red. The first transparent region lies between 1 and 3.4 microns and has a peak transmission at 2 to 2.6 microns of approximately 75 percent; the second band lies between 3.6 and 5.8 microns and has a peak transmission of 60 percent. By laminating such materials between glass, one can obtain filters with a single transmission band between 1 and 2.8 microns. By the use of powder-filter combinations, one can sufficiently scatter the shorter infra-red wave-lengths so that essentially only the second pass band remains. Transmission curves will be shown for the filters. Since the filters are made from high polymeric films, they are flexible and can be made in relatively large areas. Their chemical structure gives them a high degree of thermal stability. The materials used and the reactions involved in their formation will be discussed.

* This work has been performed under contract with the Engineer Research and Development Laboratories.

47. Reflectance and Transmittance Measurements of Thin Evaporated Metallic Films in the Infra-Red. MAX S. OLDHAM, *Naval Ordnance Laboratory.*

A reflectometer designed for use with an infra-red spectrometer is described. The arrangement permitted the

sample to be tested in parallel radiation for angles of incidence of 10 to 70 degrees. The reflected beam was compared with an uninterrupted beam so that absolute reflectances were obtained directly. Reflectance measurements were made of the component polarized perpendicular to the plane of incidence of the sample. Polarization was accomplished by two reflections from selenium at the polarizing angle of incidence. Evaporated films of various thicknesses of aluminum, platinum, gold, beryllium, silver and copper were measured in the wave-length region 1.0 to 3.5 microns. Typical results for beryllium films are presented. The variations of reflectance with angle of incidence, wave-length and film thickness are shown. Film thicknesses were measured using a modification of Tolansky's[1] interferometric method.

[1] S. Tolansky, J. Sci. Inst. 22, 161 (1945).

48. Preliminary Measurements of the Cold Flow of Silver Chloride and Thallium Bromide-Iodide.* LEWIS S. COMBES, JAMES R. TRAVIS, AND STANLEY S. BALLARD, *Baird Associates, Inc. and Tufts College.*

Measurements of a number of the physical properties of the several optical materials employed in infra-red instrumentation were reported[1] at the Detroit Meeting in October 1948. The final item undertaken during this program was the measurement of the cold flow of these materials when held under a constant load (usually less than the apparent elastic limit) for periods of many hours. To date this has been done only for small bars of three of the materials. In flexure strain, curves have been obtained for several samples of AgCl and KRS-5 under various loading conditions such that the maximum fiber stress is either less than or slightly greater than the apparent elastic limit. Comparison data have been obtained on such well-known materials as crystalline sodium chloride and Plexiglas. The data obtained thus far indicate that the cold flow behaviour of AgCl is about what might be expected for a homogeneous material, but the curves of KRS-5 show an anomalous behaviour which will be illustrated by typical curves, and discussed. The extension of this program to the measurement of strain and cold flow of circular disks ("windows") of these optical materials is now being planned.

* This work has been supported by Contract W-44-009 eng-473 between the Engineer Research and Development Laboratories, Fort Belvoir, Virginia, and Baird Associates, Inc., Cambridge, Massachusetts.

[1] L. S. Combes and S. S. Ballard, J. Opt. Soc. Am. 38, 1101A (1948).

49. Infra-Red Spectra of Argon, Krypton, and Xenon between 1.2 and 2.2 Microns.* W. R. SITTNER (Introduced by E. R. Peck), *Northwestern University.*

The infra-red spectra of high intensity condenser discharge sources have been studied by means of a recording spectrometer described by Nelson.[1] A PbS photoconductive cell was used for a detector. The probable error in the determination of wave number of the observed lines is approximately 0.1 cm^{-1}. Sixty-five lines of argon were observed for the first time, while the spectra of krypton and xenon showed 69 and 40 new lines, respectively. About three-fourths of the new lines are due to combinations of terms of the normal atom given by Humphreys and Meggers.[2] The interpretation of the remaining lines is uncertain. Some of the unusual characteristics of inert gas spectra excited in repetitive condenser discharges will be discussed

* This work was supported by the Navy Department, Bureau of Ships.

[1] R. C. Nelson, J. Opt. Soc. Am. 39, 68 (1949).
[2] Humphreys and Meggers, Bur. Stand. J. Research 10, 427 (1933); 10, 139 (1933).

50. The Infra-Red Absorption Spectra of Ten Substituted Methanes. EARLE K. PLYLER AND W. S. BENEDICT, *National Bureau of Standards.*

The infra-red absorption spectra of $CHCl_3$, $CHBr_3$, CHI_3, CH_2Cl_2, CH_2I_2, $CHBrCl_2$, $CHBr_2Cl$, $CBrCl_3$, CBr_2Cl_2, and CCl_4 have been measured in the region from 2 to 38μ. Chloroform and bromoform were investigated in the vapor state and in the liquid state. A comparison of the spectra for the two different states reveals only small shifts in the wave-lengths of the bands. The spectra of the other compounds were obtained in the liquid state or in solutions. Cell thicknesses from 0.05 mm to 2.0 mm were used. The thick cells made it possible to observe many combination bands. The observed bands have all been interpreted as fundamentals, combination and overtone bands, and difference bands. In the compounds with similar structures, the relative intensities of the various bands show regularities. The fundamentals may be assigned to different symmetry types, on the basis of a normal coordinate treatment, using force constants similar to those reported by Decius.[1]

[1] J. C. Decius, J. Chem. Phys. 16, 214 (1948).

51. Invited paper, entitled "A Color Translating Ultraviolet Microscope," BY E. H. LAND, *Polaroid Corporation.*

52. A New Family of Microscope Objectives.* DAVID S. GREY, *Research Laboratory, Polaroid Corporation.*

The Schwarzschild aplanatic pair of mirrors has been adapted for use as microscope objectives.[1] Incorporation of refractive components into the optical system provides means of obtaining large numerical apertures without use of aspheric surfaces. Apochromatic correction has been obtained over a wave-length interval much greater than is possible with purely refractive systems, and monochromatic aberrations can be corrected for larger fields of view. Primary attention is given to systems apochromatic over the region 220 mμ to 800 mμ for use in the color translating ultraviolet microscope. Results obtained with an objective of numerical aperture 0.72 corrected for this region of the spectrum are described.

* This work was supported by funds from the Office of Naval Research.

[1] C. R. Burch, Proc. Phys. Soc. (London) 59, 41 (1947).

53. Ultraviolet Light Sources.* CHARLES H. MATZ AND DWIGHT P. MERRILL, *Research Laboratory, Polaroid Corporation.*

Various ultraviolet light sources have been investigated with respect to their suitability as sources of illumination for a color translating ultraviolet microscope.[1] Since the microscope requires, ideally, illumination by relatively narrow bands of radiation centered about any chosen wave-length within the spectral region between approximately 200 and 400 millimicrons, an important desideratum

of a source is that its ultraviolet spectrum be a continuum throughout the specified range. Other characteristics to be taken into account are size, intrinsic brightness and the angle throughout which Lambert's law is obeyed. These will be discussed briefly. A simple quartz-prism, pin-hole spectrograph will be described, whereby the spectral ultraviolet brightness of a source can be evaluated in terms of the sensitivity of a photographic plate. From this relationship, without need for the expression of either brightness or sensitivity in absolute units, the exposure time required by the same source-plate combination in any photomicrographic system can be computed from the N.A., magnification, and reflection and absorption losses of the system. Several sources best suited for illumination of the microscope will be discussed and results of measurements of brightness will be reported.

* This work was supported by funds from the Office of Naval Research.
[1] E. H. Land, "A color translating ultraviolet microscope," Paper 51 above.

54. Methods of Color Translation.* R. CLARK JONES, *Research Laboratory, Polaroid Corporation.*

In general, color translation is accomplished by placing apparatus between the eye of the observer and the object viewed, such that the three color receptors in the eye of the observer effectively respond to radiation in a band of wave-lengths different from the band to which the receptors ordinarily respond. Evidently an essential part of any method of color translation is the conversion of an image in one wave-length into an image in another wave-length. This process will be termed image-conversion. In addition to the photographic method of converting an ultraviolet image into a visible image employed in the color translating microscope,[1] four other methods of image-conversion exist. The five methods employ the following devices: 1. Photographic plate or film, 2. Fluorescent screen, 3. Image tube, 4. Flying spot scanner, 5. Image orthicon. The last three are electronic devices developed for use in television. On the basis of the brightness of available ultraviolet sources, and on the basis of the visible brightness needed for the human eye to have full color discrimination, it will be shown that the odd numbered methods appear promising and worthy of development, whereas the even numbered methods appear unsatisfactory.

* This work was supported by funds from the Office of Naval Research.
[1] E. H. Land, "A color translating ultraviolet microscope," Paper 51 above.

55. Color Translating Ultraviolet Microscopy and Ultraviolet Spectrophotometry.* ELKAN R. BLOUT AND MIRIAM S. FLOWER, *Research Laboratory, Polaroid Corporation.*

Ultraviolet absorption spectrophotometry has been extensively used in the characterization and identification of many materials. We shall describe and discuss the procedures used in our laboratory for color translating ultraviolet microscopy,[1] and in particular some of its applications to biological, organic, and pharmaceutical chemistry. By taking photomicrographs of materials under controlled conditions at three different wave-lengths in the ultraviolet and then projecting simultaneously the images so obtained through three visible additive color filters, one obtains a colored representation of the material in which the color depends on its inherent ultraviolet absorption.[2] Variables involved in the use of the technique, such as control of exposure times, photographic development and specimen size, will be discussed, and an attempt made to compare the advantages and disadvantages of this method with ultraviolet absorption spectroscopy and spectrophotometry. We shall present examples and comparisons of ultraviolet spectrophotometry and color translating ultraviolet microscopy from the fields of biology and biological chemistry (tissue sections, nucleic acid, proteins and amino acids) and organic chemistry (aromatic acids, purines, pyrimidines, fibers and high-polymer films).

* This work was supported by funds from the American Cancer Society and the Office of Naval Research.
[1] E. H. Land, "A color translating ultraviolet microscope," Paper 51 above.
[2] E. M. Brumberg, *Comptes Rendus* **25**, 473 (1939).

56. Instrumental and Doppler Broadening in the Fabry-Perot Interference Pattern of Close Doublets.* P. M. GRIFFIN AND J. R. MCNALLY, JR., *Carbide & Carbon Chemicals Corporation.*

The intensity distribution in Fabry-Perot interference patterns as a function of instrumental and Doppler broadening is discussed. Merton's method,[1] in which the line shape is approximated by assuming that an exponential distribution of thermal velocities in the source gives rise to a Gaussian distribution of light in the interference fringe, was rejected as not being applicable to the Fabry-Perot instrument in agreement with the conclusions of Robertson.[2] Starting from the results of Saha[3] for a single line, an expression was developed for the intensity distribution due to a close doublet as a function of the temperature of the source, order of interference, reflection power of the interferometer plates, and the ratio of peak intensities of the two lines. This expression was applied to the green lines from a hypothetical source containing electromagnetically separated Hg^{204} with Hg^{202} as the principal impurity and investigated under the following conditions: source temperatures of 77 and 300 degrees Kelvin; reflection powers of 0.80, 0.85, and 0.90; orders of interference corresponding to plate separations 1, 2, and 3 centimeters. From these data conclusions are drawn concerning the maximum tolerable percentage of Hg^{202} in a Hg^{204} source if the green line from this source were to be used as an acceptable standard of wave-length.

* Based on work performed under contract for the Atomic Energy Commission by Carbide and Carbon Chemicals Corporation at Oak Ridge, Tennessee.
[1] T. R. Merton, Proc. Roy. Soc. (London) **A97**, 307 (1920).
[2] J. K. Robertson, Can. J. Research **4**, 305 (1931).
[3] M. N. Saha, Phys. Rev. **10**, 782 (1917).

57. Further Classification of the Spectrum of Singly-Ionized Uranium. J. R. MCNALLY, JR., *Carbon and Carbide Chemicals Corporation*, AND G. R. HARRISON, *Massachusetts Institute of Technology.*

The present status of the classification of the spectrum of singly-ionized uranium is discussed. Analysis of this spectrum was begun at MIT in 1941 but publication was withheld during the war for security reasons. During this period a preliminary analysis of the complex ion spectrum was published by Schuurmans[1] and also by Schuurmans, van den Bosch and Dijkwel.[2] The early Zeeman effect

studies at the Massachusetts Institute of Technology Spectroscopy Laboratory have been supplemented by isotope shift investigations in the Y-12 laboratories of Carbon and Carbide Chemicals Corporation. The application of IBM equipment to the classification of the spectrum has also materially aided the analysis of the complex energy structure of U II.

[1] Ph. J. C. Schuurmans, "Over de analyse van enige complexe spectra (Th. en U)." Diss. Amsterdam 1946.
[2] Ph. J. C. Schuurmans, J. C. van den Bosch, and N. Dijkwel, Ph 13, 117 (1947).

58. The Spectra of the Heavy Elements. FRANK S. TOMKINS AND MARK FRED, *Argonne National Laboratory and Armour Research Foundation.*

The spectra of the new heavy elements are characterized by great complexity similar to that well known for thorium and uranium. Consequently, description of the spectra to be adequate for term analyses and assignment of electron configurations must be quite extensive, containing complete, accurate wave-lengths and much other material. Since considerable effort and amounts of sample are required it will be some time before such descriptions are available. On the other hand it would be useful for spectrochemical analyses to have wave-lengths to 0.1A and intensities in a convenient spectral region, and this information has been collected for protactinium, neptunium, plutonium, and americium. Intensities for each line were obtained as the reciprocal of the limiting dilution at which it could be seen with the copper spark source, and therefore the same intensity scale is used for each element. Hence it could be observed that the spectrum of americium appears to stand in the same relation to those of the other heavy elements that the spectrum of europium does to those of the preceding rare earths, both elements containing relatively few lines of high average intensity. This suggests by analogy that Am I contains seven *f* electrons plus two others.

59. Photographing Spectra in the Vacuum Ultraviolet. A. L. SCHOEN AND EDWIN S. HODGE, *Kodak Research Laboratories.*

Sensitive materials for photographing the far ultraviolet spectrum usually require either a fluorescent overcoating on the emulsion or a sensitive silver halide layer in an abnormally low concentration of gelatin on the surface. The characteristics of a new photographic material of the latter type are described in this paper. The testing and the properties of this material are considered and the applications to spectrography are indicated.

60. Emulsion Calibration Paper for Quantitative Spectroscopic Analysis. HAROLD K. HUGHES AND R. W. MURPHY, *Technical Service Department, Socony-Vacuum Laboratories.*

The time devoted to collecting and plotting the required data in any of the well-known methods of emulsion calibration for quantitative spectroscopic analysis is generally an appreciable fraction of the total analytical time. This can be reduced considerably by the use of a new coordinate paper on which the plot of transmittance *versus* relative exposure is approximately a straight line for all of the common emulsions. By the use of this paper, the need for the (1—transmittance) portion is eliminated. When it can be established that the calibration on this paper is a straight line, the number of calibration points can be reduced. The new emulsion calibration paper has a logarithmic abscissa and a modified logarithmic ordinate which expands non-uniformly from about 30 percent to 97 percent transmittance. The approximate linearity of emulsion calibration curves for Eastman SA—1 films, SA—1 plates, SA—2 films, I—N plates and 33 plates, between 2 percent and 97 percent transmittance, has been verified with data from five independent laboratories. A method will be described for eliminating all emulsion calibration procedures when standards are placed on the same plate or film with unknowns.

61. A Laboratory-Cast Pin Sample for the Spectrographic Analysis of Copper-Base Alloys. E. W. PALMER, J. P. IRWIN, AND C. C. FOGG, *The American Brass Company.*

A practical and inexpensive method has been developed for preparing pins of standard size and shape from any form of metallic sample (wire, sheet, heavy bars, drillings, etc.) received for spectrographic analysis by a brass mill laboratory. The sample is reduced to fine chips, and a small portion (approx. 1 gram) remelted under argon in a specially designed graphite crucible which also serves as the mold in which the sample is solidified. The crucible and contents are heated in a small laboratory electric arc furnace. Sample pins so prepared are machined to dimensions that vary with the excitation to be used and the elements to be determined. It is shown that even for alloys containing easily oxidized or easily vaporized elements, in the amounts usually encountered, the pin sample satisfactorily reflects the composition of the material prior to remelting. Replicate analyses can be made on the same pin by remachining. Because the high conductivity of copper-base alloys makes these materials unusually sensitive to changes in electrode size and shape, this development of a standard sample makes possible, for the first time, really quantitative spectrographic work on the wide variety of forms and gauges of alloys submitted to the brass mill spectrographer.

62. An Air Interrupter for Use with an A.R.L. Spark Source. EMIL KACZOR AND KATHERINE CHAMBERLAIN, *Wayne University.*

Substitution of an air interrupter for the rotary gap on this spark source is not practical as the transformer lacks power to charge the capacitors to sparking potential several times per cycle. A separate unit is described that is powered by the transformer in the original unit. Changeover from conventional operation with the rotary gap to air interruption is rapid and convenient. An inductively coupled pick-up is also described for obtaining oscilloscope patterns indicating voltage and current conditions in the leads to the analytical gap. To study single patterns, a camera synchronizing attachment has been built that makes it possible to photograph a single trace on an ordinary oscilloscope with green medium persistence screen. An Eastman Twin Lens Reflex camera was used. The moving contact that is built into the shutter closes the circuit to charge a condenser after the leaves are fully

open. This potential is applied to the horizontal plates of the oscilloscope and produces a single sweep across the screen. The shutter time is made long enough to take advantage of the full persistence period of the trace. Fully exposed photographs of single sweeps can be obtained in this way on Verichrome film.

63. Some New Techniques in the Spectrochemical Analysis of Nonmetallic Samples. M. F. HASLER AND C. E. HARVEY, *Applied Research Laboratories.*

Several new techniques have been developed which greatly extend the range and application of spectrochemical methods in nonmetallic sample analysis. The first has to do with a method of vaporizing and collecting a nonmetallic sample in a manner which reduces it to a standard chemical and crystallographic form. By this means, samples and synthetically prepared standards can be reduced to a common form which allows analysis by various high precision spectrochemical methods. The second is a method of sparking to the edge of a rotating disk, which disk is a briquet containing a nonmetallic sample mixed with a binder. This method of sparking allows results of high precision to be obtained providing the correct binder, discharge conditions and rotational speed of the disk are employed. A combination of these two techniques has been utilized to solve the difficult problem of mica analysis. A method has been developed which allows analysis of both major and minor constituents with an accuracy of 2–3 percent of the amount present. A similar method has been used to extend alkali determinations in cement down to 0.01 percent with greatly increased accuracy, yet utilizing spectrum lines in the ultraviolet and violet.

64. The Correction of Slit-Width Errors. ARTHUR C. HARDY AND F. MANSFIELD YOUNG, *Massachusetts Institute of Technology.*

In the classical treatments[1-4] of the error that results when a continuous source is used with a monochromator having slits of finite width, arbitrary assumptions are made concerning the distribution of energy in the pass band of the monochromator. The present investigation is concerned with the general case where the energy distribution of the pass band may be any function of wave-length. As a result of this investigation, it is proposed that the effective width of the slits of a monochromator be defined by

$$w = \{24[a_2 + (a_1^2/2)]\}^{\frac{1}{2}}$$

where a_1 and a_2 are coefficients of the correction terms of the first and second order respectively. It will be shown that these coefficients can be readily found experimentally, and that in many instances automatic slit-width correction is feasible.

[1] Lord Rayleigh, Phil. Mag. 42, 441 (1871).
[2] Runge, Zeits. f. Math. 42, 205 (1897).
[3] Paschen, Wied Ann. 60, 712 (1897).
[4] Hyde, Astrophys. J. 35, 237 (1912).

65. Relation between Entrance and Exit Pupils of Telescopic Systems. IRVINE C. GARDNER, *The National Bureau of Standards.*

The definitions of the entrance and exit pupils, as commonly given, are formulated in terms of paraxial imagery only. For telescopic systems the definitions have been extended to apply to extra-axial points and to include the effects of pupil aberrations. If a telescopic system is free from distortion and an incident plane wave emerges as a plane wave free from aberrations it is shown that exact relations between conjugate chords in the entrance and exit pupils can be derived by application of principles of the wave theory. Equivalent relations can be derived by equating the flux of energy in the incident beam to that in the emergent beam. These results are applied to show that there is a necessary though small variation in resolving power for different parts of the field of a telescopic system even though it is ideally free from aberrations.

66. Resolution of Two Particles in a Bright Field by Coated Objectives. HAROLD OSTERBERG AND FRANKLYN C. WISSLER, *American Optical Company.*

It will be shown theoretically that the physical limit of resolution for two particles against a bright background is improved by coating the objective to reduce the diameter of the Airy disk below its classical value. The increase in the relative energy content of the diffraction rings which accompanies contraction of the Airy disk may be said to have a minor effect upon the physical limit of resolution but to have a deteriorating effect upon contrast of the diffraction image of the two particles. The comparative performance of two special types of coated objectives and the classical Airy type objective will be discussed. The two special types consist of objectives coated as in the method wherein an ink spot is centered at the aperture, and of objectives coated to obtain a simplified Sonine[1] diffraction pattern having contracted Airy disks. The physical limit of resolution for two non-overlapping particles decreases with increasing particle size within the range for which the approximation of the theory is valid. This physical limit depends also upon the amplitude and phase transmission of the particles.

[1] H. Osterberg and J. E. Wilkins, Jr., J. Opt. Soc. Am. 38, 668A (1948).

67. The Resolving Power of a Coated Objective, II. J. ERNEST WILKINS, JR., *American Optical Company.*

Luneberg[1] has discussed the problem of attempting to increase the resolving power of an objective by applying a coating to the aperture in such a manner that the diffraction pattern produced by the coated objective has a narrower central bright disk than is the case for an uncoated objective. In a previous paper[2] a particular type of coating was proposed for this purpose, but no attempt was made to control any other aspect of the diffraction pattern. In this paper there is described a coating leading to a diffraction pattern which has a narrower central bright disk than is the case for an uncoated objective and which further has the maximum central intensity of all possible diffraction patterns with the same size central bright disk. For an aberrationless objective free from reflection losses this coating simply produces a half-wave-length retardation with no change in amplitude over a uniquely determined part of the aperture and affects neither amplitude nor phase over the rest of the aperture.

[1] R. K. Luneberg, Mathematical Theory of Optics, Brown University, 1944.
[2] H. Osterberg and J. E. Wilkins, Jr., J. Opt. Soc. Am. 38, 668A (1948).

68. Some Remarks on Gold Treatment of Photographic Silver Halide Emulsions. F. W. H. MUELLER, *Ansco Research Laboratories.*

Earlier attempts of various investigators to increase the sensitivity of photographic emulsions by addition of colloidal silver, silver sulfide, or gold are reviewed. Koslowsky's discovery of the effect of certain gold complex salts as powerful sensitizers is described and a possible mechanism of the effect discussed. The importance of this effect for the manufacture of modern high speed and fine grain film as well as special x-ray emulsions is indicated.

BIBLIOGRAPHY: W. Jenisch, Zeits. f. wiss. Phot. **24**, 248 (1926). B. H. Carroll and D. Hubbard, Bur. Stand. J. Res. 1, 565–88 (1928). Agfa Film Plant, Wolfen, Ger. Reports Sept.-Oct. 1936, R. Koslowsky; H. Mueller. Bibliogr. of Scientific and Industrial Reports, U. S. Dept. of Commerce, Vol. 8, p. 873. PB 70053, fr. 831–50.

69. Achromatic Anti-Reflection Films. PAUL LEURGANS, *Bausch & Lomb Optical Company.* (15 min.)

The possibilities of multiple anti-reflection films effective over a broad spectral range have not been fully exploited. If the basic theory of a single anti-reflection film[1] is generalized, it becomes apparent that in principle it is possible to obtain zero reflectivity at N wave-lengths if a combination of N films is used. Two cases, $N=2$ and $N=3$, are solved after first obtaining the necessary film thicknesses by a geometrical method. For the case of a double film ($N=2$) the thickness of the top layer is a quarter wave and the thickness of the film next to the glass is a half wave. A set of film indices with which it is possible to obtain two reflectivity zeros on a glass of index 1.62 is 1.41 for the top film and 2.00 for the bottom film. The film indices depend on the glass index and on the wave-length separation between the two points of zero reflectivity. For a triple film, the film thicknesses are a quarter wave for the top film, a half wave for the middle film and three quarters for the bottom film. In this case the required film indices can also be found among available materials. For example, on a glass of index 1.52, the top film index may be 1.41, the middle index 2.12 and the bottom film index 1.72.

[1] M. Born, *Optik* (Verlag-Julius, Springer, Berlin, 1933), pp. 122–126.

70. The Measurement of Flame Temperatures. CURTIS J. HUMPHREYS AND EARLE K. PLYLER, *National Bureau of Standards.*

A method of measuring the temperatures of flames utilizing the continuous radiant energy from incandescent particles within the flame has been devised. If the particles are sufficiently small they approach thermal equilibrium with gaseous molecules. This temperature should be differentiated from that determined by measuring the characteristic molecular emission spectra from flames, giving either vibrational or rotational temperatures. The method is applicable to opaque or semi-opaque flames and can be used for transparent flames by introduction of fine particles. The method consists in measuring the intensity in the ultraviolet continuum at several different wave-lengths, which are free from molecular bands. These intensities are compared at the same wave-lengths with the continuous emission from a tungsten ribbon-filament lamp with a quartz window, which had been calibrated for a range of temperatures from 2000° to 3000°K. Methods of measuring the spectral intensities by photography and use of photocells will be discussed, including necessary corrections and precautions. Observations have been made on the oxy-acetylene welding torch flame with varying proportions of the gases. Flame temperatures have been determined in the range between 2500° and 3000°K.

71. A Radiation Slide Rule and Nomographs for the Simplification of Radiation Calculations. ALFRED H. CANADA, *General Electric Company.*

Two developments are described as time saving aids in radiation calculations. The first is a method of exponential nomograph construction[1] applicable to problems following either Lambert's or Beer's absorption laws. Nomographs either of concentration and extinction coefficient or of pressure, path length and extinction coefficient are illustrated as functions of percent transmission. The method of construction of such nomographs is described to show their applicability to many exponential functions. Such nomographs provide a simple graphical solution to many problems involving the Lambert-Beer Law. The second development is the Radiation Slide Rule[2] for the computation of black body radiation. The design and data compilation for the rule is described with sample problems to illustrate its use. A single setting of the rule at a desired temperature yields the value of radiation from a source with any emissivity in several different systems of units; the position of the radiation maximum in microns or in waves per centimeter; and the distribution of this energy, if the source is a black body, in the spectrum. The rule may also be used for temperature conversion, energy conversions and wave-length conversions to either waves per centimeter or frequency. Scales of relative luminosity, photon energies and characteristics of tungsten are also included.

[1] A. H. Canada, GE Review, p. 44, March, 1948.
[2] A. H. Canada, GE Review, p. 50, December, 1948.

Author Index of Papers

Ballard, Stanley S.—see Combes, Lewis S. and James R. Travis
Barnett, C. E. and L. D. Grady—No. 7
Barr, E. E.—No. 44
Benedict, W. S.—see Plyler, Earle K.
Benson, Nels C., Georg Hass, and Noel W. Scott—No. 31
—see Goldberg, Benjamin
Billings, B. H.—No. 45
—see Pfund, A. H. and E. J. Weichel
Bingham, R. H.—No. 38
Blout, E. R., R. S. Corley, and P. L. Snow—No. 46
— **and Miriam S. Flower**—No. 55
Bube, Richard H.—No. 13
Bullock, B. W. and S. Silverman—No. 43
Canada, Alfred H.—No. 71
Carman, P. D.—No. 32
Chamberlain, Katherine—see Kaczor, Emil
Combes, Lewis S., James R. Travis, and Stanley S. Ballard—No. 48
Corley, R. S.—see Blout, E. R. and P. L. Snow
Davidson, H. R. and L. W. Imm—No. 39
Dawson, L. H.—see Plymale, W. S., Jr.
Debye, P.—No. 34
Duntley, S. Q.—Nos. 19 and 20
Epstein, L. Ivan—No. 28
Flower, Miriam S.—see Blout, Elkan R.
Fogg, C. C.—see Palmer, E. W. and J. P. Irwin
Fred, Mark—see Tomkins, Frank S.
Gardner, Irvine C.—No. 65
Goddard, Pliny E.—see Pearlman, Donald and Franz Urbach
Godlove, I. H.—No. 40
Goldberg, Benjamin and Nels C. Benson—No. 29
Grady, L. D.—see Barnett, C. E.
Granville, Walter C. and Deane B. Judd—No. 35
Grey, David S.—No. 52
Griffin, P. M. and J. R. McNally, Jr.—No. 56
Hamly, D. H.—No. 36
Hardy, Arthur C. and F. Mansfield Young—Nos. 41 and 64
Harrison, George R.—No. 18
——see McNally, J. R., Jr.
Harvey, C. E.—see Hassler, M. F.
Hass, Georg—No. 30
——see Benson, Nels C. and Noel W. Scott
Hassler, M. F. and C. E. Harvey—No. 63
Hecht, Selig—see Hendley, Charles D.
Hendley, Charles D. and Selig Hecht—No. 24
Hodge, Edwin S.—see Schoen, A. L.
Holmes, Marian C.—see Middleton, W. E. Knowles
Hughes, Harold K. and R. W. Murphy—No. 60
Humphreys, Curtis J. and Earle K. Plyler—No. 70
Imm, L. W.—see Davidson, H. R.
Irwin, J. P.—see Palmer, E. W. and C. C. Fogg
Johnson, James S. and Ferd E. Williams—No. 14
Jones, R. Clark—No. 54
Judd, Deane B.—see Granville, Walter C.
Kaczor, Emil and Katherine Chamberlain—No. 62
Land, E. H.—No. 51
Leurgans, Paul—No. 69
Liston, Max D.—see White, John U.
MacAdam David L.—No. 25
Macht, David I., Marcus Ostro, and Stanley H. Macht—No. 33
——see Macht, David I. and Marcus Ostro
Matz, Charles H. and Dwight P. Merrill—No. 53
McNally, J. R., Jr. and G. R. Harrison—No. 57
——see Griffin, P. M.
Merrill, Dwight P.—see Matz, Charles H.
Middleton, W. E. Knowles—No. 37
—— **and Marian C. Holmes**—No. 26
Miles, Walter R.—No. 23
Mueller, F. W. H.—No. 68
Murphy, R. W.—see Hughes, Harold K.
Nagy, Elemer—No. 12
Nail, Nelson R., Franz Urbach, and Donald Pearlman—No. 11.
——see Urbach, Franz and Donald Pearlman
Nottingham, Wayne B.—No. 1
Oldham, Max S.—No. 47
Osterberg, Harold and Franklyn C. Wissler—No. 66
Ostro, Marcus—see Macht, David I. and Stanley H. Macht
Palmer, E. W., J. P. Irwin, and C. C. Fogg—No. 61
Parkinson, W. W., Jr. and Ferd E. Williams—No. 4
Patten, Stanley H. and Ferd E. Williams—No. 16
Pearlman, Donald, Pliny E. Goddard, and Franz Urbach—No. 9
——see Nail, Nelson R. and Franz Urbach
——see Urbach, Franz and Nelson R. Nail
Peckham, R. H.—No. 3
Pfund, A. H., E. J. Weichel, and B. H. Billings—No. 27
Plyler, Earle K. and W. S. Benedict—No. 50
Plyler, Earle K.—see Humphreys, Curtis J.
Plymale, W. S., Jr. and L. H. Dawson—No. 2
Ratliff, Floyd—see Riggs, Lorrin A.
Riggs, Lorrin A. and Floyd Ratliff—No. 21
Rosenbaum, Alma—see Studer, Frank J.
Schoen, A. L. and Edwin S. Hodge—No. 59
Scott, Noel W.—see Benson, Nels C. and Georg Hass
Shrader, Ross E.—No. 15
Silverman, S.—see Bullock, B. W.
Sittner, W. R.—No. 49
Sloan, Louise L.—No. 22
Snow, P. L.—see Blout, E. R. and R. S. Corley
Studer, Frank J. and Alma Rosenbaum—No. 6
Tomkins, Frank S. and Mark Fred—No. 58
Travis, James R.—see Combes, Lewis S. and Stanley S. Ballard
Urbach, Franz, Nelson R. Nail, and Donald Pearlman—Nos. 10 and 17
——see Nail, Nelson R. and Donald Pearlman
——see Pearlman, Donald and Pliny E. Goddard
Weichel, E. J.—see Pfund, A. H. and B. H. Billings
White, John U. and Max D. Liston—No. 42
Wilber, D. T.—No. 5
Wilkins, J. Ernest, Jr.—No. 67
Williams, Ferd E.—No. 8
——see Johnson, James S.
——see Parkinson, W. W., Jr.
——see Patten, Stanley H.
Wissler, Franklyn C.—see Osterberg, Harold
Young, F. Mansfield—see Hardy, Arthur C.